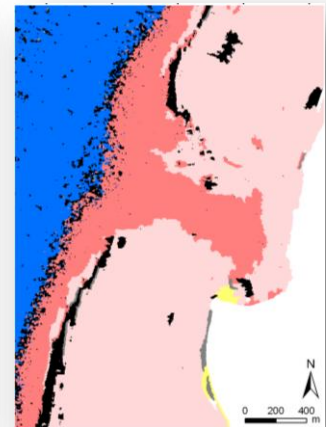
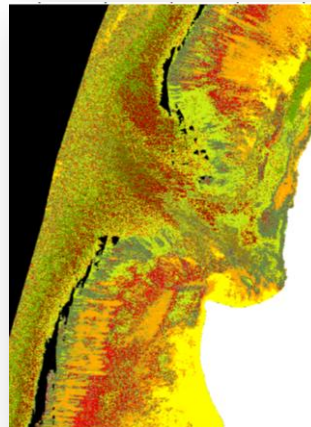
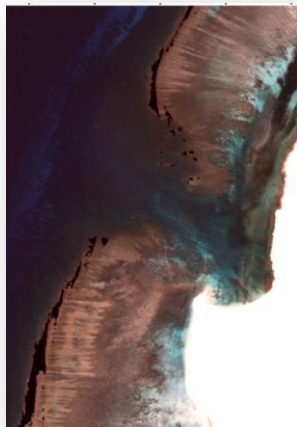


Ningaloo Collaboration Cluster: Habitats of the Ningaloo Reef and adjacent coastal areas determined through hyperspectral imagery

Halina T. Kobryn, Kristin Wouters and Lynnath E. Beckley
Ningaloo Collaboration Cluster Final Report No.1b
June 2011



Ningaloo Collaboration Cluster: Habitats of the Ningaloo Reef and adjacent coastal areas determined through hyperspectral imagery

Halina T. Kobryn, Kristin Wouters and Lynnath E. Beckley

Ningaloo Collaboration Cluster Final Report No.1b

June 2011



This report is an outcome from the Ningaloo Collaboration Cluster – a partnership between Murdoch University, The University of Western Australia, the Australian National University, The University of Queensland, Edith Cowan University, Curtin University of Technology, the Sustainable Tourism Cooperative Research Centre and CSIRO's Wealth from Oceans Flagship. The Cluster is funded through CSIRO's Flagship Collaboration Fund and the partners' in-kind support.
www.csiro.au/partnerships/NingalooCluster

Enquiries should be addressed to:

Dr Halina T. Kobryn (H.Kobryn@murdoch.edu.au) (0893602411)
School of Environmental Science, Murdoch University, Perth, WA

Distribution list

Neil Loneragan, Ningaloo
Collaboration Cluster Leader

Tom Hatton, WfO Flagship
Director

Bill de la Mare, CSIRO Cluster
Representative

Copyright and Disclaimer

© 2011 CSIRO To the extent permitted by law, all rights are reserved and no part of this publication covered by copyright may be reproduced or copied in any form or by any means except with the written permission of CSIRO.

Important Disclaimer

CSIRO advises that the information contained in this publication comprises general statements based on scientific research. The reader is advised and needs to be aware that such information may be incomplete or unable to be used in any specific situation. No reliance or actions must therefore be made on that information without seeking prior expert professional, scientific and technical advice. To the extent permitted by law, CSIRO (including its employees and consultants) excludes all liability to any person for any consequences, including but not limited to all losses, damages, costs, expenses and any other compensation, arising directly or indirectly from using this publication (in part or in whole) and any information or material contained in it.

ISBN 978-0-86905-951-7

Contents

1	Overview	1
1.1	Benefits and managements implications	3
1.2	Further Developments	4
1.3	Acknowledgements.....	4
1.4	Planned Publications	5
1.5	Communications	5
1.5.1	Presentations	5
1.5.2	Student Projects.....	6
1.5.3	Data Accessibility (Data Summary).....	7
1.5.4	Meta data description.....	7
1.5.5	Who is the custodian of the data.....	7
1.5.6	Raw data and data products description.....	7
2	Benthic habitat, topographic and geomorphic classifications of Ningaloo reef with hyperspectral imagery	9
2.1	Introduction	9
2.2	Methods	11
2.2.1	HyMap data acquisition.....	11
2.2.2	Field data collection	14
2.2.3	Preprocessing HyMap data.....	18
2.2.4	Field data processing	19
2.2.5	Class selection.....	21
2.2.6	Separation of the field data into training and validation sets:	22
2.2.7	Spectral analysis of image-derived spectra	22
2.2.8	Pixel-based benthic cover classification approach.....	24
2.2.9	Post-classification	27
2.2.10	Validation	30
2.2.11	Topographic and geomorphic classifications	31
2.3	Results.....	35
2.3.1	Spectral analysis of field spectra and selection of class components	35
2.3.2	Spectral analysis of image-derived spectra	37
2.3.3	Image classification results	38
2.3.4	Probability images.....	41
2.3.5	Mosaics and masks	42
2.3.6	Thematic generalisation.....	43
2.3.7	Spatial generalisation.....	54
2.3.8	Spatial statistics	56
2.3.9	Validation results.....	72
2.3.10	Topographic classification.....	73
2.3.11	Geomorphic classification	83
2.4	Discussion	90
2.4.1	Spectral analysis.....	90
2.4.2	Classification approach.....	92
2.5	Summary and conclusions.....	96
3	Hyperspectral imagery for landscape characterisation along the coast of the Ningaloo Marine Park, Western Australia	99
3.1	Introduction	99
3.1.1	Overview of the study area	99
3.1.2	Ningaloo coastline and off-road vehicles	102

3.1.3	Remote sensing of soils and vegetation.....	107
3.2	Methods	110
3.2.1	Study area.....	110
3.2.2	Data Processing.....	111
3.2.3	Analysis of the bare sediment component of the landscape	112
3.2.4	Soil analysis	120
3.2.5	Spectral analysis of field samples	120
3.2.6	Hyperspectral image processing	121
3.2.7	Statistical analysis.....	122
3.2.8	Other geographic data	123
3.2.9	Classification of roads and tracks.....	123
3.2.10	Cumulative length of roads/tracks	124
3.2.11	Densities of roads/tracks	124
3.3	Results	127
3.3.1	Bare sediment component of the landscape	127
3.3.2	Spectral Angle Mapper Classifications	135
3.3.3	Principal Component Analysis.....	142
3.3.4	Vegetation cover	144
3.3.5	Lengths and densities of roads and tracks.....	153
3.3.6	Cumulative length and densities of roads/tracks in pastoral stations	156
3.3.7	Land tenure and vegetation.....	174
3.3.8	Vegetation around accommodation nodes.....	182
3.3.9	Vegetation in coastal strip and adjacent to sanctuary zones.....	182
3.4	Discussion.....	184
3.4.1	Sources of variance within field measurements	184
3.4.2	Discrimination of sediment types.....	185
3.4.3	Distribution patterns within sediment classifications.....	185
3.4.4	Tracks and roads	186
3.5	Conclusion	190
	References	192
	Appendix A	204
	Appendix B	205
	Appendix C	206
	Appendix D	207
	Appendix E.....	208
	Appendix F.....	210
	Appendix G	211

1 OVERVIEW

This study had two components, namely, mapping of the marine habitats of Ningaloo Reef and characterising the landscape of coastal areas adjacent to along the Ningaloo Marine Park.

Marine habitats

In relation to marine habitats in the shallow (<20m) regions of Ningaloo Reef, this project had three objectives. Firstly, it aimed to develop a high-resolution characterisation of the reef and shallow water habitats to provide the basis for future, multiple-use management and planning of the area. Second objective was focused on description of the biodiversity values, and the third on the identification of biodiversity hotspots.

This report focuses mainly on the first objective and the latter two objectives are reported separately by Mike van Keulen and Mark Langdon (Habitats and biodiversity of Ningaloo Reef lagoon. Part 1c: Biodiversity and Ecology) and by Greg A. Skilleter, Neil R. Loneragan, Halina T. Kobryn, Ayax Diaz-Ruiz and Ali McCarthy (Part 1d: Assessing invertebrate biodiversity on Ningaloo Reef: Validation of habitat surrogacy).

Using hyperspectral data (bottom reflectance) we were able to retrieve a very detailed characterisation of marine substrates in the Ningaloo Marine Park, at a 3.5 x 3.5 m pixel resolution. Globally, this data set is one of the most extensive for a coral reef system and covers over 300 km of coastline, extending seamlessly from the 20 m depth contour to 2 km inland. In general, the unique spectral characteristic of each pixel (made up by objects within it), combined with information from field validation, allowed us to classify the imagery into different habitats or thematic layers. To ensure validity and spatial consistency of the final habitat classes, we undertook spectral separability analysis of the image-derived spectra. Final class labels were derived at five different thematic levels, from three broad (biotic, abiotic and mixed), through medium detail describing 13 classes of habitats, to detailed coral form information combined with the other components (algae or abiotic). Accuracy assessment (overall and per-class) was completed with the overall accuracy of 74 % at the detailed 4a class (this level has 21 classes). Post-classification smoothing, masking and generalisations were undertaken to ensure visually effective products without loss of the information.

The classification process was driven by spectral reflectance data and also by the field data. Classification of hyperspectral imagery over shallow lagoons generated a number of data sets. The outputs of image analysis contain final classification categories with look-up tables as well as per-pixel probability layers and overall percentage cover of corals, macroalgae and sediment. This final classification data set can be displayed in different ways depending on the user requirements.

For selected areas, bathymetry data retrieved from the Modular Inversion and Processing System (MIP) processed hyperspectral imagery were analysed to create combined depth, aspect and slope images to assist in understanding the distribution of benthic cover types. Maps of geomorphic features for selected areas were generated using an object-oriented classification approach which combined topographic variables and habitat maps.

The overall summary showed that the majority (54 %) of the cover is composed of macroalgal and turfing algae communities, while hard and soft coral cover (>10 % per pixel) represents only 7 % of the mapped area (762 km²). There were 5 854 ha of coral mosaics mapped along the Ningaloo Reef. The single largest coral mosaic type was continuous tabulate coral (2 155 ha or 37 % of all corals).

The majority of the coral classes (66 %) were a mix of dense to continuous tabulate coral, sparse digitate coral, soft coral and sparse submassive and massive corals. Continuous to patchy digitate and tabulate coral made up approximately 10 % of the coral cover, while “blue tip” *Acropora* was approximately 8.5 %. The majority of the hard coral occurred as either very dense (continuous >90 %) cover or as patchy distribution (20-45 %). Approximately 15 200 ha (21 %) of the mapped habitats were in close proximity to the shore (0-500 m). Some 14 % of the coral communities mapped were located close to shore. Approximately half of the coral communities are located within the sanctuary zones of the Ningaloo Marine Park.

While sand dominated the most popular snorkelling areas at Turquoise Bay, Coral Bay and Gnaraloo, they had quite different coral cover within 500 m of the most common entry point to the water. Turquoise Bay had the largest proportion of coral and Gnaraloo the least. Of the three locations, Coral Bay area had the largest proportion of macroalgae mosaics.

This project has shown that it is possible to map coral reef habitats over large areas using hyperspectral remote sensing with multiple flight lines and that this technique is well suited for semi-automated mapping tasks in clear water, coastal environments.

Terrestrial mapping

The main aim of the terrestrial analysis was to map the extent of vegetation and off-road vehicle tracks along the coast at Ningaloo using hyperspectral remote sensing. The specific objectives were to:

- Provide broad classification of the vegetation along the Ningaloo coast with particular attention to live (photosynthetically active) shrubs and trees
- Examine the spatial density of off-road vehicle tracks in the Ningaloo region and their possible impacts on vegetation
- Investigate the relationship between track density, total track length and land tenures, and
- Determine the number of tracks providing access to sanctuary zones of the Marine Park in order to evaluate latent risks if visitor numbers were to increase.

The Ningaloo coastline in the remote northwest of Western Australia is a popular tourist destination, attracting thousands of visitors to its coastline to enjoy fishing, camping, snorkelling, wildlife viewing and four-wheel drive activities. In order to protect the unique coastal environment that is attracting so many visitors, careful planning and monitoring of the coastal roads and access points to beaches is required to minimize any degradation of the natural resources.

Hyperspectral remote sensing is a non-invasive tool that can provide information on landforms, vegetation and ground cover that might be missed by other remote sensing tools. The study included different management zones, landscapes and ecosystems and certain areas were validated in the field to check the vegetation types and presence of tracks or roads.

As the popularity of Ningaloo Reef and the Cape Range National Park as tourist destinations increases, the associated increase in tourist-related traffic will potentially create a soil erosion risk on the peninsula, which may lead to accelerated sediment build-up in the Ningaloo Reef lagoons as well as loss of coastal plant cover in an already sparsely vegetated area.

This study aimed to classify the distribution of all distinct, bare, terrestrial cover types within the 2006 HyMap Ningaloo survey area, based on the variations in their physical and chemical properties. The study area was approximately 2 km inland from the mean high water mark, extending from Red Bluff

in the south to Exmouth in the north. Through analysis of the sediment distribution maps produced, the study attempted to detect areas vulnerable to erosion and sedimentation. Sixteen bare terrestrial surface types were identified by applying ENVI's Spectral Angle Mapper to the corrected and masked reflectance data. These surfaces were validated by measuring key soil properties and environmental variables and field spectrometry of 36 soil samples. Principal Component Analysis determined that mean reflectance, moisture content and iron content were the main sources of variation within the dataset. Hyperspectral imagery was found to be an effective means of classifying and mapping sediment distribution.

This study also examined the spatial density of off-road vehicle tracks in the Ningaloo region and investigated the relationship between track density, total length and land tenures. Results were analysed within five land tenures along the coast (miscellaneous crown reserves, National Park, freehold land, unallocated crown land and pastoral leases). The longest total cumulative distance of tracks (802.3 km) and the highest track density (9.7 km per km²) were found on pastoral leases. In contrast, Cape Range National Park had the lowest roads/tracks density at 0.3 km per km². The analysis also showed that tracks densities were high at tourist accommodation nodes and certain camp sites. The type of land tenure appeared to be extremely important as it defines the management arrangements along the coast.

The relationships between broad vegetation communities and coastal tracks and land tenure, distance to shore and accommodation nodes were also investigated. The results showed that the type and amount of vegetation potentially impacted by four-wheel drive tracks varied along the coast according to vegetation association distribution and land tenure. Tourist accommodation also has impact on surrounding vegetation. Finally, the number of access tracks was greater in coastal areas not vested in the Department of Environment and Conservation but significantly, leading to one of the sanctuary areas, Winderabandi. These findings help identify indicators for monitoring and evaluating future developments of the Ningaloo coastal region.

1.1 Benefits and managements implications

Effective management and monitoring of large Marine Protected Areas require detailed baseline data on distribution of benthic habitats (as a surrogate for marine biodiversity). Large areas with complex bathymetry and clear waters such as the Ningaloo Marine Park (NMP) in Western Australia naturally lend themselves to the application of optical remote sensing as a means of gathering data on benthic cover and bathymetry. This high resolution baseline data (thematic maps and per-class probability layers) can assist managers and scientists with the following:

- Designing and implementing effective monitoring programs for the coral assemblages
- Designing and implementing extensive biodiversity surveys with the opportunity to develop linkages between benthic cover type and plant and animal distribution. Development of surrogacy indicators between habitat type and biota found in the field should be given a high priority
- Gaining a better understanding of the relationship between benthic cover and topographic variables such as depth, slope and aspect.

The derived hyperspectral dataset for the terrestrial areas has the potential to provide an indication of the effectiveness of hyperspectral techniques for monitoring and managing the prevailing network of roads and minor tracks along Ningaloo's coastline. This could assist the Department of Environment and Conservation (DEC) with future assessments of the appropriate level of access and use of the

Ningaloo coastal environment and the potential physical impact of vehicular traffic on the vulnerable coastal communities.

1.2 Further Developments

The following list summarises further analyses of the data generated in this project that would be valuable for researchers and managers working in the area:

- Detailed analysis of the relationship between biodiversity surrogacy at different levels should be undertaken. With this very detailed data set it should be possible to link field-based surveys and explore the relationships at different thematic levels and different per-class probability thresholds. Studies on fish grazing, as part of Ningaloo research in the WA Marine Science Institution (WAMSI) will also benefit greatly from the results of this work
- More extensive analyses should be undertaken on the relationships between presence/absence of different benthic cover types and topographic and geomorphic variables derived from the bathymetry
- An atlas (preferably hard copy for those users who are not used to GIS and image processing) of the main thematic maps created in this study would be highly beneficial to the managers and scientists working in the area
- Parts of such an atlas would also form a valuable teaching resource as most map-based, teaching materials in Australia are based on information from the Great Barrier Reef
- Further research is needed to examine at the level of thematic detail and spatial scale which can be extracted from the data set and the level of detail that is necessary for monitoring purposes (especially coral)
- With further field work focused on algae, the current data set can be further reprocessed for more detailed description of macroalgae, turfing algae and possibly seagrasses.

1.3 Acknowledgements

The collection of hyperspectral data was funded by BHP-Billiton and coordinated by the Australian Institute of Marine Science. We especially thank Dr Andrew Heyward for facilitating the funding arrangements and Dr Peter Hausknecht (formerly with HyVista Corporation) for the liaison, commitment and support with the data queries.

We thank Murdoch University for in-kind support, CSIRO Wealth from Oceans and BHP Billiton for funding and acknowledge support from HyVista Corporation and EOMAP.

CSIRO staff: Dr Mick Haywood and Dr Russ Babcock assisted in providing field validation data and provided valuable feedback on the results. Murdoch University staff, Dr Nicole Pinnel and students, Dr Matt Harvey, Mark Langdon and Kim Marrs provided substantial assistance with the fieldwork. We are very grateful for your contributions.

1.4 Planned Publications

- Vital statistics of the marine habitats in Ningaloo Marine Park (Kobryn, H.T., Beckley, L.E and Wouters, K., journal: *Coral Reefs*, draft in development)
- Benthic cover mapped using spectral and topographic variables (Kobryn, H.T., Wouters, K. and Beckley, L.E., journal: *Photogrammetric Engineering and Remote Sensing*, draft in development)
- Coastal tracks of the Ningaloo coast, relationship with tenure, management and geographic variables (Kobryn, H.T., Beckley, L.E. and others, draft in development)
- Distribution and characterisation of bare and vegetated landscape component of the Ningaloo coast using hyperspectral imagery. (Kobryn, H.T. and others, draft in development)

1.5 Communications

1.5.1 Presentations

Heege T., Hausknecht, P., Kobryn H.T. 2007. *Hyperspectral Seafloor Mapping And Direct Bathymetry Calculation Using Hymap Data From The Ningaloo Reef And Rottnest Island Areas In Western Australia*, European Association of Remote Sensing Laboratories Symposium, Oud Sint-Jan, Bruges, Belgium.

Heege T., Kiselev, V., Heblinski, J., Miksa, S., Pinnel, N., Hausknecht, P. P., Kobryn, H.T. 2007. *Physically based data processing of multi- and hyperspectral remote sensing data. From inland to marine applications*. European Association of Remote Sensing Laboratories Symposium, Bolzano, Italy.

Heege, T., Kobryn, H.T., Heblinski J., Harvey, M. and McDonald A. 2008. *Standardized sea floor and water depth mapping using optical airborne and satellite data*, 14th Australasian Remote Sensing Conference, Darwin, NT.

Heege, T., Heblinski, J., Kobryn, H., Wouters, K., Pinnel, N., Reinartz, P. 2009. *Standardized Sea Floor And Water Depth Mapping Using Optical Airborne And Satellite Data*, IEEE International Geoscience & Remote Sensing Symposium, Cape Town, Africa.

Kobryn H., Pinnel N., Heege T., Beckley, L.E., Harvey, M. and Long, S. 2008. *Mapping The Habitats And Biodiversity Of Ningaloo Reef, Western Australia Using Hyperspectral Imagery*, 11th International Coral Reef Symposium “Reefs for the Future”, Ft. Lauderdale, Florida, USA.

Kobryn, H.T., Wouters, K., Beckley, L.E., Pinnel, N. and Heege, T. 2009. *Making sense of hyperspectral remotely sensed habitat data for Ningaloo Marine Park, Western Australia*, Australian Marine Sciences Association Conference, Adelaide, SA.

Kobryn, H.T., Wouters, K., Beckley, L.E., Pinnel, N. and Heege, T. 2009. *Marine benthic habitats of Ningaloo Reef: mapping and derivation from hyperspectral remote sensing*. Australian Coral Reef Society Annual Conference, Darwin, NT.

Kobryn, H.T., Wouters, K., Beckley, L.E. and Heege, T. 2010. *Habitat mapping with hyperspectral remote sensing. Ningaloo Marine Park*. WAMSI Show and Tell, Perth WA.

Kobryn, H.T., Wouters, K., Beckley, L.E. and Heege, T. 2009. *Habitat mapping with hyperspectral remote sensing. Ningaloo Marine Park*. Wealth from Ocean Integration Workshop, Perth WA.

Kobryn, H.T., Pinnel, N. van Keulen, M., Beckley, L.E., Harvey, M.M., Hausknecht, P. and Hayward, P. 2007. *Through the looking glass! Revealing the habitats and biodiversity of Ningaloo Reef using hyperspectral imagery*. Australian Coral Reef Society Annual Conference, Fremantle, WA.

Kobryn, H. T., Pinnel, N., Beckley, L. E. Harvey, M., Mike van Keulen, M., Heege , T. and Hausknecht, P. 2007. *Habitats and biodiversity of Ningaloo Reef. Mapping the habitat components and bathymetry with hyperspectral remote sensing*. Australian Coral Reef Society Annual Conference, Fremantle, WA.

Kobryn, H.T., Wouters, K., Beckley, L.E., Pinnel, N. 2009. *Mapping the marine benthic habitats of Ningaloo Reef lagoon*, Ningaloo Symposium, Exmouth, WA.

Pinnel N., Kobryn, H.T., Heege, T., Harvey M., Beckley, L.E. 2008. *A Hyperspectral, remote-sensing approach to spectral discrimination of marine habitats at Ningaloo Reef, Western Australia*. 11th International Coral Reef Symposium “Reefs for the Future”, Ft. Lauderdale, Florida, USA.

Pinnel, N., Kobryn, H.T., Heege, T., Harvey, M.M., Beckley, L. E. van Keulen, M., Collins, L. and Hausknecht P. 2007. *Spectral discrimination of marine habitats at Ningaloo Reef, Western Australia*. Australian Coral Reef Society Annual Conference, Fremantle, WA.

Pinnel N., Kobryn, H., Heege T., Harvey M., Long S., Fitzpatrick, B., Twiggs, E., Beckley L. and van Keulen, M. 2008. *A large scale hyperspectral approach for coral reef habitat mapping at Ningaloo Marine Park, Western Australia*, 14th Australasian Remote Sensing and Photogrammetry Conference, Darwin, NT.

Wouters, K., Kobryn, H.T., Heege, T. and Beckley, L.E. 2009. *Mapping marine benthic habitats and topographic structures of Ningaloo Reef at varying thematic and spatial resolutions using different classification approaches and hyperspectral remote sensing*. Australian Coral Reef Society Annual Conference, Darwin.

Wouters, K., Kobryn, H.T., Heege, T. and Beckley, L.E., 2010. *Ningaloo Reef- combining hyperspectral and topographic information to classify geomorphic features*. WAMSI Show and Tell, Perth WA.

1.5.2 Student Projects

Luisa D’Andrea, 2007. *Using hyperspectral imagery to map vegetation condition and ground cover of the coastal area at Coral Bay, WA*, MSc thesis Murdoch University, Australia, 67pp.

Jess Bunning, 2008. *Hyperspectral techniques to detect off-road vehicle tracks along the Ningaloo coastline*, MSc thesis Murdoch University, Australia, 70pp.

Denis Rouillard, 2008. *The use of hyperspectral imagery in mapping marine and terrestrial sediment distribution on the Cape Range Peninsula*, MSc thesis Murdoch University, Australia, 126pp.

Simon Wee Beng Huat , 2009. *Extent and density of roads and tracks along the Ningaloo coastline, North West Australia*, MSc thesis Murdoch University, Australia, 61pp.

Julien Noyer, 2010. *Spatial patterns of 4WD tracks along the coast of Ningaloo, Australia*, 3rd year BSc project, 34pp.

1.5.3 Data Accessibility (Data Summary)

This study produced three main data sets for the area covered by the 2006 airborne hyperspectral HYMAP survey extent:

- Marine benthic habitat including per-class probability
- Terrestrial cover including vegetation indices and green shrub cover
- Tracks and roads

Further information about these data sets and access to them can be obtained from Dr Halina T. Kobryn, School of Environmental Science, Murdoch University, Western Australia (0893602411, email: H.Kobryn@murdoch.edu.au).

1.5.4 Meta data description

Documentation files (“Readme” files) have been produced for all data sets created and are part of the GIS data file directory structure.

1.5.5 Who is the custodian of the data

Access and further information about these data set can be obtained from Dr Halina T. Kobryn, School of Environmental Science, Murdoch University, Western Australia (0893602411, email: H.Kobryn@murdoch.edu.au).

1.5.6 Raw data and data products description

Raw data for this project included airborne hyperspectral HyMap imagery flown in 2006 and are described in the methods section of this report and Appendix A.

2 BENTHIC HABITAT, TOPOGRAPHIC AND GEOMORPHIC CLASSIFICATIONS OF NINGALOO REEF WITH HYPERSPETRAL IMAGERY

Authors: Halina T. Kobryn, Kristin Wouters, Lynnath E. Beckley, Thomas Heege and Nicole Pinnel

2.1 Introduction

Coral reefs are iconic ecosystems which create diverse habitat mosaics and support a wide range of organisms (Spalding *et al.* 2001). Globally, Australia boasts the largest coral reef ecosystems, in the Great Barrier Reef (GBR) as well as one of the world's largest fringing reefs along the Ningaloo coast (UNEP/IUCN 1988, Spalding *et al.* 2001). Ningaloo is a part of a diverse reef system of the Indian Ocean and one of the least disturbed (Spalding *et al.* 2001). The area has been protected by Ningaloo Marine Park since 1987 and nominated for World Heritage status in January 2010 (Commonwealth of Australia 2002, DEWHA, 2010). Ningaloo Reef lies in close proximity to the mainland and extends over nearly 300 km along the northwest coast of Western Australia. It lies along the narrowest section of the Australian continental shelf, with the depth contour of 200 m less than 20 km offshore and is the longest fringing reef on any west coast of a continent (Collins *et al.* 2003).

While some corals (scleractinian and soft corals) are present in the Exmouth Gulf, most of the recent formations fringe the western shores of Exmouth Peninsula (UNEP/IUCN 1988, Short 1999, Short and Woodroffe 2009). Although most of the reef area (including the Muiron Islands to the north) has been protected under state and federal laws (UNEP/IUCN 1988), it still faces many threats.

Threats to the coral reef in the region include natural events such as cyclones, pests and diseases as well as human-induced factors which include regional mining and exploration (mostly oil and gas), shipping, fishing and tourism. Some threats are of a more global nature such as coral bleaching and pests transported by marine vessels (Bryant *et al.* 1998, CALM and MPRA 2005). Monitoring and management activities require comprehensive data to allow for efficient planning and management (Spalding *et al.* 2001). Challenges for management include timely response to any adverse events such as oil spills or ship stranding and planning in the light of changing climates and associated ocean conditions such as warming and acidification (Spalding *et al.* 2001). Understanding complexity of the ecosystems and their interactions requires baseline data which include bathymetry and habitat maps.

Habitat maps derived from various remote sensing instruments have become widely used in marine monitoring and management in the past two decades. Reasons for this increasing use have been lower costs of the data, more user-friendly software for image processing, better methods for deriving habitat maps from remotely sensed data, as well as growing awareness by the managers and decision makers of the usefulness of these data for conservation, planning, monitoring and management (Green *et al.* 2000). Effective management and monitoring of large marine protected areas requires detailed baseline data on the distribution and abundance of benthic habitats. Large areas with clear waters such as the Ningaloo Marine Park (NMP) in Western Australia naturally lend themselves to the application of optical remote sensing as a means of gathering data on coral reef habitats.

The current habitat mapping base of the NMP, generated by the Department of Environment and Conservation (DEC), includes only very general habitat classes based on visual interpretation of aerial photos (Bancroft and Sheridan 2000, CALM and MPRA 2005). Cassata and Collins (2001), using visual interpretation of aerial images, attempted more detailed mapping of benthic habitats of Ningaloo, but limited this to a few selected sections of the reef, mostly confined to the sanctuary

zones. Thus, no attempt has yet been made to generate a detailed habitat map covering a large area of the NMP or to integrate the information about the reef with the data along the adjacent coastal area.

Considering that spatial information has the potential to change management approaches (Costello *et al.* 2010) and that remote sensing can be employed relatively cost-effectively for large, mostly inaccessible areas, it seems logical that detailed habitat maps produced using large spatial, remotely sensed datasets are a feasible option for improved monitoring and management of the NMP.

Satellite or airborne remote sensing has increasingly been employed to map coral reef communities worldwide (Green *et al.* 1996, Holden and LeDrew 1998, Hochberg and Atkinson 2000, Mumby *et al.* 2001, Mumby and Edwards 2002, Roelfsema *et al.* 2002, Andrefouet *et al.* 2003, Hochberg and Atkinson 2003, Karpouzli 2004, Andrefouet and Guzman 2005, Purkis *et al.* 2005, Riegl and Purkis 2005, Harborne *et al.* 2006, Purkis *et al.* 2006, Purkis *et al.* 2008).

While a range of these studies used high spatial resolution data, e.g. IKONOS (Andrefouet *et al.* 2003, Hochberg and Atkinson 2003, Riegl and Purkis 2005, Purkis *et al.* 2005, Purkis *et al.* 2008) or Quickbird (Mishra *et al.* 2007), most studies using high spectral resolution data have been limited to investigating field spectroscopy rather than airborne hyperspectral data. These studies have demonstrated that discrimination is possible between *in situ* hyperspectral reflectance measurements of corals from algae (Hochberg and Atkinson 2000, Hochberg *et al.* 2003, Mumby, 2004), coral growth forms or species (Lubin *et al.* 2001, Hedley and Mumby 2002, Hedley 2004, Kutser 2006) and healthy from bleached coral (Holden and LeDrew 1998, Myers *et al.* 1999) through the use of narrow spectral bands. These are capable of discriminating subtleties in spectra between substrates, providing the use of specific absorption features not retrievable from medium resolution multispectral data (Andrefouet *et al.* 2002, Hochberg and Atkinson 2003).

Further techniques have been employed in these studies to increase the detectability of spectral differences between reef substrates. These have included clustering, principal component and linear discriminant analyses (Holden and LeDrew 1998, Andrefouet *et al.* 2004, Hochberg and Atkinson 2000), as well as derivative analyses, which highlight differences in the shape of spectral reflectance curves rather than in illumination variations (Hedley *et al.* 2004, Mumby *et al.* 2001, Holden and LeDrew 1998, Hochberg *et al.* 2003).

Only a few studies have attempted mapping of coral reef substrates or communities using airborne hyperspectral data, such as CASI (Mumby and Edwards 2002, Andrefouet *et al.* 2004), AAHIS (Hochberg and Atkinson 2000), AAHIS and AVIRIS (Hochberg and Atkinson 2003) or AISA Eagle (Mishra *et al.* 2007), though not of large areas or a whole reef system.

One of the acknowledged drawbacks of existing airborne hyperspectral instruments and, in fact, most remote sensing imagery for coral reef mapping is their spatial resolution. Even with the high spatial resolution of multispectral sensors such as Ikonos, Quickbird or the hyperspectral CASI, which are able to map at scales of < 3 m (Purkis 2008), small patches of most reef substrata are still beyond the resolution of existing remote sensors. Very fine-scale structures in coral reefs cannot be resolved (Phinn *et al.* 2003) and the heterogeneity and structural complexity leads to problems with mixed pixels as a result of poor spatial resolution (Dobson and Dustan 2000, Maeder *et al.* 2002). For instance, Andrefouet *et al.* (2002) concluded that bleached and non-bleached coral colonies would only be distinguishable in pixels of 0.01 m², which currently do not exist in commercial remote sensing instruments.

Hedley *et al.* (2004) acknowledged this mixed pixel factor in coral reefs by creating "mixture groups to represent various realistic scenarios of change in reef communities" using *in situ* spectral measurements of different combinations of substrates. Purkis (2005) used a small number of mixed classes to classify coral and non-coral assemblages. Addressing the issue of mixed pixels using currently available airborne and satellite sensors would require classifying not only biologically uniform benthic component/substrate pixels, but also pixels comprising a realistic mix of substrate types occurring in coral reefs.

Therefore, a combination of techniques was used in this study to map pure as well as mixed reef habitats representative of the Ningaloo Reef. Techniques involved spectral analyses of *in situ*, as well as image-derived spectra. This spectral separability analysis facilitate the selection of classes, fuzzy logic to generate probability images for each habitat class and enable the analysis of classes with equally high probabilities, and development of a semi-automated supervised classification using derivatives and based on underwater visual census field data of benthic cover percentages.

2.2 Methods

2.2.1 HyMap data acquisition

HyMap data with 125 spectral bands between 450 - 2500 nm and an average spectral resolution of 15 nm were acquired over 10 days in April and May 2006 at 3.5 m ground resolution. The total area of the survey covered 3 400 km², encompassing Ningaloo reef to a depth of approximately 20 m, as well as the coastal strip adjacent to the Ningaloo Marine Park (Figure 1 and 2). For further details on HyMap acquisition, refer to the HyMap data acquisition report (Appendix A).

Data used in the marine habitat mapping consisted of bottom reflectance and bathymetry. These were retrieved from the HyMap data, after extensive processing by HyVista and EOMAP in collaboration with Murdoch University, to remove atmospheric, sun glitter, air/water interface and water column effects (Appendix B). Data processing steps for the terrestrial component are covered in the next section and Appendix D. All data processing was carried out on georeferenced mosaics of data blocks (Figure 2 and 3).

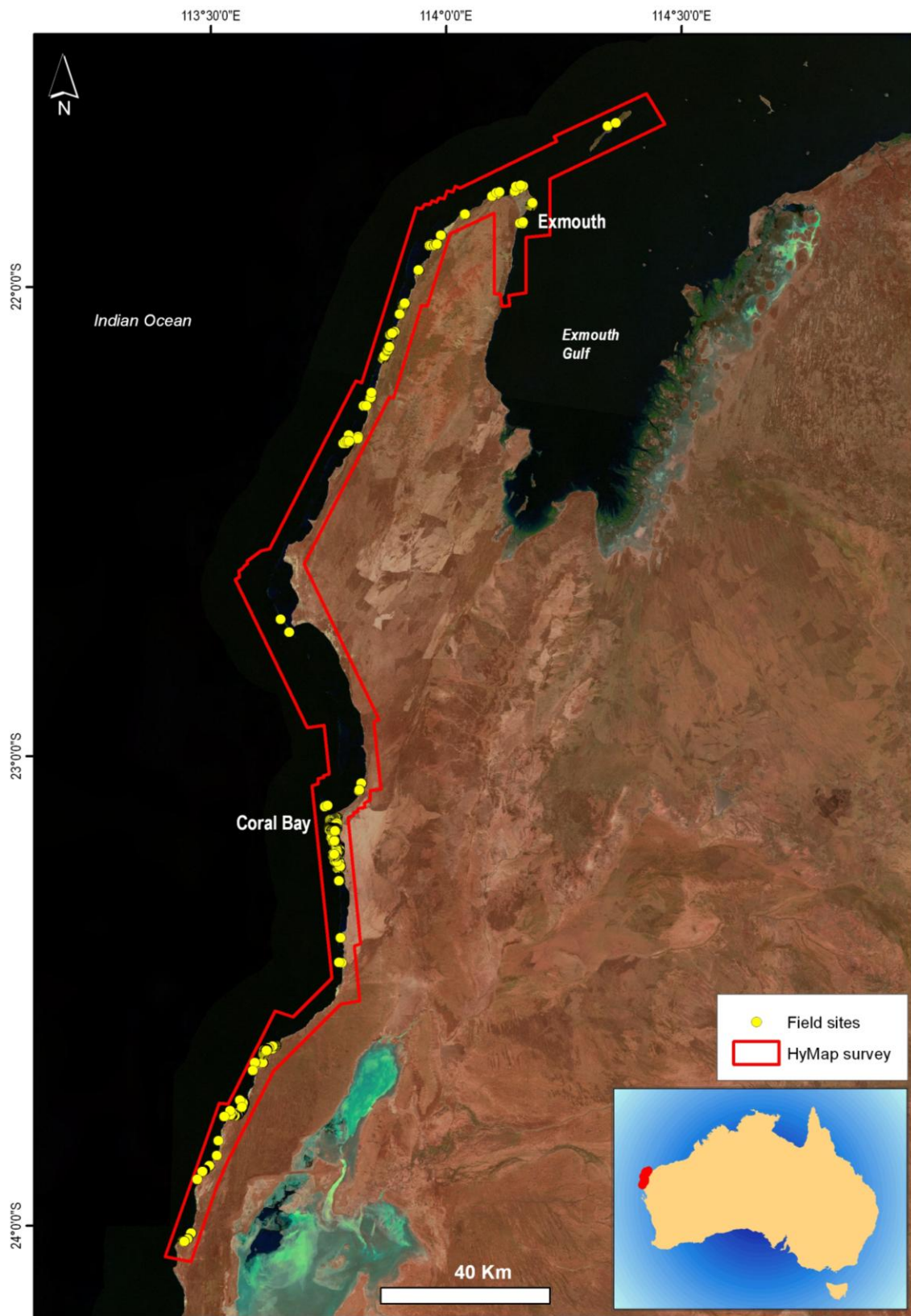


Figure 1: Extent of the HyMap survey and location of the field sites over Ningaloo Reef in Australia.

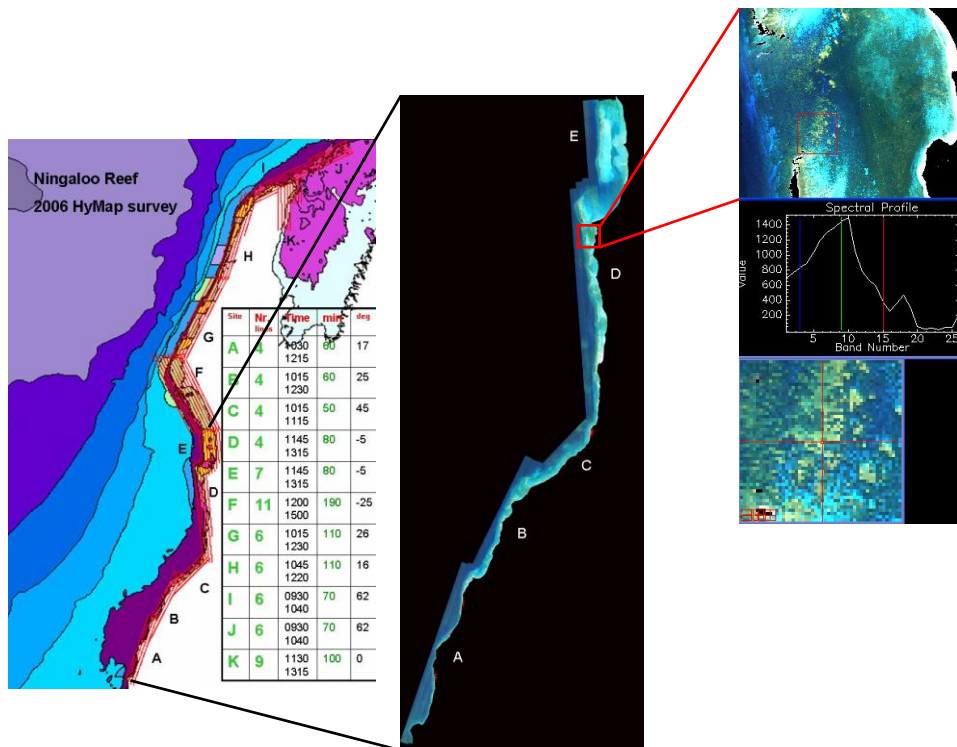


Figure 2. Overview of the HyMap mission at Ningaloo (left) showing data blocks A-K, mosaic of flight lines for blocks A-E depicting subsurface reflectance (middle) and subsets of block D (near Coral Bay) depicting different coverage (coral, shallow water, deeper water, sediments) and spectral reflectance plot from a single 3.5x3.5 m pixel (right).

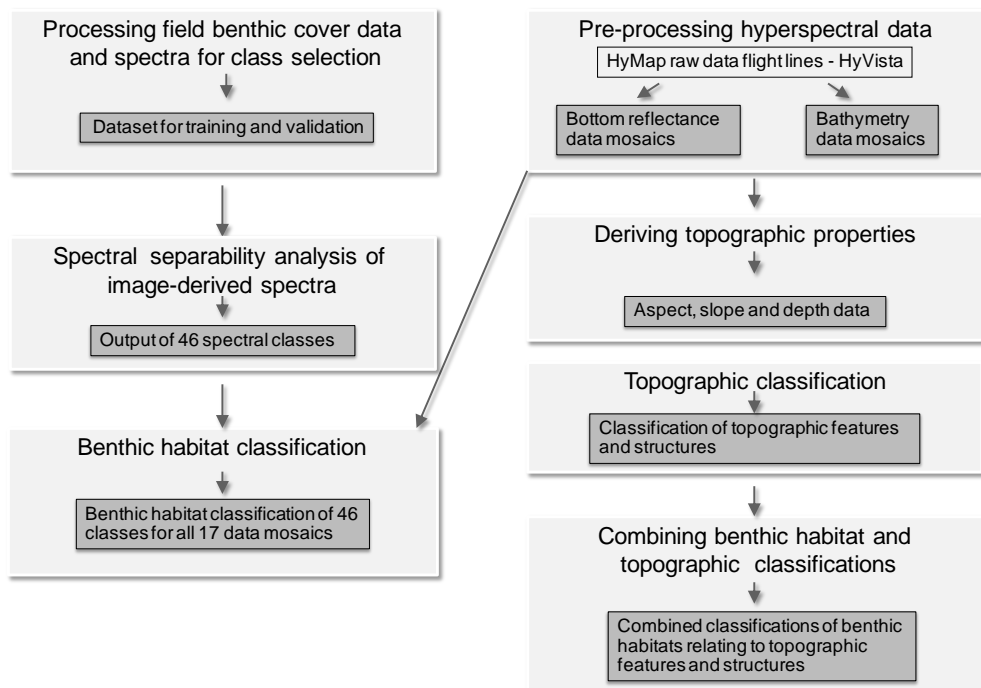


Figure 3. Overview of the methods for airborne and field data processing.

2.2.2 Field data collection

Airborne data processing and development of the image classification and validation were supported by ten field trips in different parts of the Ningaloo Reef between 2006 and 2009 (Figure 1). During these field trips two types of data were collected:

1. Underwater spectra for a range of substrates, often single species of coral or algae but also abiotic components such as sand, limestone pavement and other spectrally uniform benthic components (to determine the degree of spectral separability between habitat components)
2. High resolution benthic cover data of uniform as well as mixed benthic habitats at a pixel (3.5 m x 3.5 m) and megaquadrat (9 m x 9 m) scales

Underwater spectral measurements

Spectral reflectance from different substrate types including sand, coral and brown algae were collected *in situ* to assess the range of spectral variability that may be found in each cover type (Figure 4). A specific sampling strategy was adopted to measure the spectral reflectance of as many homogenous substrates as possible to characterise the spectral signatures of each. Data collection was performed following the methods described in Hochberg and Atkinson (2000, 2003).

The choice of substrates to measure was based initially on the benthic codes described by Page *et al.* (2001) and included biotic substrates such as hard and soft corals, macro- and turf algae as well as abiotic substrates such as sand and limestone pavement which occur widely throughout the reef. Different growth forms for some species of corals were also included, on the expectation that these growth forms could be spectrally separated due to differences in brightness as a result of varying texture and morphology.



Figure 4. Diver collecting underwater spectra of coral using Ocean Optics spectrometer.

Data collection

For each single reflectance measurement, spectral radiances were collected underwater of the desired substrates using an Ocean Optics USB 2000 portable spectrometer fitted with a 30 m fibre-optic cable with a diameter of 400 μm and a whole acceptance angle of 22.4° (wavelength range 330–850 nm), which was operated by a laptop computer located on the boat.

Spectral data were collected in pairs, the upwelling radiance from the target component and the corresponding downwelling radiance. To enable reflectance calculations, the same viewing geometry was used for the target and for a standard calibration panel placed adjacent to the target substrate. This setup allowed both spectra (target and calibration panel) to be acquired within 1–2 seconds. The time lapse between calibration panel and target reflectance measurements was minimized to reduce discrepancies due to changing light conditions. The measurements were meant to retrieve the pure spectra for end-member identification. A dark current measurement was collected before and after each dive, which was subtracted from all subsequent spectral measurements to correct for the light signal when the detector array is closed.

The Teflon reflectance panel was calibrated by Curtin University against a Labsphere Spectralon standard in air and a correction factor f was applied to calculate the reflectance spectra.

Data processing

The spectra were converted to absolute reflectance values using the following formula:

$$R_{USB2000} = f * \frac{DN_{target}}{DN_{panel}}$$

Reflectance measurements from the USB 2000 were calculated by dividing the digital count (DN) measured by the spectrometer with panel reference measurement and multiplying by a panel calibration factor f (provided by Curtin University). The reflectance spectra were processed to a spectral resolution of 1 nm intervals over the wavelength range 400–750 nm and also resampled to match the spectral response of the 2006 HyMap sensor. Ten individual spectra per sample were averaged to ensure optimal signal to noise ratio and the random measurements covered the range of variance within the homogenous substrate type. Analysis of spectral separability was undertaken through the calculation of median, mean, standard deviation as well as first and second derivatives by use of least square (Savitzky – Golay) polynomial smoothing filter of 9 nm width and an order of 3 (Demetriades-Shah *et al.* 1990).

Underwater photographs were taken to accompany each set of measurements for a given target and geographical locations were recorded with a Garmin GPS unit. Species present, percentage cover estimates and water depth were also recorded at each location.

Underwater benthic cover estimates

Single point, quadrat and transect sampling were undertaken to create the initial habitat classes and to drive the image classification and accuracy assessment (validation) of the airborne data. Between 2006 and 2009, habitat type and percentage cover were described at nearly 3 500 locations in Ningaloo Marine Park. Field work was limited by accessibility of the 300 km long reef, but much effort was made to cover a wide range of ecologically variable areas of the reef (Figure 1). The

majority of field data were collected by Murdoch University staff and students, with some also contributed by CSIRO scientists engaged in an extensive biological project.

Two methods of sampling have been used to determine benthic substrate components: transects and nested quadrats. The transect method consisted of extending a 100 m transect line (fibreglass measuring tape) and noting the substrate categories and their percentage cover within adjacent 3 m x 3 m quadrat along the line. Benthic substrate categories followed the descriptions used by the Australian Institute of Marine Science protocols for long-term monitoring (Page *et al.* 2001) (Table 1).

The nested quadrat method involved setting up a 9 m x 9 m quadrat (mega-quadrat) in a north-south orientation on the seabed and sub-dividing this quadrat into nine 3 m x 3 m sub-quadrats. Key points within the mega-quadrat were marked using weighted floats (Figure 5). Benthic substrate categories (as per Page *et al.* 2001) and percent composition of those categories for the mega-quadrat and then each sub-quadrat were recorded by the diver. A photograph of a 0.5 m x 0.5 m sub-sample in the south-west corner of each sub-quadrat was taken.

Location was established using Garmin GPS at the start and end of each transect and in the centre of each nested quadrat as well as in five sub-quadrats, in the order of 5, 1, 3, 9, 7 (quadrat 1 is located in the SW corner of the mega-quadrat) (Figure 5). Additional, GPS-referenced points were also collected to identify significant and isolated features on the seabed (e.g. significant changes in bottom type and isolated patch reefs and bommies).

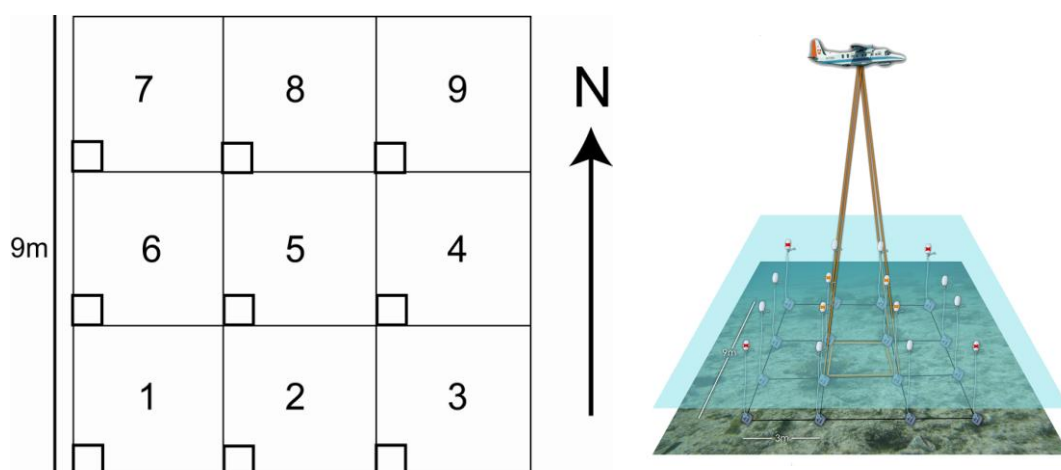


Figure 5. Layout of nested quadrat design (left) indicating orientation, order of sampling and location of sub-quadrats and photo-quadrats. GPS points are taken in the centre of sub-quadrats 1, 3, 5, 7 and 9. The graphic on the right indicates the relationship between the nested quadrat and the remote sensed imagery (3.5 m pixel size).

Transect data were also collected by CSIRO staff as part of another project. The data consisted of benthic cover and respective percentages per whole transect (~100 m long) and the geographic location of the starting point of each transect. These data were used for areas not covered by the Murdoch data, e.g. along the forereef and in more remote areas such as Murion Islands.

Table 1. Benthic cover types and their codes in Murdoch field data of Ningaloo Reef based on Page *et al.* (2001).

Name	Code
Branching <i>Acropora</i>	ACB
Branching <i>Acropora</i> "blue tip"	ACBT
Digitate <i>Acropora</i>	ACD
Encrusting <i>Acropora</i>	ACE
Submassive <i>Acropora</i>	ACS
Tabulate <i>Acropora</i>	ACT
Bottlebrush <i>Acropora</i>	ACX
Coralline Algae	CA
Branching non- <i>Acropora</i>	CB
Digitate non- <i>Acropora</i>	CD
Encrusting non- <i>Acropora</i>	CE
Foliaceous non- <i>Acropora</i>	CF
Massive coral	CM
Mushroom coral	CMR
Submassive coral	CS
Recently dead coral	DC
<i>Dictyota</i>	DY
<i>Halimeda</i> spp.	HA
Intact Dead Coral	IDC
Branching IDC	IDC-B
Tabulate IDC	IDC-T
Digitate IDC	IDC-D
Massive IDC	IDC-M
Limestone pavement	LP
Macroalgae	MA
<i>Padina</i>	PA
Rubble	R
Sand	S
Sand and Microalgae	SA
Soft Coral	SC
Seagrass	SG
<i>Sargassum</i>	SR
Sponge	Sp
Turf Algae	TA
<i>Ulva</i>	UL

2.2.3 Preprocessing HyMap data

HyMap flight lines were processed by HyVista Corporation to include radiance calibration at the sensor, atmospheric and geometric corrections. For further details on HyMap pre-processing, refer to the HyMap data acquisition report (Appendix A) and EOMAP processing report (Appendix B). The calibrated sensor radiance flight lines were individually processed by the German collaborator EOMAP using the physics-based Modular Inversion and Processing System (MIP) (Heege and Fischer 2000, Heege *et al.* 2003, Heege and Fischer 2004). This step was focused on corrections for atmospheric effects, sun glitter and bidirectional above- and underwater effects, resulting in subsurface reflectance images.

This step was followed by geo-referencing and mosaicking of the individual subsurface reflectance flight lines by HyVista Corporation to generate 17 image data blocks based on their acquisition date and geographical proximity. The correction of water column-related effects on the mosaicked flight lines was subsequently performed using MIP software to retrieve the bathymetry and sea floor reflectance data, used later as an input for the benthic habitat classification (Figure 6).

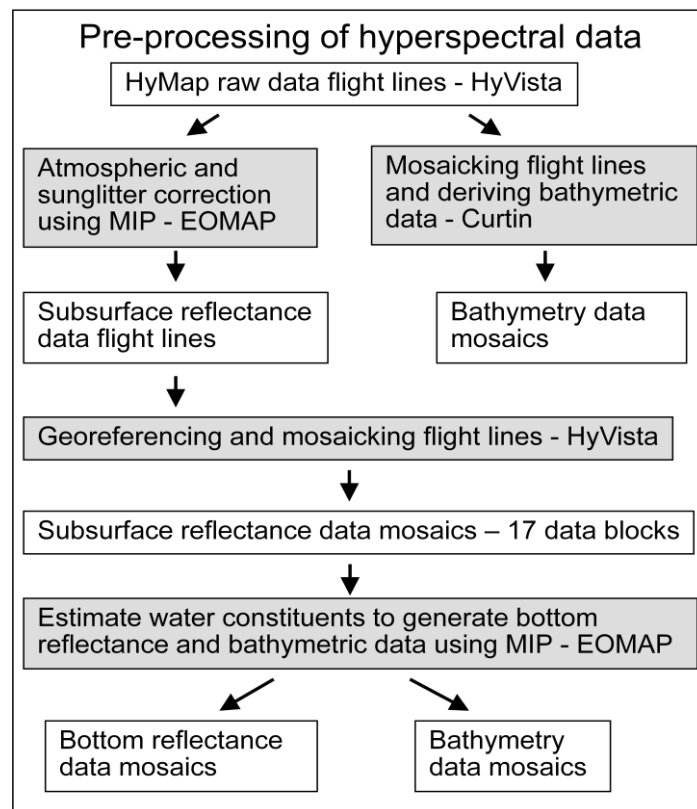


Figure 6. Pre-processing of the HyMap data to retrieve bottom reflectance and bathymetry of Ningaloo Reef.

Several issues arose during pre-processing:

- Due to the large area (on the ground) and file size of some mosaics, they had to be split further from the original 11 blocks, thereby resulting in 17 blocks; block A (split into A1 and A2), block F1 (split into F11 and F12), block F2 (split into F21 and F22), block G (split into G1 and G2) and block H (split into H1 and H2).
- During georeferencing of the flight lines, all image data blocks were projected to UTM Zone 49 S. However, as three mosaics were actually located outside of Zone 49 S, they had to be

reprojected to the correct UTM Zone 50 S. As a small fraction of one block was located in UTM Zone 49 S and the majority in Zone 50 S, the small fraction was slightly cropped. The cropped part of the image was also covered by the neighbouring image block, so that continuous coverage was preserved.

- As terrestrial image data had not entirely been removed in all subsurface reflectance image blocks when previously masking land and water (Appendix B), these areas had to be masked again using a range of values determined through trial and error from two HyMap bands (band 4 using values <300 and band 26 using values >4 000, image data type 16 bit integer) and replaced with the value 0.

2.2.4 Field data processing

Field data were used to create a classification hierarchy, habitat class labels and for the accuracy assessment. Data from several field trips as well as CSIRO data were combined into one database. A number of inconsistencies in the field data were corrected for. This included position, thematic label and consistency in percentage cover estimates. A more detailed summary of these steps is provided in Appendix C.

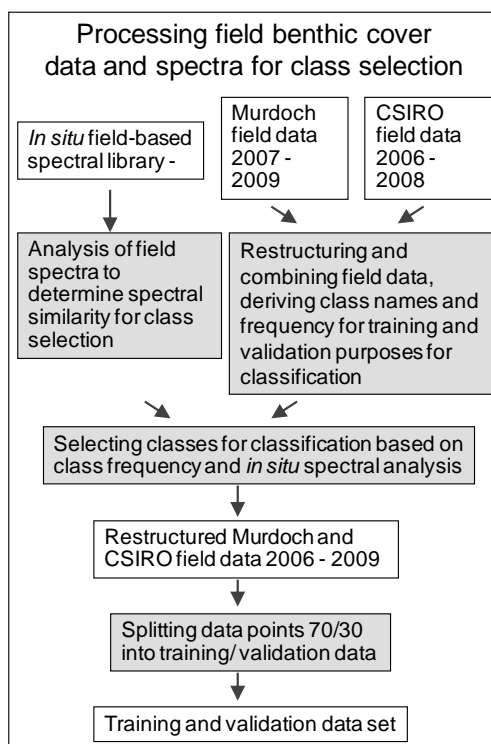


Figure 7. Processing steps for field spectra and field validation data at Ningaloo Reef.

Habitat classes were based on the type and percentage of substrate cover determined in the field. Habitat class labels were made up of a combination of the single benthic components in relation to their percentage in the sample area, as well as the analysis of *in situ* field spectra as an indicator of which single components were separable. Ecological relevance of labels was also taken into account, with the focus on the dominant biotic component. Label prefix was added describing the proportion of that component relative to the less dominant biotic components, as well as to the abiotic components. Following the labelling of all field data points, the final class selection was based on the frequency of occurrence of ground truth points per class in the dataset, since a minimum number of points per class

was required for training and validation of the classification. The final points were subsequently randomly stratified in approximately 70 % for training purposes and 30 % for validation purposes.

Generating the field reference dataset based on spectral analysis and logical habitat class combinations

After combining datasets, a second dataset was generated based on spectral analysis of *in situ* spectra (to determine the combination or exclusion of components for the classification), as well as logical combinations (such as grouping hard coral, macroalgal and dead coral subcategories to form ‘base’ classes, each with a percentage cover value as a sum of the subcategories). A number of benthic classes found in the field (Table 1) were aggregated, resulting in the final 15 benthic components (Table 2):

- Hard coral subcategories were grouped into “HC”: ACB, ACBT, ACD, ACE, ACS, ACT, ACX, CB, CD, CE, CF, CM, CMR, CS, but were kept separate for more detailed habitat class description
- ACB, ACD and ACT were changed to CB, CD and CT as the field data were assumed to have inaccuracies regarding the correct identification of coral genera (*Acropora* vs. Non-*Acropora*).
- Intact dead coral subcategories were grouped into “IDC”: DC, IDC, IDC-B, IDC-D, IDC-M, IDC-T
- Macroalgal subcategories were grouped into “MA” (coralline and turf algae were not included): MA, SR, HA, PA, DY, UL.

As each field data point was described using up to nine benthic codes and their respective percentage covers, the next step was to assign a label to each benthic class, with the aim of subsequently combining these labels to form a class name per data point. This was done to generalise the existing data structure and capture uniform and mixed benthic components. The hierarchy used was based on the percentage cover ranging from 90 % or more (continuous cover), 50-90 % (dominant category) and two types of mixed classes (less than 50 % cover) (Table 3).

Table 2. Selected habitat class components at Ningaloo Reef, modified from benthic codes used in the field (see also Table 1).

Habitat class name	Code
Branching coral	CB
“blue tip” coral (<i>Acropora</i>)	CBT
Digitate coral	CD
Encrusting coral	CE
Submassive coral	CS
Tabulate coral	CT
Massive coral	CM
Foliaceous coral	CF
Turfing algae or macroalgae-covered dead coral or rubble	TA- or MA-covered IDC or R
Limestone pavement	LP
Macroalgae (consisting largely of <i>Sargassum</i>)	MA
Rubble	R
Sand	S
Soft coral	SC
Turf algae	TA

Table 3. Summary of the benthic category labelling approach using class label and percentage cover for Ningaloo Reef.

Class label	Description	Example
Continuous classes	If the dominant percentage cover $\geq 90\%$, the point could be considered to be pure benthic substrate, so the remaining percentage cover values were disregarded and the dominant category name received the prefix "Continuous"	Category 1 (most dominant) is limestone pavement (LP) with 95 % cover, category 2 is hard coral (HC), with 5 %, resulting in the label "Pure limestone pavement" label and category 2 input disregarded
Mixed classes with one category dominant	If the dominant component is biotic and its percentage lies between 50- 90 % and the difference between the highest and second highest percentage values ≥ 30 , the remaining percentage values were included and the dominant category name received the prefix "Dominant"	Category 1 is limestone pavement (LP) with 70% cover, category 2 is hard coral with 25 % cover, resulting in the label "Dominant limestone pavement" label and the second label of hard coral for category 2
Mixed classes with categories equal	If the difference between the dominant percentage and a lower percentage ≤ 20 , they are considered equal; and will each receive the prefix "equal" if the sum of the equal percentages $\geq 90\%$ (the latter was done to avoid two categories of, for instance 40% and 30 % to be defined as equal, when the difference to the rest of the percentages $> 20\%$ and these would thus be disregarded)	Category 1 is limestone pavement with 50 % cover, category 2 is hard coral with 45 % cover, therefore $\text{SumCover1} + \text{Cover2} = 95\% \rightarrow$ category 1 was assigned a label "equal limestone pavement" and category 2 received label "equal hard coral"
Mixed classes that do not fall into the above categories	Mixed classes that do not fall into the above categories (i.e. not pure, no mixed class with one dominant category, no equal categories): categories remain in the order they are in and receive the prefix "1", "2", "3", etc. depending on their percentage value	Category 1 is limestone pavement with 60 %; category 2 is hard coral with 35 % cover, category 3 is sand with 5 % cover, therefore category 1 received label "1-limestone pavement", category 2 received label "2-hard coral" and category 3 received label "3-S"

Benthic habitat classes were assigned simpler descriptions in the final classification product using the following logic:

- Biotic component descriptor was moved to the beginning of the label, e.g. "Equal-limestone pavement/Equal-macroalgae" became "Patchy macroalgae with limestone"
- If in the mixed classes, the dominant category was abiotic, then the biotic categories received the prefix "Sparse" and was used at the beginning of the label, e.g. "Dom-LP/HC/MA" ("Dominant limestone pavement with hard coral and macroalgae" became "Sparse hard coral and macroalgae with limestone pavement" (note that structure of the lookup table allows the end user to see the full details of the class label and it is also possible to create new class labels)
- Where there was a hard coral component, the single hard coral growth forms were listed at the end of the label, e.g. "Dominant hard coral with sand (with hard coral = Continuous tabulate coral)".

2.2.5 Class selection

Following the assignment of class names to each data point, the frequency of classes was determined. As a result of the high number of classes in the dataset, the number of classes selected for classification was reduced based on the frequency of classes. Only classes with a high enough frequency (at least 3 points) were considered, resulting in approximately 1 500 points from the original 3 500 field data points. Classes that were over-represented, e.g. sand, with frequencies over 15, were randomly reduced (based on spatial distribution) to decrease the classification time, while

still keeping sufficient variance in the data, resulting in approximately 600 points for classification and validation.

2.2.6 Separation of the field data into training and validation sets

The 600 final points were split into approximately 70 % for training and 30 % for validation purposes. Random stratification (each class was treated independently), was used to allow for all classes to be represented in the training and validation datasets and not lose classes with low frequencies or over represented classes with the highest frequencies. This was performed using SPSS software.

2.2.7 Spectral analysis of image-derived spectra

Before the 600 training sites representing final habitat classes could be used for classification, it was necessary to undertake spectral separability analysis of spectra derived from images at those 600 locations (Figure 8).

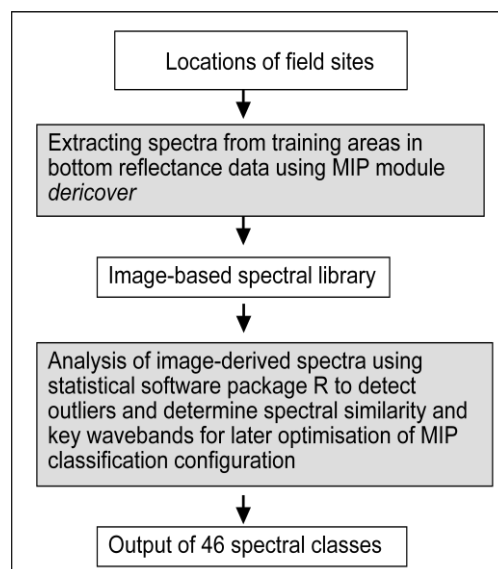


Figure 8. Summary of steps to create spectral classes for image classification of Ningaloo Reef.

Image processing steps are explained later in the report, but it is important to mention here that, for image-derived spectra, we have used a measure known as bottom reflectance which is the proportion of light reaching the sensor after the atmospheric, water/air interface and water column and depth properties have been corrected for. In short, it is the reflectance from the substrates as if the influences of the atmosphere and water were completely removed.

Spectral analysis of image-derived spectra was necessary for three reasons. Firstly, we needed to check for any remaining geographic position error in the image and field data that was previously not identified despite extensive manual cross-checking. Secondly, there was a possibility of spectral similarity of classes comprising different, but spectrally similar reef components, found to be separable in the analysis of *in situ* spectra, but which would possibly not be separable using the lower HyMap 15 nm resolution and in part smaller spectral range. Finally, we needed to check for spectral variation within the field reference points describing same habitat classes.

A multivariate spectral analysis was performed on image-derived spectra to examine habitat class separability, detect outliers and potentially regroup classes. The statistical software package R (R

Development Core Team 2008) was used to analyse the class separability, detect outliers and potentially regroup similar classes.

The first step consisted of extracting spectra from the bottom reflectance images using the software MIP based on the location of the training points:

- The line/column of each point in the respective images was derived based on the coordinates of the points and the upper left corner of respective image (Easting/Northing), as this information was needed as input in MIP
- Using the derived line/column information, image-based spectra were collected from the image pixel in text format at the exact location of the training point
- Spectra collected from the different images were then combined, i.e. the spectral ranges of points of the same class but collected from different image blocks were added together into one text file, with the class definition consisting of the spectral range per image band (wavelength)

The second step involved the spectral analysis of extracted spectra using principal component analysis, hierarchical clustering and a distance index.

Principal component analysis (PCA) is a commonly used method to reduce redundancy in multi- or hyperspectral data. Correlated variables, in this case spectral bands, are transformed into a smaller number of uncorrelated variables, which each represent a linear combination of the original data values accounting for the maximal variability. To analyse hyperspectral data, PCA can be used to discriminate between classes and identify key and redundant wavebands. Further applications include identifying possible outliers, as well as groups of highly collinear variables. PCA transformed data can also be viewed in a two-dimensional space to graphically illustrate variations between and within groups of points in the data. The R package “vegan” (Oksanen *et al.* 2009) and functions “rda” as well as “ordiplot”, “ordiellipse” and “ordispider” were used to perform PCA on the image-derived spectra and to graphically view PCA results in order to:

- detect possible outliers assigned to the incorrect class as a result of GPS error of the training data
- identify spectral bands that were highly correlated and exclude these redundant features that would not contribute to, or may have an adverse effect upon, the classification process using MIP
- determine spectral variations within and between, classes viewed in two-dimensional space, thus illustrating potential separability of classes

Hierarchical clustering involves joining the spectral measurements of the classes sequentially according to similarity to determine spectral distinction between classes and identify outliers. This results in a cluster dendrogram showing families of clusters which themselves contain other clusters. R package “Stats” (R Development Core Team 2008) with function “hclust” was used to apply cluster analysis to the image-derived spectra using Euclidian distance in order to support the results of PCA analysis in terms of detecting possible outliers and determining spectral distinction between and within classes.

The Jeffries-Matusita (JM) distance is commonly used in remote sensing as a measure of statistical separation between pairs of classes. It represents the average distance between two class density functions and is asymptotic to the value of 2.0 with increasing class separability. Thus, the larger the distance, the higher the probability of correct separation of classes, with a value of 2.0, representing 100 % separability. A threshold of ≥ 1.90 was used to indicate spectral separation. The R package “MASS” (Venables and Ripley 2002) and a modified R code (Appendix E) were used to apply the JM

distance to spectra. This allowed us to quantify the spectral separation between class pairs that had previously been identified as spectrally similar in the PCA and cluster analysis, applied to a selected number of key wavebands determined using PCA.

Spectral separability analysis was performed on all training and validation points. However, care was taken that only very obvious outliers were deleted from the validation dataset, so as not to bias the accuracy assessment or decrease the already relatively low number of points for some classes.

Following the spectral analysis, the dataset was modified accordingly, e.g. apparent outliers were deleted and spectral similarity between particular classes was noted. Some of the affected habitat classes and problems encountered due to class similarity included sand in deep depressions classified as a mix of hard coral and dead coral or as limestone pavement, very bright, white sand misclassified since no training data existed for this substrate and classes containing macroalgae components classified as mix of hard coral and dead coral or as continuous dead coral and vice versa.

These issues were addressed by adding training and validation points for sand based on areas that were known to consist of very bright sand (e.g. at Turquoise Bay in image data block H1 and slightly darker sand near Mangrove Bay in image data block H2). In addition, the spectra of hard and dead coral classes were compared with spectra of classes containing macroalgae component and key wavebands were determined to enhance separation of these classes.

The 67 habitat classes determined by class frequency were reduced to 46 final classes following the spectral analysis as a result of deleting outlier points, thereby reducing the number of points in some classes to below three and therefore making them unusable as a training class. High spectral similarity between some classes was used as a basis for thematic generalisations of these classes and the fuzzy logic validation approach.

2.2.8 Pixel-based benthic cover classification approach

The habitat mapping was performed on the HyMap bottom reflectance images using a supervised classification approach based on the spectral signatures resulting from the spectral analysis and using the Modular Inversion and Processing System (MIP) software. The MIP classification module incorporates fuzzy logic and 1st and 2nd order derivatives in addition to reflectance data.

The first step involved generating rule sets per class that included the spectral class ranges as input for the classification. For this, the MIP module “deriformat” was used to reformat the class spectra into the correct format for the later classification (Figure 9).

This resulted in four new files generated per class in addition to the input class spectra file: a file containing only the reflectance data, a file containing only the first derivative, a file containing only the second derivative (each with the average value per spectral band and the standard deviation), as well as a configuration file containing the information of the reflectance, first and second derivatives in a different format.

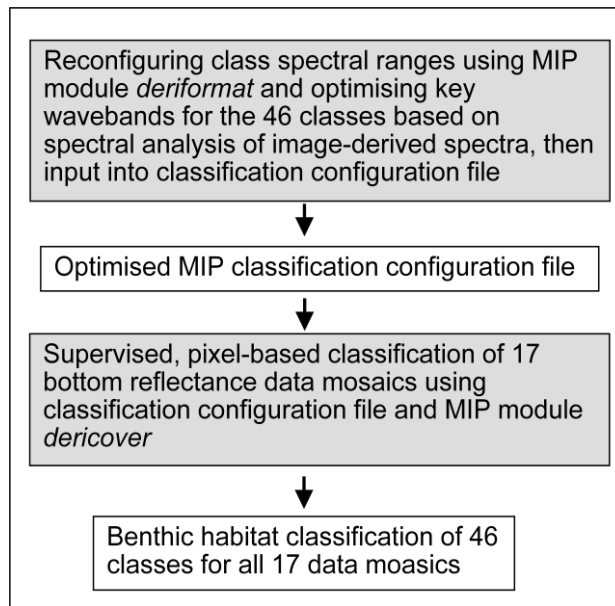


Figure 9. Summary of steps in benthic habitat classification at Ningaloo Reef.

The contents of the class configuration files were added to an overall classification configuration file (Figure 10), which was used as input for the classification. This file included other parameters that can be changed accordingly, such as weighting factors for wavelength intervals and the minimum probability for derivation analysis (Figure 11). The parameter “Deriweight” can be modified per class and for single wavelengths in order to enhance or suppress certain classes.

26chans	456.6	456.6	471.5	471.5	487.9	487.9
Name	QDEV	2STDABW	QDEV	2STDABW	QDEV	2STDABW
Pure-S	33.6774	19.3079	36.0863	20.0760	39.1268	20.9268

Figure 10. Example of a text file containing the average value per spectral band and the standard deviation of the reflectance for class “Pure-S” (90% or more cover of sand).

```

!Use Derivation for inversion: wavelength are interpreted as channels, if WAVEL<0
-real/number -real[nm] -number minvalue maxvalue real not_read
Minvalue & Maxvalue are Half-width-values for gaussian function of target values
DERIWAWE Halfwidth Derivation Minvalue Maxvalue Deriweight DERI_codename (Len=10, in KAPITOLS):
456.6 3.0 0 4.89 6.98 1 Pure-MA
471.5 3.0 0 6.55 8.67 1 Pure-MA
487.9 3.3 0 8.18 10.00 1 Pure-MA
502.7 3.0 0 8.29 11.50 1 Pure-MA
517.4 2.9 0 9.12 12.90 1 Pure-MA
532.8 3.1 0 10.20 14.90 1 Pure-MA
547.5 2.9 0 12.10 17.10 1 Pure-MA
562.1 2.9 0 14.30 19.70 1 Pure-MA
576.9 3.0 0 16.40 22.80 1 Pure-MA
591.7 3.0 0 20.60 26.70 1 Pure-MA
606.6 3.0 0 18.00 25.60 1 Pure-MA
621.2 2.9 0 15.70 23.10 1 Pure-MA
635.4 2.8 0 14.50 22.20 1 Pure-MA
649.9 2.9 0 13.90 21.20 1 Pure-MA
664.5 2.9 0 10.80 17.40 1 Pure-MA
464.1 8.2 1 0.296E-01 0.120E+00 1 Pure-MA
479.7 9.0 1 0.421E-01 0.102E+00 1 Pure-MA
495.3 8.1 1 0.365E-01 0.100E+00 1 Pure-MA
510.1 8.1 1 0.700E-01 0.120E+00 1 Pure-MA
525.1 8.5 1 0.820E-01 0.127E+00 1 Pure-MA
540.1 8.1 1 0.126E+00 0.158E+00 1 Pure-MA
554.8 8.0 1 0.139E+00 0.180E+00 1 Pure-MA
569.5 8.1 1 0.160E+00 0.241E+00 1 Pure-MA
584.3 8.1 1 0.132E+00 0.292E+00 1 Pure-MA
599.2 8.2 1 -0.180E+00 -0.598E-01 1 Pure-MA
613.9 8.0 1 -0.199E+00 -0.149E+00 1 Pure-MA
628.3 7.8 1 -0.114E+00 -0.416E-01 1 Pure-MA
657.2 8.0 1 -0.330E+00 -0.137E+00 1 Pure-MA
671.8 8.0 1 -0.100E+00 0.686E-02 1 Pure-MA
700.7 8.0 1 -0.153E+01 0.799E+00 1 Pure-MA
472.3 17.2 2 -0.248E-02 0.293E-02 1 Pure-MA
487.1 17.2 2 -0.204E-02 0.194E-02 1 Pure-MA
502.7 16.2 2 -0.286E-03 0.332E-02 1 Pure-MA
517.7 16.6 2 0.535E-03 0.219E-02 1 Pure-MA
532.5 16.6 2 0.109E-02 0.316E-02 1 Pure-MA
547.4 16.1 2 0.293E-03 0.216E-02 1 Pure-MA
562.2 16.2 2 0.152E-02 0.325E-02 1 Pure-MA
576.9 16.3 2 -0.238E-02 0.433E-02 1 Pure-MA
591.8 16.3 2 -0.273E-01 -0.198E-01 1 Pure-MA
606.5 16.2 2 -0.754E-02 -0.159E-02 1 Pure-MA
621.0 15.8 2 0.314E-02 0.107E-01 1 Pure-MA
635.6 15.8 2 -0.142E-02 0.660E-02 1 Pure-MA
650.0 16.0 2 -0.208E-01 -0.658E-02 1 Pure-MA
693.6 15.9 2 -0.135E+00 0.508E-01 1 Pure-MA
708.0 16.0 2 -0.220E+00 0.105E+00 1 Pure-MA
456.6 3.0 0 24.10 44.40 1 Pure-S
471.5 3.0 0 27.40 48.00 1 Pure-S
487.9 3.3 0 31.20 52.10 1 Pure-S
502.7 3.0 0 35.10 56.50 1 Pure-S
517.4 2.9 0 35.60 60.30 1 Pure-S
532.8 3.1 0 37.40 65.30 1 Pure-S
547.5 2.9 0 40.30 71.40 1 Pure-S
562.1 2.9 0 43.60 78.00 1 Pure-S
576.9 3.0 0 47.90 87.20 1 Pure-S
591.7 3.0 0 54.80 97.70 1 Pure-S
606.6 3.0 0 43.20 88.50 1 Pure-S

```

Figure 11: Example of a classification configuration file, showing two classes “Pure-MA” (90 % or more cover of macroalgae) and “Pure-S” (90 % or more cover of sand).

Using one configuration file guaranteed homogenous benthic cover classification results over the whole dataset by using consistent input spectral signatures of the classes, as well as allowing a more automated and standardised approach. It also ensured the option to apply the retrieved spectral signatures to future air- and satellite- based acquisitions in the same standardized approach, resulting in comparable classifications.

The second step involved the actual classification of image data blocks using the MIP module “dericover” and the classification configuration file. The resulting classification image included:

- the final classification image which is a result of the highest class probabilities with class values per pixel based on their order in the configuration file, e.g. if class “Pure-S” was the third class in order in the configuration file, all pixels classified as “Pure-S” would receive the value 3
- Single class probability images as a result of fuzzy logic approach.

As mentioned previously, the parameter “deriweight” in the classification configuration file could be modified per class and spectral band. As a result of the suppression of classes with a relatively narrow spectral range by other classed with a relatively large spectral range, the suppressed classes were given a higher “deriweight” value, particularly for key wavebands determined in the PCA analysis

that could enhance the separability of classes. This was applied in particular to hard coral classes, since the relatively small number of training points as well as homogeneity of these classes resulted in relatively narrow spectral ranges. Habitat classes with a higher number of training points and more heterogeneous nature of the substrate (e.g. mixed classes) afforded more spectral domination, thereby suppressing the narrow range classes. The “deriweight” setting was determined iteratively through trial and error by modifying the value and classifying a number of image subsets of fairly variable bottom cover, e.g. coral dominated subsets as well as macroalgae dominated subsets. The weights ranged between 0.1 and 9 and are normalized internally by the algorithm.

While the modification of the “deriweight” values decreased the degree of misclassification, several classes still dominated due to their large spectral range. As a result, all available classes were classified in one run, rather than classifying basic classes in a first run and consequently splitting these into their respective subclasses, since generating basic classes would have involved combining a range of classes and thus enlarging the ranges even more, leading to increased spectral overlap and misclassification.

Due to the increased attenuation at longer wavelengths (as a result of absorption by water), the spectral class ranges were restricted to the visible HyMap wavelengths, with several classes limited to a maximum of only 600 nm due to the location of their training data at greater water depth, resulting in higher absorption by water and subsequently smaller spectral range.

Using these spectral class ranges, the classification nevertheless yielded consistent results down to approximately 15 - 20 m depth due to the mostly clear waters of Ningaloo Reef. The classification procedure automatically takes into account values at wavelength, which can be considered to carry reasonable information of the sea floor reflectance with respect to the transmission of light in the water column. Spectral bands carrying unreliable/insufficient information about the seafloor were masked by the water column correction module of MIP due to the retrieved water depth and estimated scattering and absorbing properties in the water column.

For visualisation, the classification and single class probability images were colour coded using ENVI's density slice tool and subsequently saved as class images (GeoTIFF). The class images were then imported into ArcMap to generate maps.

2.2.9 Post-classification

Following the image classification, several post-classification steps were applied to the habitat data, including merging of the image data blocks, masking inconsistencies in deeper water areas, calculating the class statistics for spatial distribution and generalising the classification on thematic and spatial levels.

Mosaics

The 17 classified data blocks were merged into a single mosaic using ENVI image processing software, based on individual data block sizes of approximately 30 Mb. Due to some classification differences between image data blocks, the overlapping image borders were cropped manually prior to mosaicking in order to allow a smooth transition between image blocks.

Masking was performed on the mosaic using a combination of a deep water mask and contextual editing in order to eliminate areas with insufficient spectral signal that resulted in inconsistent classification results, i.e. “noisy” or speckled. To achieve this, the classified data were masked to a depth of 20 m using bathymetric information derived from HyMap pre-processing. Using ENVI, the

bathymetry images were cropped at 20 m depth and then generalised using a majority filter to de-speckle and generate smooth borders along the 20 m depth contour line. This was then exported as a mask and applied to the habitat images. Further masking was performed in selected areas through contextual editing, as regions between 15 – 20 m depth as well as overlap regions between image blocks still showed partially inconsistent results.

Thematic generalisation

In a very detailed (and potentially complex) dataset it is useful to organise the way data are described and displayed. Some end-users may only need to see the data in a highly generalised way, for example, where coral, algae, sand, limestone pavement and their main mixes occur. Other users may want see only where different forms of coral or dense stands of macroalgae are present. Detailed biodiversity studies may require all 46 benthic classes resulting in a complex map with a very long legend. While more sophisticated users can create their own thematic subsets through the database query in GIS, this requires some familiarity with databases and can potentially be quite slow due to the large file size. To facilitate wider access and use of the data, several, hierarchical, thematic levels were created for the classification map by generalising and combining habitat classes in a look-up table, which could be linked to the classification image using ArcGIS, in order to show different levels of habitat detail. This allowed for the final classification map set to be displayed at different thematic levels depending on the user requirements through the look-up table, which acts as a “thematic filter”.

After extensive consultation with the range of potential users (e.g. ecologists, biologists, managers, planners) and trying to anticipate future uses of the data, the 46 habitat classes were organised at five levels and sub-levels. The logic of the lookup table was from the simplest (most general) to the most detailed (complex) description in terms of the number of benthic components while also allowing capture of the continuum of cover density from very high (continuous ~100 %) to very sparse (<20 %) cover (Figure 12).

The structure of the hierarchical scheme was as follows:

- Level 1 (Simple) consisted of three classes: “Abiotic”, “Biotic” and “Mixed”
- Level 2 was made up of basic classes, where “Abiotic”, “Biotic” and “Mixed” classes from level 1 were split into their components based on the percentage of cover of the components and where respective hard coral, macroalgae and dead coral components were grouped
 - Level 2a (Basic classes) excluded the abiotic descriptor for the mixed classes (for example, “hard coral”)
 - Level 2b (Basic classes with abiotic descriptor) included the abiotic descriptor for the mixed classes (for example, “hard coral with limestone pavement”)
- Level 3 included the description of the degree of cover (continuous, dominant, patchy or sparse)
 - Level 3a included the degree of cover, but excluded the abiotic descriptor, for example “dominant hard coral”. Where there was no biotic component, the degree of cover was also shown for purely abiotic components, e.g. “continuous limestone pavement”
 - Level 3b included the degree of cover, as well as the abiotic descriptor, for example “dominant hard coral with limestone pavement”

- Level 4 included the abiotic descriptor, degree of cover and specified hard coral components (growth forms)
 - Level 4a was labelled with the same format of level 3b, but with the hard coral components (growth forms) added at the end of the label, for example “dominant hard coral with limestone pavement (where hard coral was the dominant tabulate coral with digitate coral, encrusting coral and submassive coral)”
 - Level 4b included all the degrees of cover as percentage ranges (rather than word description), for example “hard coral (65-90 %) with limestone pavement (10-35 %) (hard coral consisted of tabulate coral (50-85 %) with digitate coral (5-20 %), encrusting coral (5-20 %) and submassive coral (5-20 %))”
- Level 5 provided information solely on the hard coral components (degree of cover and form), for example “Dominant tabulate coral with digitate coral encrusting coral and submassive coral”.

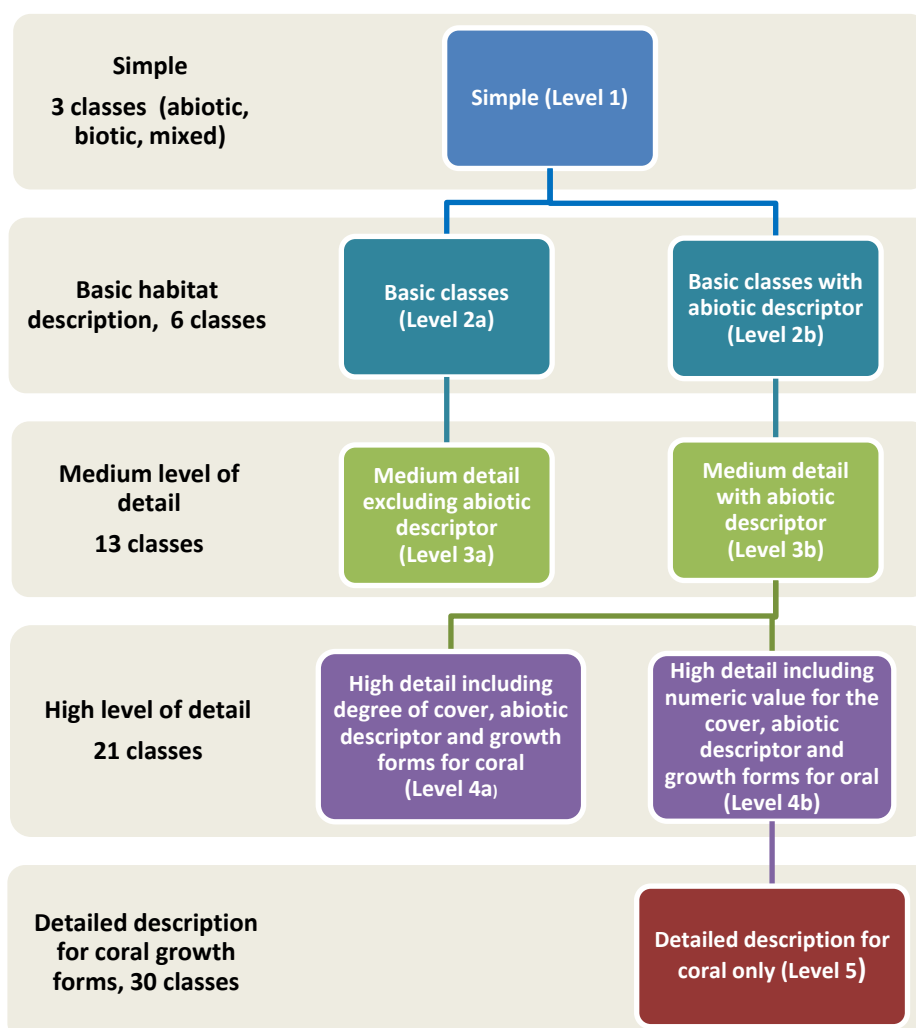


Figure 12. Illustration of the hierarchical system of the classification levels in the Ningaloo Reef benthic habitats look-up table.

Spatial generalisation

In addition to thematic generalisations, spatial generalisations were performed in order to deliver reduced data file sizes, decreased spatial detail (for users who do not require full pixel scale

(3.5 m x 3.5 m) spatial resolution of the data) and more smoothed appearance of class boundaries (decreased speckle, or “salt and pepper effect”). Majority filters with varying kernel sizes (3x3, 5x5, 7x7 and 9x9) and equal weights were applied using ENVI’s Post Classification module, thereby reducing the number of single pixels of one class by merging with neighbouring pixels of another class, resulting in different spatial resolutions per classification level.

Spatial statistics

Following mosaicking and masking, the spatial statistics of the classes were calculated in ENVI to analyse the distribution and abundance of benthic habitats across different geographic domains (e.g. whole mosaic, sanctuaries, popular snorkeling areas and near shore areas).

Raster and vector data products

ENVI was used for class colour allocation using the density slice tool prior to exporting the images as classification type files for further use in ArcMap (e.g. to generate maps). These classification type files were then saved as Geotiff format in ENVI.

In ArcMap, the raster files were additionally converted to vector format (shape files). These format choices (raster and shape file) make the data directly portable to common GIS packages such as ArcMap.

Appropriate look-up tables with the afore-mentioned thematic levels could be linked to both the raster and vector files in ArcMap to generate maps with a legend showing the different levels of habitat detail and standard legend colours. It was not practical to save the joined lookup tables with the data sets as this increased the typical size of a 30 km long mosaic from ~300 Mb to 1.5 Gb. As there were 17 such mosaics, a choice of temporary table join was a more practical solution.

Additional processing was performed on the habitat classification data to support various biodiversity studies (University of Queensland, Murdoch University and CSIRO).

2.2.10 Validation

An accuracy assessment of the classification results was performed using approximately 105 validation points. These were randomly stratified for the classes, so that both frequently and less frequently occurring classes were represented in the validation data in similar proportions, overrepresentation of frequently occurring classes would lead to bias.

Despite exclusion of obvious outliers, not all points assumed to be outliers were deleted and therefore further positional accuracy errors inherent to GPS data were still assumed to exist in the validation data. As the error was intensified through the use of the relatively small pixel size and thus reference site (e.g. a GPS point with an error of 5 – 10 m being located several pixels outside of the reference site), a larger area around each validation point was considered for the accuracy assessment. A radius of 10 m was generated around each validation area and the classification values extracted for each pixel located within the radius. If the same class as the validation class occurred within the radius, then the accuracy was accepted as correct.

Due to the high spectral similarity and thus “fuzziness” of classes (Gopal and Woodcock 1994, Congalton and Green 2008) a fuzzy accuracy assessment approach was selected. This involved

accepting accuracy as correct if the validation and classified areas were fuzzy (spectrally similar). Determining which classes were fuzzy was based on the results of the spectral analysis (e.g. showing that certain coral growth forms were spectrally similar), logical conclusion (e.g. similar degrees of cover of same class component could be grouped together), as well as ecological relevance (e.g. despite the similarity and thus fuzziness of “continuous soft coral” and “continuous digitate coral”, these classes were not combined due to their ecological relevance) (Table 4).

Table 4. Examples of accepted class membership in Ningaloo Reef hyperspectral data.

Type of class fuzziness	Examples
Similar degree of cover of one class component	Validation area is class “Sparse MA with S” and classified area is “Patchy MA with S”
One or some class component(s) of mixed classes are the same and other(s) are different	Validation area is class “Patchy MA with S” and classified area is “Patchy MA with LP and S”
Certain coral growth forms spectrally and texturally similar	Validation area is class “Continuous branching coral” and classified area is “Continuous digitate coral”

Validation was performed for thematic levels 2a and 4a using the afore-mentioned radius and fuzzy approach, with two degrees of fuzziness selected for level 4a (high degree of fuzziness, i.e. a larger number of classes are considered fuzzy).

2.2.11 Topographic and geomorphic classifications

In addition to the benthic habitat classification, topographic and geomorphic classifications were performed using the HyMap data and an object-oriented classification approach. Object-oriented classification involves segmenting the image prior to classification, whereby pixels with similar values are combined to form objects, which are then classified (Lillesand *et al.* 2008).

Whereas the bottom reflectance images were employed to generate the habitat maps, the topographic variables were created using the bathymetry derived during the same processing step as the bottom reflectance (Appendix B).

The aims of generating the topographic and geomorphic classifications were to:

- Provide detailed topographic and geomorphic maps for selected study areas to trial this method for different habitats and topographic settings in the Ningaloo Reef
- Determine and compare the spatial statistics of the topographic and geomorphic classes for the study areas
- Test whether a rule set would be applicable to different topographic regions without changing the input parameters in the rule set

Deriving topographic variables

ENVI’s topographic modelling tool was used to calculate the topographic features of “aspect” and “slope”. In conjunction with depth these were used to define topographic classes (Figure 13). Aspect, slope and depth were selected due to their ability to characterise typical and dominant reef features and could be split into logical knowledge-based classes, e.g. an aspect ranging from 45° – 135° is known to be East-facing, a slope ranging from 30° – 90° is accepted as steep and depths ranging from 5 – 20 m were considered deep for a fringing coral reef.

The topographic variables in ENVI's topographic modelling tool were calculated "by fitting a quadratic surface to the digital elevation data for the entered kernel size and taking the appropriate derivatives" (ENVI 2009). The kernel size can be modified in order to extract multi-scale topographic information.

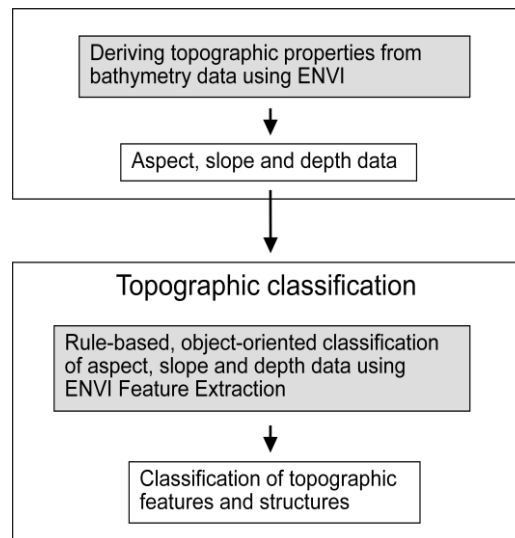


Figure 13. Overview of steps leading to image classification based on topographic variables at Ningaloo Reef.

The spatial resolution of the slope and aspect images was the same as that of the Hymap data they were derived from, i.e. 3.5 m. As this was considered to be too fine-scale to detect large objects such as lagoonal slopes, the slope and aspect images were generated using a 9x9 kernel size, hence, input features for the segmentation needed to be larger prior to segmentation. Since the changing of kernel size uses a majority filter (not average), a more realistic value was achieved for large features. The result were similarly sized objects when applying the segmentation to large homogeneous features.

Aspect, slope and depth images (the latter represented by the raw bathymetry images) were then combined into one image file using ENVI's layer stack tool. The resultant image with three bands representing slope, aspect and depth, respectively, were then used to classify topographic classes using ENVI's Feature Extraction.

Topographic classification and development of rule set

Since ENVI's Feature Extraction employs object-oriented classification methods, the input image was segmented in the first step, i.e. split into objects consisting of similar pixels. In the first step, the image bands to be used for segmentation were selected and included all topographic bands, i.e. slope, aspect and depth, as well as the land mask.

With the segmentation scale set to 10 (range was 0-100), a relatively small object size could be created and dealt with the issue of the false aspect calculation using the average of the pixel values within the object. Merging object scale was also set to the value of 10 (again scale 0-100). Once objects were generated, their spatial, spectra and textural attributes were selected. In this step, only spectral features, (i.e. referring to the input band values), were calculated, as the aim was to use only the aspect, slope and depths values that were contained in the input bands. As the classification would be driven by knowing which class ranges to use to define topographic classes, a supervised classification approach was selected and the class ranges defined in a rule set. Classes were created as part of the rule set and the class ranges defined for the classes (Table 5).

Table 5. Definition of rule set and the class ranges using bathymetry data of Ningaloo Reef.

Rule definition	
1	If avgband_1 > 30.0 AND avgband_2 [225.0, 315.0] AND avgband_3 < -50.0, then object belongs to "W_steep_deep".
2	If avgband_1 < 30.0 AND avgband_2 [45.0, 135.0] AND avgband_3 > -50.0, then object belongs to "E_flat_shallow".
3	If avgband_2 > 315.0 AND avgband_1 < 30.0 AND avgband_3 > -50.0, then object belongs to "N_flat_shallow".
4	If avgband_1 < 30.0 AND avgband_3 > -50.0 AND avgband_2 [0.0, 45.0], then object belongs to "N_flat_shallow".
5	If avgband_1 > 30.0 AND avgband_2 [135.0, 225.0] AND avgband_3 < -50.0, then object belongs to "S_steep_deep".
6	If avgband_1 < 30.0 AND avgband_2 [225.0, 315.0] AND avgband_3 > -50.0, then object belongs to "W_flat_shallow".
7	If avgband_1 [30.0, 89.9598] AND avgband_2 [45.0, 135.0] AND avgband_3 < -50.0, then object belongs to "E_steep_deep".
8	If avgband_1 [30.0, 89.9598] AND avgband_2 > 315.0 AND avgband_3 < -50.0, then object belongs to "N_steep_deep".
9	If avgband_1 [30.0, 89.9598] AND avgband_2 [0.0, 45.0] AND avgband_3 < -50.0, then object belongs to "N_steep_deep".
10	#If avgband_1 < 30.0 AND avgband_2 [135.0, 225.0] AND avgband_3 > -50.0, then object belongs to "S_flat_shallow".
11	If avgband_1 > 30.0 AND avgband_2 [225.0, 315.0] AND avgband_3 > -50.0, then object belongs to "W_steep_shallow".
12	If avgband_1 < 30.0 AND avgband_2 [225.0, 315.0] AND avgband_3 < -50.0, then object belongs to "W_flat_deep".
13	If avgband_1 > 30.0 AND avgband_2 [45.0, 135.0] AND avgband_3 > -50.0, then object belongs to "E_steep_shallow".
14	If avgband_1 < 30.0 AND avgband_2 [45.0, 135.0] AND avgband_3 < -50.0, then object belongs to "E_flat_deep".
15	If avgband_1 > 30.0 AND avgband_2 > 315.0 AND avgband_3 > -50.0, then object belongs to "N_steep_shallow".
16	If avgband_1 > 30.0 AND avgband_2 [0.0, 45.0] AND avgband_3 > -50.0, then object belongs to "N_steep_shallow".
17	If avgband_1 < 30.0 AND avgband_2 > 315.0 AND avgband_3 < -50.0, then object belongs to "N_flat_deep".
18	If avgband_1 < 30.0 AND avgband_2 [0.0, 45.0] AND avgband_3 < -50.0, then object belongs to "N_flat_deep".
19	If avgband_1 > 30.0 AND avgband_2 [135.0, 225.0] AND avgband_3 > -50.0, then object belongs to "S_steep_shallow".
20	If avgband_1 < 30.0 AND avgband_2 [135.0, 225.0] AND avgband_3 < -50.0, then object belongs to "S_flat_deep".
21	If avgband_2 < 0.0 AND avgband_3 [-50.0, -1.0], then object belongs to "Noaspect_flat_shallow".
22	If avgband_2 < 0.0 AND avgband_3 < -50.0, then object belongs to "Noaspect_flat_deep".

Eight classes were created using topographic variables (Table 6). The rule set was applied to the input image to generate the topographic classification. The final step involved selecting the output type for the classification result either as a vector file (shapefile) with the option of exporting all object attributes, and/or raster (ENVI type). We found that the rule set was transferable to all study areas, as the same topographic ranges applied regardless of the topographic characterisation of the area.

We encountered a limitation using ENVI's (4.7) Feature Extraction regarding the image size. Depending on the number of bands used and pixel size, only relatively small subsets could be processed, of approximately 900 lines x 600 columns.

Table 6. Class ranges using aspect, slope and depth variables for Ningaloo Reef.

Name	Definition
E-facing	45° - 135° aspect
N-facing	315° - 360° and 0° - 45° aspect
S-facing	135° - 225° aspect
W-facing	225° - 315° aspect
Flat	0° - 30° slope
Steep	30° - 90° slope
Shallow	0 - 5 m depth
Deep	deeper than 5 m depth

Geomorphic classification and development of rule set

In contrast to the topographic classification, an additional input file, the habitat map was used for the geomorphic classification. As with the topographic classification, all bands, including slope, aspect, depth, land mask and the habitat map, were selected for the segmentation (Figure 14).

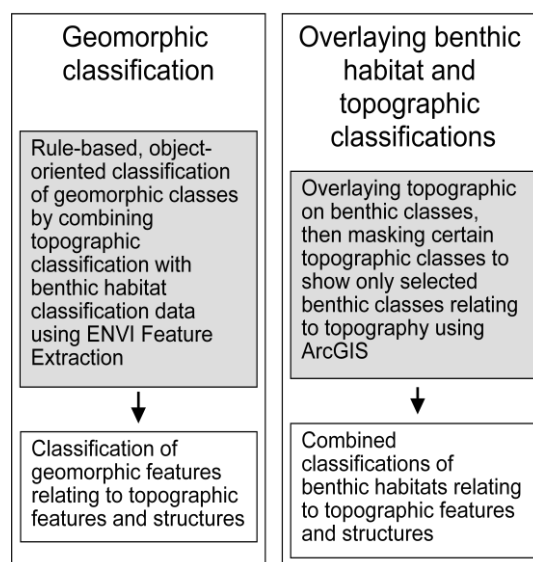


Figure 14. Steps to combine topographic and geomorphic classes with benthic habitats for mapping of the Ningaloo Reef.

The segmentation and merge scales were set to 20 or 30 and 70 or 80, depending on the study area and no thresholding was performed. All object attributes (spatial, spectral or textural) were calculated in the development of the rule set. Since developing the rule set required knowledge of the object attributes, but texture or spatial attributes (such as roundness) were not known, these were further investigated. This was done by displaying selected attributes as an image with objects fitting into a given range of attribute values showing up with higher brightness values. In this way, suitable attributes as well as their ranges could be determined more easily for each class. In the next step, the required classes were defined in the rule set which was also transferable to the other study areas with satisfactory results (Table 7). The object-oriented classification was performed using the defined rule set, which was also transferrable to the other study areas with satisfactory results.

Table 7. Rule set for geomorphic classes developed using topographic and habitat classes for the Ningaloo Reef.

Class	Rule definition
1 (0.800)	If area > 8000.0000 AND tx_variance < 9.0000 AND tx_entropy > 0.1858 AND maxband_1 < 40.0000 AND minband_3 > -100.0000 AND avgband_4 [20.0000, 29.0000] AND stdband_4 < 10.0000 AND stdband_1 < 10.0000, then object belongs to "Sand (flat lagoonal)".
2 (1.000)	If area [600.0000, 1500.0000] AND length [20.0000, 1000.0000] AND convexity < 1.2000 AND roundness < 0.5483 AND majaxislen > 54.7999 AND minaxislen < 40.0000 AND tx_range < 15.6671 AND avgband_1 > 15.0000 AND avgband_4 [29.0000, 29.0000] OR avgband_4 [19.0000, 19.0000], then object belongs to "Sand (lagoonal slopes)".
3 (1.000)	If elongation > 4.0000 AND majaxislen > 100.0000 AND minaxislen < 38.0000, then object belongs to "Sand (lagoonal slopes)".
4 (1.000)	If maxband_3 < -55.0000, then object belongs to "Forereef and deep lagoonal".
5 (0.700)	If maxband_3 [-70.0000, -10.0000] AND minband_3 [-150.0000, -20.0000] AND avgband_4 NOT [28.5000, 29.5000] AND area > 50.0000, then object belongs to "backreef and shallow lagoonal".
6 (1.000)	If maxband_3 > -20.0000 AND minband_3 > -50.0000 AND avgband_4 NOT [28.5000, 29.5000] AND tx_range NOT [8.1237, 12.7657], then object belongs to "reef flat and very shallow lagoonal".

2.3 Results

2.3.1 Spectral analysis of field spectra and selection of class components

The results of the spectral analysis of *in situ* spectra, which were subsequently used to combine or exclude components for class labelling, showed very clear separation of the main biotic and abiotic habitat components at Ningaloo Reef.

The dominant coral genus in the field data was *Acropora* but genera of the same colour were not differentiated due to lack of spectral distinction. Instead, corals were separated based on growth forms of branching, digitate and tabulate as well as their colour. All corals showed highest spectral variability in the region between 570-595 nm. Tabulate corals showed an overall higher reflectance than branching corals as a result of texture and shadowing effects, while digitate corals were found to have a relatively high reflectance, but less defined peaks at 570 nm and 600 nm than tabulate corals (Figure 15).

Hard corals could be distinguished based on their colour. All corals had a reflectance trough at 675 nm (chlorophyll presence). Brown coloured corals, including massive corals showed a triple peak feature at 570, 600 and 650 nm. Distinct “blue tip” *Acropora* had a strong absorption feature at approximately 580 nm with a sharp peak between 630 nm and 650 nm, a wide flat peak between 450 nm and 520 nm and a plateau between 620-650 nm. Despite a relatively small number of field points including “blue tip” *Acropora*, this class was included due to its ecological significance and relatively wide distribution.

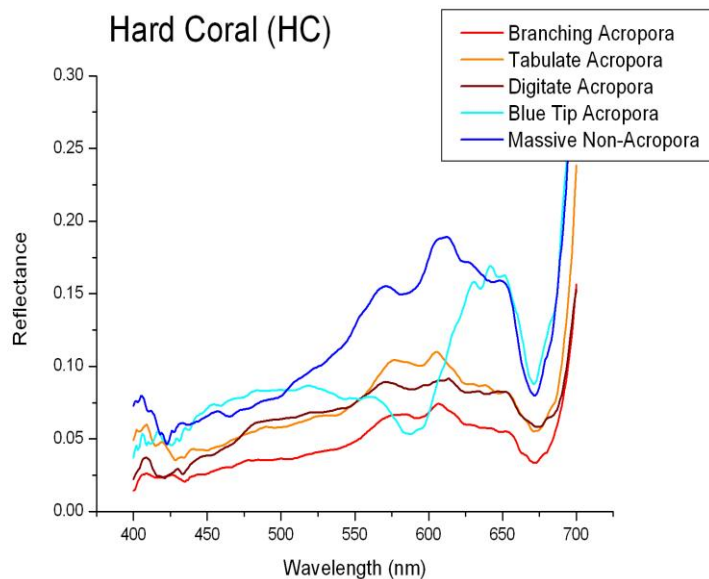


Figure 15. Field measurements of spectral reflectance (mean values) for selected hard corals at Ningaloo Reef.

The findings showed that, despite adequate separability of dead, white coral from healthy coral or abiotic substrates (sand and pavement) (Figure 16), there was an insufficient number of points in the field data where bleached or recently dead corals were found as cover-forming over a whole pixel or even covering a sufficient area of a pixel to be included as a benthic class component. In the field, cover-forming dead coral over a whole pixel was always found to be already covered by turfing algae or macroalgae. As a result, even though they were detectable in the imagery, recently dead or bleached coral was not included in the classification. Instead, the code was modified to include turfing algae or macroalgae cover on dead coral or coral rubble.

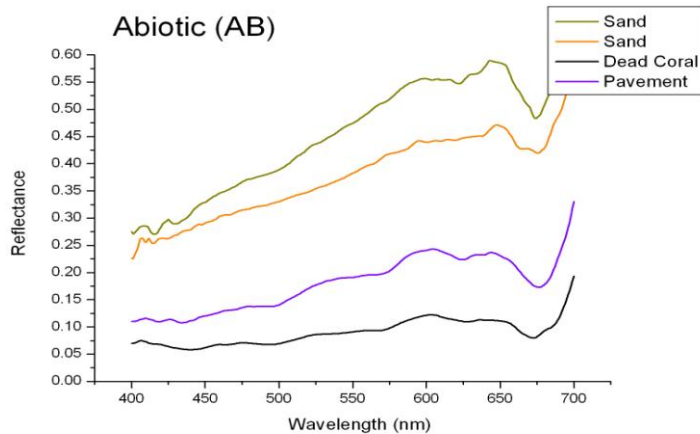


Figure 16. Field measurements of spectral reflectance for a range of abiotic benthic components (mean values) found along the Ningaloo Reef.

Of the three basic forms of algae, namely crustose calcareous algae, turf algae and fleshy macroalgae, only the fleshy macroalgae was found at the pixel cover-forming distribution. All algae (except coralline) had a reflectance feature at 420-435 nm and between 570- 600 nm. *Sargassum* also had a strong peak at 600 nm. While several macroalgal subcategories (*Sargassum*, *Padina*, *Dictyota* and *Ulva*) could be spectrally distinguished (Figure 17), all categories apart from *Sargassum* occurred either very infrequently in the field data or did not form large enough cover within a pixel to be considered. Similarly, coralline algae did not show up frequently enough in the field data and were not used in the final classification. Of the measured algal types, *Sargassum* was found to have a similar reflectance curve to brown coral with peaks at 570 nm and 600 nm, but with a more defined absorption feature just before the third peak at 650 nm.

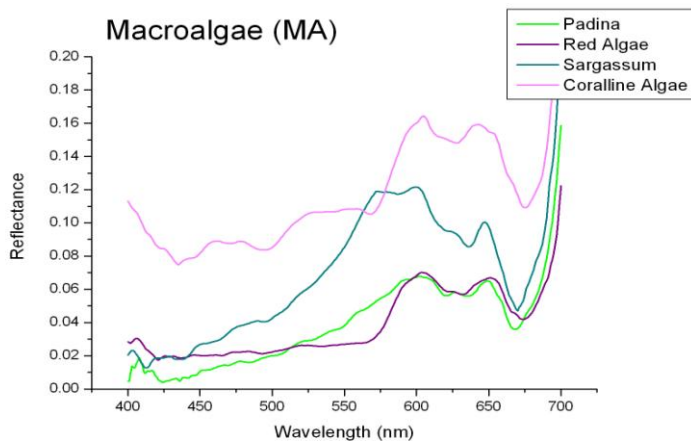


Figure 17. Field measurements of spectral reflectance (mean values) for selected macroalgae found at Ningaloo Reef.

Based on the results of the analysis of *in situ* spectra as well as the occurrence of reef components in the field data, the initial benthic code list from Page *et al.* (2001) was partly modified. Intact dead coral or coral rubble included algal cover, *Sargassum* was separated from macroalgae and “blue tip” *Acropora* was included as a new benthic code (Table 1).

2.3.2 Spectral analysis of image-derived spectra

The results of the image-derived spectral analysis were expected to show far less class differentiation than the *in situ* spectra due to the lower spectral resolution of 15 nm versus 3 nm as well as the smaller spectral range because of the attenuation at longer wavelengths.

The results of the PCA and hierarchical cluster analysis on the image-derived spectra for the continuous coral classes (with > 90 % dominance within the pixel) showed a high spectral similarity for continuous branching, digitate, massive and soft coral, despite the spectral differences visible in the *in situ* spectral signatures (Figure 18). Soft coral and digitate coral were found to have a JM index of 1.46.

The continuous tabulate coral class was found to have a relatively large spectral range partly overlapping with the continuous branching and digitate coral classes using PCA and cluster analysis; however, on applying the JM distance, they were found to be separable with an index of 2. Continuous tabulate coral and class dominant tabulate coral with digitate coral were not separable with a JM distance = 1.3.

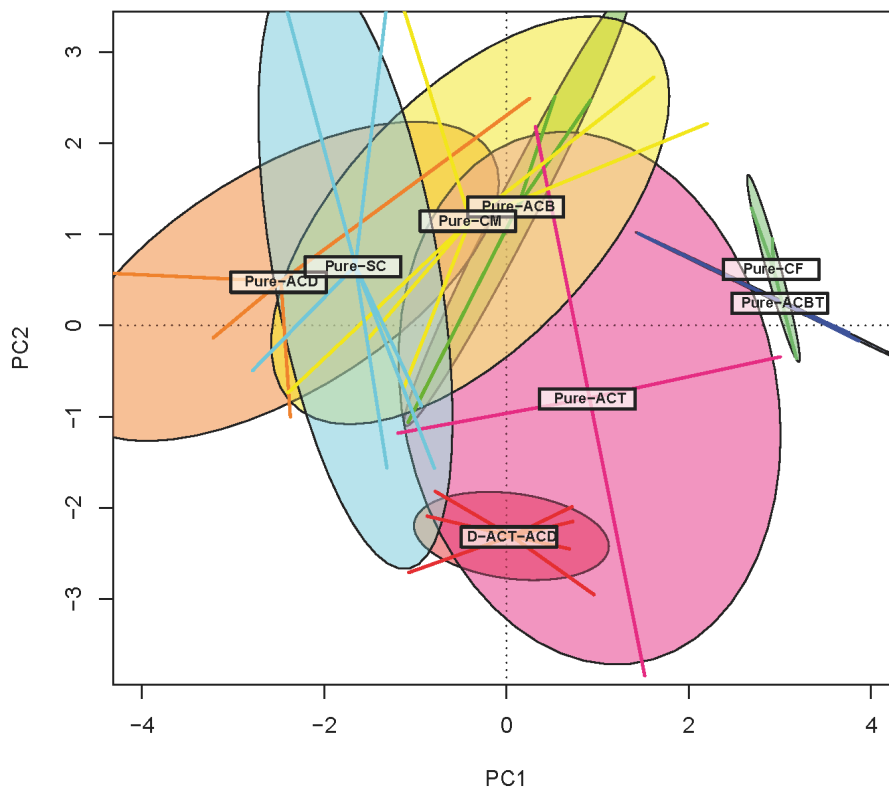


Figure 18. PCA transformed data viewed in a two-dimensional space showing continuous (near 100% cover) coral classes (referred to as “Pure”) from Ningaloo Reef.

Continuous macroalgae and several coral classes had an apparent high similarity using PCA and cluster analysis and on applying the JM distance, were found to have a separation of 1.87. Since the coral and macroalgae classes are both ecologically relevant and the JM distance was close to the accepted value for separation of 1.9, the classes were considered separable.

Classes that included the same components with a similar degree of cover were found to be spectrally similar, such as dominant or continuous cover of the same component, e.g. dominant macroalgae with sand and dominant macroalgae.

Classes where the biotic cover was sparse or patchy had a low spectral influence on the class, were often not separable, e.g. sparse hard coral with limestone pavement and sparse hard coral with sand, where limestone pavement and sand have large brightness differences. These results were used to determine the “fuzziness” between classes during final accuracy assessment.

2.3.3 Image classification results

The operational approach to classification which used a single training set, a single software configuration file and was run on georeferenced data blocks (as opposed to individual flight lines) proved successful. The overall processing time of the 17 data blocks was approximately 3 - 4 full days. Results of the overall probability image, i.e. the actual classification image, as well as the single class probability images are presented in the next sections.

Habitat maps

The classification resulted in 46 habitat classes documented in the configuration file. Figure 19 and Figure 20 show the subsurface reflectance (show near-normal colour composite) and classification outputs, respectively, of area near Coral Bay with two subsets zooming into areas with varied habitats. Figure 21 depicts the legend with 46 habitat classes (the benthic codes can be obtained from Table 2). As the data blocks were classified prior to mosaicking and masking, deep water areas are still visible. Presentation of the data as pairs of subsurface reflectance and habitats allows the user to have a better idea of the locations of different reef components and coastal features.

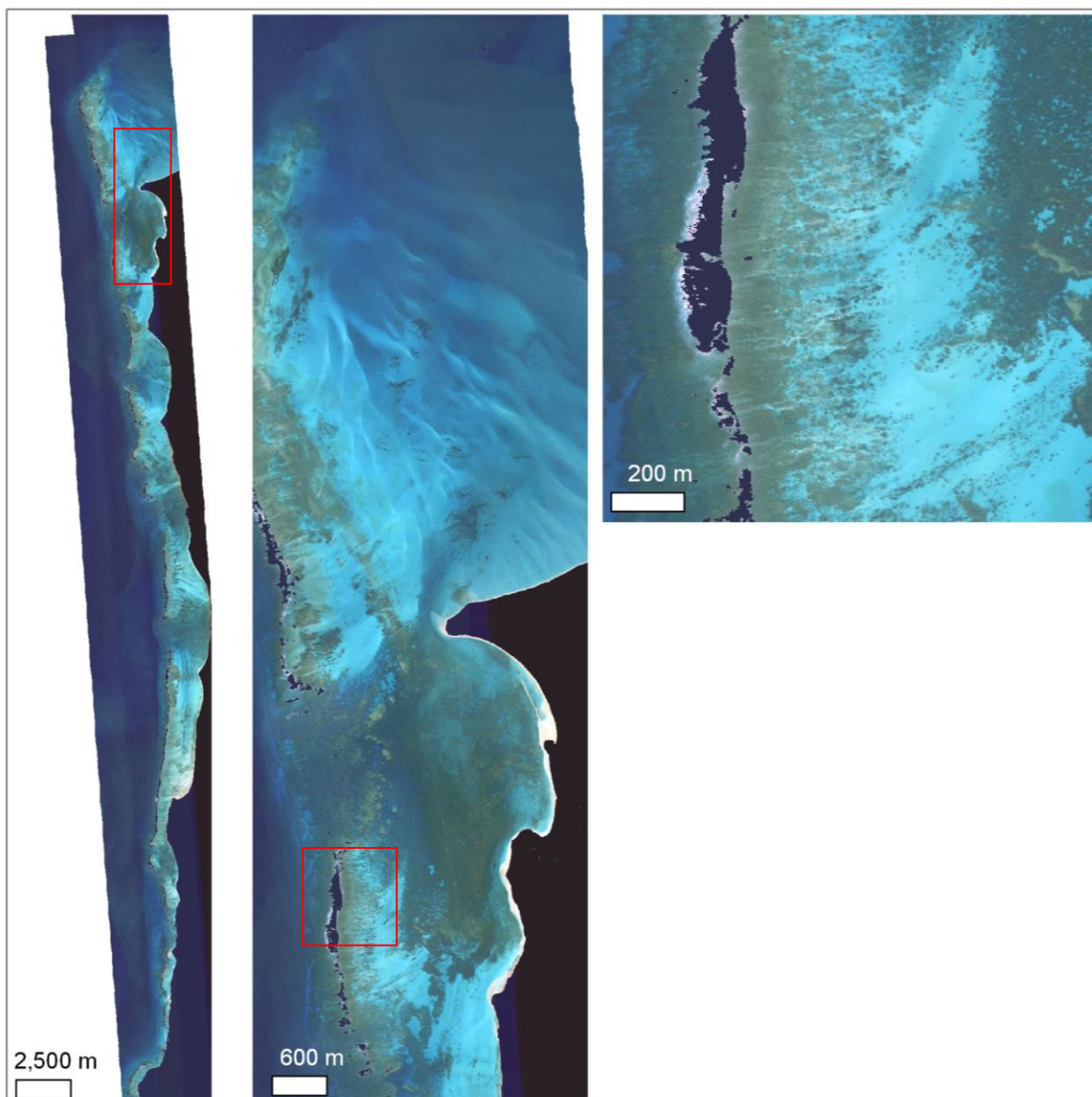


Figure 19. Example of HyMap RGB image for the block D, including Coral Bay area at Ningaloo Reef. Red boxes show boundaries of enlarged images, from left to the right.

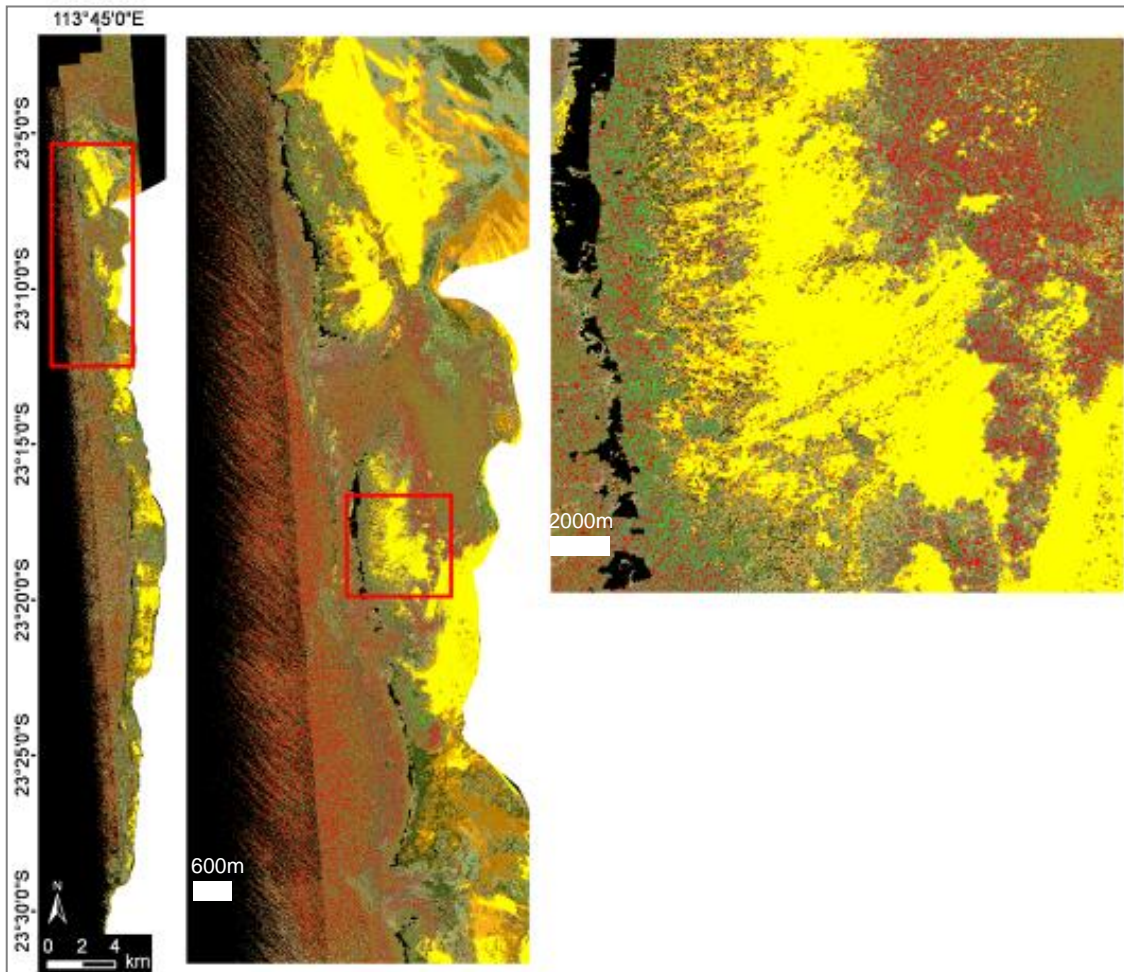


Figure 20. Example of the classification map for the block D, including the Coral Bay area at Ningaloo Reef. The legend is shown in Figure 21. Red boxes show boundaries of enlarged images, from left to the right. Note that deep water areas west of the forereef have not been masked and edges of blocks, especially at the northern extent are clearly visible.

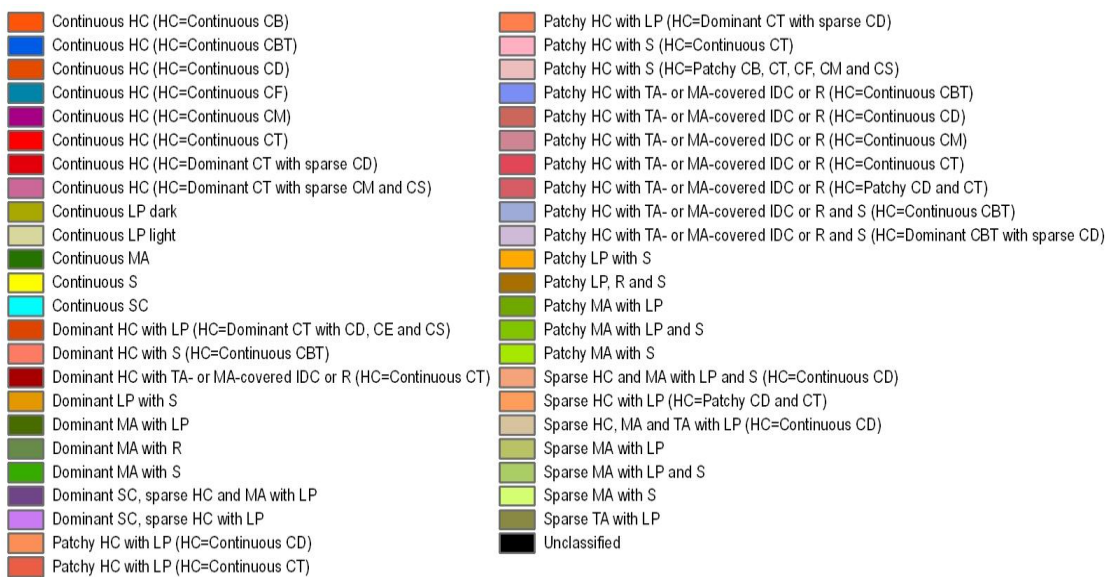
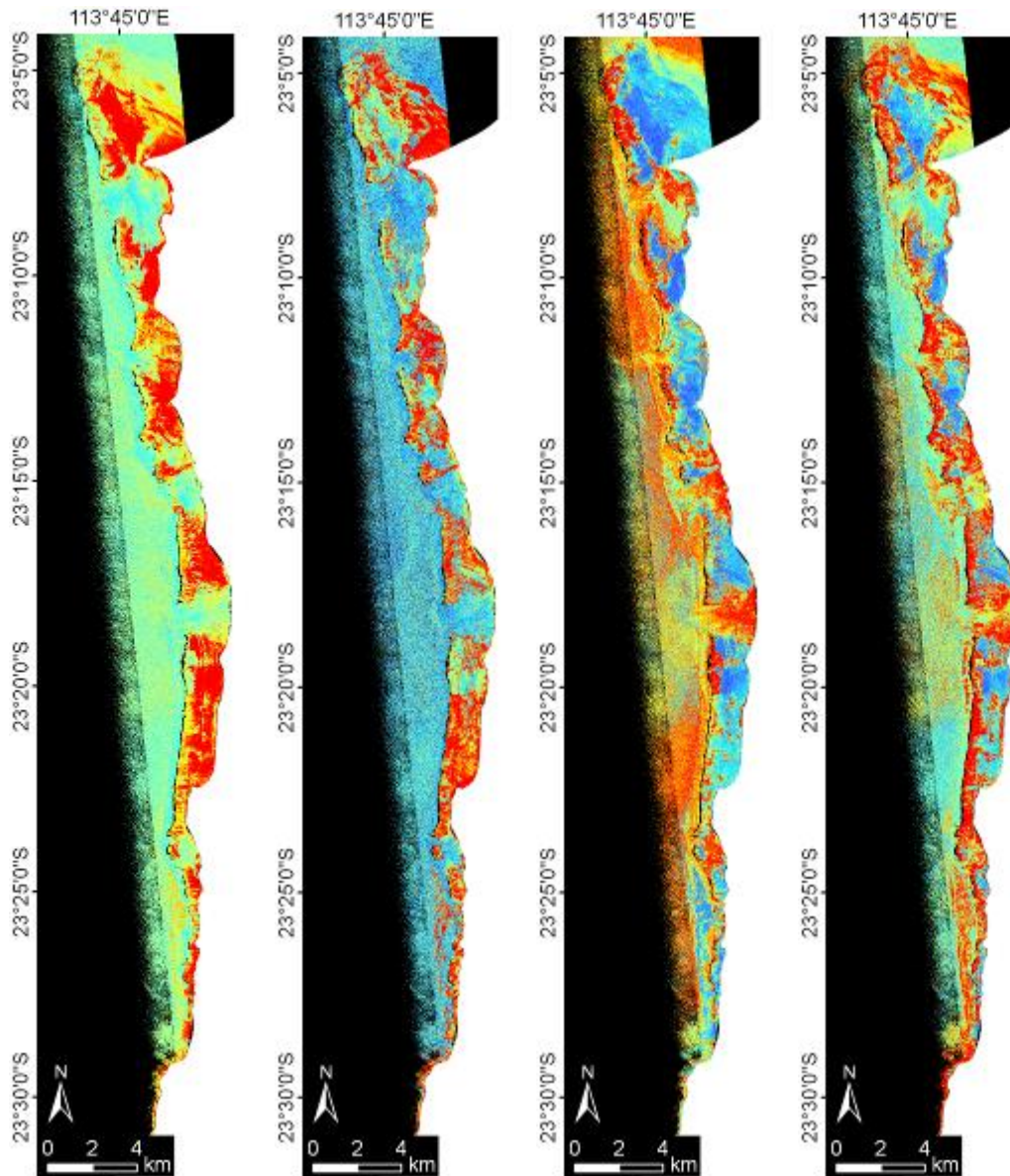


Figure 21. Legend showing the habitat classes relating to map in Figure 20. Abbreviations for benthic codes correspond to those in Table 2.

2.3.4 Probability images

Individual per-class probability images were generated during data processing. Examples of single class probability images for four spectrally different classes are shown for the Coral Bay area (block D) (Figure 22).



Legend

Probability value [%]

100

0

No data

Land mask

Figure 22. Single class probability images of data block D showing percentage probability for the following classes 'continuous sand', 'continuous limestone pavement', 'continuous digitate coral' and 'continuous macroalgae' (from left to right).

Spatial distribution of the class “continuous sand” can be seen to correspond well to the classification results in Figure 20, with continuous limestone pavement as well as continuous digitate coral and continuous macroalgae having similar probabilities. This type of output would be of interest to the users who want to analyse only a particular thematic subset of the data or investigate the influence of different probability thresholds on the analysis. These probability maps allow, for example, to combine only those classes which include a coral component into a single multi-band file to analyse distribution of coral dominated mosaics.

2.3.5 Mosaics and masks

While some users only work in a small area, contained within a single data block, others might need the full, merged dataset for the entire length of the reef. The 17 classified data blocks merged into a single mosaic resulted in a file size of approximately 5 Gb (despite an average block size of 30 Mb). This large size was the result of the overall geographic dimensions and pixel resolution of the dataset after mosaicking, as shown in Figure 23.

Following masking using bathymetry input (combination of the deep water mask and contextual editing), a large proportion of the HyMap imagery was excluded, particularly in areas with very narrow lagoons, such as in the southern part of the reef (Figure 23).

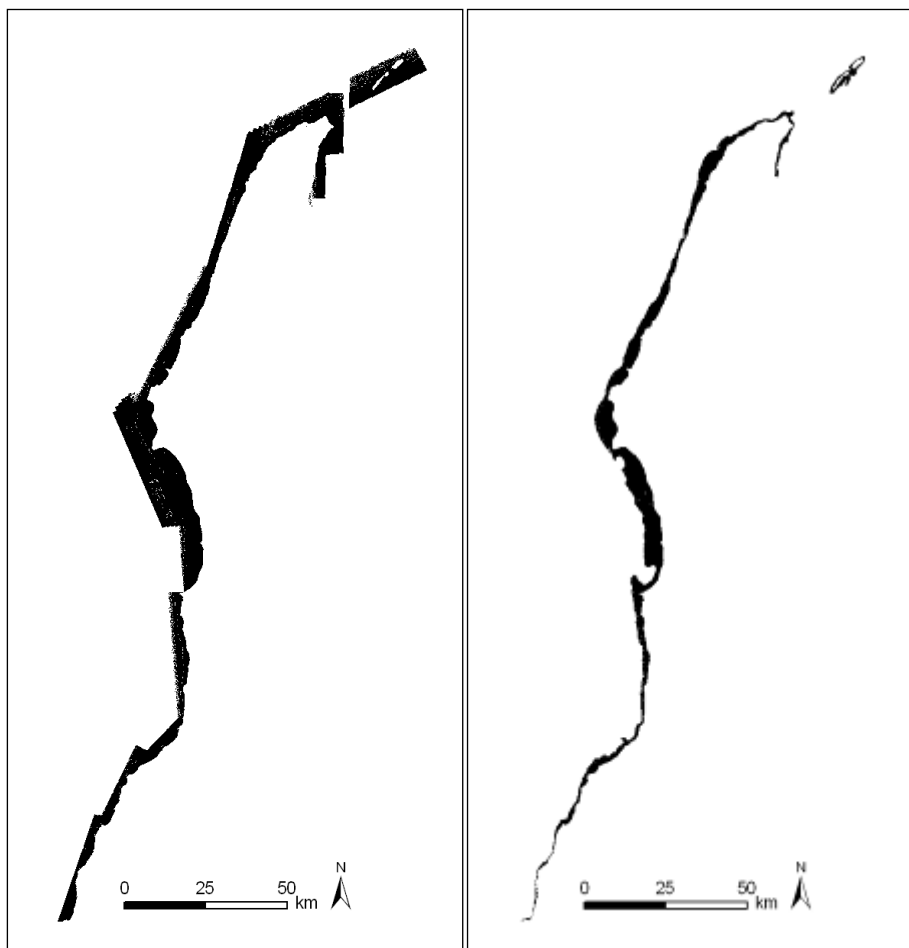


Figure 23. Mosaic of classified image blocks for the whole reef (left) and the same mosaic after the depth mask had been applied (right). Note the narrow reefs in the south compared to the central areas of the Ningaloo Reef.

2.3.6 Thematic generalisation

Five thematic classification levels and sub-levels were created with varying degrees of benthic cover detail, ranging from a basic level with three classes (biotic, abiotic and mixed) to the most detailed with 46 habitat classes (consisting of all benthic components and hard coral growth forms in pure or mixed states) for level 5. Examples of all levels are shown for Turquoise Bay area (Figure 24). The maps were generated using ArcMap, where the look-up table with different levels was linked to the classification image to generate the respective habitat maps at different levels of detail.

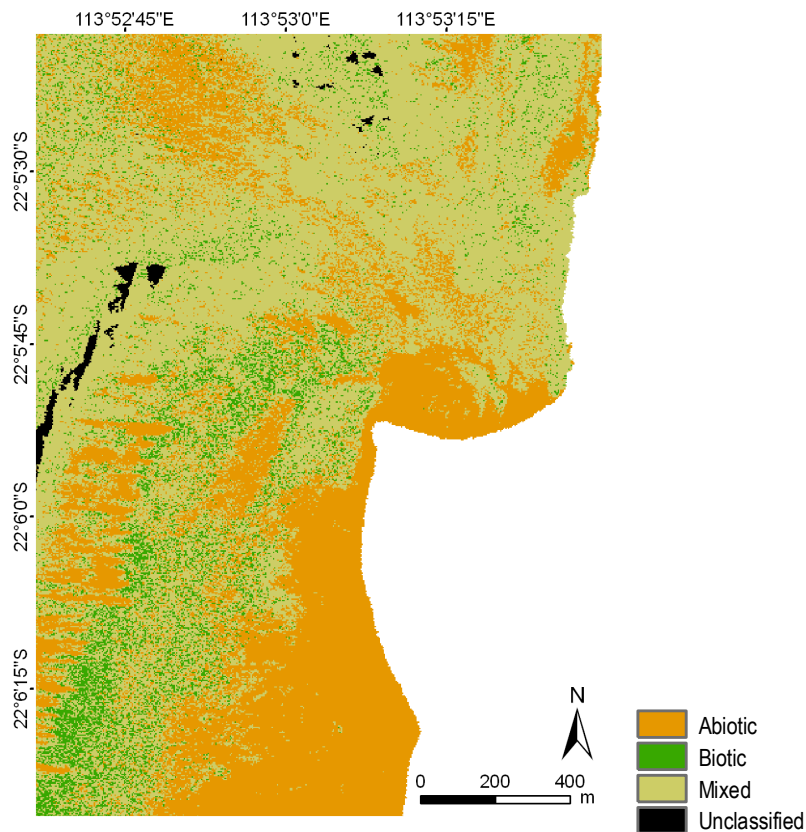


Figure 24. Example of benthic habitats for the Turquoise Bay area at the thematic classification level 1.

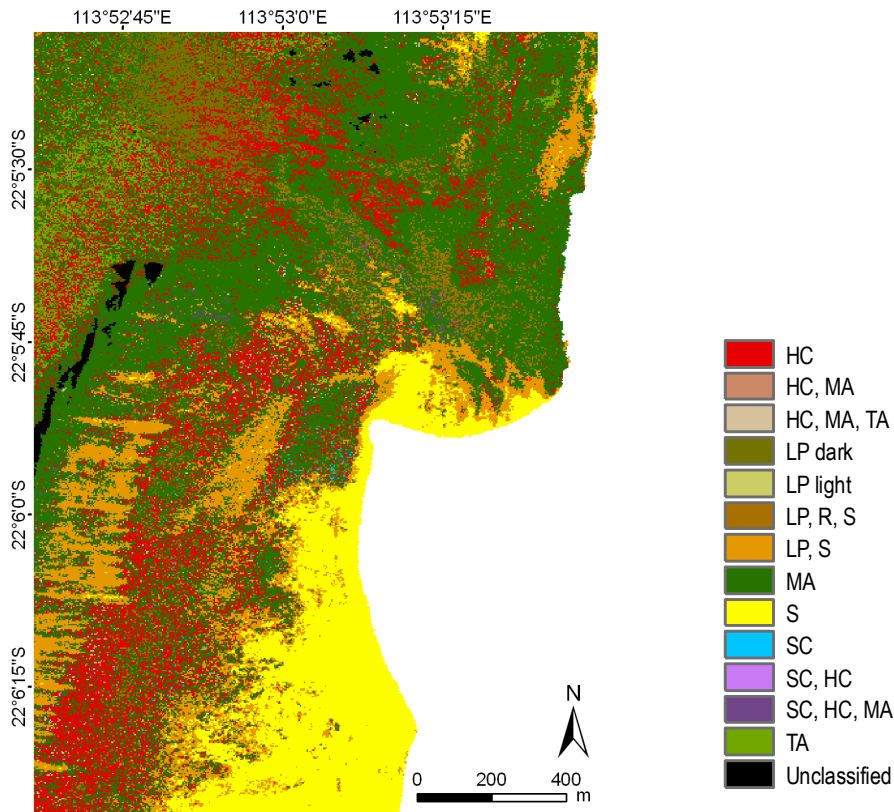


Figure 25. Example of benthic habitats for the Turquoise Bay area at the thematic classification level 2a. Legend uses codes explained in Table 1.

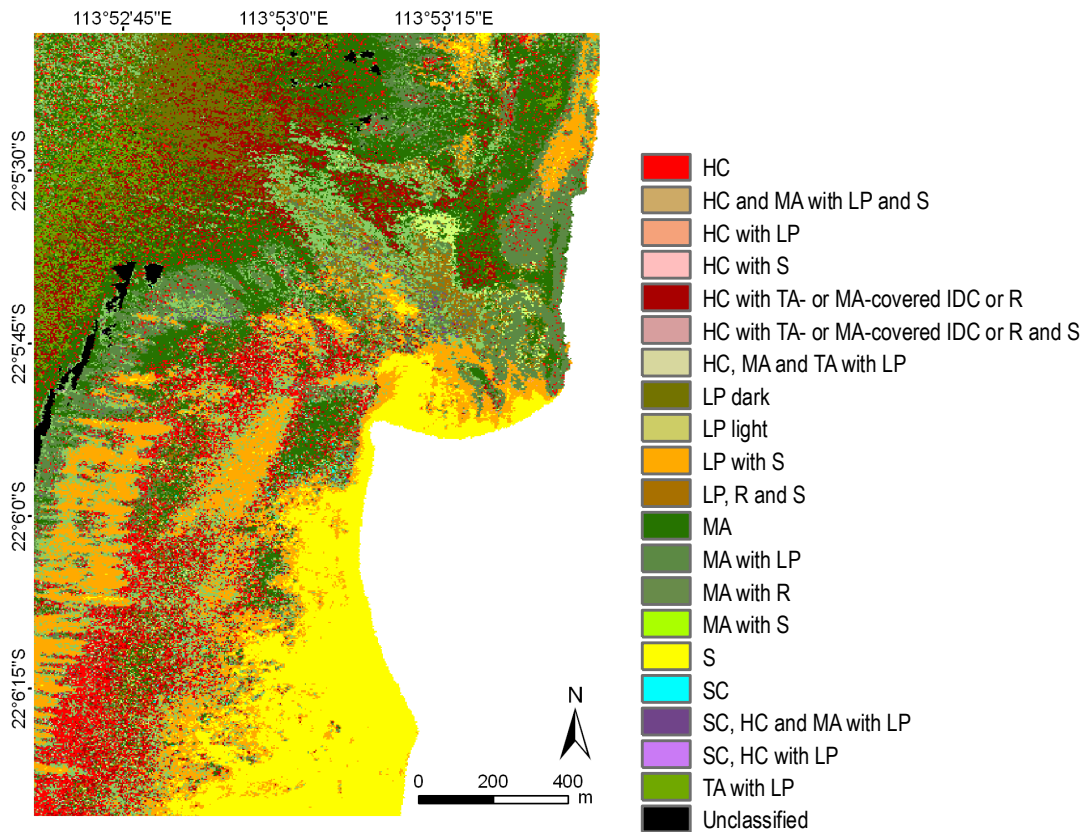


Figure 26. Example of benthic habitats for the Turquoise Bay area at the thematic classification level 2b. Legend uses codes explained in Table 1.

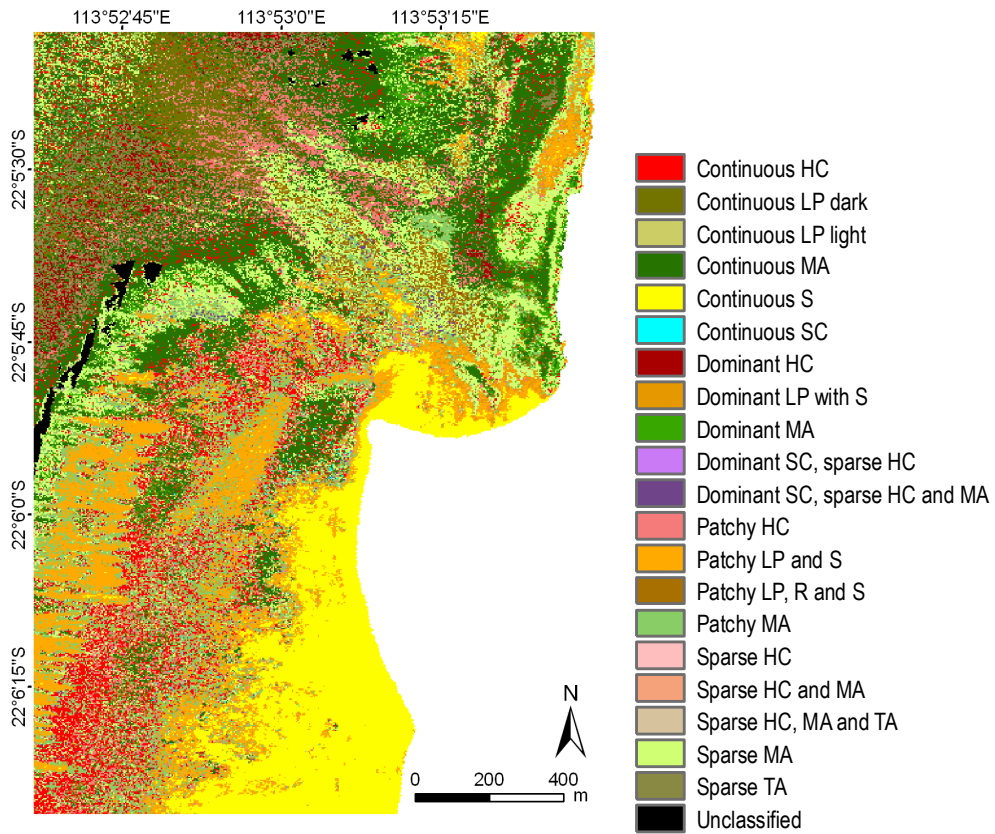


Figure 27. Example of benthic habitats for the Turquoise Bay area at the thematic classification level 3a. Legend uses codes explained in Table 1.

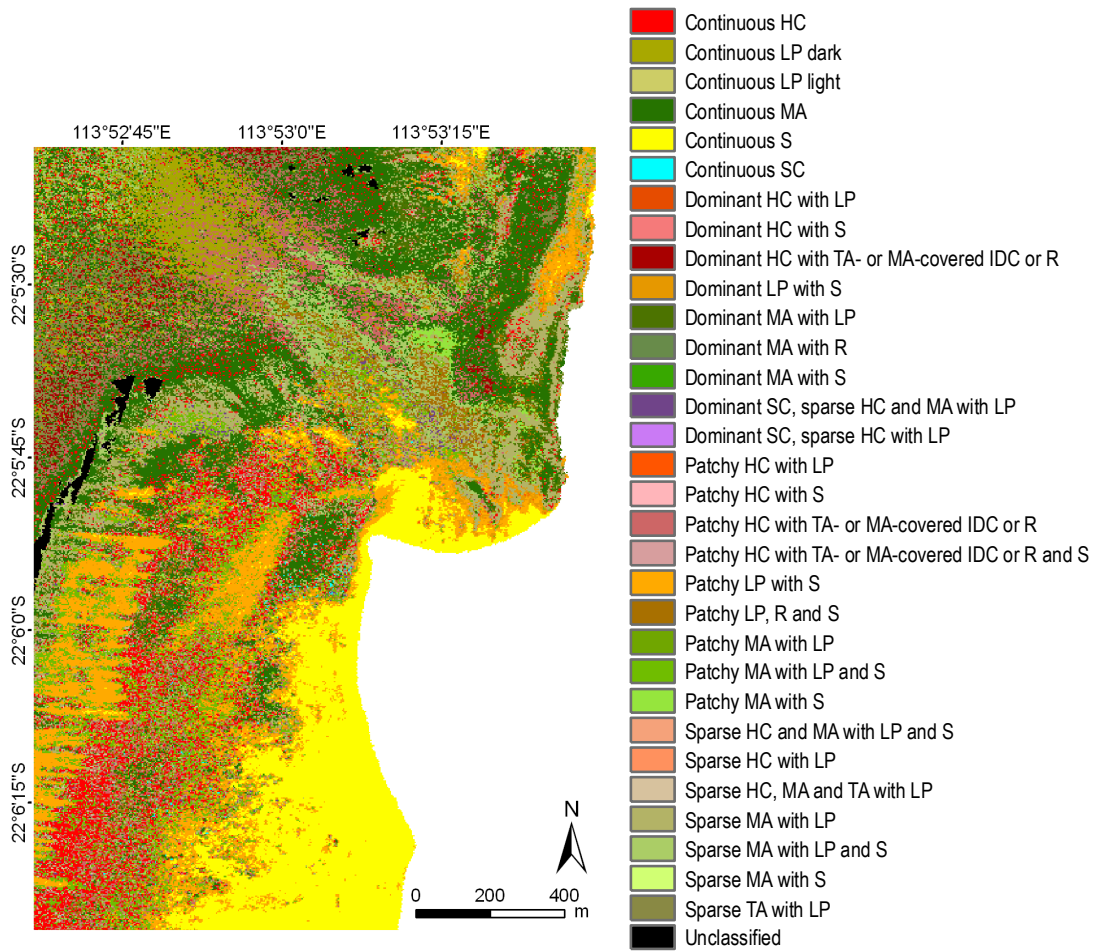


Figure 28. Example of benthic habitats for the Turquoise Bay area at the thematic classification level 3b. Legend uses codes explained in Table 1.

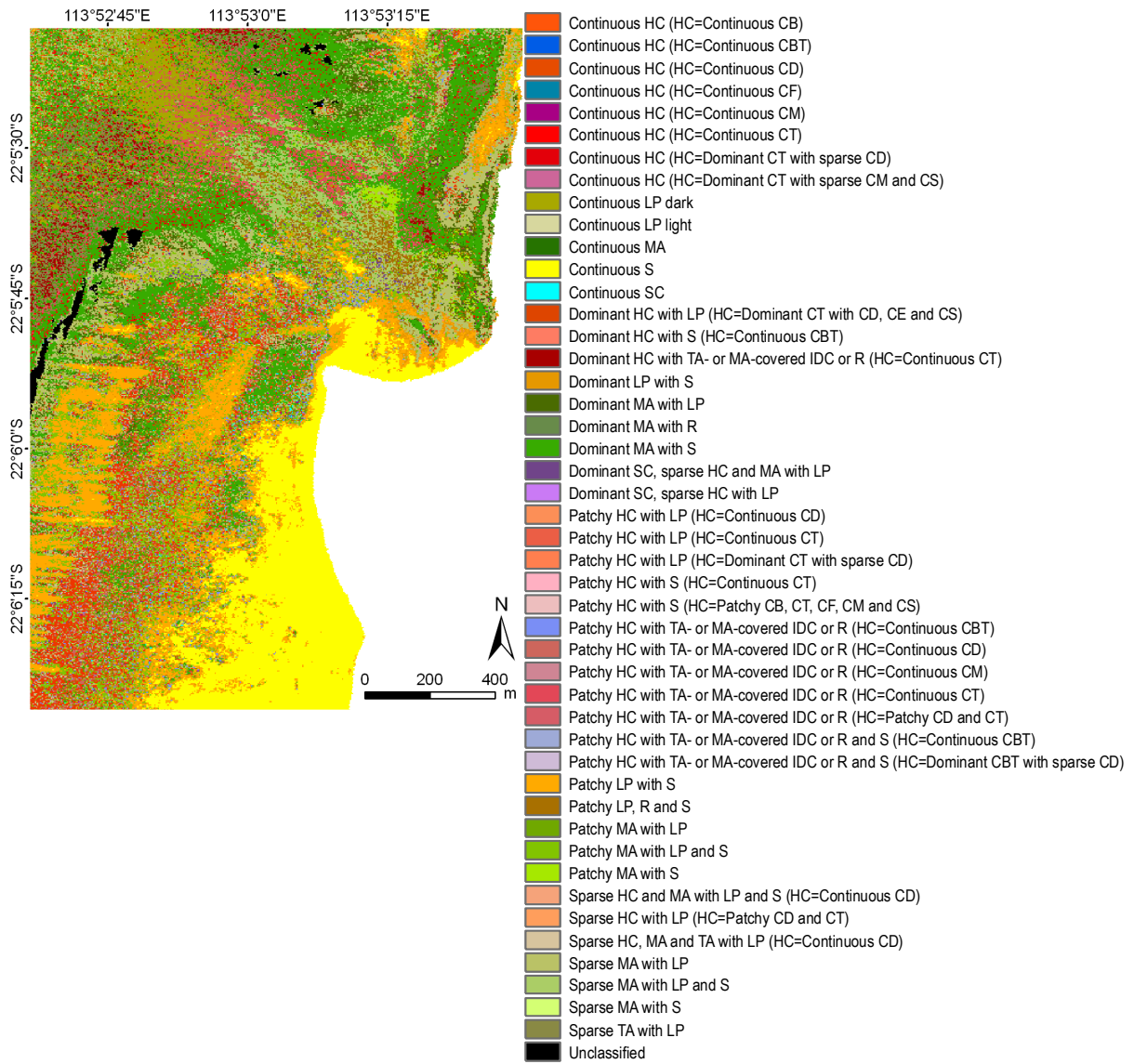


Figure 29. Example of benthic habitats for the Turquoise Bay area at the thematic classification level 4a with the legend, using codes explained in Table 1.

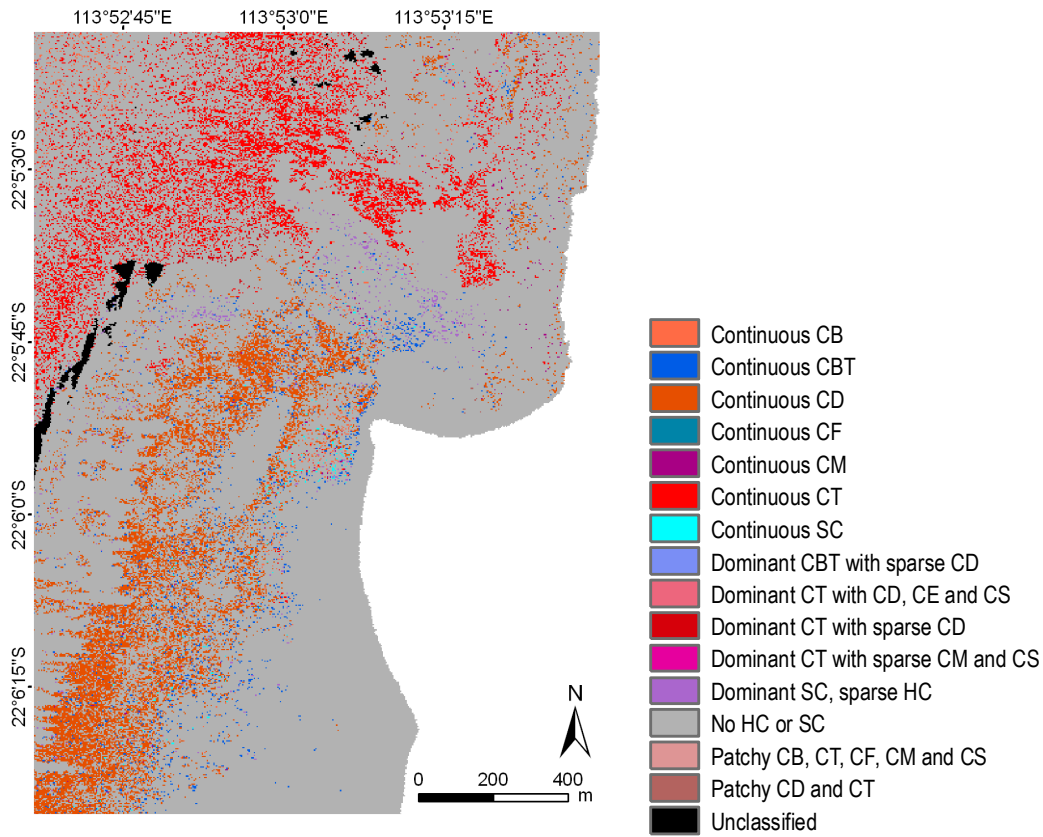


Figure 30. Example of benthic habitats for the Turquoise Bay area at the thematic classification level 5, showing only information about hard or soft coral classes. Grey areas on the map do not contain any coral component discernible within a pixel. Legend uses codes explained in Table 1.

Table 8. Lookup table for marine habitat maps at different levels of detail for biotic and abiotic descriptors and degree of cover at Ningaloo Reef. Codes are explained in Table 1.

Value	Level1	Level2a	Level2b	Level3a	Level3b	Level4a	Level5
0	Unclassified	Unclassified	Unclassified	Unclassified	Unclassified	Unclassified	Unclassified
1	Abiotic	LP, S	LP with S	Dominant LP with S	Dominant LP with S	Dominant LP with S	No HC
2	Mixed	MA	MA with S	Sparse MA	Sparse MA with S	Sparse MA with S	No HC
3	Mixed	HC	HC with TA- or MA-covered IDC or R	Dominant HC	Dominant HC with TA- or MA-covered IDC or R	Dominant HC with TA- or MA-covered IDC or R (HC=Continuous CT)	Continuous CT
4	Mixed	HC	HC with LP	Dominant HC	Dominant HC with LP	Dominant HC with LP (HC=Dominant CT with CD, CE and CS)	Dominant CT with CD, CE and CS
5	Mixed	HC	HC with S	Dominant HC	Dominant HC with S	Dominant HC with S (HC=Continuous CBT)	Continuous CBT
6	Mixed	HC	HC with LP	Sparse HC	Sparse HC with LP	Sparse HC with LP (HC=Patchy CD and CT)	Patchy CD and CT
7	Mixed	HC, MA	HC and MA with LP and S	Sparse HC and MA	Sparse HC and MA with LP and S	Sparse HC and MA with LP and S (HC=Continuous CD)	Continuous CD
8	Mixed	HC, MA, TA	HC, MA and TA with LP	Sparse HC, MA and TA	Sparse HC, MA and TA with LP	Sparse HC, MA and TA with LP (HC=Continuous CD)	Continuous CD
9	Mixed	MA	MA with LP	Sparse MA	Sparse MA with LP	Sparse MA with LP	No HC
10	Mixed	MA	MA with LP and S	Sparse MA	Sparse MA with LP and S	Sparse MA with LP and S	No HC
11	Mixed	TA	TA with LP	Sparse TA	Sparse TA with LP	Sparse TA with LP	No HC
12	Mixed	MA	MA with LP	Dominant MA	Dominant MA with LP	Dominant MA with LP	No HC
13	Mixed	MA	MA with R	Dominant MA	Dominant MA with R	Dominant MA with R	No HC
14	Mixed	MA	MA with S	Dominant MA	Dominant MA with S	Dominant MA with S	No HC
15	Mixed	HC	HC with TA- or MA-covered IDC or R	Patchy HC	Patchy HC with TA- or MA-covered IDC or R	Patchy HC with TA- or MA-covered IDC or R (HC=Continuous CD)	Continuous CD
16	Mixed	HC	HC with S	Patchy HC	Patchy HC with S	Patchy HC with S (HC=Continuous CT)	Continuous CT
17	Abiotic	LP, R, S	LP, R and S	Patchy LP, R and S	Patchy LP, R and S	Patchy LP, R and S	No HC
18	Mixed	HC	HC with TA- or MA-covered IDC or R	Patchy HC	Patchy HC with TA- or MA-covered IDC or R	Patchy HC with TA- or MA-covered IDC or R (HC=Continuous CM)	Continuous CM
19	Abiotic	LP, S	LP with S	Patchy LP and S	Patchy LP with S	Patchy LP with S	No HC
20	Mixed	HC	HC with TA- or MA-covered IDC or R and S	Patchy HC	Patchy HC with TA- or MA-covered IDC or R and S	Patchy HC with TA- or MA-covered IDC or R and S (HC=Dominant CBT with sparse CD)	Dominant CBT with sparse CD
21	Mixed	HC	HC with TA- or MA-covered IDC or R and S	Patchy HC	Patchy HC with TA- or MA-covered IDC or R and S	Patchy HC with TA- or MA-covered IDC or R and S (HC=Continuous CBT)	Continuous CBT
22	Mixed	HC	HC with LP	Patchy HC	Patchy HC with LP	Patchy HC with LP (HC=Dominant CT with sparse CD)	Dominant CT with sparse CD
23	Mixed	HC	HC with LP	Patchy HC	Patchy HC with LP	Patchy HC with LP (HC=Continuous CD)	Continuous CD
24	Mixed	HC	HC with LP	Patchy HC	Patchy HC with LP	Patchy HC with LP (HC=Continuous CT)	Continuous CT
25	Mixed	HC	HC with S	Patchy HC	Patchy HC with S	Patchy HC with S (HC=Patchy CB, CT, CF, CM and CS)	Patchy CB, CT, CF, CM and CS

26	Mixed	HC	HC with TA- or MA-covered IDC or R	Patchy HC	Patchy HC with TA- or MA-covered IDC or R	Patchy HC with TA- or MA-covered IDC or R (HC=Patchy CD and CT)	Patchy CD and CT
27	Mixed	HC	HC with TA- or MA-covered IDC or R	Patchy HC	Patchy HC with TA- or MA-covered IDC or R	Patchy HC with TA- or MA-covered IDC or R (HC=Continuous CBT)	Continuous CBT
28	Mixed	HC	HC with TA- or MA-covered IDC or R	Patchy HC	Patchy HC with TA- or MA-covered IDC or R	Patchy HC with TA- or MA-covered IDC or R (HC=Continuous CM)	Continuous CM
29	Abiotic	S	S	Continuous S	Continuous S	Continuous S	No HC
30	Mixed	MA	MA with LP	Patchy MA	Patchy MA with LP	Patchy MA with LP	No HC
31	Mixed	MA	MA with LP and S	Patchy MA	Patchy MA with LP and S	Patchy MA with LP and S	No HC
32	Mixed	MA	MA with S	Patchy MA	Patchy MA with S	Patchy MA with S	No HC
33	Abiotic	LP light	LP light	Continuous LP light	Continuous LP light	Continuous LP light	No HC
34	Abiotic	LP dark	LP dark	Continuous LP dark	Continuous LP dark	Continuous LP dark	No HC
35	Biotic	SC	SC	Continuous SC	Continuous SC	Continuous SC	Continuous SC
36	Mixed	SC, HC, MA	SC, HC and MA with LP	Dominant SC, sparse HC and MA	Dominant SC, sparse HC and MA with LP	Dominant SC, sparse HC and MA with LP	Dominant SC, sparse HC
37	Biotic	HC	HC	Continuous HC	Continuous HC	Continuous HC (HC=Continuous CBT)	Continuous CBT
38	Biotic	HC	HC	Continuous HC	Continuous HC	Continuous HC (HC=Continuous CF)	Continuous CF
39	Mixed	SC, HC	SC, HC with LP	Dominant SC, sparse HC	Dominant SC, sparse HC with LP	Dominant SC, sparse HC with LP	Dominant SC, sparse HC
40	Biotic	HC	HC	Continuous HC	Continuous HC	Continuous HC (HC=Dominant CT with sparse CD)	Dominant CT with sparse CD
41	Biotic	HC	HC	Continuous HC	Continuous HC	Continuous HC (HC=Dominant CT with sparse CM and CS)	Dominant CT with sparse CM and CS
42	Biotic	HC	HC	Continuous HC	Continuous HC	Continuous HC (HC=Continuous CB)	Continuous CB
43	Biotic	HC	HC	Continuous HC	Continuous HC	Continuous HC (HC=Continuous CD)	Continuous CD
44	Biotic	HC	HC	Continuous HC	Continuous HC	Continuous HC (HC=Continuous CT)	Continuous CT
45	Biotic	HC	HC	Continuous HC	Continuous HC	Continuous HC (HC=Continuous CM)	Continuous CM
46	Biotic	MA	MA	Continuous MA	Continuous MA	Continuous MA	No HC

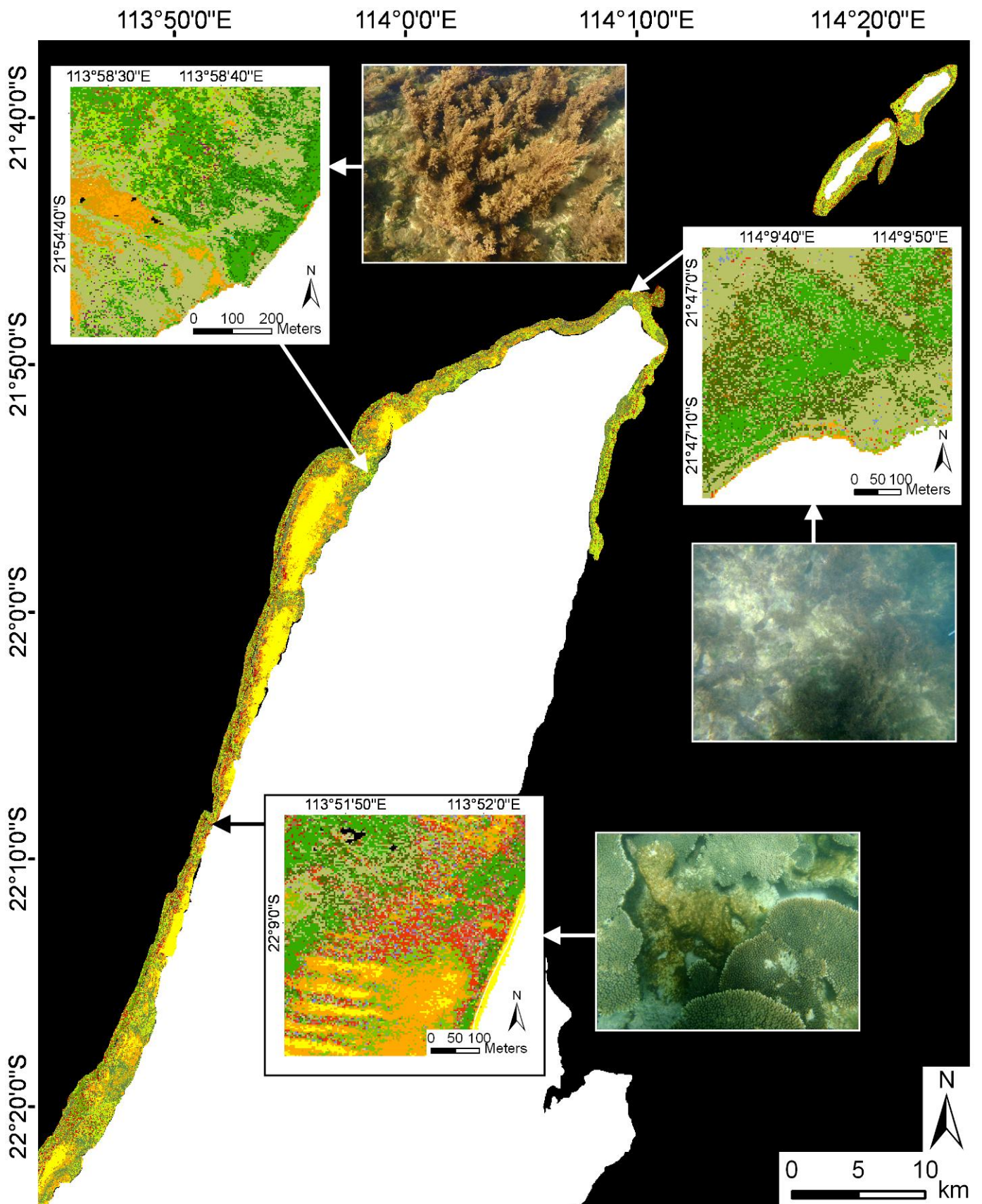


Figure 31. Overview of the northern part of the Ningaloo Reef with insets illustrating detailed habitat maps for areas dominated by macroalgal (upper inset) and coral mosaics (lower inset). Legend from Figure 28 applies. Land has been masked (white). Underwater photographs illustrate typical substrate components of macroalgae and plate coral.

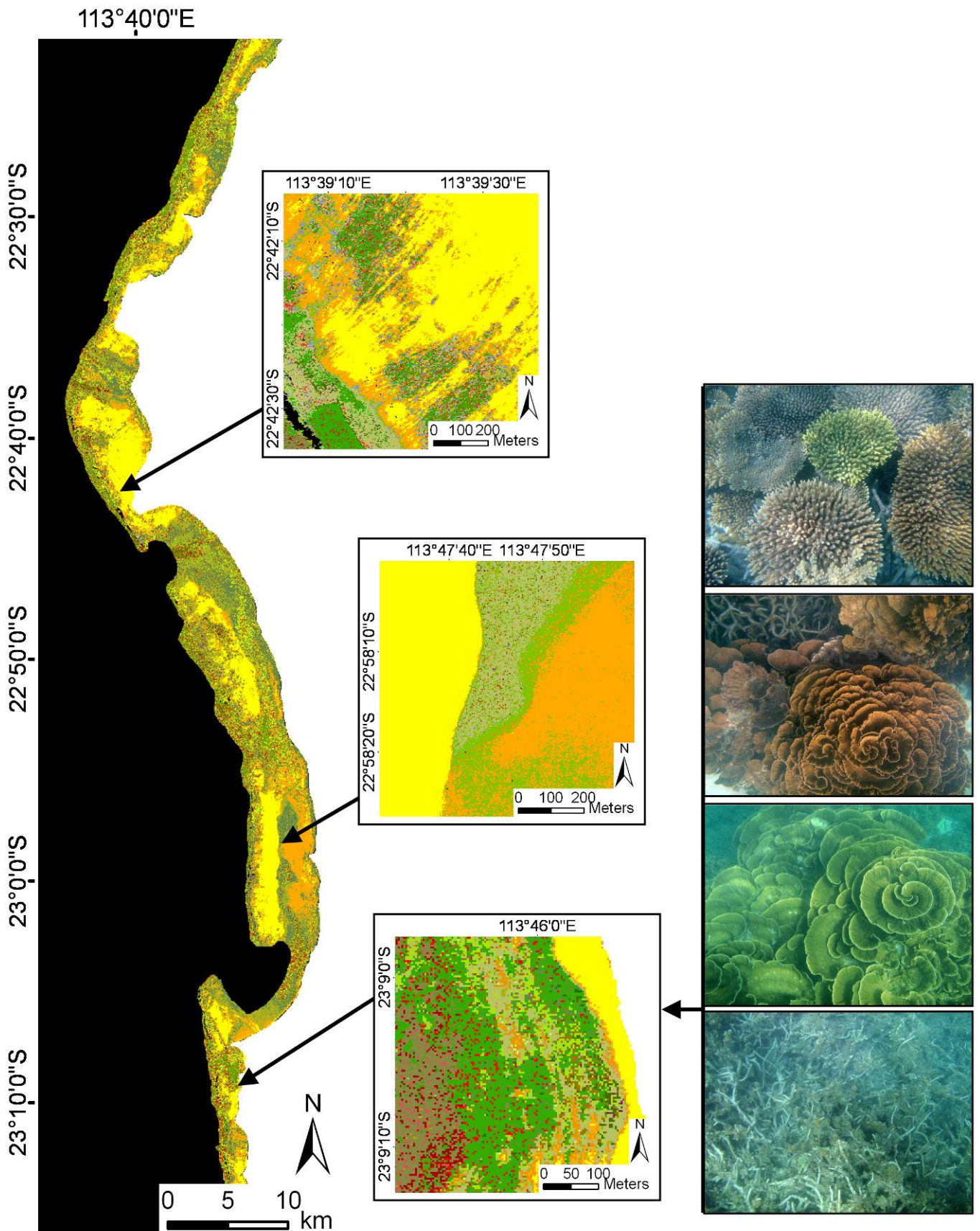


Figure 32. Overview of the central part of the Ningaloo Reef with insets illustrating detailed habitat maps for areas dominated by macroalgae, limestone and sand (upper inset and middle) and coral mosaics (lower inset). Legend from Figure 28 applies. Land has been masked (white). Underwater photographs illustrate typical substrate components of digitate, foliose and branching coral (with macroalgae).

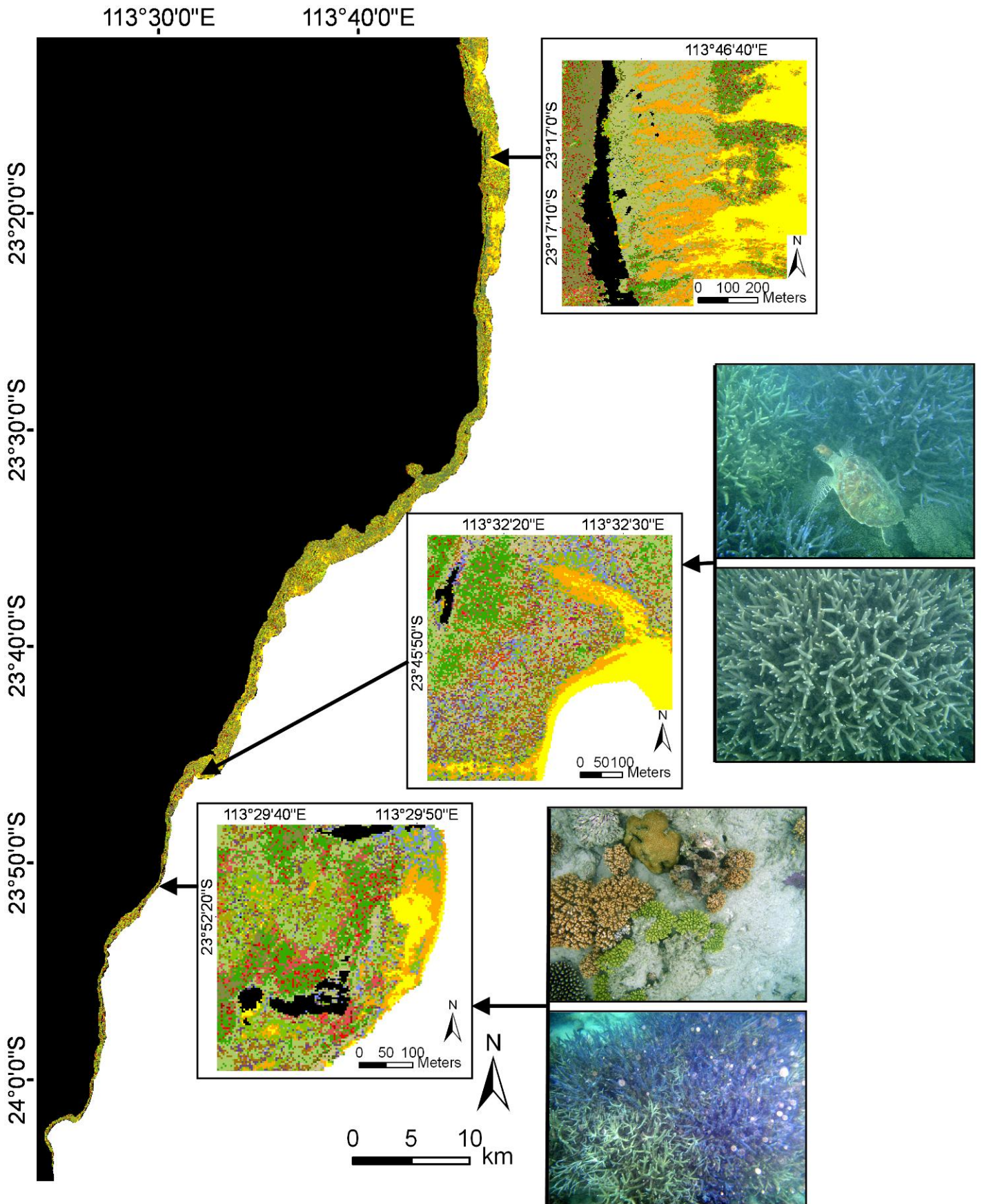


Figure 33. Overview of the southern part of the Ningaloo Reef with insets illustrating detailed habitat maps for areas dominated by macroalgae, limestone and sand (upper inset) and coral mosaics (middle and lower inset). Legend from Figure 28 applies. Land has been masked (white). Underwater photographs illustrate typical substrate components of soft, digitate, branching coral (with macroalgae) and "blue tip" *Acropora*.

2.3.7 Spatial generalisation

Some applications of the habitat maps may require simpler spatial boundaries and lower overall resolution (spatial, i.e. larger pixel size and thematic, i.e. fewer classes). For example, a hard copy display of the entire dataset at even an A0 poster format would not require or show every pixel in the data set. The decrease in spatial detail and smoothing of class boundaries are visible in Figure 34 which depicts the non-generalised image compared to these with majority filter with 5x5 and 9x9 kernel sizes applied. The generalisation resulted in an overall increase in area of dominant classes that form spatially homogenous cover while less dominant classes covering small areas, i.e. only a few neighbouring pixels, decreased in total area.

Hard coral classes which had sparse distribution and occurred in small patches (2-3 pixels at a time) showed a decrease in total area. Homogenous classes such as limestone pavement which covered large areas increased as a result of spatial generalisation. One reason for this pattern is that hard coral classes were within a “mosaic” of limestone pavement and or macroalgae. The continuous sand class, however, did not increase substantially, as it was a fairly homogeneous class, not interspersed with other classes (Table 9). Hence, while spatial generalisation produces a smoother, less noisy output, it should never be used for calculations or detailed analysis.

Table 9. Example of changes in areas of highly fragmented classes with the increased kernel size in spatial generalisations of the habitat maps for the Ningaloo Reef.

Class name	Area (km ²)				
	original resolution	3x3 kernel	5x5 kernel	7x7 kernel	9x9 kernel
Continuous hard coral	12.63	4.09	1.63	1.40	1.15
Continuous dead coral	14.25	8.76	6.90	6.63	6.23
Continuous limestone pavement	783.02	1,096.75	1,266.99	1,284.91	1,302.08
Continuous macroalgae	0.55	0.29	0.14	0.11	0.08
Continuous sand	130.73	130.57	132.92	133.65	134.90
Continuous soft coral	0.81	0.33	0.14	0.12	0.09

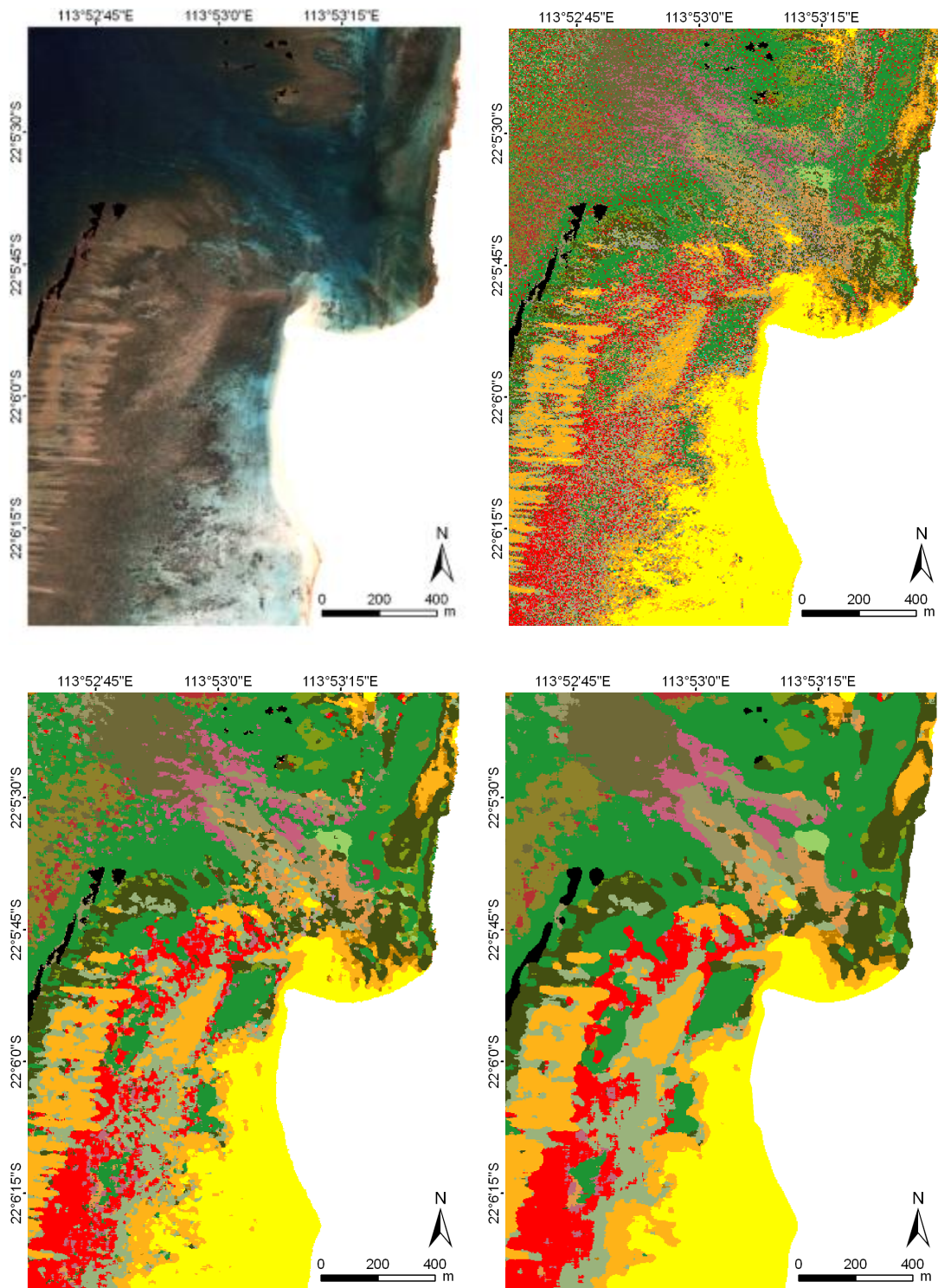


Figure 34. Spatial generalisations using majority filters (Turquoise Bay). Top left: HyMap RGB image. Top right: non-generalised classification image. Bottom left: majority filter using 5x5 kernel size. Bottom right: majority filter using 9x9 kernel size.

2.3.8 Spatial statistics

The summary statistics of areas of the classes were calculated at the full resolution data to determine the distribution and proportions of the 46 benthic habitats across different geographic domains. This was done for the whole mosaic, near shore areas (500 m buffer), sanctuary zones and popular swimming and snorkelling areas. This study mapped 761.7 km² of the reef which included 5 854 ha of coral mosaics (classes containing coral from 20-100% cover) (7.6 %), 51 % of macro- and turfing algae and 41 % of sand and limestone pavement (Table 10 and Table 11). Approximately 50 % of the areas mapped were in sanctuary zones (383 km²) and 21 % of the mapped area was within 500 m distance from the mean high water mark (Table 11).

Table 10. Spatial statistics (in % and hectares) for all classes containing hard coral (from sparse to continuous) for the whole Ningaloo Reef (full mosaic and depth masked images).

Level 5 classes	%	Area (ha)
Continuous branching coral	2.603	152.429
Continuous "blue tip" coral	8.548	500.527
Continuous "blue tip" coral, or dominant "blue tip" coral with sparse digitate coral	0.074	4.356
Continuous digitate coral	7.131	417.465
Continuous digitate coral or patchy digitate coral and tabulate coral	10.013	586.242
Continuous tabulate coral, continuous digitate coral or patchy digitate coral with tabulate coral)	31.274	1831.08
Continuous tabulate coral, continuous digitate coral, or dominant tabulate coral with sparse digitate coral	0.908	53.159
Continuous tabulate coral, dominant tabulate coral with sparse digitate coral or with sparse massive coral and submassive coral	38.164	2234.49
Continuous tabulate coral, or patchy branching coral, tabulate coral, foliaceous coral, massive and submassive coral)	0.053	3.111
Continuous foliaceous coral	0.003	0.151
Continuous massive coral	0.812	47.553
Dominant tabulate coral with digitate coral, encrusting coral and submassive coral	0	0.013
Patchy digitate coral and tabulate coral	0.416	24.354
<i>Total for coral mosaics</i>	<i>100.00</i>	<i>5854.93</i>

There were 5 854 ha of coral mosaics mapped along the Ningaloo Reef. Single largest coral mosaic was continuous tabulate coral (2 155 ha or 36.7 % of all corals). The majority of the coral classes (66 %) were a mix of dense to continuous tabulate coral, sparse digitate coral, soft coral and sparse submassive and massive corals. Continuous to patchy digitate and tabulate coral made up approximately 10 % of the coral cover, while "blue tip" *Acropora* was approximately 8.5 %. The majority of the hard coral occurred as either very dense (continuous >90 %) cover or as patchy distribution (20-45 %) (Table 10). Proportions of the main benthic components were approximately the same in the study area, nearshore water (up to 500 m offshore) and in combined sanctuary zones (Table 11, Table 12 and Table 13). Some coral assemblages were more commonly found near shore (up to 500 m), for example, class "Dominant soft coral, sparse hard coral and macroalgae with limestone pavement" made up 15 % of the nearshore environment compared to ~10 % in the study area or 8 % in the sanctuary zones. Similarly, percentage cover of the "patchy hard coral with turf or macroalgae-covered dead coral or rubble (hard coral = Continuous "blue tip" coral)" class within the 500 m buffer was 15 % compared to ~9 % for the whole study area or sanctuary zones.

When examining the results for the sanctuary zones it must be remembered that some zones lie well beyond the area covered by this survey as they extend to water beyond the 20 m depth cut-off value. Corals at Ningaloo do occur beyond the 20 m depth as the photic depth extends to over 50m. Bateman sanctuary zone had the largest proportion of hard coral classes, followed by Murat, Mandu and Maud. Bateman had twice the percentage cover coral compared to the whole study area (14 % vs. 8 %), whereas Murat, Mandu and Maud had between 7.6-6.5 % coral cover) (Table 14 and Figure 36). Lakeside sanctuary zone had the least coral cover (0.06 %) (despite a few prominent coral bommies) with majority being sand (92 %). Bundegi, Murat and Tantabiddi sanctuary zones had the largest proportion of macroalgae mosaics while most southern sanctuary zones of Turtles, Gnaraloo and 3-Mile had the largest proportion of limestone pavement within the area mapped in this study (Figure 36).

Maps of all sanctuary zones are shown in Figure 37-Figure 54 for thematic level 2b, presented in the order from north to south, while more detailed maps of subsets of selected sanctuary zones and selected popular swimming and snorkelling areas are shown in Figure 55- Figure 65 and Figure 63-63, for level 4a (see legends for classification levels 2b and 4a in Figure 24). These detailed classification maps reveal different patterns of habitat distribution.

While sand dominated the most popular snorkelling areas at Turquoise Bay, Coral Bay and Gnaraloo, they had quite different coral cover within 500m of the most common entry point to the water. Turquoise Bay had the largest proportion of coral and Gnaraloo the least. Of the three locations, Coral Bay area had the largest proportion of macroalgae mosaics (Figure 66Figure 65).

Table 11. Summary of areas (ha) and percentage of all 46 habitat classes for the whole of Ningaloo Reef (mosaicked and depth masked images), 500 m buffer (along Ningaloo Reef shoreline) and sanctuary zones (summary for all zones).

Habitat classes		Whole reef		500m buffer		Sanctuary zones	
Code	Class label	%	(ha)	%	(ha)	%	(ha)
1	Dominant limestone pavement with sand	5.945	4527.631	7.929	1310.065	5.606	2151.893
2	Sparse macroalgae with sand	0.051	38.967	0.088	14.488	0.058	22.275
3	Dominant hard coral with turf or macroalgae-covered dead coral or rubble (hard coral = Continuous tabulate coral)	0.855	651.505	0.367	60.657	0.992	380.974
4	Dominant hard coral with limestone pavement (hard coral = Dominant tabulate coral with digitate coral, encrusting coral and submassive coral)	0.000	0.013	0.000	0.001	0.000	0.009
5	Dominant hard coral with sand (hard coral = Continuous "blue tip" coral)	0.005	3.935	0.006	1.012	0.005	1.937
6	Sparse hard coral with limestone pavement (hard coral = Patchy digitate coral and tabulate coral)	0.032	24.354	0.078	12.844	0.030	11.557
7	Sparse hard coral and macroalgae with limestone pavement and sand (hard coral = Continuous digitate coral)	0.012	9.054	0.023	3.720	0.008	3.200
8	Sparse hard coral, macroalgae and turf algae with limestone pavement (hard coral = Continuous digitate coral)	0.161	122.302	0.129	21.377	0.132	50.841
9	Sparse macroalgae with limestone pavement	12.899	9824.228	18.593	3071.910	12.574	4826.701
10	Sparse macroalgae with limestone pavement and sand	6.032	4594.521	4.130	682.285	7.134	2738.376
11	Sparse turf algae with limestone pavement	4.928	3753.682	2.355	389.053	5.714	2193.296
12	Dominant macroalgae with limestone pavement	0.811	617.393	1.655	273.394	0.800	307.126
13	Dominant macroalgae with rubble	0.053	40.252	0.085	14.035	0.044	16.758
14	Dominant macroalgae with sand	13.103	9979.345	12.969	2142.612	13.043	5006.782
15	Patchy hard coral with turf or macroalgae-covered dead coral or rubble (hard coral = Continuous digitate coral)	0.138	105.104	0.101	16.672	0.145	55.809
16	Patchy hard coral with sand (hard coral = Continuous tabulate coral)	0.000	0.123	0.000	0.025	0.000	0.059
17	Patchy limestone pavement, rubble and sand	3.431	2613.165	4.323	714.226	3.869	1485.355
18	Patchy hard coral with turf or macroalgae-covered dead coral or rubble (hard coral = Continuous massive coral)	1.411	1074.361	0.770	127.178	1.716	658.702
19	Patchy limestone pavement with sand	8.687	6616.480	10.293	1700.535	6.550	2514.255
20	Patchy hard coral with turf or macroalgae-covered dead coral or rubble and sand (hard coral = Dominant "blue tip" coral with sparse digitate coral)	0.006	4.296	0.004	0.650	0.006	2.152
21	Patchy hard coral with turf or macroalgae-covered dead coral or rubble and sand (hard coral = Continuous "blue tip" coral)	0.000	0.060	0.000	0.022	0.000	0.022
22	Patchy hard coral with limestone pavement (hard coral = Dominant tabulate coral with sparse digitate coral)	0.000	0.243	0.001	0.107	0.000	0.110
23	Patchy hard coral with limestone pavement (hard coral = Continuous digitate coral)	0.069	52.907	0.135	22.284	0.063	24.200
24	Patchy hard coral with limestone pavement (hard coral = Continuous tabulate coral)	0.000	0.009	0.000	0.002	0.000	0.002
25	Patchy hard coral with sand (hard coral = Patchy branching coral, tabulate coral, foliaceous coral, massive coral and submassive coral)	0.004	2.988	0.002	0.274	0.003	1.235

26	Patchy hard coral with turf or macroalgae-covered dead coral or rubble (hard coral = Patchy digitate coral and tabulate coral)	0.000	0.116	0.000	0.007	0.000	0.048
27	Patchy hard coral with turf or macroalgae-covered dead coral or rubble (hard coral = Continuous "blue tip" coral)	0.652	496.282	0.805	132.920	0.639	245.288
28	Patchy hard coral with turf or macroalgae-covered dead coral or rubble (hard coral = Continuous massive coral)	0.000	0.077	0.000	0.011	0.000	0.032
29	Continuous sand	19.489	14843.565	17.590	2906.178	19.667	7549.627
30	Patchy macroalgae with limestone pavement	0.030	22.471	0.050	8.211	0.029	11.268
31	Patchy macroalgae with limestone pavement and sand	10.461	7967.336	8.602	1421.263	10.074	3867.176
32	Patchy macroalgae with sand	2.606	1984.547	4.199	693.708	2.714	1041.869
33	Continuous limestone pavement light	0.000	0.252	0.000	0.051	0.000	0.135
34	Continuous limestone pavement dark	3.517	2678.458	1.204	198.901	3.853	1479.192
35	Continuous soft coral	0.007	4.961	0.007	1.126	0.006	2.477
36	Dominant soft coral, sparse hard coral and macroalgae with limestone pavement	0.769	585.795	0.824	136.156	0.675	259.217
37	Continuous hard coral (hard coral = Continuous "blue tip" coral)	0.000	0.310	0.000	0.036	0.001	0.197
38	Continuous hard coral (hard coral = Continuous foliaceous coral)	0.000	0.151	0.000	0.012	0.000	0.072
39	Dominant soft coral, sparse hard coral with limestone pavement	0.001	0.447	0.000	0.064	0.001	0.211
40	Continuous hard coral (hard coral = Dominant tabulate coral with sparse digitate coral)	0.104	79.288	0.041	6.828	0.125	48.131
41	Continuous hard coral (hard coral = Dominant tabulate coral with sparse massive coral and submassive coral)	0.000	0.180	0.000	0.038	0.000	0.087
42	Continuous hard coral (hard coral = Continuous branching coral)	0.200	152.429	0.104	17.231	0.174	66.891
43	Continuous hard coral (hard coral = Continuous digitate coral)	0.376	286.109	0.250	41.369	0.389	149.432
44	Continuous hard coral (hard coral = Continuous tabulate coral)	2.829	2155.022	1.523	251.609	2.938	1128.008
45	Continuous hard coral (hard coral = Continuous massive coral)	0.062	47.476	0.126	20.803	0.045	17.317
46	Continuous macroalgae	0.264	201.367	0.639	105.622	0.175	67.153
	<i>Total</i>	<i>100.00</i>	<i>76163.554</i>	<i>100.000</i>	<i>16521.575</i>	<i>100.000</i>	<i>38387.453</i>

Table 12. Summary of areas of four selected combined habitat classes for the whole Ningaloo Reef (depth masked images), 500 m buffer (along shoreline) and sanctuary zones (summary for all zones).

Combined habitat classes	Whole reef		500m buffer		Sanctuary zones	
	%	[ha]	%	[ha]	%	[ha]
Continuous hard coral	7.693	5 859.897	5.296	875.035	8.093	3 108.217
Continuous sand	19.489	1 4843.57	17.590	2 906.178	19.667	7 549.627
Dominant to continuous macroalgae with limestone pavement, rubble or sand	51.238	3 9024.11	53.365	8 816.581	52.359	20 098.780
Continuous limestone pavement	3.517	2 678.710	1.204	198.952	3.854	1 479.327

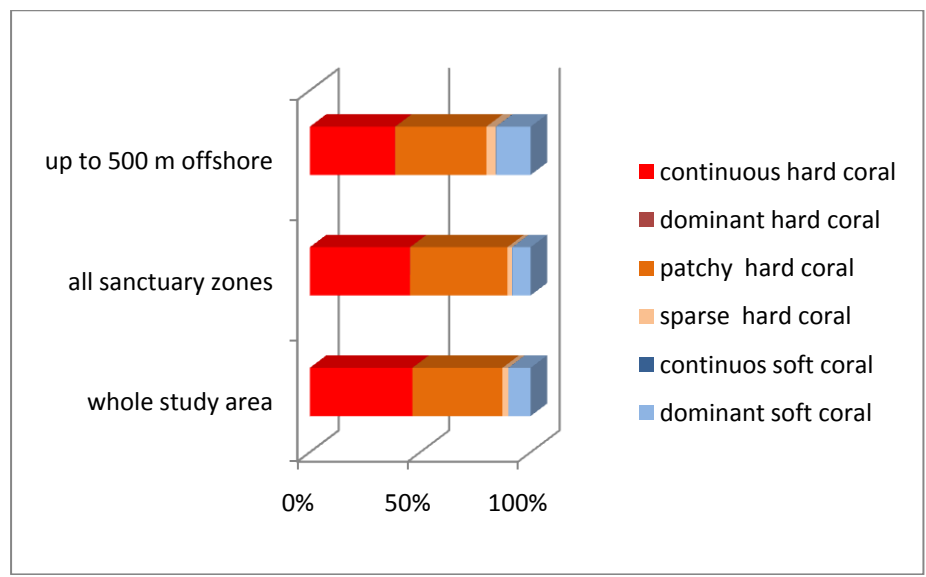


Figure 35. Coral-dominated classes (percentage) summarised for the whole Ningaloo Reef (0-20 m depth), within the 500 m buffer (along full length of the shoreline) and in sanctuary zones (summary for all zones 0-20 m depth).

Table 13. Summary of areas for coral mosaics within the whole study area, up to 500m from the shore and in sanctuary areas mapped for the Ningaloo Reef (<20 , depth) sorted by area and proportion covered from largest to smallest.

Coral mosaic	Area (ha)			Area (%)		
	whole area	500m buffer	sanctuary zones	whole area	500m buffer	sanctuary zones
Continuous hard coral (hard coral = Continuous tabulate coral)	2155.022	251.609	1128.008	36.7488	28.7328	36.2661
Patchy hard coral with turf or macroalgae-covered dead coral or rubble (hard coral = Continuous tabulate coral)	1074.361	127.178	658.702	18.321	14.5232	21.1776
Dominant hard coral with turf or macroalgae-covered dead coral or rubble (hard coral = Continuous tabulate coral)	651.505	60.657	380.974	11.1099	6.92680	12.2485
Dominant soft coral, sparse hard coral and macroalgae with limestone pavement	585.795	136.156	259.217	9.98935	15.5485	8.33396
Patchy hard coral with turf or macroalgae-covered dead coral or rubble (hard coral = Continuous "blue tip" coral)	496.282	132.92	245.288	8.46292	15.1789	7.88614
Continuous hard coral (hard coral = Continuous digitate coral)	286.109	41.369	149.432	4.87892	4.72418	4.80432
Continuous hard coral (hard coral = Continuous branching coral)	152.429	17.231	66.891	2.59932	1.96771	2.15058
Sparse hard coral, macroalgae and turf algae with limestone pavement (hard coral = Continuous digitate coral)	122.302	21.377	50.841	2.08557	2.44117	1.63456
Patchy hard coral with turf or macroalgae-covered dead coral or rubble (hard coral = Continuous digitate coral)	105.104	16.672	55.809	1.79230	1.90388	1.79429
Continuous hard coral (hard coral = Dominant tabulate coral with sparse digitate coral)	79.288	6.828	48.131	1.35207	0.77973	1.54744
Patchy hard coral with limestone pavement (hard coral = Continuous digitate coral)	52.907	22.284	24.2	0.90220	2.54475	0.77804
Continuous hard coral (hard coral = Continuous massive coral)	47.476	20.803	17.317	0.80959	2.37562	0.55675
Sparse hard coral with limestone pavement (hard coral = Patchy digitate coral and tabulate coral)	24.354	12.844	11.557	0.41530	1.46673	0.37156
Sparse hard coral and macroalgae with limestone pavement and sand (hard coral = Continuous digitate coral)	9.054	3.72	3.2	0.15440	0.42481	0.10288
Continuous soft coral	4.961	1.126	2.477	0.08460	0.12858	0.07964
Patchy hard coral with turf or macroalgae-covered dead coral or rubble and sand (hard coral = Dominant "blue tip" coral with sparse digitate coral)	4.296	0.65	2.152	0.07327	0.07422	0.06919
Patchy hard coral with turf or macroalgae-covered dead coral or rubble and sand (hard coral = Dominant "blue tip" coral with sparse digitate coral)	4.296	0.65	2.152	0.07326	0.07422	0.06919
Dominant hard coral with sand (hard coral = Continuous "blue tip" coral)	3.935	1.012	1.937	0.06710	0.11556	0.06228
Patchy hard coral with sand (hard coral = Patchy branching coral, tabulate coral, foliaceous coral, massive coral and submassive coral)	2.988	0.274	1.235	0.05095	0.03129	0.03971
Dominant soft coral, sparse hard coral with limestone pavement	0.447	0.064	0.211	0.00762	0.00731	0.00678
Continuous hard coral (hard coral = Continuous "blue tip" coral)	0.31	0.036	0.197	0.00529	0.00411	0.00633

Patchy hard coral with limestone pavement (hard coral = Dominant tabulate coral with sparse digitate coral)	0.243	0.107	0.11	0.00414	0.01222	0.00354
Continuous hard coral (hard coral = Dominant tabulate coral with sparse massive coral and submassive coral)	0.18	0.038	0.087	0.00307	0.00434	0.00280
Continuous hard coral (hard coral = Continuous foliaceous coral)	0.151	0.012	0.072	0.00258	0.00137	0.00232
Patchy hard coral with sand (hard coral = Continuous tabulate coral)	0.123	0.025	0.059	0.00210	0.00286	0.00190
Patchy hard coral with turf or macroalgae-covered dead coral or rubble (hard coral = Patchy digitate coral and tabulate coral)	0.116	0.007	0.048	0.00200	0.00080	0.00154
Patchy hard coral with turf or macroalgae-covered dead coral or rubble (hard coral = Continuous massive coral)	0.077	0.011	0.032	0.00131	0.00126	0.00103
Patchy hard coral with turf or macroalgae-covered dead coral or rubble and sand (hard coral = Continuous "blue tip" coral)	0.06	0.022	0.022	0.00102	0.00251	0.00071
Dominant hard coral with limestone pavement (hard coral = Dominant tabulate coral with digitate coral, encrusting coral and submassive coral)	0.013	0.001	0.009	0.00022	0.00011	0.00029
Patchy hard coral with limestone pavement (hard coral = Continuous tabulate coral)	0.009	0.002	0.002	0.00015	0.00023	6.43E-05

Table 14. Summary of areas of the four main combined habitat classes for individual sanctuary zones at Ningaloo Reef to depths of 20 m.

Sanctuary zones	Continuous hard coral classes		Continuous sand class		Dominant to continuous macroalgae with limestone pavement, rubble or sand classes		Continuous limestone pavement classes	
	%	ha	%	ha	%	ha	%	ha
Bundegi	5.623	17.499	0.007	0.021	36.286	112.918	0.027	0.085
Murat	7.567	5.272	0.005	0.004	32.899	22.923	0.199	0.138
Lighthouse Bay	2.541	11.113	0.261	1.139	17.238	75.383	5.626	24.602
Jurabi	1.12	7.526	16.089	108.121	12.166	81.759	0.629	4.23
Tantabiddi	2.351	1.177	9.229	4.621	29.408	14.723	0.245	0.123
Mangrove Bay	2.705	25.923	49.816	477.362	7.06	67.653	0.039	0.374
Lakeside	0.06	0.005	92.41	7.606	0.268	0.022	0	0
Mandu	7.484	91.951	12.106	148.742	21.148	259.83	2.602	31.968
Osprey	4.523	125.532	10.724	297.597	19.682	546.192	1.249	34.66
Winderabandi	3.811	163.615	14.645	628.647	15.272	655.587	1.78	76.414
Cloates	2.76	555.123	25.023	5033.786	11.089	2230.729	4.142	833.26
Bateman	14.391	74.606	1.042	5.401	23.664	122.68	13.764	71.357
Maud	6.564	131.157	19.133	382.281	22.606	451.689	2.188	43.72
Pelican	5.099	122.155	16.465	394.476	17.379	416.384	3.74	89.597
Cape Farquar	3.161	66.576	2.307	48.597	14.16	298.243	9.486	199.783
Gnaraloo	1.79	3.137	2.294	4.022	7.063	12.381	15.596	27.338
3 Mile	3.31	3.225	6.212	6.054	10.045	9.789	13.243	12.905
Turtles	2.573	4.466	1.695	2.941	9.086	15.771	17.038	29.574

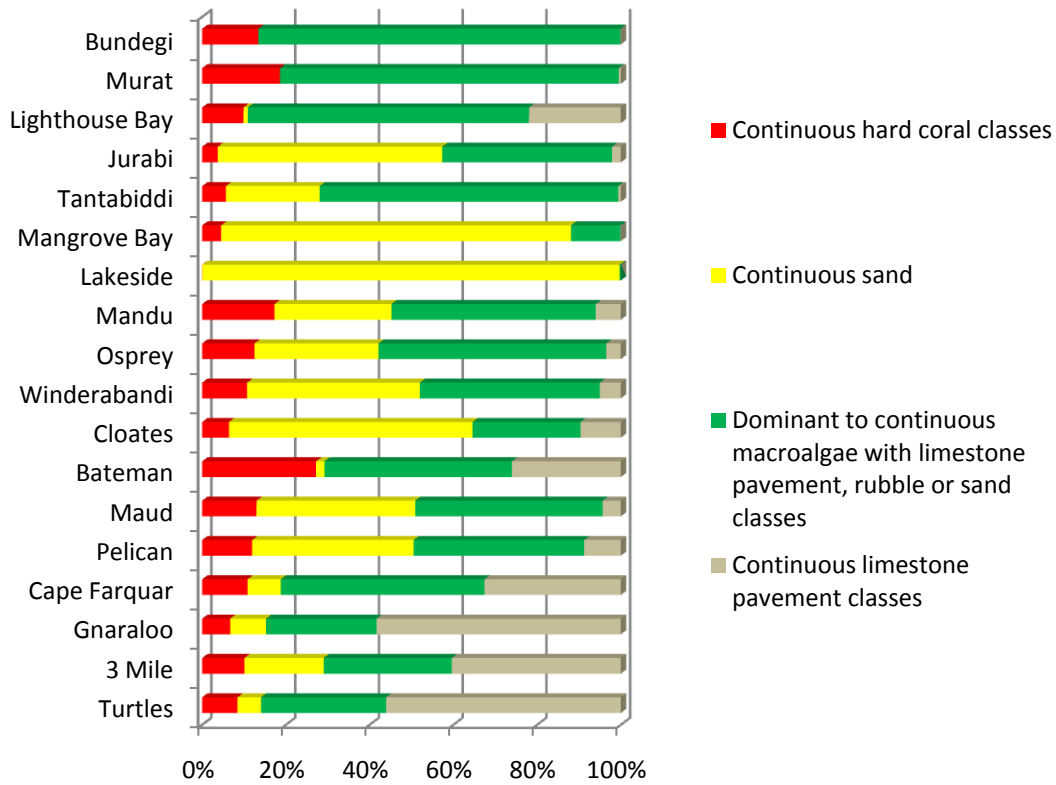


Figure 36. Summary of main benthic mosaics for all mapped sanctuary areas from north to south along the Ningaloo Reef coast.

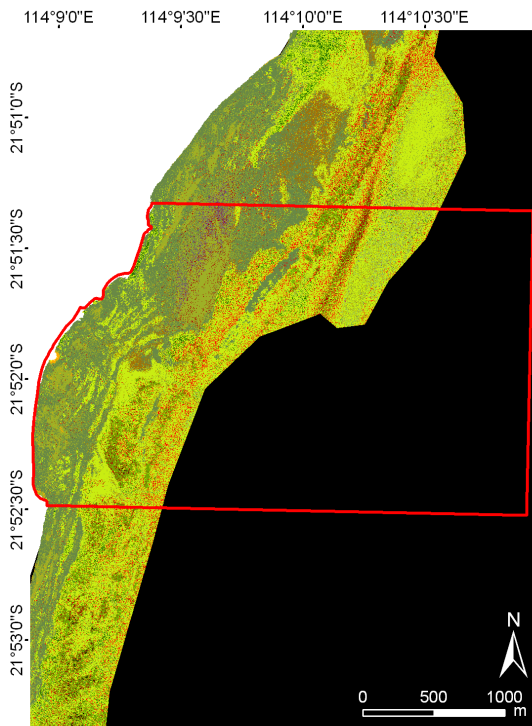


Figure 37. Benthic habitats for Bundegi sanctuary zone at classification level 2b.

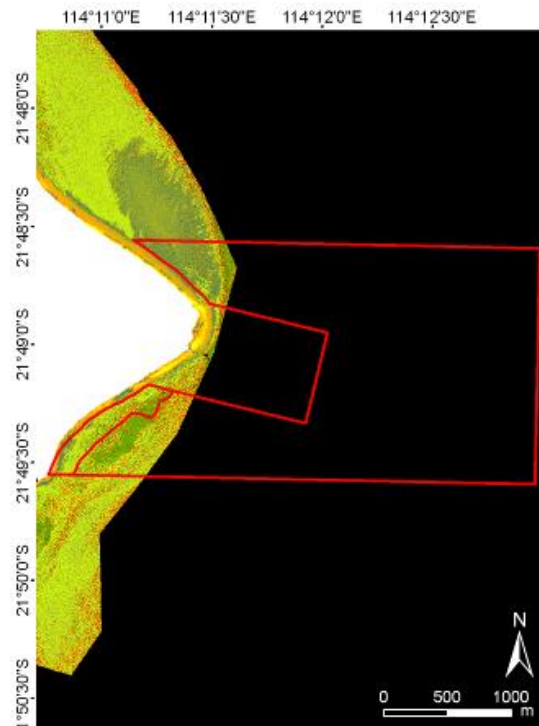


Figure 38. Benthic habitats for Murat sanctuary zone at classification level 2b.

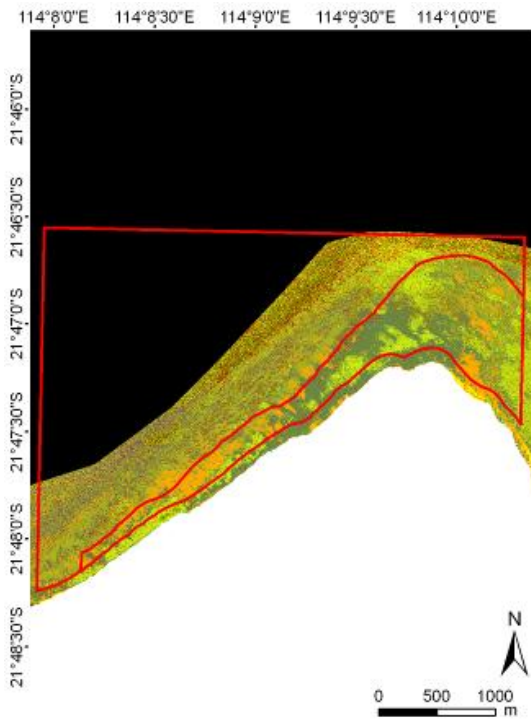


Figure 39. Benthic habitats for Lighthouse sanctuary zone at classification level 2b.

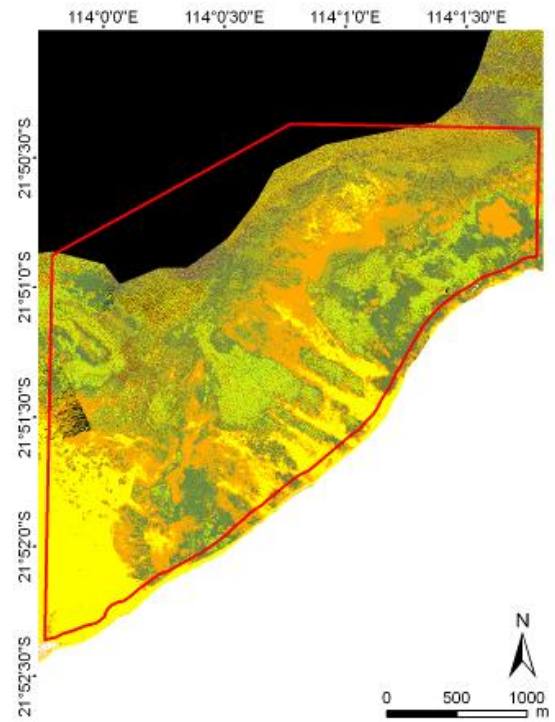


Figure 40. Benthic habitats for Jurabi sanctuary zone at classification level 2b.

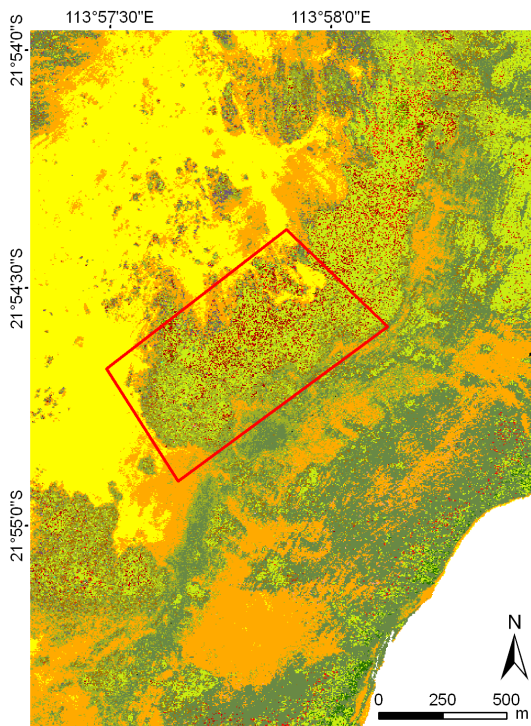


Figure 41. Benthic habitats for Tantabiddi sanctuary zone at classification level 2b.

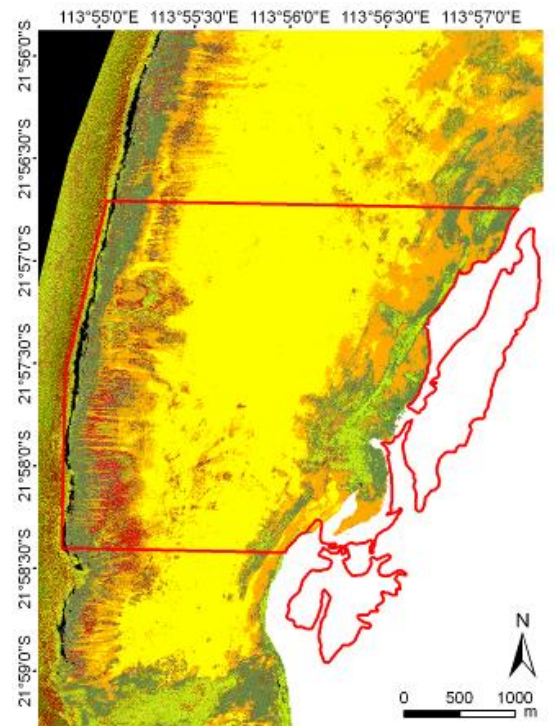


Figure 42. Benthic habitats for Mangrove sanctuary zone at classification level 2b.

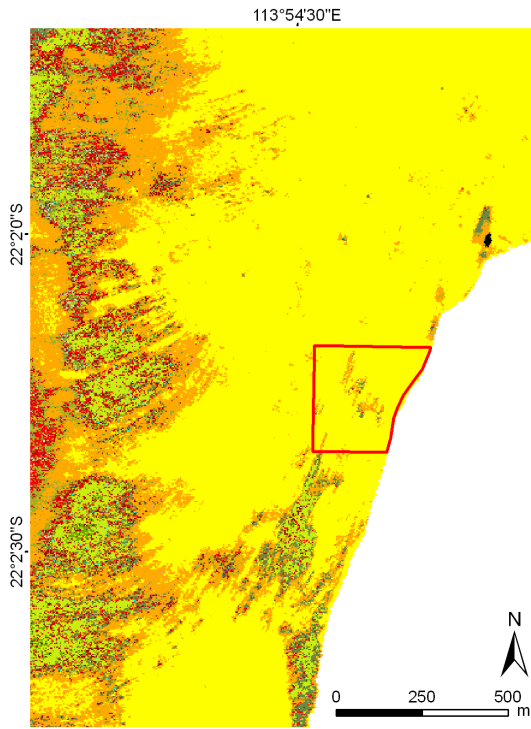


Figure 43. Benthic habitats for Lakeside sanctuary zone at classification level 2b.

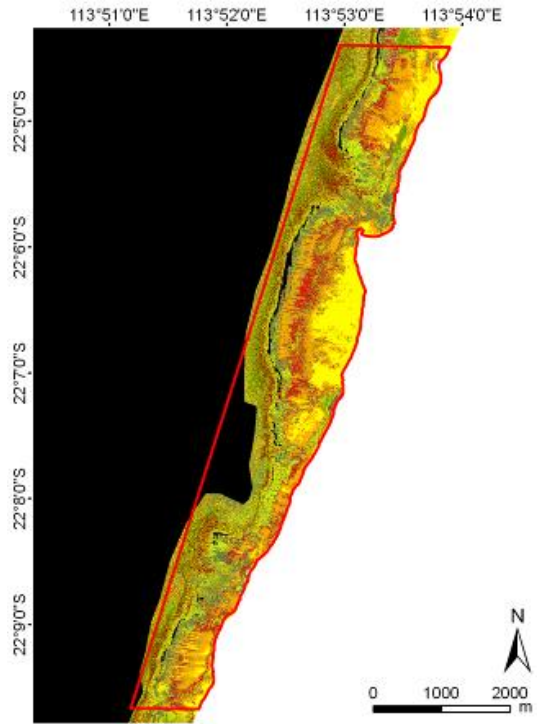


Figure 44. Benthic habitats for Mandu sanctuary zone at classification level 2b.

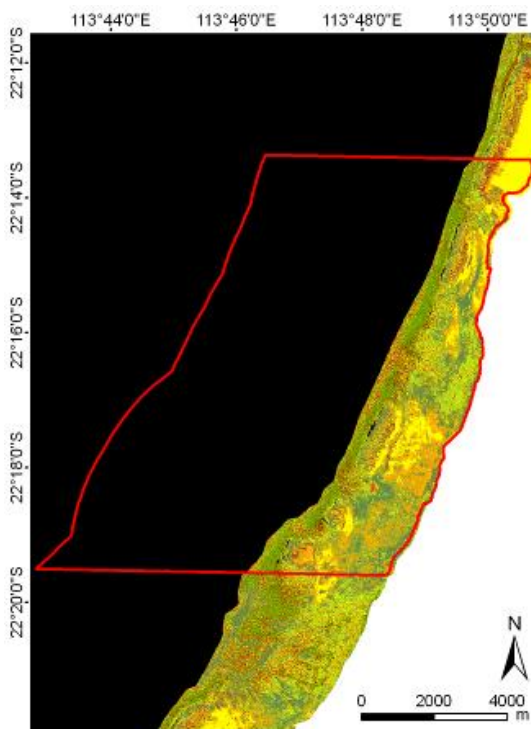


Figure 45. Benthic habitats for Osprey sanctuary zone at classification level 2b.

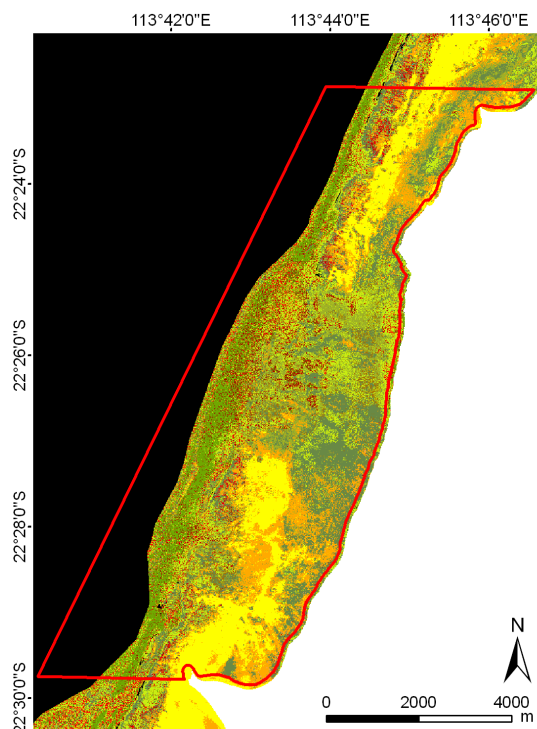


Figure 46. Benthic habitats for Winderabandi sanctuary zone at classification level 2b.

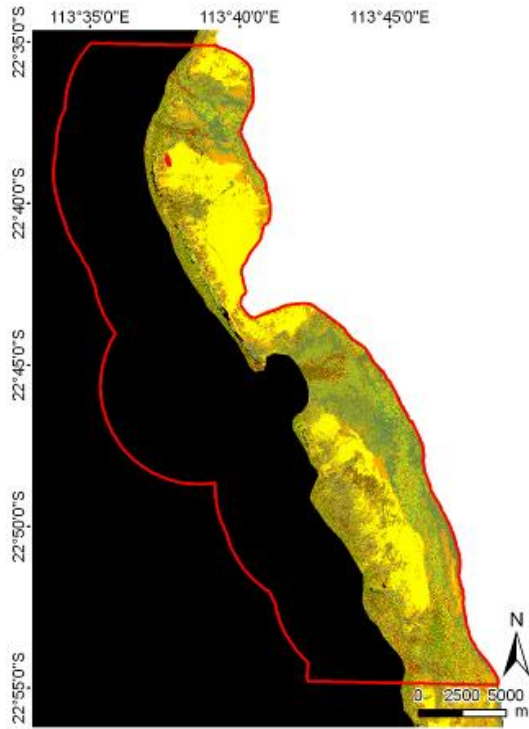


Figure 47. Benthic habitats for Cloates sanctuary zone at classification level 2b.

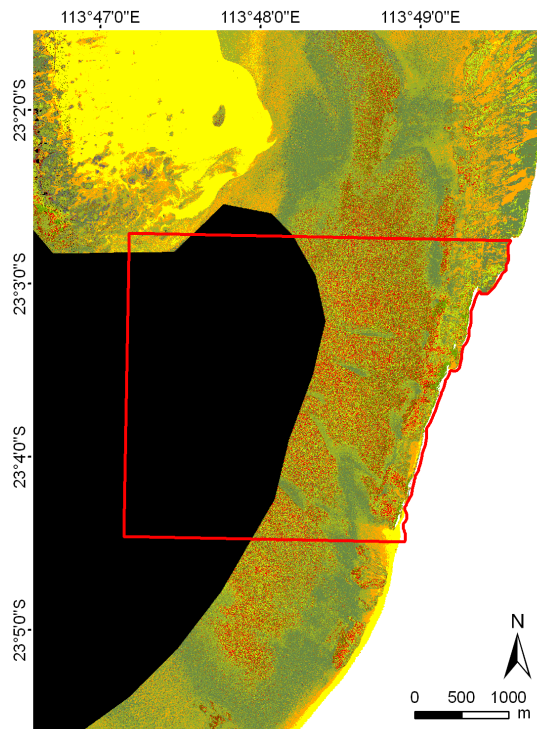


Figure 48. Benthic habitats for Bateman sanctuary zone at classification level 2b.

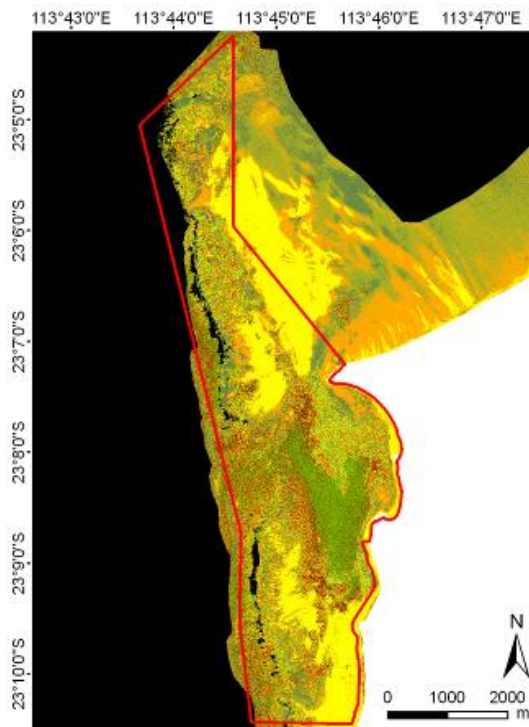


Figure 49. Benthic habitats for Maud sanctuary zone at classification level 2b.

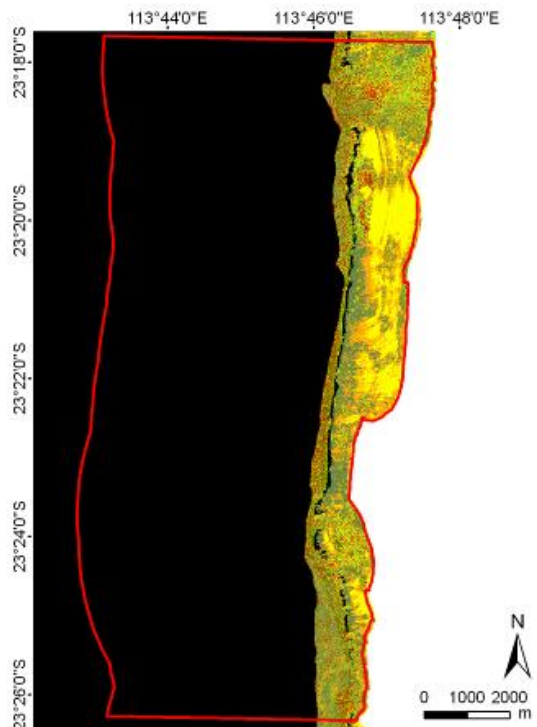


Figure 50. Benthic habitats for Pelican sanctuary zone at classification level 2b.

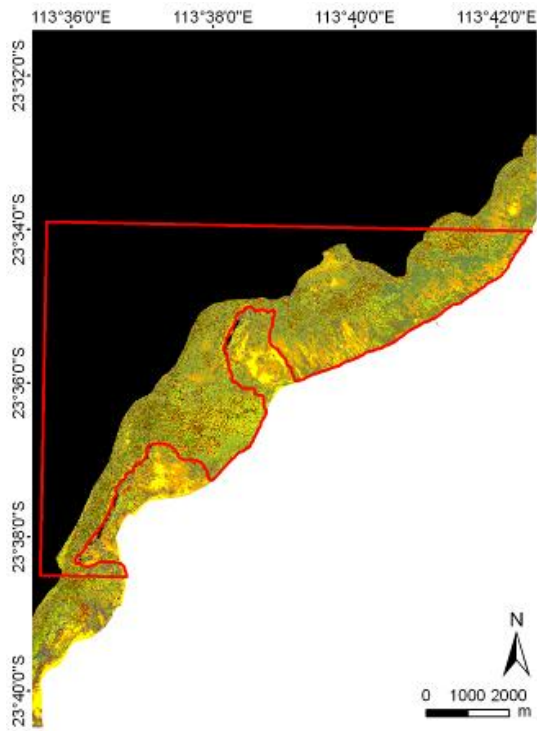


Figure 51. Benthic habitats for Cape Farquhar sanctuary zone at classification level 2b.

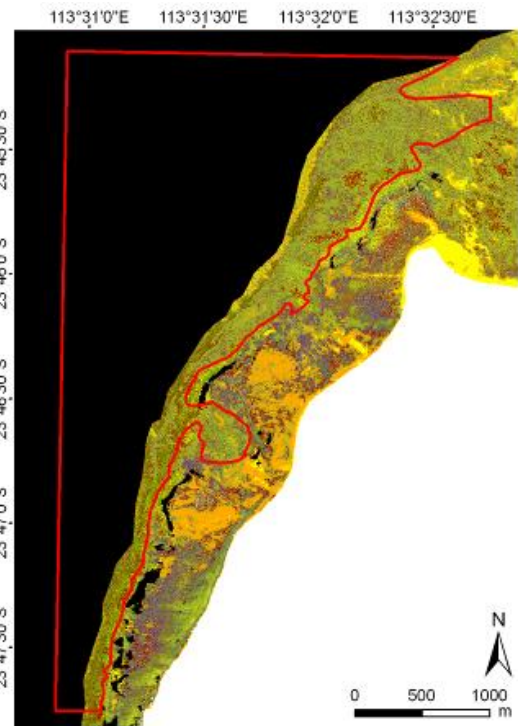


Figure 52. Benthic habitats for Gnaraloo sanctuary zone at classification level 2b.

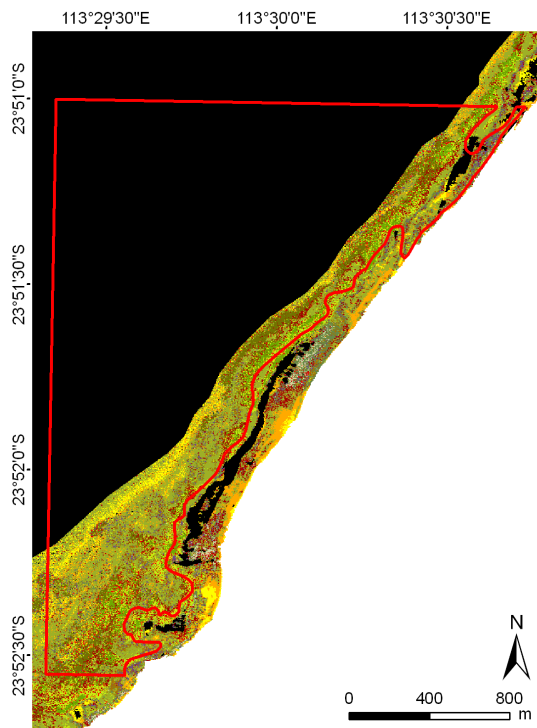


Figure 53. Benthic habitats for 3 Mile sanctuary zone at classification level 2b.

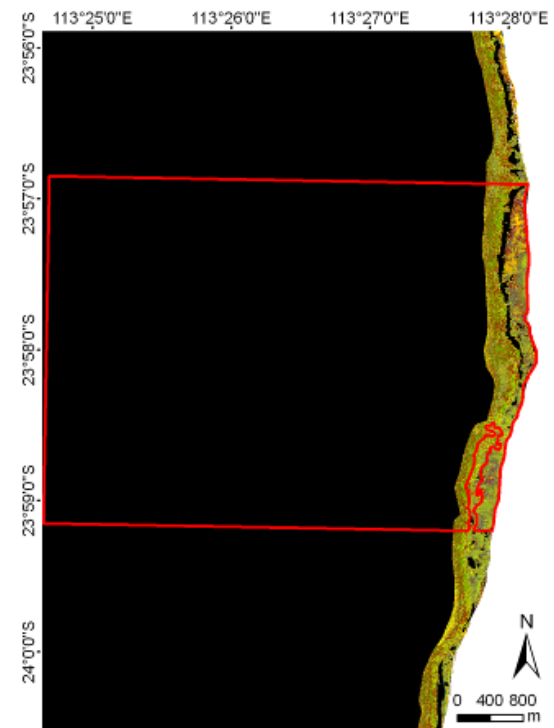


Figure 54. Benthic habitats for Turtles sanctuary zone at classification level 2b.

Detailed habitat maps for sanctuary zones

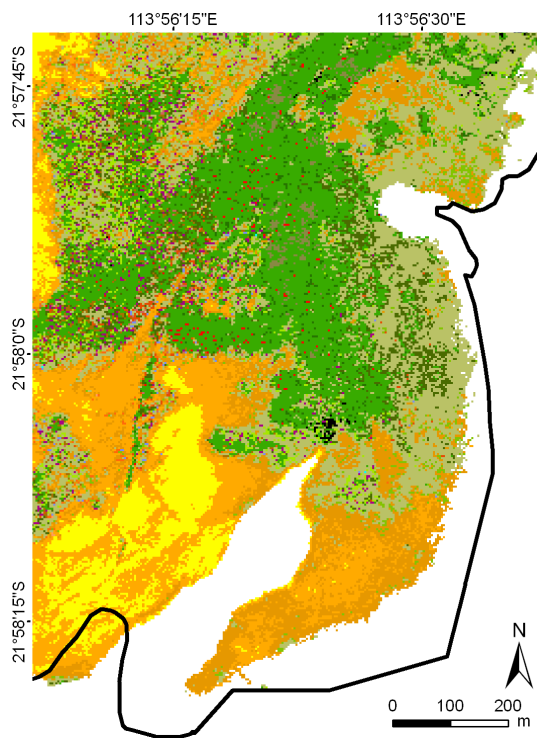


Figure 55. Subset of Mangrove Bay sanctuary zone at classification level 4a.

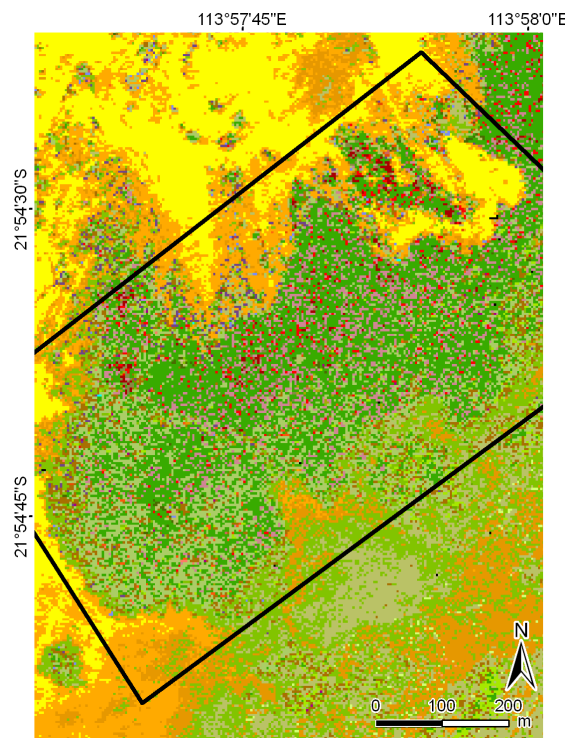


Figure 56. Subset of sanctuary zone Tantabiddi at classification level 4a.

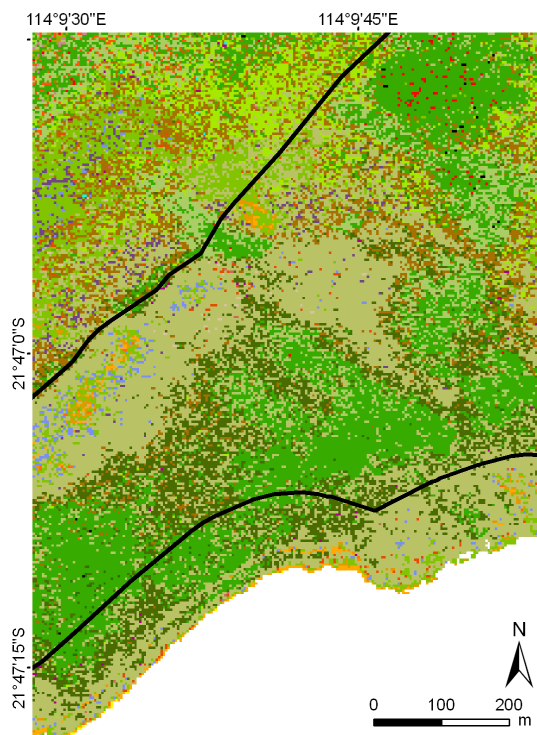


Figure 57. Subset of sanctuary zone at Lighthouse Bay at classification level 4a.

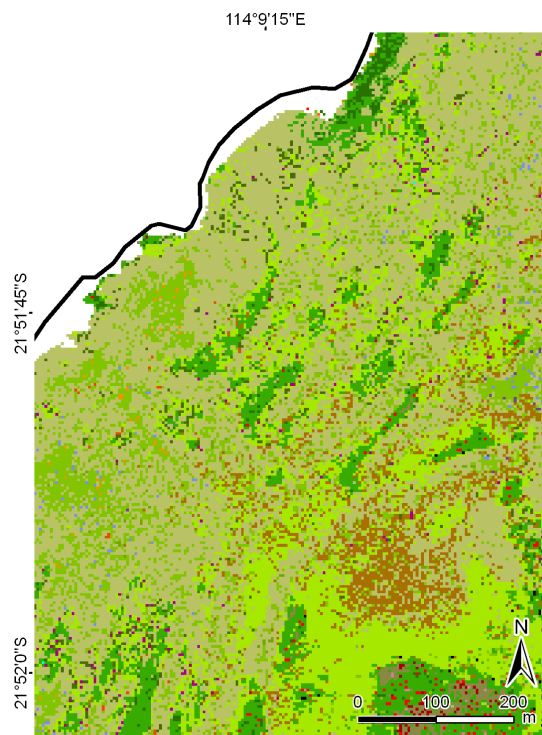


Figure 58. Subset of Bundegi sanctuary zone at classification level 4a.

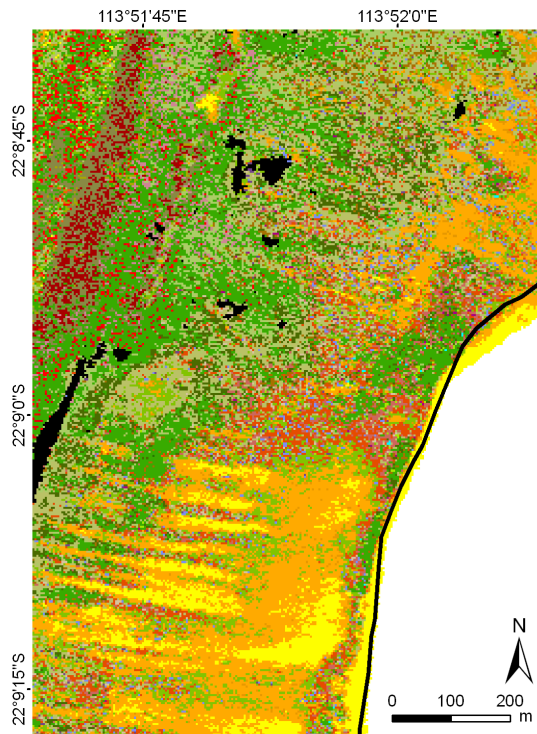


Figure 59. Subset of Mandu sanctuary zone at classification level 4a.

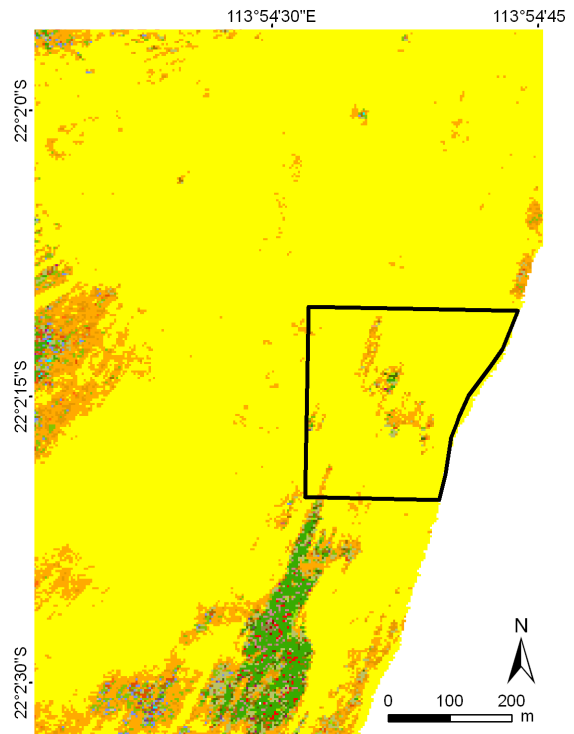


Figure 60. Subset of Lakeside sanctuary zone at classification level 4a.

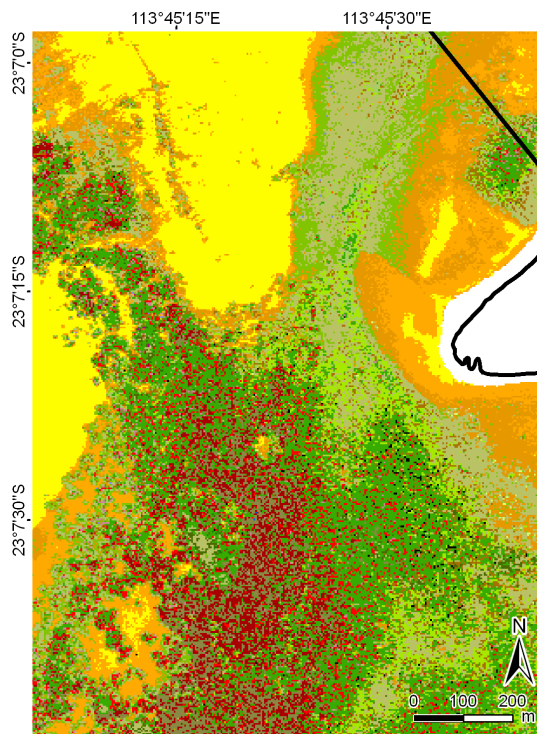


Figure 61. Subset of Maud sanctuary zone at classification level 4a.

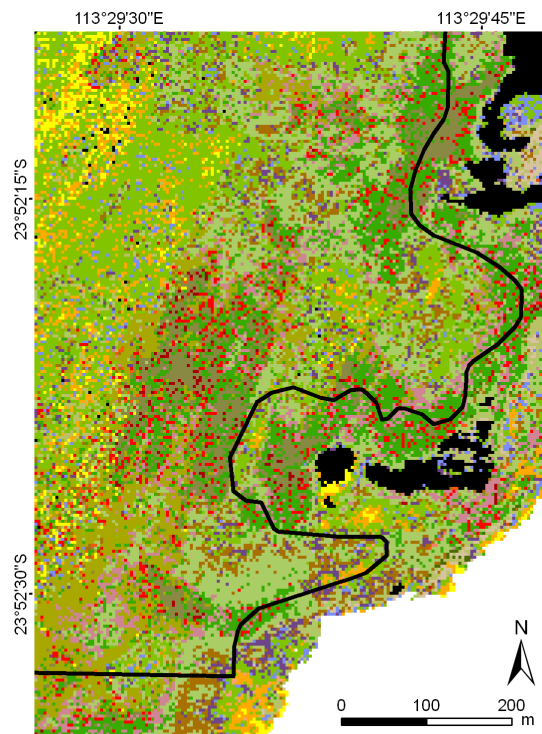


Figure 62. Subset of 3 Mile sanctuary zone at classification level 4a.

Detailed habitat maps for popular snorkelling areas

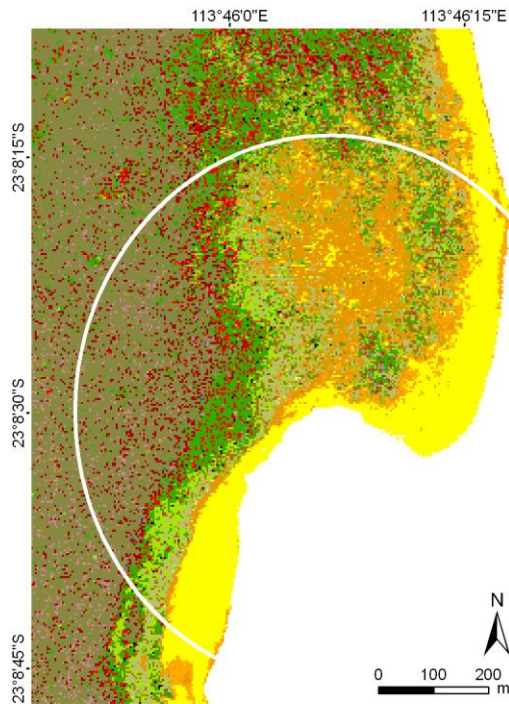


Figure 63a. Habitat map for snorkelling area in Coral Bay at classification level 4a. Buffer of 500m is shown in white.

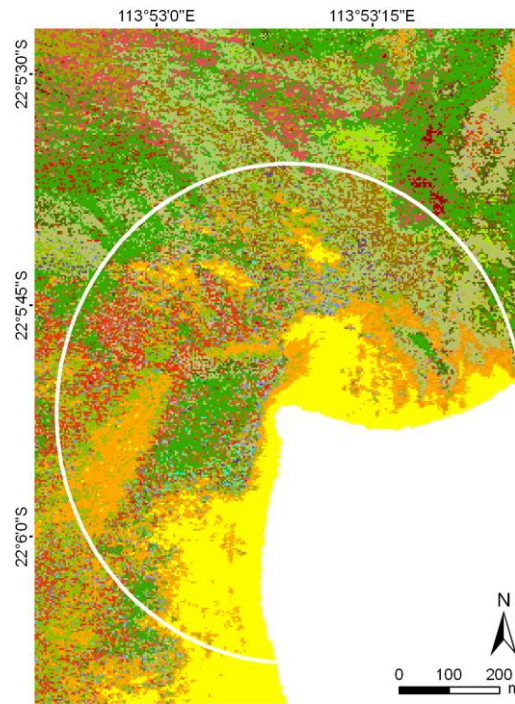


Figure 64. Habitat map for snorkelling area in Turquoise Bay at classification level 4a. Buffer of 500m is shown in white.

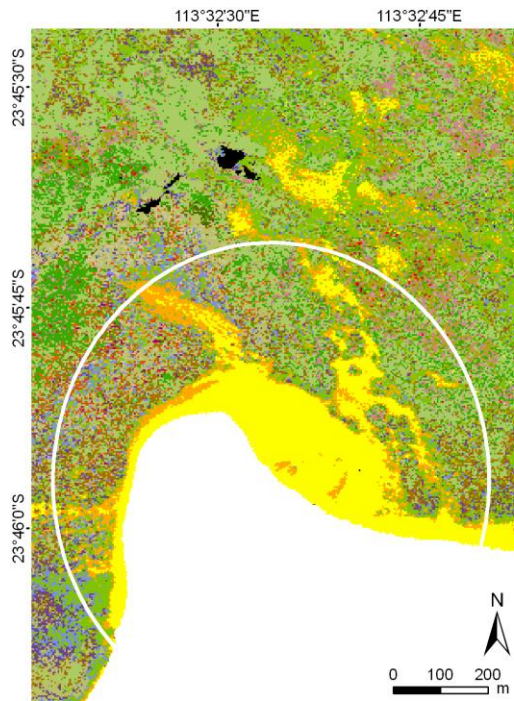


Figure 65. Habitat map for Gnarraloo snorkelling area at classification level 4a. Buffer of 500m is shown in white.

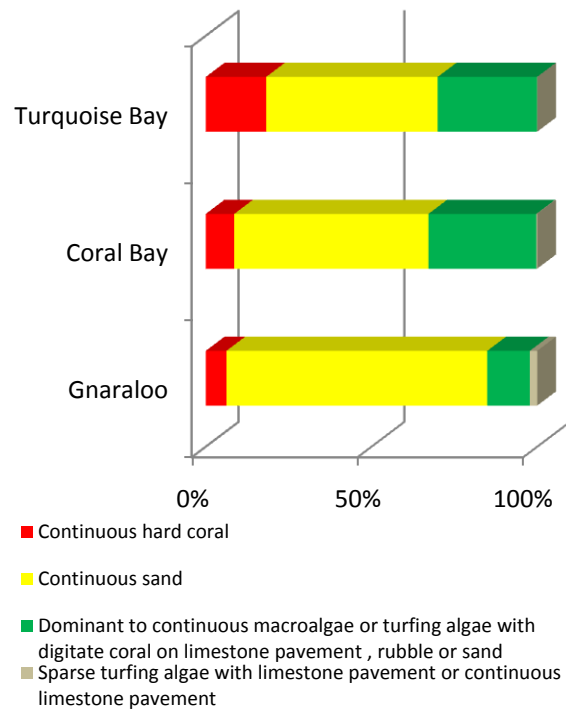


Figure 66. Summary of habitat classes for three popular snorkelling areas at Ningaloo up to 500 m offshore.

2.3.9 Validation results

The overall accuracy using the 10 m radius and fuzzy logic approach was calculated at 83.81 % for level 2a, 70.48 % for level 4a (higher number of fuzzy classes) and 63.81 % for level 4a (lower number of fuzzy classes).

Validation performed for level 4a showed, as expected, that the higher degree of fuzziness resulted in a higher overall accuracy than the lower degree of fuzziness, with the highest results for level 2a. The classes considered as acceptable for a correct accuracy are presented in Table 15.

Table 15. Confusion matrix of accuracy assessment for level 4a (high number of fuzzy classes). The upper table shows the validation points, while the lower table shows the percentages. The value in the bottom right cell of each table is the sum of the diagonal.

		Validation classes (1-46)													
		1	3	4	5	7	12	16	20	29	35	37	40	42	Σ
Classified image (1-46)	1	38	0	0	0	0	0	0	0	0	0	0	0	0	38
	3	4	2	0	0	0	1	0	0	0	0	0	0	0	7
	4	6	0	4	0	0	0	0	0	0	0	0	0	0	10
	5	1	0	0	1	0	0	0	0	0	0	0	0	0	2
	7	2	0	0	0	3	0	0	0	0	0	0	0	0	5
	12	1	0	0	0	0	8	0	0	0	0	0	0	0	9
	16	2	0	0	0	0	2	0	0	0	0	0	0	0	4
	20	1	0	0	0	0	2	0	4	0	0	0	0	0	7
	29	0	0	0	0	0	0	0	0	4	0	0	0	0	4
	35	1	0	0	0	0	0	0	0	0	6	0	0	0	7
	37	0	0	0	0	0	2	0	0	0	0	0	0	0	2
	40	1	0	0	0	0	1	0	0	0	0	0	4	0	6
	42	4	0	0	0	0	0	0	0	0	0	0	0	0	4
	Σ		61	2	4	1	3	16	0	4	4	6	0	4	0

		Validation classes (1-46)													
		1	3	4	5	7	12	16	20	29	35	37	40	42	Σ
Classified image (1-46)	1	36.19	0.00	0.00	0.00	0.00	0.00	0.00	0.00	0.00	0.00	0.00	0.00	0.00	36.19
	3	3.81	1.90	0.00	0.00	0.00	0.95	0.00	0.00	0.00	0.00	0.00	0.00	0.00	6.67
	4	5.71	0.00	3.81	0.00	0.00	0.00	0.00	0.00	0.00	0.00	0.00	0.00	0.00	9.52
	5	0.95	0.00	0.00	0.95	0.00	0.00	0.00	0.00	0.00	0.00	0.00	0.00	0.00	1.90
	7	1.90	0.00	0.00	0.00	2.86	0.00	0.00	0.00	0.00	0.00	0.00	0.00	0.00	4.76
	12	0.95	0.00	0.00	0.00	0.00	7.62	0.00	0.00	0.00	0.00	0.00	0.00	0.00	8.57
	16	1.90	0.00	0.00	0.00	0.00	1.90	0.00	0.00	0.00	0.00	0.00	0.00	0.00	3.81
	20	0.95	0.00	0.00	0.00	0.00	1.90	0.00	3.81	0.00	0.00	0.00	0.00	0.00	6.67
	29	0.00	0.00	0.00	0.00	0.00	0.00	0.00	0.00	3.81	0.00	0.00	0.00	0.00	3.81
	35	0.95	0.00	0.00	0.00	0.00	0.00	0.00	0.00	0.00	5.71	0.00	0.00	0.00	6.67
	37	0.00	0.00	0.00	0.00	0.00	1.90	0.00	0.00	0.00	0.00	0.00	0.00	0.00	1.90
	40	0.95	0.00	0.00	0.00	0.00	0.95	0.00	0.00	0.00	0.00	0.00	3.81	0.00	5.71
	42	3.81	0.00	0.00	0.00	0.00	0.00	0.00	0.00	0.00	0.00	0.00	0.00	0.00	3.81
	Σ		58.10	1.90	3.81	0.95	2.86	15.24	0.00	3.81	3.81	5.71	0.00	3.81	0.00

2.3.10 Topographic classification

Combination of bathymetry and its simple derivatives of slope and aspect in an object-oriented classification resulted in a map combining all three variables. Results for mapping of these topographic features, the overlay of topographic classification over single habitat classes and the geomorphic classification are illustrated here using selected study areas, together with the spatial statistics of the topographic and geomorphic maps per study site and class (Figure 67).

Topographic classification showed clear patterns corresponding to shallow flat lagoons, steep slopes of channels and undulating surfaces of sandy and limestone bottom types (Figure 69 - Figure 73). These areas were quite different to each other (width of the lagoon, range of depths, slopes and aspect) and it could be used to test applicability of a single rule set for object-oriented classification.

The wide channel between the North and South Muiron Islands was shown particularly clearly, by the aspect and depth data and the final topographic classification (Figure 69). Evident were also extensive (nearly 300 m wide) east and west facing slopes in the shallower waters as well as secondary channels in the south eastern part of the image (north facing). West facing, gentle slopes in the shallow water accounted for 17.5 % of the area and west facing, gentle slopes in the deep water, another 14 %. Third and fourth largest areas were in east and south facing flat and shallow settings (12 % each) (Figure 67).

The Turquoise Bay example highlighted a mosaic of surfaces facing a range of directions, all in shallow water, with distinct west facing slopes parallel to the shore north of the swimming area. This area was characterised by a flat, and very shallow lagoon as well as a reef channel known to have strong currents, but was found to be surprisingly shallow out beyond the reef crest (less than 5 m depth) and then dropping off steeply along the forereef approximately 200 m seawards of the reef crest. Over 23 % of that area was in west facing, flat and shallow environment. The second largest topographic setting (22 %) was facing east, flat and shallow. The third largest area was characterised by south facing slopes, flat and shallow settings (Figure 67 and Figure 70).

Bateman Bay showed drowned drainage features, particularly well described in the aspect image, while depth data showed extensive drowned sections of the bay, with the northern extent having a characteristic southern aspect in the topographic features map. Bateman Bay had extensive west facing, quite flat, deep (18 %) and shallow (17 %) areas as well as south facing flat deep (15 %) and shallow areas (11 %). Of all study areas, Bateman Bay had the largest proportion of flat surfaces, both in the deep and shallow waters (Figure 67 and Figure 71).

The Point Maud area was characterised by small, circular features in the southern section due to the presence of bommies and relatively heterogeneous reef structure, while the northern section was more homogeneous and comprised of fairly flat, sandy plains and slopes. The Point Maud area had a large proportion of west facing flat and deep areas (15 %) as well as east and west facing flat, shallow topographic settings (~13 % each). This area was quite flat with a further 21 % in south facing, gentle sloping shallow and deep areas.

Gnaraloo Bay had a narrow and shallow lagoon up to the reef crest and an extensive flat sandy substrate along the coastline, becoming more heterogeneous outside of the shallow

lagoon with larger differences in slope and depth (due to the occurrence of large bommie-like structures). The Gnaraloo subset was characterised by west facing slopes, with equal proportions being gentle and deep, steep and deep and gentle and shallow. There was also a nearly equal proportion of east facing slopes, in the same depth and slope ranges (~30 % of total).

From the point of view of sampling design it is often important to consider topographic setting and the information where particular topographic settings can be found can assist and save a lot of time in the field. For instance, if one needed to sample in west facing, flat shallow or deep areas, the largest areas were located in Bateman Bay, whereas extensive east facing flat and deep areas exist in Maud study area.

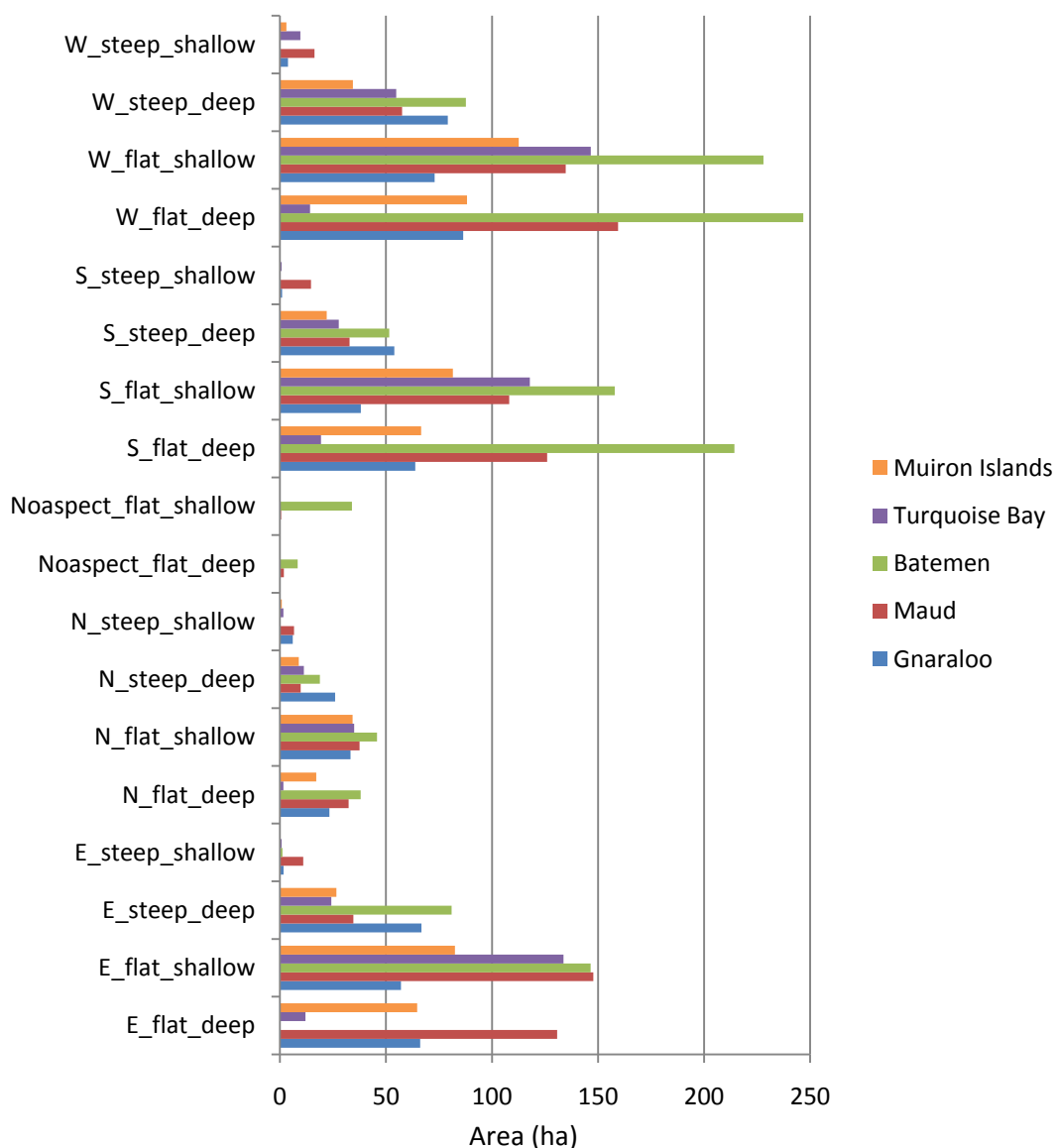


Figure 67. Summary of the areas (hectares) of topographic classes in five data subsets along the Ningaloo Reef.

The overlay of selected single habitat classes over topographic classification highlights the value of processing the data for both habitat maps and bathymetry. This is illustrated with just one example for Turquoise Bay area which shows topographic setting of sand dominated

habitats, all in shallow water, on gentle slopes and mostly facing west. Macroalgae mosaics, on the other hand, while also present in mostly very shallow water, were found on the west and east facing gentle slopes within the lagoon as well as the east and west facing slopes of the back reef (Figure 74). The wide channel in the reef was quite shallow with clear delineation of the gentle slopes. Limestone pavement was only present in extensive patches within the shallow channel (Figure 75) while coral cover was patchy and present both, inside (east facing gentle slopes) and outside the lagoon (west facing gentle sloping areas).

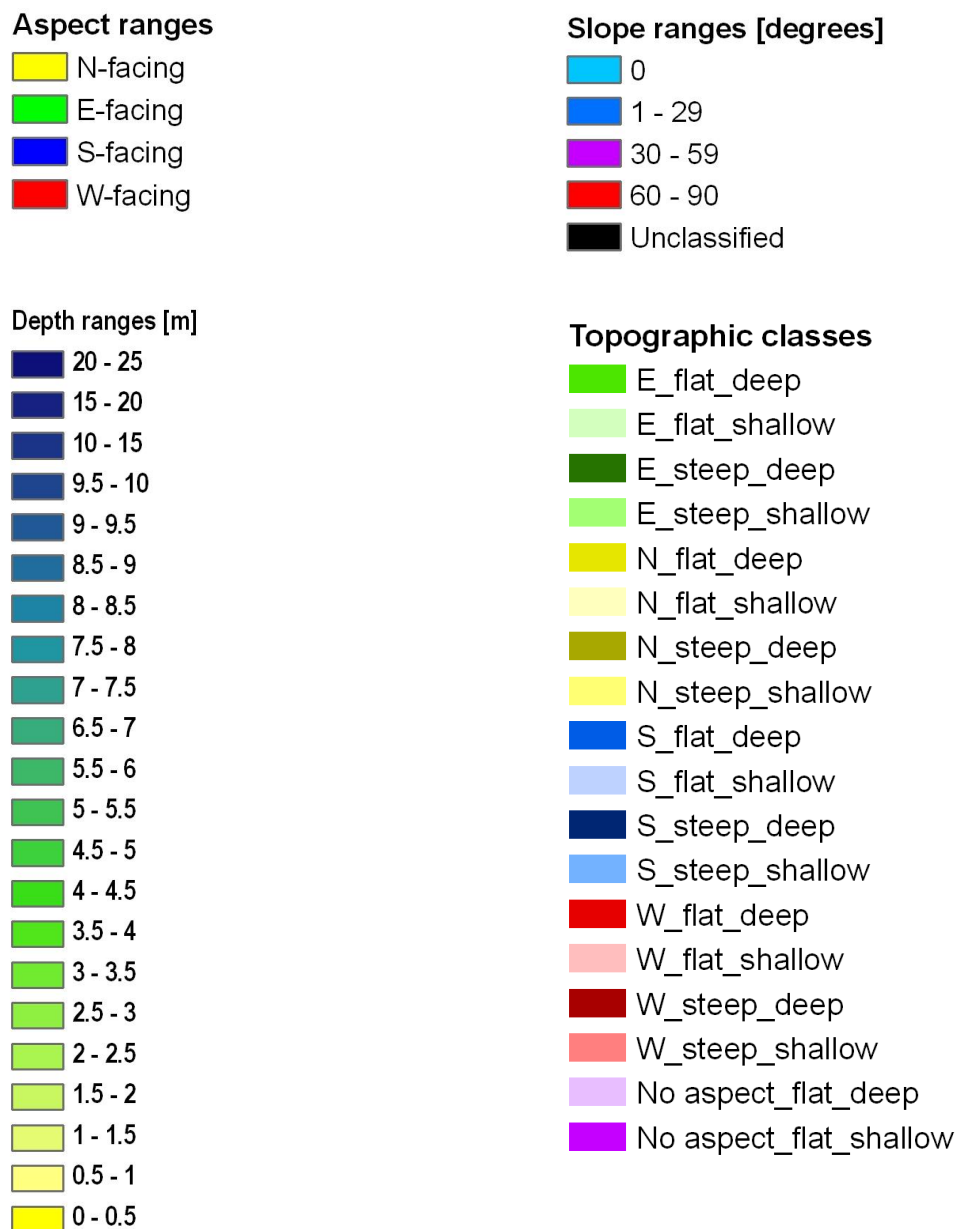


Figure 68. Legends for aspect, slope, depth and final topographic classes at Ningaloo Reef. This legend applies to Figure 69-Figure 73.

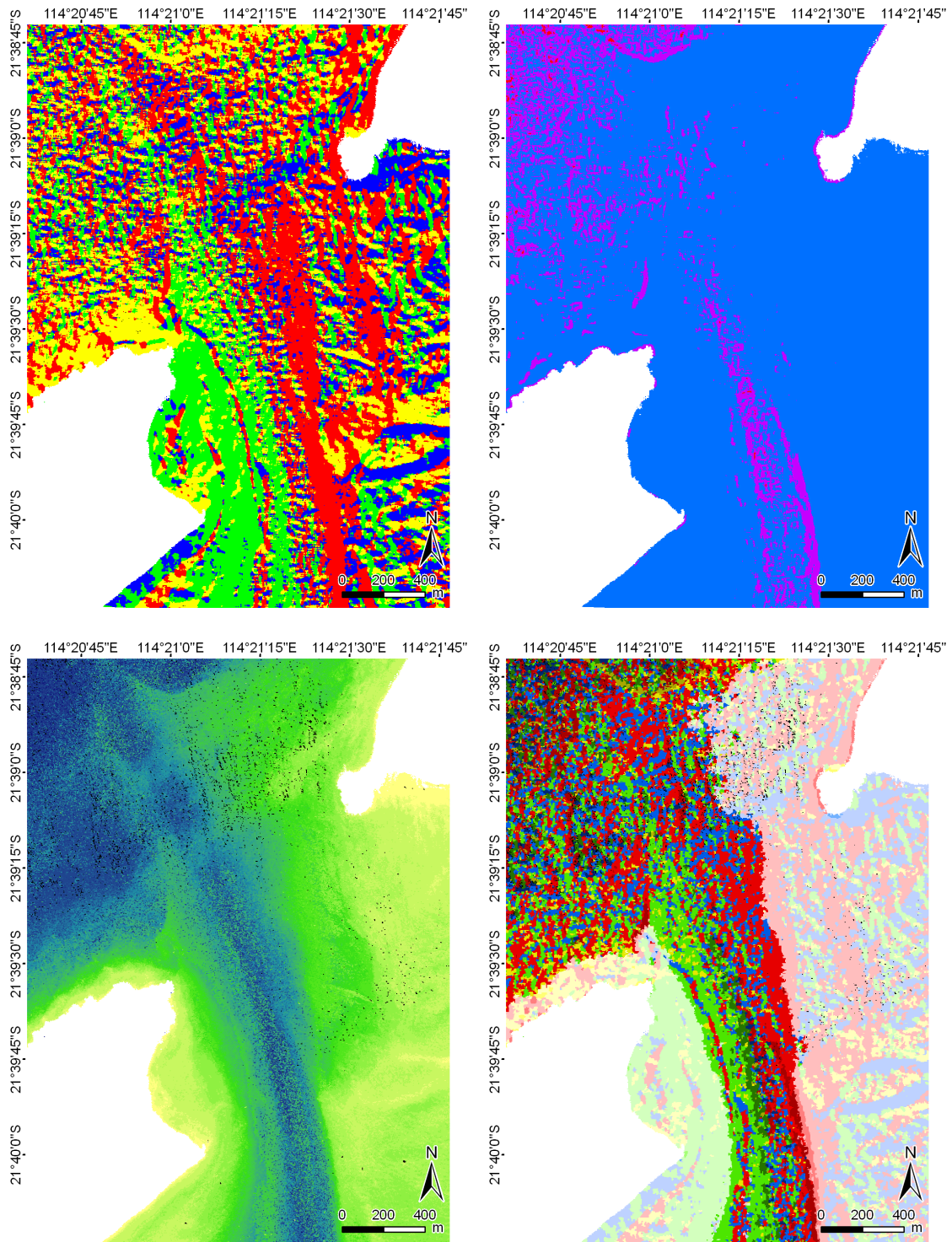


Figure 69. Aspect (top left), slope (top right), depth (bottom left) and resultant topographic classification (bottom right) for study area Muiron Islands. Legends in Figure 68 apply.

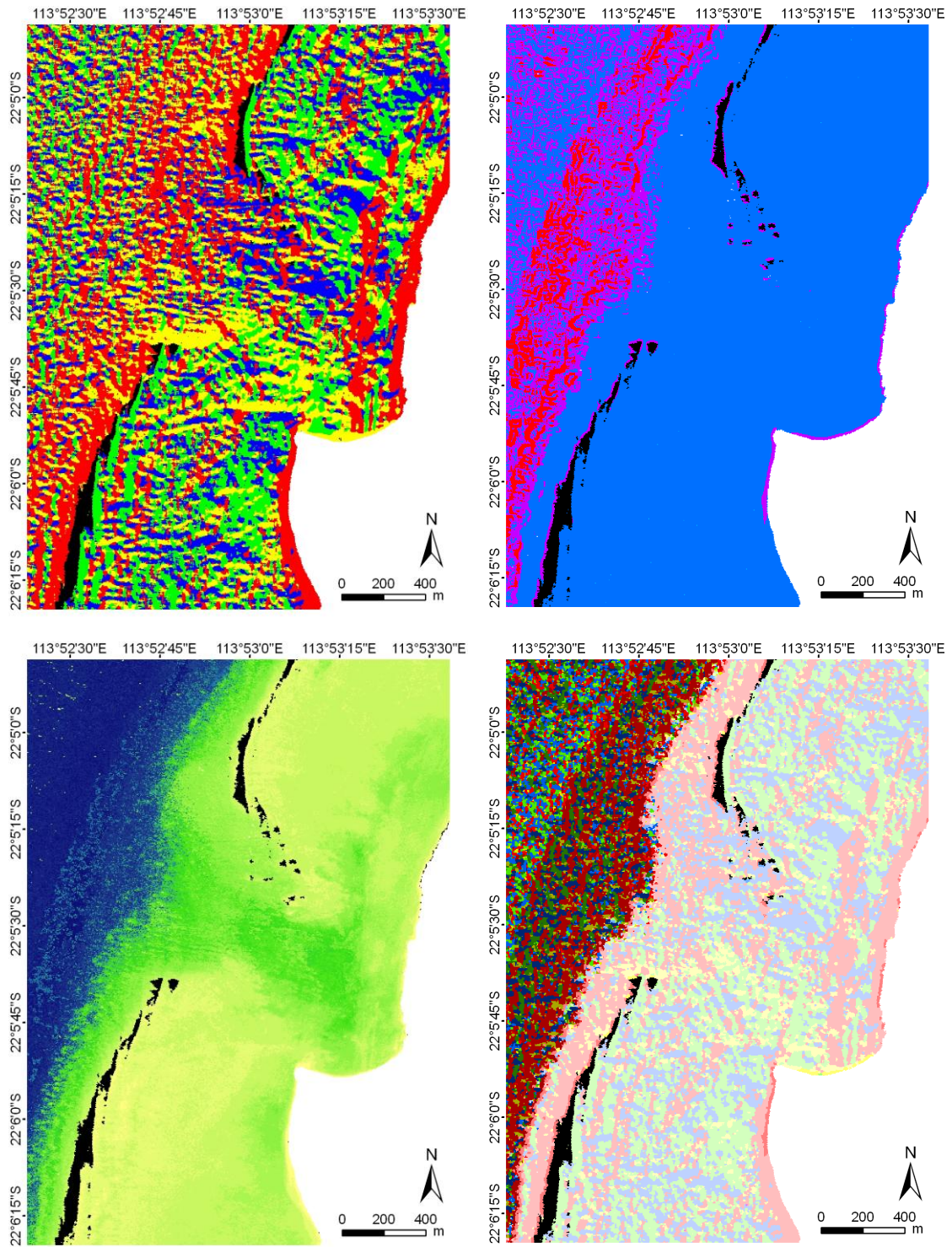


Figure 70. Aspect (top left), slope (top right), depth (bottom left) and resultant topographic classification (bottom right) for study area at Turquoise Bay. Legends in Figure 68 apply.

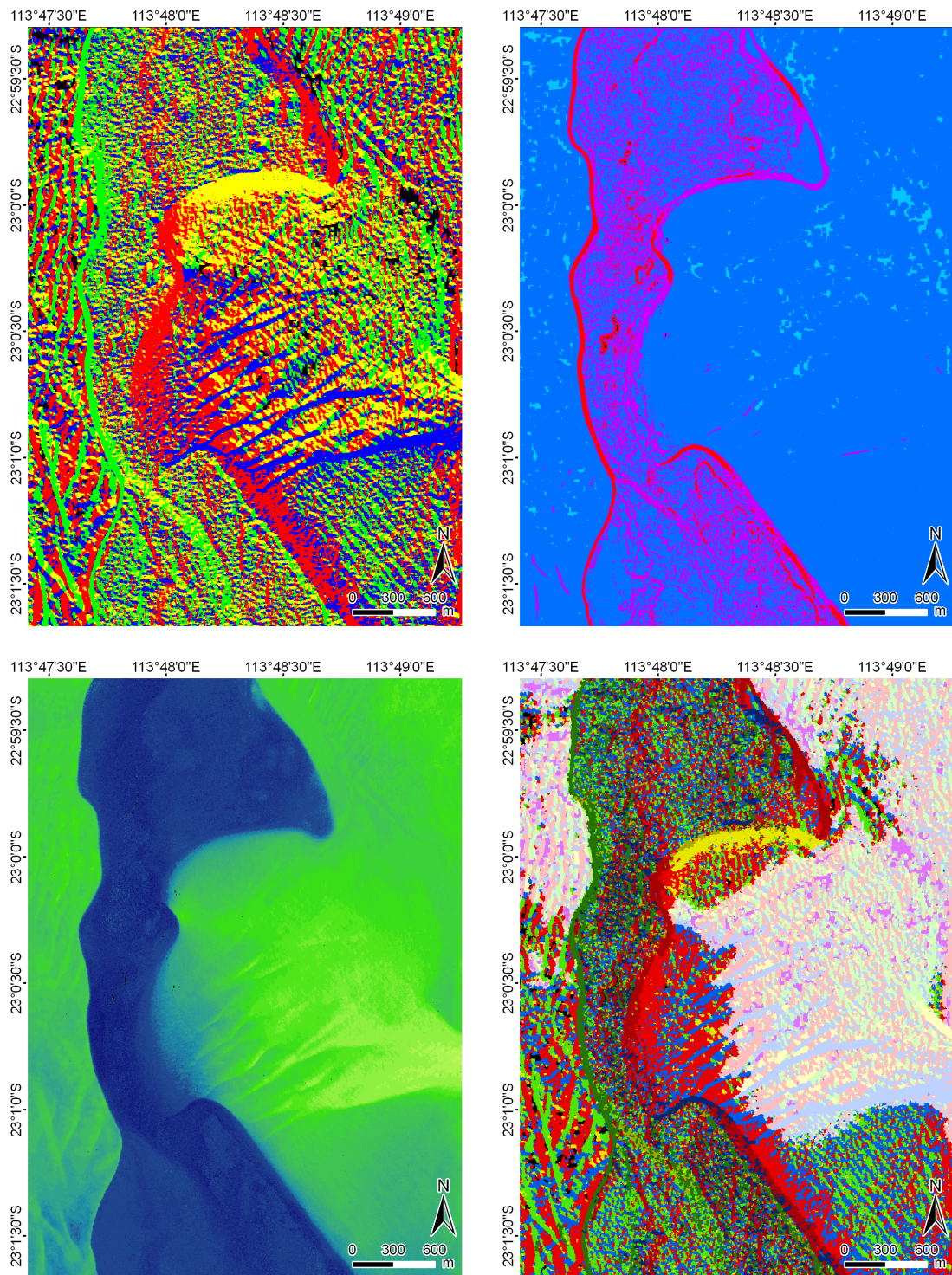


Figure 71. Aspect (top left), slope (top right), depth (bottom left) and resultant topographic classification (bottom right) for study area in Bateman. Legends in Figure 68 apply.

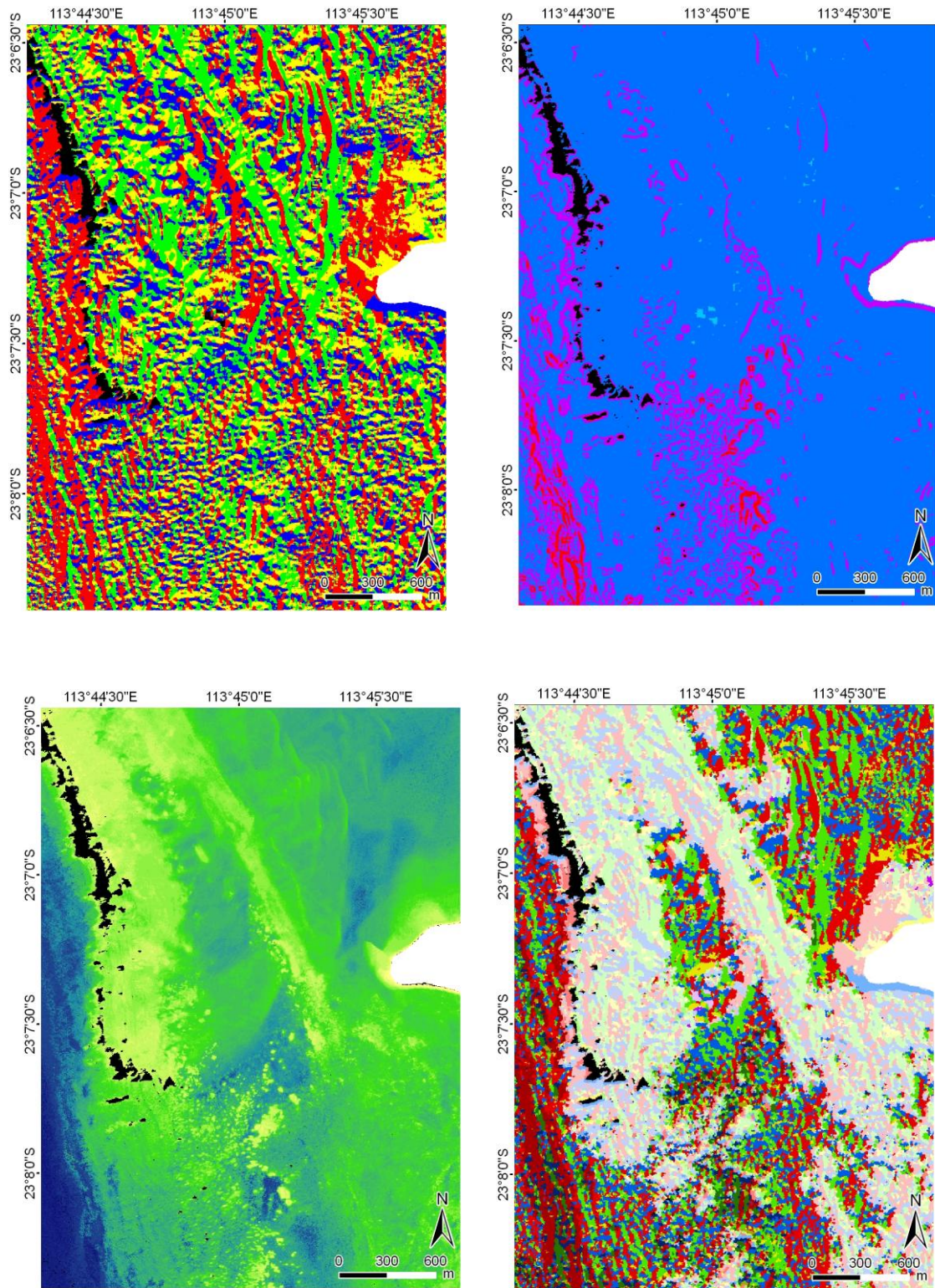


Figure 72. Aspect (top left), slope (top right), depth (bottom left) and resultant topographic classification (bottom right) for study area at Point Maud. Legends in Figure 68 apply.

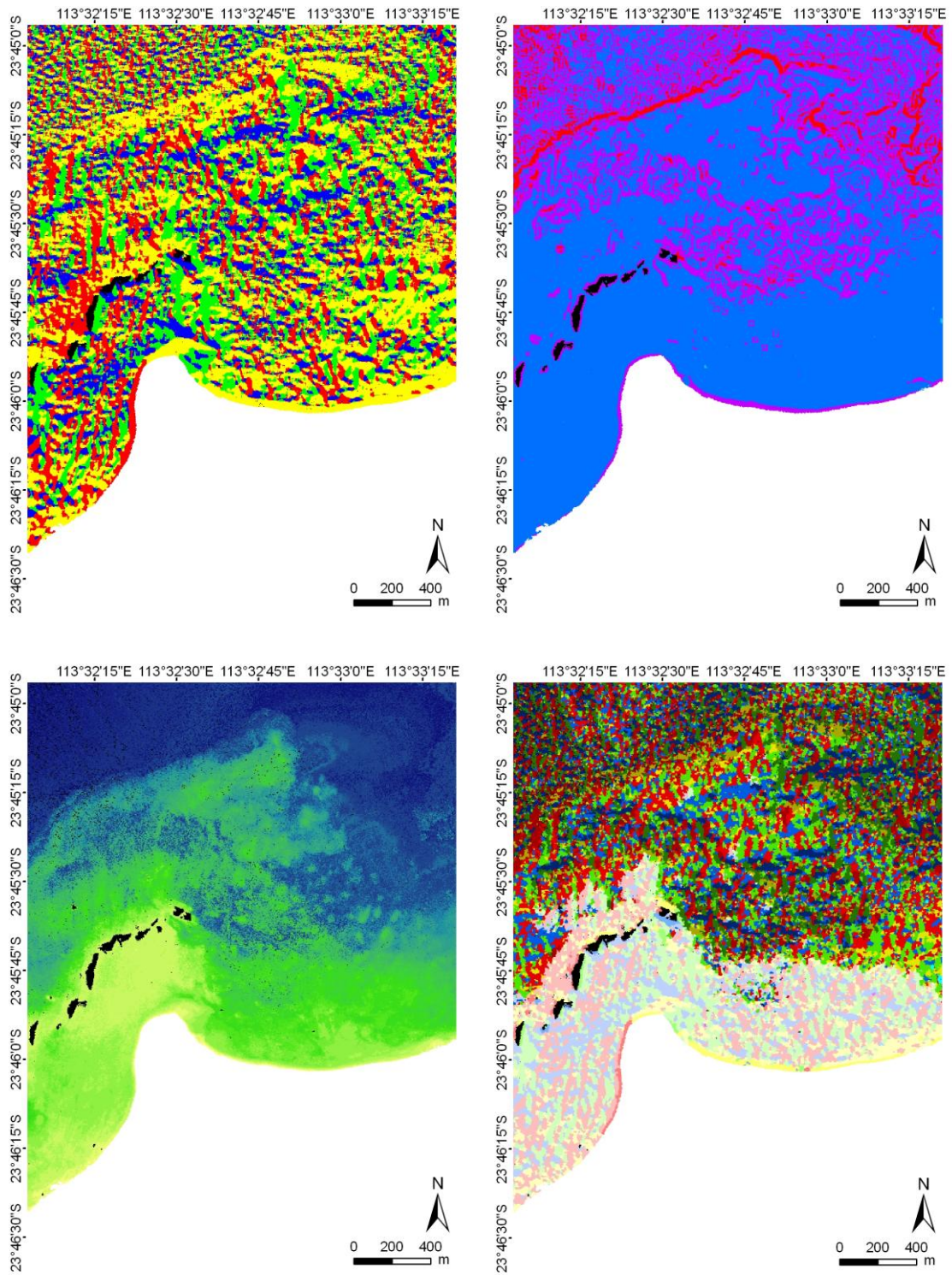
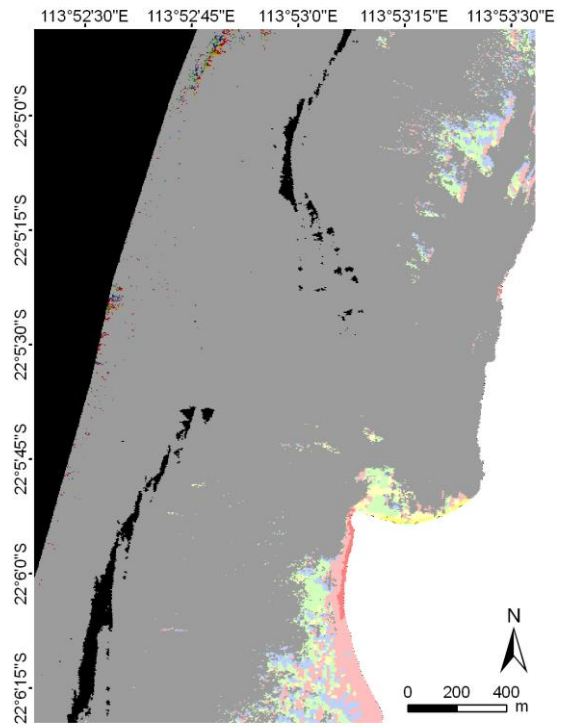
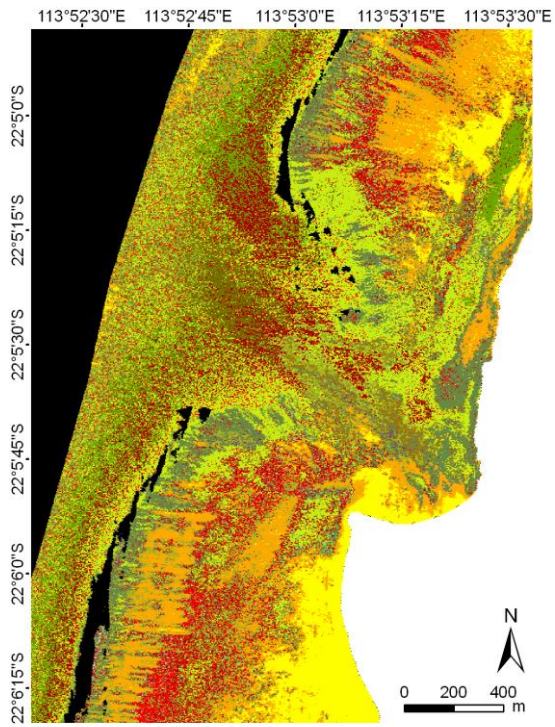


Figure 73. Aspect (top left), slope (top right), depth (bottom left) and resultant topographic classification (bottom right) for study area at Gnaraloo. Legends in Figure 68 apply.



- HC
- HC and MA with LP and S
- HC with LP
- HC with S
- HC with TA- or MA-covered IDC or R
- HC with TA- or MA-covered IDC or R and S
- HC, MA and TA with LP
- LP dark
- LP light
- LP with S
- LP, R and S
- MA
- MA with LP
- MA with R
- MA with S
- S
- SC
- SC, HC and MA with LP
- SC, HC with LP
- TA with LP
- Unclassified

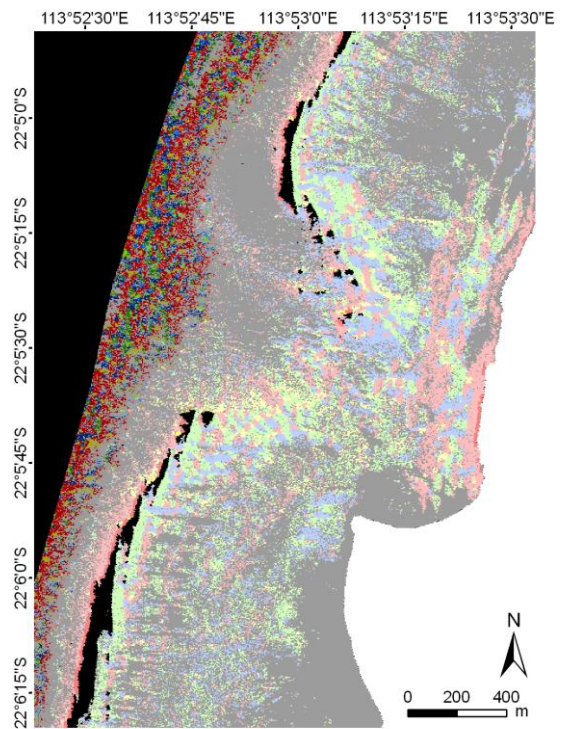
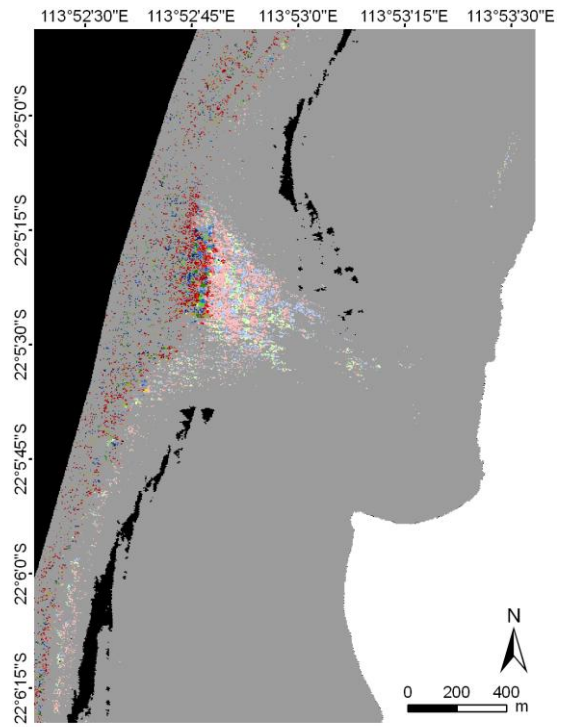
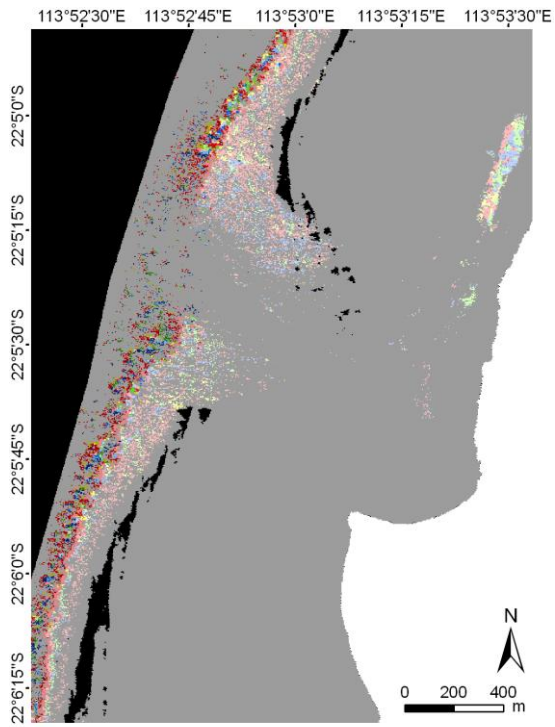


Figure 74. Habitat map for Turquoise Bay and overlay of topographic categories for single habitat classes, sand (top right) and macroalgae (bottom right). Topographic class legend is displayed in Figure 75.



Topographic classes

- E_flat_deep
- E_flat_shallow
- E_steep_deep
- E_steep_shallow
- N_flat_deep
- N_flat_shallow
- N_steep_deep
- N_steep_shallow
- S_flat_deep
- S_flat_shallow
- S_steep_deep
- S_steep_shallow
- W_flat_deep
- W_flat_shallow
- W_steep_deep
- W_steep_shallow
- No_aspect_flat_deep
- No_aspect_flat_shallow

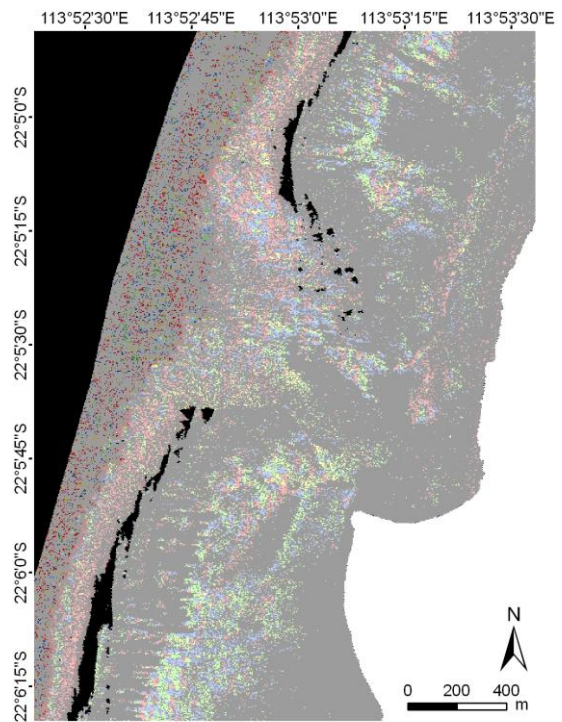


Figure 75. Distribution of single habitat classes in different topographic settings for Turquoise Bay; turfing algae and limestone pavement top left, limestone pavement top right and hard coral at bottom right.

2.3.11 Geomorphic classification

The multi-scale, object oriented classification successfully extracted reef and lagoonal features of interest. The rule set developed using topographic variables and habitat classification allowed five, quite different areas from distant parts along the coast to be consistently classified into five broad classes described as:

- Sand or limestone pavement (flat lagoonal)
- Sand or limestone pavement (lagoonal slopes)
- Coral and algal communities (deep forereef and other deep areas)
- Coral and algal communities (backreef/shallow forereef and other shallow areas)
- Coral and algal communities (reef flat and very shallow areas)

While other combinations and different numbers of classes are possible, we have demonstrated here that the approach of object oriented classification is possible even in very different topographic settings.

Based on these five classes, the Muiron Islands area was characterised by a deep channel between the two islands, forereef, deep lagoonal environments, reef flats and very shallow lagoonal settings (~32 % each), both with coral and algal communities present in the channel between the two islands and on the slopes. There was not much sand in this area (<2 %) (Figure 76 and Figure 77).

Turquoise Bay with had a wide, flat lagoon (nearly 1.6 km wide), dominated by coral and algal communities (reef flat and very shallow areas) (42 %), with another 36 % in the coral and algal communities (deep forereef and other deep areas) and coral and algal communities (backreef/shallow forereef and other shallow areas) classes. Reef channel was surprisingly shallow out beyond the reef crest (less than 5 m depth), but dropping off steeply along the forereef approximately 200 m seawards of the reef crest (Figure 76 and Figure 78).

Just over 60 % of Bateman Bay had sand in flat lagoonal environments, with another 35 % with coral and algal communities (deep forereef and other deep areas). A deep water region dominates the central part of the study area, while on the eastern part a submerged drainage pattern is clearly noticeable. Edges of the deep water feature are covered with sand and limestone pavement (lagoonal slopes) (Figure 76 and Figure 79).

Maud sanctuary area was characterised by small, circular features in the southern section due to the presence of bommies and relatively heterogenous reef structure, while the northern section was more homogeneous and comprised fairly flat sandy plains and slopes. The Maud area was mostly assigned to coral and algal community classes (backreef/shallow forereef and other shallow areas) (55 %) and further 15 % in forereef and deep lagoonal environments with coral and macroalgae mosaics. Two large areas of flat lagoonal sand can also be seen to the north and east of Point Maud. (Figure 76 and Figure 80).

Gnaraloo Bay had a narrow and shallow lagoon up to the reef crest and an extensive flat sandy substrate along the coastline, becoming more heterogeneous outside of the shallow lagoon with larger differences in slope and depth (due to the occurrence of large bommie-like structures). This part of the Ningaloo coast is characterised by very narrow lagoons, here only approximately 500 m wide. Two single largest classes in Gnaraloo were coral and algal

communities (deep forereef and other deep areas) coral and algal communities (backreef/shallow forereef and other shallow areas) (52 % combined) (Figure 76). Those shallow coral communities on the reef flat can be clearly seen in the western part of Figure 81. Nearshore sand in shallow lagoons can also be seen as a large contiguous habitat.

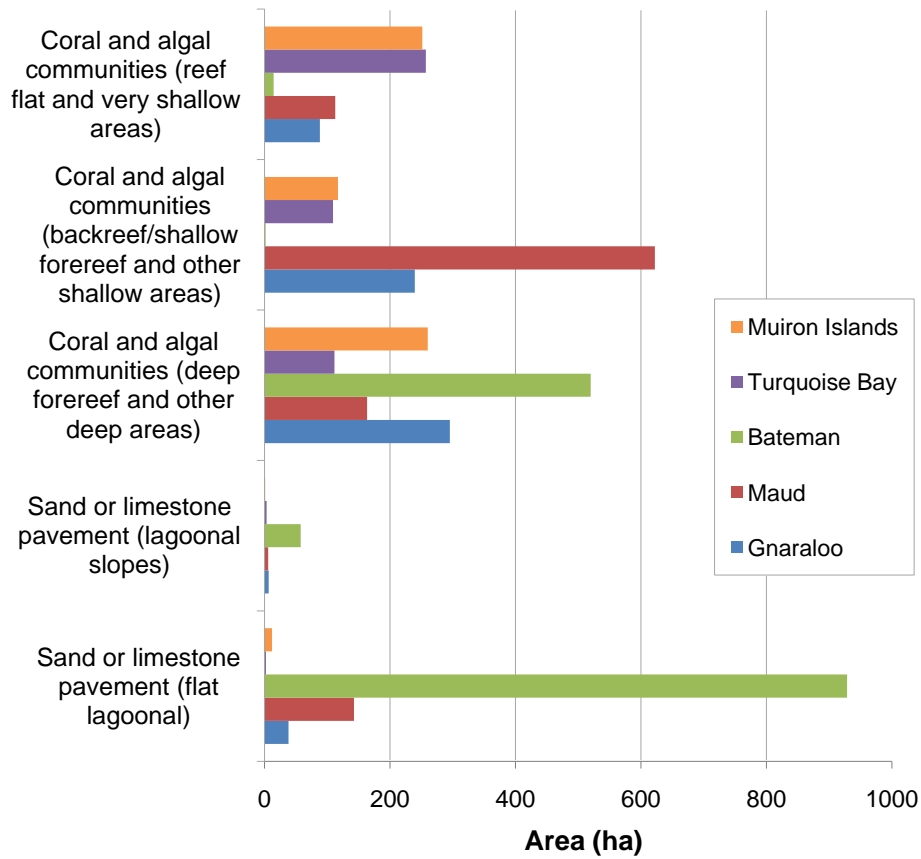


Figure 76. Summary of areas of geomorphic classes mapped within the five study areas along Ningaloo Reef.

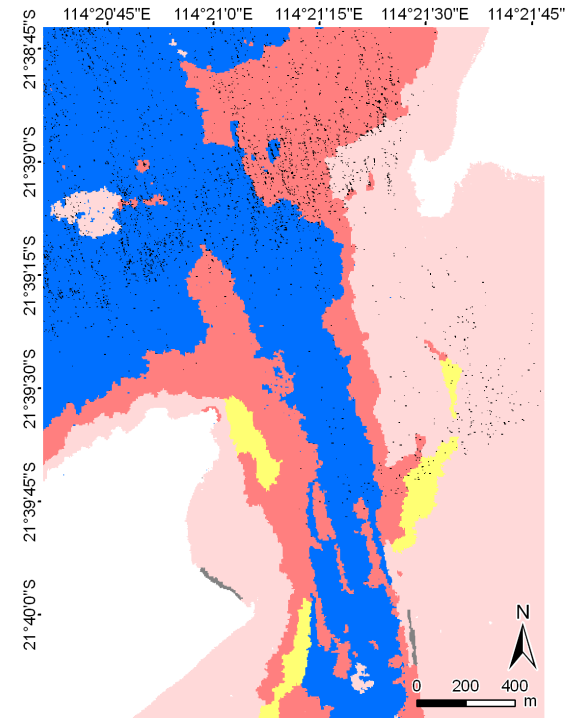
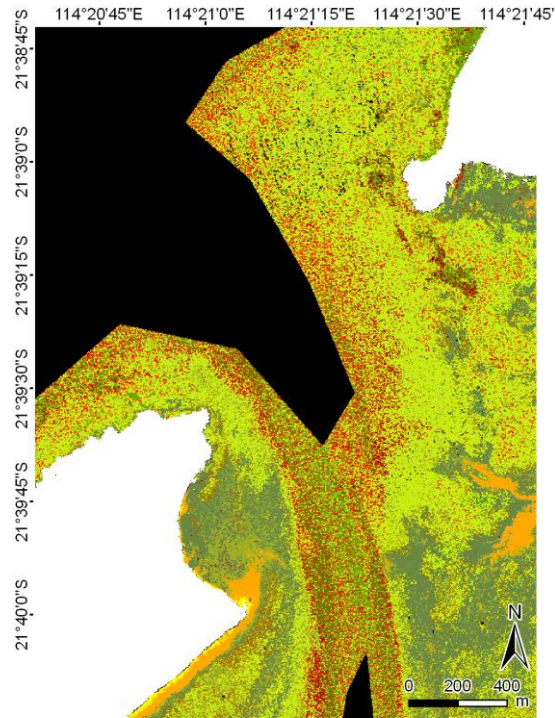
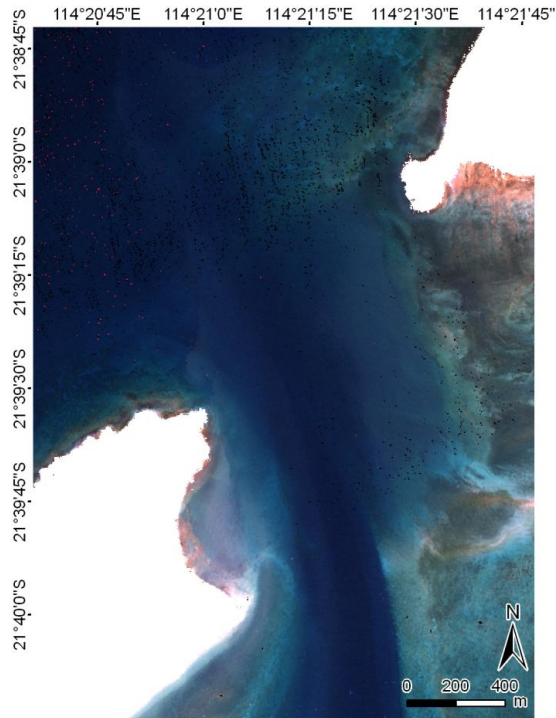
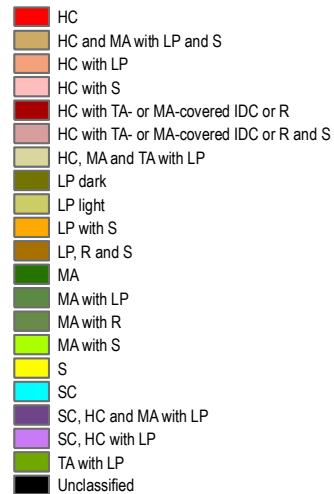


Figure 77. Muiron Island area shown as subsurface reflectance (left), habitat map (centre) and geomorphic classes (right). Note that while habitat map classes were masked at 20m depth, geomorphic classification was carried out beyond that masked region.



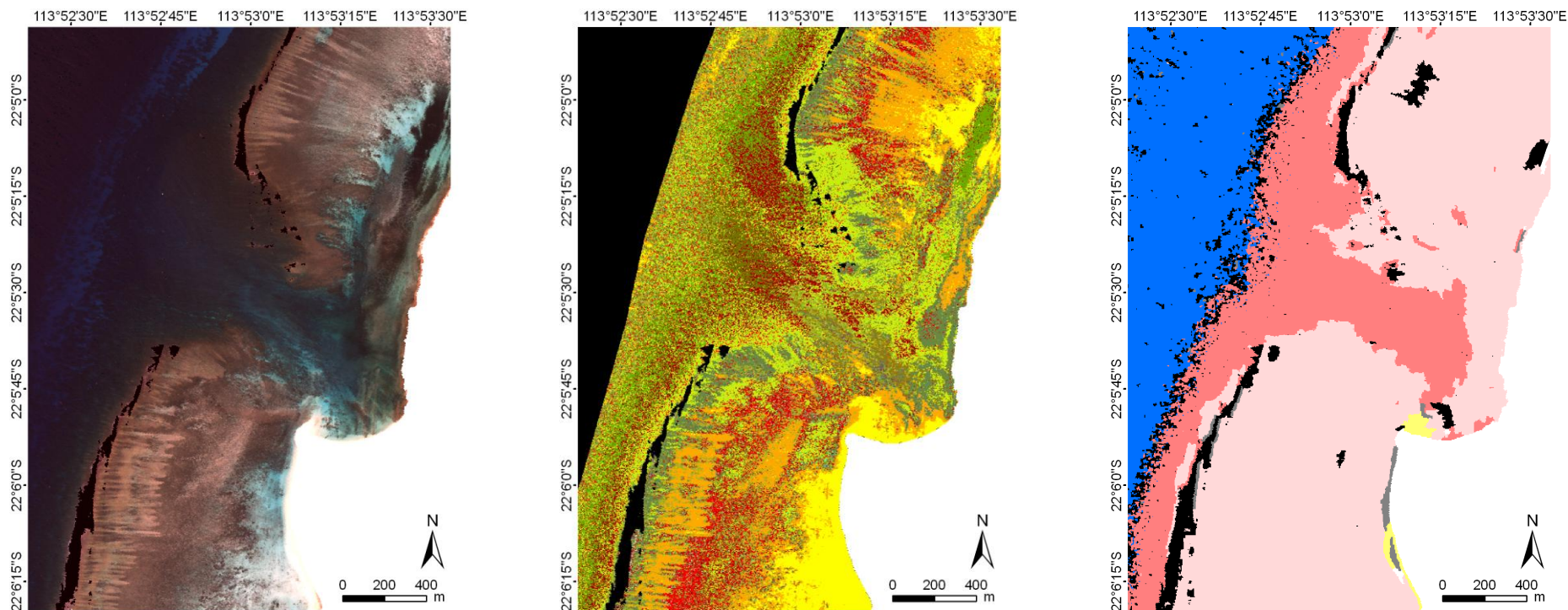


Figure 78 Turquoise Bay area shown as subsurface reflectance (left), habitat map (centre) and geomorphic classes (right).

- HC
- HC and MA with LP and S
- HC with LP
- HC with S
- HC with TA- or MA-covered IDC or R
- HC with TA- or MA-covered IDC or R and S
- HC, MA and TA with LP
- LP dark
- LP light
- LP with S
- LP, R and S
- MA
- MA with LP
- MA with R
- MA with S
- S
- SC
- SC, HC and MA with LP
- SC, HC with LP
- TA with LP
- Unclassified

- Coral and algal communities (reef flat and very shallow areas)
- Coral and algal communities (backreef/shallow forereef and other shallow areas)
- Coral and algal communities (deep forereef and other deep areas)
- Sand or limestone pavement (flat lagoonal)
- Sand or limestone pavement (lagoonal slopes)
- Unclassified

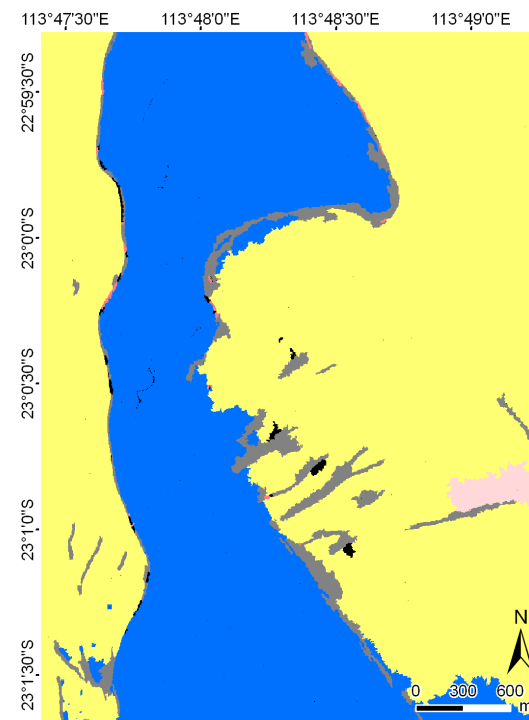
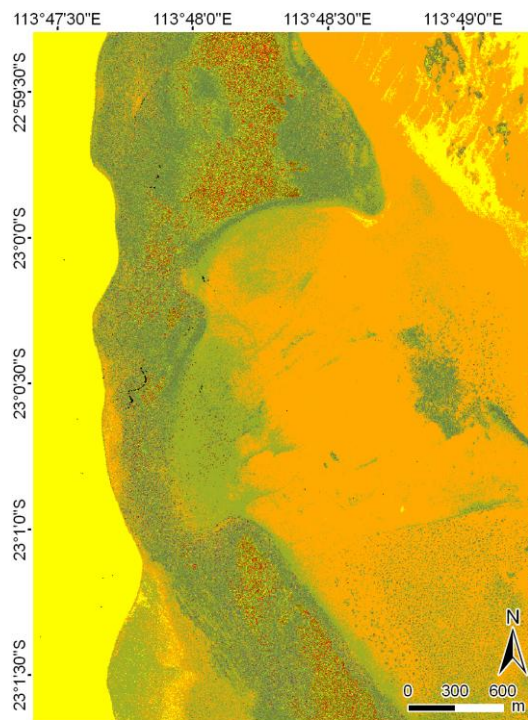
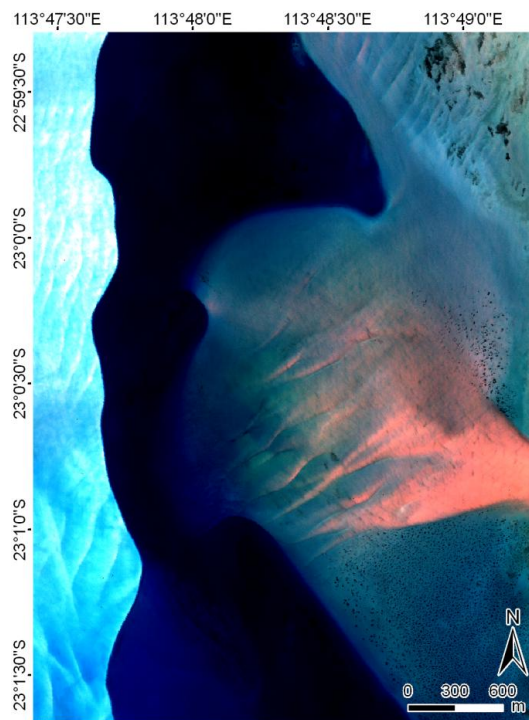


Figure 79. Bateman Bay area shown as subsurface reflectance (left), habitat map (centre) and geomorphic classes (right).

- HC
- HC and MA with LP and S
- HC with LP
- HC with S
- HC with TA- or MA-covered IDC or R
- HC with TA- or MA-covered IDC or R and S
- HC, MA and TA with LP
- LP dark
- LP light
- LP with S
- LP, R and S
- MA
- MA with LP
- MA with R
- MA with S
- S
- SC
- SC, HC and MA with LP
- SC, HC with LP
- TA with LP
- Unclassified

- Coral and algal communities (reef flat and very shallow areas)
- Coral and algal communities (backreef/shallow forereef and other shallow areas)
- Coral and algal communities (deep forereef and other deep areas)
- Sand or limestone pavement (flat lagoonal)
- Sand or limestone pavement (lagoonal slopes)
- Unclassified

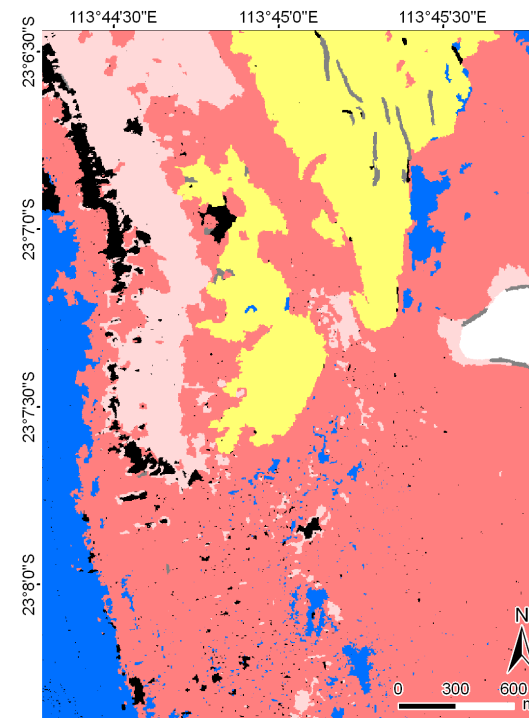
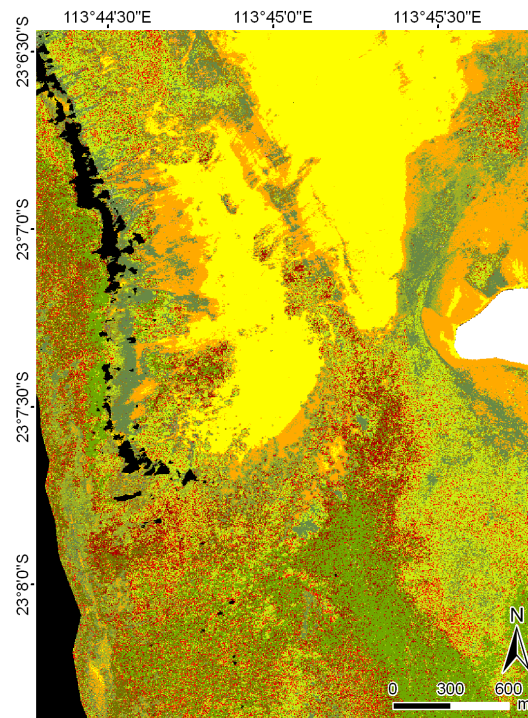
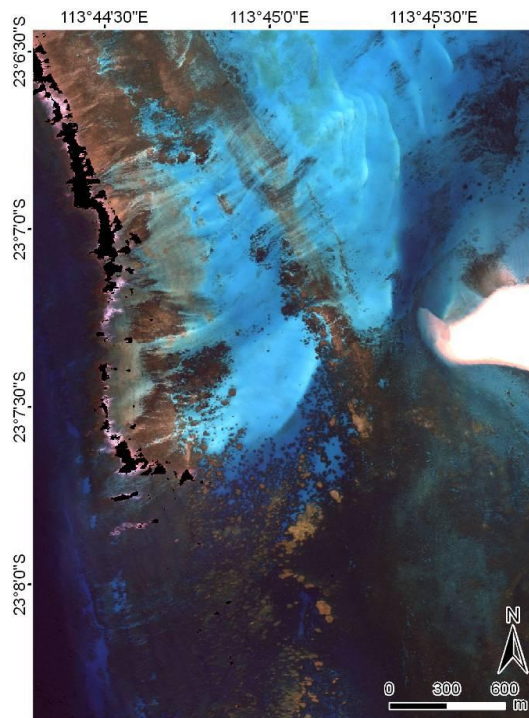


Figure 80. Northern Coral Bay (Maud) area shown as subsurface reflectance (left), habitat map (centre) and geomorphic classes (right).

- HC
- HC and MA with LP and S
- HC with LP
- HC with S
- HC with TA- or MA-covered IDC or R
- HC with TA- or MA-covered IDC or R and S
- HC, MA and TA with LP
- LP dark
- LP light
- LP with S
- LP, R and S
- MA
- MA with LP
- MA with R
- MA with S
- S
- SC
- SC, HC and MA with LP
- SC, HC with LP
- TA with LP
- Unclassified

- Coral and algal communities (reef flat and very shallow areas)
- Coral and algal communities (backreef/shallow foreereef and other shallow areas)
- Coral and algal communities (deep foreereef and other deep areas)
- Sand or limestone pavement (flat lagoonal)
- Sand or limestone pavement (lagoonal slopes)
- Unclassified

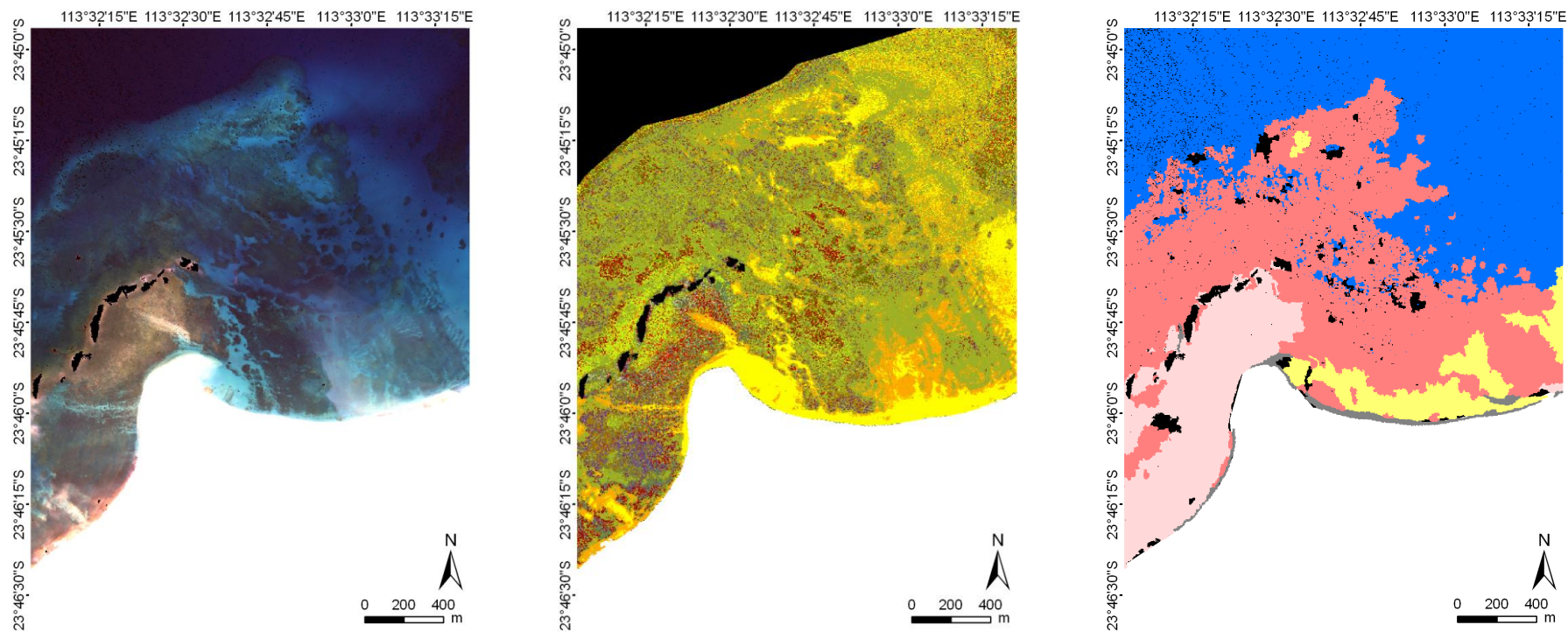


Figure 81. Gnaraloo Bay area shown as subsurface reflectance (left), habitat map (centre) and geomorphic classes (right).

- HC
- HC and MA with LP and S
- HC with LP
- HC with S
- HC with TA- or MA-covered IDC or R
- HC with TA- or MA-covered IDC or R and S
- HC, MA and TA with LP
- LP dark
- LP light
- LP with S
- LP, R and S
- MA
- MA with LP
- MA with R
- MA with S
- S
- SC
- SC, HC and MA with LP
- SC, HC with LP
- TA with LP
- Unclassified

- Coral and algal communities (reef flat and very shallow areas)
- Coral and algal communities (backreef/shallow foreereef and other shallow areas)
- Coral and algal communities (deep foreereef and other deep areas)
- Sand or limestone pavement (flat lagoonal)
- Sand or limestone pavement (lagoonal slopes)
- Unclassified

2.4 Discussion

This study successfully demonstrated utility of high resolution airborne optical remote sensing over a very large area to map marine habitats using operational methods. Data processing used in the study allowed for extraction of highly detailed benthic habitat classification as well as seamless bathymetry for marine waters up to 20 m depth. This detection limit is consistent with previous work on coral reefs elsewhere (e.g. Hochberg *et al.* 2003). Corrections to the remote sensing data were implemented with operational methods which used standardized parameters and were processed on a stand-alone desktop computer. Data were successfully processed on whole mosaics (up to five flight lines), enabling rapid implementation of a single classification approach for the whole study area. This approach allows for future processing of additional data sets and comparisons over time for selected areas.

2.4.1 Spectral analysis

Spectral data and site descriptions, including cover type and percentage cover were collected between 2006 and 2009, as it was not possible to collect all field data around the time of HyMap acquisition. There were several reasons for this, namely, logistics and costs, size of the area, and the airborne data collection schedule, (which depended on weather conditions) making simultaneous collection of field data difficult. However, the majority of data points were collected around the same season (April) with similar algal growth conditions. Data were obtained at locations with fairly homogenous cover type, therefore ensuring their representativeness and allow for any positional errors (McCoy 2005).

While the *in situ* spectra collection was limited to areas accessible to divers (spectrometer was based on the boat) or shore sampling, it provided sufficient background information which informed early decisions on the direction of the classification framework, including spectral separability between different benthic components (“pure” and mixed). Underwater spectral data were collected mostly in the northern and central parts of the Ningaloo Reef.

Analysis of field spectra in the early part of the project allowed for formulation of a clear approach to the development of the classification scheme. Benthic habitats of the Ningaloo Reef are highly diverse and mixed. Creation of the spectral library allowed for determination of the degree of separability of the dominant spectral components within the benthic cover. Methods employed in this study allowed for detailed site description, photographs and spectra to be obtained *in situ*, especially important in marine protected areas.

Spectral analysis of the image spectra using the PCA and JM distance allowed for exact measures of separability to be determined, thus eliminating subjectivity in the final class selection. PCA and JM distance were deemed appropriate as image spectra were from corrected imagery. This approach provided a good basis for refining or regrouping classes before final classification which used reflectance and the first two derivatives.

Field spectra were collected from a wide range of substrates and represented “pure” substrate types or their components, not spectral mixes which typically exist at the pixel level in the remote sensing data set. Earlier studies by Hedley and Mumby (2002) and Hedley *et al.* (2004) noted that field spectra often were unlikely to capture the full spectral variability of benthic habitats since large variability

(due to season, for example) exists even at species level. Results from the spectral separability analysis of the field spectra were very similar to previous studies on corals, algae and abiotic substrates including blue corals (e.g. Holden and LeDrew 1998, Joyce and Phinn 2003, Hochberg *et al.* 2003, Stephens *et al.* 2003). In particular, Joyce and Phinn (2003) showed clear separation between field spectra of *Montipora* spp., *Porites* spp., macroalgae (*Chlorodesmis fastigata*) and sediments containing benthic microalgae. All the brown corals sampled at Ningaloo exhibited a characteristic reflectance feature at 570 nm, also reported in previous studies (Hochberg and Atkinson 2003, Hochberg *et al.* 2003). In a study by Mumby *et al.* (2004), an airborne CASI instrument with 1 m² pixels and 10 broad spectral bands allowed for spectral separation between *Porites* spp., living *Pocillopora* spp., recently and old dead *Porites* spp. and *Pocillopora* spp. as well as *Halimeda* spp. and coralline red algae. Depth of water and subsequent attenuation of the signal was however a major limitation in that particular study. Nearly all peaks in coral and algae occurred in narrow wavelength ranges, sometimes as broad as 20 nm, but often of the order of 10 nm (Hochberg *et al.* 2003). Multispectral instruments could not separate some of the information classes and this is where hyperspectral instruments have a definite advantage. Many living reef components share similar pigments and, therefore, the spectral separability of non-living components is often confounded by the presence of the epilithic algal film or turf algae (Hedley and Mumby 2002, Hedley *et al.* 2004). While studies such as Hochberg *et al.* (2003) separated corals according to colour only, we additionally attempted to split brown corals into growth forms, such as branching, digitate and tabulate, as it was found that different contrasting and shadowing, particularly between tabulate and branching/digitate corals, texture and morphology resulted in differences in brightness.

The selection of benthic classes for the final classification was largely based on frequency of occurrence of that substrate in the field data set as well as spectral separability. Effort was made to cover different areas along the reef from the southern, narrow reef areas, characterized by near-shore limestone plateaus, to the central wide lagoonal areas, with extensive coral cover, to the northern areas, dominated by macroalgae and limestone pavements.

As previously mentioned, mapping species of macroalgae, turfing or coralline algae was not a priority for this project, however a number of field spectra of commonly occurring species have been collected. In the classification scheme, all algae were grouped only on the basis of their percentage cover within a quadrat (pixel), rather than using species. This was mostly because, apart from *Sargassum* sp., all other algae, whether turfing, fleshy or coralline, occurred in highly mixed assemblages. Green *et al.* (2000) noted that from the coastal management perspective, it often is very valuable to map algal communities in detail. Such maps could facilitate better understanding and management of their biodiversity as well as interactions with coral communities, especially important in areas of periodic or chronic disturbance. With further fieldwork, the current hyperspectral dataset for Ningaloo Reef could be reprocessed to enhance the level of description for algal communities. Harvey (2009) achieved high accuracies and separation between canopy and turfing algae using the same instrument and pre-processing approach in an area dominated by various algae and seagrasses around Rottneest Island, 900 km south of Ningaloo.

Certain benthic components such as coralline algae were not used in the final classification as they were infrequent in the field data or taking up only a small fraction of the pixel area. Most coralline algae were found on the very shallow reef flats. These areas were not sufficiently accessible to collect enough data for classification and validation. Similarly, although spectral library results showed good separation between different macroalgae and turfing algae, and live and dead corals, there were very

few homogenous pixels in the airborne data to allow for such detailed classes to be included. Lack of extensive cover by recent dead coral was supported by the findings of long term monitoring investigation in Ningaloo by Long (2007) who found very only small percentage of recently dead coral in the Coral Bay area. Older dead coral specimens were all overgrown by macroalgae (Long 2007). Andréfouët *et al.* (2001) concluded in their study on remote sensing detection of dead corals that bleached and non-bleached corals could only be mapped with pixels of about 0.01 m² and very high spectral resolution sensors were needed to separate spectra of some corals and macroalgae (Joyce and Phinn 2003). Barott *et al.* (2009) achieved a high degree of separation between field spectra of different taxa of coral and algae. The study by Hochberg *et al.* (2003) noted that in order for remote sensing to be applied more widely in coral reef studies, better understanding of spectral separability of the basic benthic cover types is needed.

Due to data being acquired in autumn, some of the main cover-forming algae had a yellow or brown colouration, resulting in some misclassification of the coral classes, in particular tabulates. The occurrence of *Sargassum* as well as other algae on large cover-forming patches of coral resulted in a partially overlapping spectral ranges of *Sargassum* and coral classes, thus leading to some misclassifications. *Sargassum* had a strong spectral similarity to coral, evident in the field spectra, with reflectance peaks near 600 nm and 650 nm, as also found by (Hochberg and Atkinson 2000; Hochberg and Atkinson 2003). However, *Sargassum* was also found to have a peak at 570 nm as coral, a spectral feature absent in *Padina*, red algae and coralline algae.

2.4.2 Classification approach

The hierarchical classification approach used in this study reflected typical, complex reef mosaics of coral, various algae, sand and pavement, and thus it was logical to classify the images first into basic biotic and abiotic components and then to further organise them at more detailed levels within these broad classes. This approach was similar to the scheme used by Harvey *et al.* (2007) in the temperate areas at Rottneest Island, off the Western Australian coast. Using the same instrument, that study showed good separation between seagrasses, canopy and turfing algae and abiotic components of the marine benthos (Harvey *et al.* 2007; Harvey 2009).

Spectral analysis of the image derived spectra prior to image classification allowed for refinements in final class definitions such as some classes for example, with the same biotic or abiotic components may need to be merged. While some classes (for example “blue tip” *Acropora*) were very different from other branching corals, a number of classes containing a low percentage of coral and more than 50 % of algae were spectrally very similar. The very high spectral resolution of the sensor highlighted variability in spectral properties of abiotic cover types such as sand and pavement from the northern to the southern extent of the study area. Large spectral variability of sand was mostly due to grain sizes and mineralogical composition which varies along the coast (Cassata and Collins 2008). For the final classification, all spectral sub-classes representing sand were merged.

Benthic classifications generated during this study fit into the two most complex habitat classifications described by Green *et al.* (2000): definition of habitats through quantification of biotic assemblages and also a classification system which combined more than one type of information, in this case, topographic variables and biotic assemblages. Some classification maps can encompass as many as five basic information units, for example surficial geology, sub-benthos, benthic biology, geform and water column information (FGDC 2010).

Through expert visual aerial photo-interpretation, the previous habitat map for the Ningaloo Marine Park identified 13 broad habitats, which included the pelagic zone (Bancroft and Sheridan 2000). Coral reef and general reef communities were divided into classes based on their depth/tide regime (intertidal, shallow, low relief, lagoonal, seaward). Classes mapped by Bancroft and Sheridan (2000) broadly correspond to the output from the object oriented classification which combined benthic cover and topographic variables and created 12 information classes (in contrast to 46 classes in the habitat mapping at the highest level of detail).

Hierarchical design of the benthic classification developed here was driven primarily by the end-user needs, some requiring only medium level descriptive resolution, while others, more detailed information. This hierarchy, of course, also reflects the uncertainty in the classification and its subsequent accuracy. The advantage of the hierarchical arrangement method used here was that it was based on operational processing of remotely sensed data and standard, quadrat-based fieldwork, both easily reproducible and quantitative. Class names incorporate both description and percentage cover, hence, any future changes in percentage cover beyond $\pm 10\%$ are going to be measurable. In addition, the classification scheme developed here captured gradients of various biotic assemblages, in particular, at thematic levels 3 and 4.

The approach of using a look-up table for the final habitat maps to organise the 46 thematic classes allows users to create their own legends, with either mostly descriptive or quantitative or semi-quantitative labels. This approach also accommodates the fact that the definitions of habitats always have some arbitrary component in class labelling (Green *et al.* 2000). Presence of both qualitative and quantitative descriptions for the class labels goes some way towards ensuring that these maps can be interpreted easily, are unambiguous, and reflect the quantitative and qualitative characteristics of the habitats captured through the fieldwork.

A good classification scheme should aim to accommodate a broad range of users' needs and their technical backgrounds (Green *et al.* 2000). Habitat maps for Ningaloo Reef while large in terms of file sizes, have been created using GeoTiff format, an industry standard for raster files and have been made available either as a whole-reef file or as geographic subsets or mosaics.

Many classification schemes based on reef geomorphology have been already developed and compared to the habitat classification schemes, and there seems to be a lot more consistency and standardisation for this approach (Kuchler 1986, Holthus and Maragos 1995, Cassatta and Collins 2008). Lidz *et al.* (2006), in a study of Florida Keys reefs, used 22 thematic classes with descriptive labels. Some of these biotic components such as seagrasses were given an additional descriptor indicating abiotic substrate component, for example: "seagrass on lime mud" and "seagrass on carbonate sand". This was similar to the system used in current study, although less complex. Studies such as Hochberg *et al.* (2003) separated corals according to colour only, this study additionally classified often similarly coloured corals based on growth form such as branching, digitate and tabulate. Texture and morphology had a spectral influence on brightness because of different contrasting and shadowing, particularly between tabulate and branching or digitate corals.

A number of previous studies have mapped coral cover using a semi-quantitative approach such as density (Zainal *et al.* 1993, Ahmad and Neil 1994). These studies described the coral cover as "low", "medium" and "high" density. Bour *et al.* (1996) provided percentage density (intervals) for coral cover. This is similar to the current study and probably the most realistic if the area of study is large and quite diverse. In a study of Pacific Ocean Islands, Dalleau *et al.* (2010) created 10 coarse and 56

detailed classes which incorporated information on depth, exposure, percentage cover of algae, coral and seagrasses, taxonomy and geomorphology. They reported accuracy of mapping as greater than 75 %. In a multi-temporal study of Florida Keys with Landsat TM, Dustan *et al.* (2001) examined community shifts over time in very broad terms, from coral to algal dominated. These studies used a mix of classification approaches and data sets, including multitemporal data and enabled biologists to study shifts in coral communities in space and time. What is crucial is that the logic of the classification scheme that allows for comparisons to be made between locations and over time.

The choice of classifier is always an important one as the conventional ‘‘hard’’ spectral classification schemes are problematic when applied to mixed substrate pixels because each pixel must be assigned to a single substrate category. With the fuzzy logic approach used in this study, classes with equally high probabilities could be analysed and revised.

Previous studies examined a linear unmixing approach (assumes reflectance of the pixel to have a linear relationship to the sum of the end-member spectra (Mather 1999, Settle and Drake 1993, Hedley *et al.* 2004)). Limitation of this approach in large studies is the need for a comprehensive spectral library of the benthic substrates, very unlikely and possibly not practical for an area as large as Ningaloo Reef. As previously mentioned, many studies have shown that large spectral variability exists even with the same species of benthic cover types (Hedley and Mumby 2002, Hedley *et al.* 2004). In addition, spectral mixing may not follow the simple linear model (Hedley *et al.* 2004). Therefore, the spectral unmixing approach was not chosen due to insufficient number of field spectra covering the range of possible reef components collected in the field. At a practical level, there was a substantial time constraint in that activity (diving and boating) and while we could have pursued collection of additional spectra, this would have been intrusive (extracting reef biota in a marine park) further, there were possible effects on the spectral behaviour of corals and algae for the duration of exposure to the air in order to follow Hedley (2004)’s approach of creating representative mixed classes.

Results of the accuracy assessment, while ranging from 64% from the most detailed data set to 84 % for the medium detailed maps, were in the range of accuracies reported in similar studies elsewhere. Other studies using multi- and hyperspectral sensors which classified habitats to at least eight classes, all reported overall accuracies above 70 % (e.g. Schweizer *et al.* 2005, Zharikov *et al.* 2005, Mishra *et al.* 2007, Wabnitz *et al.* 2008, Harvey 2009). Lower accuracies in some classes can be attributed primarily to the spectral similarity between coral types and between coral and algal types as a result of similar reflectance and absorption features. This was particularly the case with patchy and sparse distributions of macroalgae.

If any future follow up studies consider mapping algae, including fleshy macroalgae as a priority, we recommend, sea and weather conditions permitting, to collect the airborne data in season, where *Sargassum* and other algae are still young (i.e. spring), in order to maximise the separability. However, in this study acquisition time was strongly dependant on instrument availability as well as weather conditions, which were deemed most suitable in April, at the end of the typical macroalgae peak growing season. Any future mapping of algae, including turf algae and crustose calcareous algae, an important reef cementing material, would require additional field work either collecting field spectra or locating areas which have these as the dominant cover types (for example reef crest and reef flats).

Current airborne or satellite systems do not yet offer spatial or spectral resolutions to map coral reef communities at the species level (Joyce and Phinn 2003) and further work is needed in understanding spectral separability of the different benthic components (Hochberg *et al.* 2003). While better sensors will address this, spectral interactions specifically between spectrally mixed substrates are far more complex than their terrestrial equivalents and more research is needed to allow integrations of remote sensing research into studies on coral health, condition and process monitoring (Joyce and Phinn 2003). Currently, for operational projects, regional-scale, including change mapping, rely on multispectral satellites such as Landsat TM, QuickBird or SPOT (e.g. Kuchler *et al.* 1986, Zainal *et al.* 1993, Bour *et al.* 1996, Call *et al.* 2003, Vanderstraete *et al.* 2006, Benfield *et al.* 2007, Palandro *et al.* 2008).

Results of this study will support ongoing and future research on basic biological processes on the reef such as chlorophyll content, photosynthetic capacity and nutrient cycling. In this study, consideration was taken to ensure operational effectiveness of the approach and suitability as baseline mapping and as a long term monitoring tool for large areas.

Unlike the terrestrial environment, very few studies have explored sensitivity of thematic and spectral scales in regard to benthic habitat maps, in particular in their ability to capture seascape metrics. In a recent study, Kendall and Miller (2008) showed that maps with coarser spatial resolutions mapped rare benthic classes poorly compared to more dominant classes. Patchily distributed habitats declined in area more quickly than clumped distributions. This concurs with the finding of the current study where, especially coral classes, declined in area as spatial aggregation increased. This has clear implications when choosing spatial and thematic scales for mapping and survey designs based on such data sets.

The two main advantages of optical remote sensing for this study have been, firstly, the ability to seamlessly map benthic cover and bathymetry across the whole system of lagoons, including very shallow waters over coral normally inaccessible to acoustic surveys. Clear, shallow waters along the Ningaloo coast naturally lend themselves to such optical remote sensing methods. The second advantage was coverage of the coastal terrestrial component, adjacent to the reef which allowed for mapping tracks, vegetation cover and bare areas in the landscape.

Findings from this study can be used for management and monitoring. A number of possible indicators include coral cover, cover of the macroalgae, sand, limestone or rubble. Some of the past studies which mapped large scale reef systems focused on geomorphic aspects (Ahmed and Neil 1994) or biological studies (e.g. Andréfouët and Payri 2001, Roelfsema *et al.* 2002). Very few studies reported in the literature have mapped very large areas of coral reefs using remote sensing. One such study by Lidz *et al.* (2006) in the Florida Keys used aerial photomosaics and expert visual photo-interpretation approach to map a survey area similar in size to the current study (3 140 km²) and mapped 19 benthic communities. Lidz *et al.* (2006) supplemented their visual interpretation with the data from hydrographic survey (bathymetry) and created maps of seabed habitats and topography, similar to what the current study has achieved by combining benthic classes and topographic classes into one classification using object oriented classification. The advantage of the approach adopted here is that, once a single rule set was developed, it was transferable to other parts of the reef without further intervention by the operator, making it a more objective and repeatable approach. Analysis of the combined habitat and bathymetry (with its derivatives) dataset illustrates that many areas along the reef may be uniform in cover type, yet exist in different bathymetric settings (slope, aspect as well

as depth) and conversely, areas highly uniform in morphology may have different cover types. These two data sets complement each other. As data sets such as the one created for the Ningaloo Reef become more widely available, it should provide more impetus to evaluations using landscape ecological theory, already well advanced in terrestrial environments (Kendall and Miller 2007).

Digital data sets and maps, such as those created during this study are effective tools to help understanding past (Lidz *et al.* 2006, Dustan *et al.* 2001) and current distributions of reefs (Cassatta and Collins 2008). The ability to visualise the reef settings, patterns of distributions and degree to which different parts of the reef are connected are vital in designing surveys and monitoring programs. This study also delivered a comprehensive data set describing the adjacent coastal environment including vegetation cover and tracks, important in understanding patterns of human access and potential impacts from human activities. Future work could examine in more detail spatial patterns, distribution along the reef and relative sizes of particular benthic cover subsets. This could be undertaken in combination with bathymetry and its derivatives generated during this study. An example of such investigation could be algae grazing halos which exist along the coast, at scales ~ 100-200 m in diameter. Additional data sets such as exposure to prevailing winds and currents, turbidity, position in relation to major bathymetric features (channel passes, slopes, flat-bottomed lagoons) and geomorphology could aid in our understanding of the distribution of biota.

With the advent of satellite-based hyperspectral sensors, more cost-effective and repeatable classification methods will become possible. However, the relatively low (~20 m) spatial resolution of new hyperspectral satellites will not be able to identify fine-scale reef structures and as many “pure” pixels of different habitat types. Transferring the classification scheme to current multispectral sensors with a higher spatial resolution may be possible, but would require down-sampling due to lower spectral resolution and would possibly result in a loss of spectral information and ultimately fewer habitat classes.

2.5 Summary and conclusions

Effective management and monitoring of large marine protected areas requires detailed baseline data on distribution of benthic habitats. Large areas with complex bathymetry and very clear waters such as at Ningaloo Reef naturally lend themselves to the application of optical remote sensing as a means of gathering data on benthic cover and depth. An airborne hyperspectral remote sensing mission of the Ningaloo Reef was flown in April 2006 over 10 days to acquire data over 3 400 km², at 3.5 m pixel resolution, using 125 bands in the visible to near infrared range of the electromagnetic spectrum and 21 bands sensing over the water areas.

Hyperspectral data have been corrected for the influences of the atmosphere, air-water interface, water depth and water constituents (phytoplankton, suspended matter and Gelbstoff absorption) using the physics-based Modular Inversion and Processing System (MIP). Bottom reflectance in the visible range (450-900 nm) have been used to detect and map the distribution of 46 benthic classes such as sand, limestone pavement, rubble, macroalgae and different coral types/growth forms such as tabular, branching, digitate and soft corals. Classification of bottom properties was achieved by linear spectral unmixing and refined by combined fuzzy logic and derivative classification techniques.

The outputs of image analysis contain final classification categories as well as per-pixel probability layers and overall percent cover of corals, macroalgae and sediment. Benthic categories have been

organised into abiotic and biotic components, and then split further into sand, limestone pavement, several coral cover categories and macroalgae dominated classes. These were organised through a look-up table into five thematic information class levels.

Field trips were conducted to collect underwater spectra of dominant, cover forming benthic components and to acquire high resolution benthic cover data for training and validation of the final benthic cover maps. Quadrat, transect and single point sampling approaches were used to collect nearly 3 500 field validation points. Accuracies of classification range from 70 % or higher depending on the class and class generalisation level. Bathymetry data have been processed to create slope and aspect images to assist in understanding the distribution of benthic cover types. Further, combined depth, aspect and slope images can be used in an object-oriented classification to create topographic classes which can aid in understanding of the habitat distribution as well as, for example, designing stratified sampling schemes for detailed biodiversity studies or long-term monitoring.

This study has mapped 762 km² of the Ningaloo Reef which was comprised of 7.6 % of coral, 51.5 % of algae and 41 % of sand and limestone pavement. Tabulate corals dominated all other coral categories (36.7 %) and the majority (66 %) of coral distribution was as classes made up of mixes of dense to continuous tabulate coral, sparse digitate coral, soft coral and sparse submassive and massive corals. Continuous to patchy digitate and tabulate coral made up approximately 10 % of the coral cover, while “blue tip” *Acropora* was approximately 8.5 %. The majority of the hard coral occurred as either very dense (continuous >90 %) cover or as patchy distribution (20-45 %). A number of coral assemblages were more commonly found near the shore (up to 500 m offshore), for example class “Dominant soft coral, sparse hard coral and macroalgae with limestone pavement” made up 15 % of the near shore environment compared to ~10% in the study area or 8 % in the sanctuary zones. Within the mapped areas (up to 20 m depth), Bateman sanctuary zone had the largest proportion of hard coral classes, followed by Murat, Mandu and Maud. Bateman had twice the percentage cover coral compared to the whole study area (14 % vs. 8 %), whereas Murat, Mandu and Maud had between 6.5-7.6 % coral cover). Lakeside Sanctuary zone had the least coral cover (0.06%) with majority being sand (92 %). Bundegi, Murat and Tantabidi sanctuary zones had the largest proportion of macroalgae mosaics while most southern sanctuary zones, Turtles, Gnaraloo and 3-Mile, had the largest proportion of limestone pavement within the area mapped in this study.

Topographic and geomorphic classification identified valuable applications which combined slope, aspect and substrate into one seamless data set. The rule set developed for the Ningaloo Reef was tested on five different areas and allowed consistent mapping of these seascapes. From the point of view of sampling design, monitoring or biodiversity surveys is it often important to consider topographic setting as this information can assist and save a lot of time in the field. The overlay of single habitat classes over topographic classification highlighted the value of processing data for both, habitat and bathymetry in one, seamless process.

This application shows that it is possible to map coral reef habitats over large areas and that hyperspectral remote sensing is well suited for automated mapping tasks. This baseline data can be used for ongoing and future monitoring programs using the same or simpler satellite-based multispectral sensors such as QuickBird or WorldView2 to detect change over areas of interest. Hyperspectral sensors provide a non-invasive and cost-effective approach to mapping and monitoring the extent and condition of reefs over large areas because of their capability to identify reef components on the basis of their spectral response.

Habitat classes were described quantitatively and the hierarchical approach to habitat classification facilitates access and use by end-users with different requirements for thematic detail. This includes per-class probability maps. The current classification provides hierarchical structure for benthic components and a simpler, flat structure for topographic variables and a classification which combines topographic and benthic variables developed for a range of areas along the reef.

3 HYPERSPECTRAL IMAGERY FOR LANDSCAPE CHARACTERISATION ALONG THE COAST OF THE NINGALOO MARINE PARK, WESTERN AUSTRALIA

Halina T. Kobryn, Lynnath E. Beckley, Viki Cramer, Dennis Rouillard, Peter Hausknecht, Jessica Bunning, Simon Wee, Julien Noyer and Luisa D'Andrea

3.1 Introduction

Acquisition of hyperspectral data for mapping of the marine habitats of the Ningaloo Reef provided a unique opportunity to extend this mapping to the adjacent coastal area. It is highly relevant to map vegetation cover, sediment, tracks and coastal access points given that human use of the area is growing and likely to increase (DEWHA 2010, Smallwood *et al.* 2011). The main aim of this part of investigation was to examine the landscape along the coast at Ningaloo using hyperspectral remote sensing. The specific objectives were:

- To provide broad classification of the vegetation along the Ningaloo coast with particular attention to shrubs and trees
- Map vegetation condition such as vegetation greenness, plant senescence, moisture stress and the distribution of vegetation cover including mangroves, coastal vegetation and bare substrate type
- Delineation of tracks through the dune systems and adjacent coastal plain
- To examine the spatial density of off-road vehicle tracks in the Ningaloo region and investigate the relationship between track density, total track length and land tenures
- To evaluate the potential impacts of four-wheel drive vehicles on vegetation communities of the Ningaloo coast.
- Determine the number of tracks providing access to sanctuary zones of the Ningaloo Marine Park in order to evaluate latent risks if visitors' numbers were to increase.

Arid coastal areas of the Ningaloo Reef have been mapped in this project in a sequence which corresponds to the above objectives (i.e. soils, vegetation and tracks) and will be introduced in the following section. A brief introduction about the climate, geology, soils and vegetation is followed by introduction to impacts of 4WD vehicles on the coastal environment and finally, remote sensing methods for mapping landscape components of soils and vegetation.

3.1.1 Overview of the study area

Climate

The hot and arid climate of the Ningaloo coast contrasts with warm, semi-arid conditions in the south. The mean annual rainfall at Cape Range is approximately 300 mm and is largely exceeded by the evaporation rate of 1700-3050 mm (Bureau of Meteorology 2011). Due to this difference, run-off is very low and associated with high rainfall cyclonic events (Bureau of Meteorology 2011). The

frequency of these events is likely to increase due to climate change, resulting in an increase in associated problems of erosion (Pachauri and Reisinger 2007).

Geology and geomorphology

The whole Ningaloo coast lies within the southern Carnarvon Basin geological region and is characterised by limestone features, unstable dune systems, sand, coastal plains and outwash alluvial plains (Wyrwoll *et al.* 1993, WAPC 1996, Collins *et al.* 2003). The Cape Range geological province includes important mineral resources including limestone, oil and gas. Large areas of the coast are characterized by unstable dune systems and are susceptible to disturbance, especially the Cape Range ridge dunes and coastal dunes (Collins *et al.* 2003). The most significant geological structure of the northern Ningaloo coast is the Cape Range with its anticline structure which extends over 100 km along the length of the peninsula, the dissected plateau, gorges, extensive cave system and marine deposits (Wyrwoll *et al.* 1993, Allen 1993, Department of Planning and Infrastructure 2004).

The geology of the western Cape Range slopes is dominated by calcarenite Miocene formations, with the three major units being Tulki limestone, Vlaming sandstone and the Pilgramunna formation (Wyrwoll *et al.* 1993). The unique karst geomorphology of the range has been produced by the erosion of these carbonate rocks (Allen 1993, Boulton *et al.* 2003). There are also major iron ore deposits in the region, which contribute to the above average iron concentration of marine sediments (Alongi *et al.* 1996). The most prominent rock types on the terraced lower slopes are the quartzose calcarenite Milyering member and the relict coralgall Jurabi member, both of Pleistocene age (Van de Graaff *et al.* 1980). The coastal plain is occupied by the more recent Tantabiddi coralgall deposit, which is partly covered by alluvial fans of Pleistocene and Holocene ages. The active dunes and beaches consist of quartzose calcarenite (Wyrwoll *et al.* 1993).

Soils

Red deep sand is the dominant soil type on the coastal plain of the Exmouth soil province, with some red loamy earth found on the alluvial fans and the escarpment, calcareous deep sands on the coastal dunes and calcareous shallow loams at higher elevations (Tille 2006). The geomorphic surveys conducted at Ningaloo (Hesp and Morrissey 1984, Hesp 1986) are the only recorded studies showing the detailed spatial distribution of Cape Range soils, however, conventional soil maps are poorly suited for use in conjunction with high resolution landscape data obtained in digital terrain analyses (Zhu 1997).

Vegetation

The Ningaloo Coast lies within the Eremaean Botanical Province (the arid zone), the largest botanical province in Western Australia (Erickson *et al.* 1973, Beard 1990). The province overlaps two climatic regions, the winter rainfall region and summer rainfall region. Therefore, it is biologically rich with flora from temperate, tropical and arid biogeographic provinces that are unique to the area, with some 20 endemic taxa (Beard 1990, Keighery and Gibson 1993). The vegetation is dominated by grasslands, low woodlands, coastal strand vegetation, low shrublands and mangroves (Erickson *et al.* 1973, Beard 1990, Keighery and Gibson 1993). The regional vegetation survey and mapping was undertaken by Beard (1975) and later by Payne *et al.* (1980). Beard (1975, 1990) described the vegetation as a mix of *Acacia* shrublands with hummock grasses (*Triodia* and *Plechtrachne*) in the

understorey. Trees are generally absent except in watercourses, including gorges of the Cape Range in the north.

Ningaloo's coastal biological communities are characterized by fragile Holocene dunal habitats, hard coastal limestone platform with grasslands and arid perennial shrubs. The main types are represented by *Acacia*, *Eremophila*, *Cassia*, *Atriplex*, *Triodia* and *Eucalyptus* (Erickson *et al.* 1973, Keighery and Gibson 1993, Wajon 2008).

The beach habitat of Ningaloo consists of carbonate sand, often covering limestone (Cassata and Collins 2008). The beach is mostly unvegetated, however, flora such as spinifex (*Spinifex longifolius*) is quite common. Small stands of *Acacia coriacea* and *Acacia rostellifera* with clumps of *Atriplex* sp. form the shrubby component of the dune vegetation (Erickson *et al.* 1973, Keighery and Gibson 1993).

The saltmarsh habitat is located along the intertidal and supratidal shores of low energy coastlines and consists of muddy or silty terrigenous sediment (Bancroft and Sheridan 2000). It contains salt-tolerant plants and low shrubs mixed with bare salt flats. Common saline communities include *Atriplex vesicaria* and several other low shrubs of the Chenopodiaceae family (*Rhagodia* sp., *Salsola kali*, *Sueda* sp., *Trelkeldia* sp.) (Erickson *et al.* 1973, Keighery and Gibson 1993).

Ningaloo's mangal habitat, such as at Mangrove Sanctuary and Yardie Creek that are depicted in Figure 82, contain the common *Avicennia marina*, *Rhizophora stylosa* and *Bruguiera exaristata* mangroves. They typically grow in the upper intertidal zone on essentially muddy, silty clay substrate (Alongi *et al.* 2000). The mangrove roots provide substrates for various gastropods (e.g. *Natica*, *Cerithium*, *Stombus*) and mangrove crabs (*Scylla serrata*) (Bancroft and Sheridan 2000). Burrowing worms and insects also inhabit the area and the mangal habitat provides refuge for the juveniles of various fish species (Cassata and Collins 2008).



Figure 82.a) Mangal habitat at Yardie Creek b) and at Mangrove Sanctuary, Ningaloo.

Invasive plants in the region include grasses such as buffel grass (*Cenchrus ciliaris*) introduced for grazing which replaced much of the *Triodia* grasslands along the coast (Keighery and Gibson 1993) (Figure 83).



Figure 83. Buffel grass invasion near Mandu Mandu in Cape Range National Park, Ningaloo.

3.1.2 Ningaloo coastline and off-road vehicles

Over recent years, Australia has witnessed a significant increase in the sales and usage of four-wheel drive vehicles and Sports Utility Vehicles (SUVs) (Federal Chamber of Automotive Industries 2011). They have become more readily available and affordable to meet growing demands from adventurous customers, including tourists and a younger retiree market, who desire to tackle mud, sand, gravel and water areas where standard vehicles fail to access (Taylor 2001). A record of 1 049 982 vehicles (truck, standard cars, etc.) was sold in Australia in 2007, which marked a 9.1 % increase over 2006. In 2010 1 035 574 vehicles were sold, 10.5 % increase on 2009. Of the additional sales 31 % were SUVs and 17 % were 4x4 pick-ups, comprising a major proportion of the overall market growth and generating a lot of economic activity through sales and rentals (Federal Chamber of Automotive Industries 2011).

Leisure activities along coastal areas frequently involve the use of off-road vehicles being driven over beaches and sand dunes (Harvey and Caton 2003, Defeo *et al.* 2009). For many years their detrimental long-term effect on coastal habitats, organisms and ecosystems has been a controversial issue in Australia and throughout the world (Godfrey and Godfrey 1980). As early as the 1970s, the impact of off-road vehicles on Australian coastlines was recognized by the Government as causing disturbance to wildlife and damage of wilderness, including loss of vegetation resulting in soil erosion (House of Representatives 1977). Similarly, Australian ecologists and environmental groups have been alarmed by the potential impact of off-road vehicles on sensitive ecosystems (e.g. Schlacher *et al.* 2007). Sadly, although the ecological attributes of beaches and dunes are publicly less known compared to their social and economic aspects, their disappearance risks creating catastrophic and irreversible consequences to vital ecosystem functions, biodiversity and habitat (Godfrey and Godfrey 1980).

In Western Australia, over 80 % of all tourism and recreation occurs in the coastal zone (Priskin 2003a, Harvey and Caton 2003). The Ningaloo coastline in the remote northwest of Western Australia has recently transformed into a highly popular tourist destination for international, domestic and interstate visitors eager to explore the Ningaloo coastline (CALM and MPRA 2005). This rise in

tourism has generated additional employment opportunities, adding to the fishing, agriculture and Defence Department jobs (Wood and Dowling 2002, Wood and Glasson 2005). The Ningaloo community needs to effectively manage the pressures from escalating visitations in order to conserve resources and achieve long-lasting benefits from tourism. The near shore waters, foreshore and coastal hinterland of the Ningaloo coastline offer a superb diversity of recreational opportunities for tourists (CALM and MPRA 2005). Approximately 200 000 people visited Ningaloo in 2004, partaking in a range of coastal activities including wildlife viewing, boating, fishing, diving, snorkelling, camping, touring and four wheel-driving (Western Australian Planning Commission 2004) (Figure 84). People's entitlement to access the beach and foreshores is naturally presumed by tourists (Kay *et al.* 1997) and to support rising visitation and associated expectations, accommodation and tourist operators have expanded. However, to achieve sustainable tourism, better planned access to coastal areas is required, for, although recreation in coastal areas is distributed over a vast area, significant degradation of coastal nodes has occurred at locations of high human intensity (WAPC 2004).

Degradation is the result of littering, trampling of vulnerable habitat, insensitive disposal of human waste and damage to coastal environments by four-wheel drive and other off-road vehicles. Remote natural areas are particularly susceptible to the impacts of four-wheel drive recreation, creating complex coastal management issues (Priskin 2003a, Defeo *et al.* 2009). As visitor numbers rise, there is risk of increasing environmental degradation, particularly on the more popular foreshore nodes or adjacent to marine access points (CALM and MPRA 2005).



Figure 84. Example of recreational activities, fishing along the rocky shores along the Ningaloo coast (left), Tantabiddi boat ramp (top right) and typical coastal camp at Ningaloo (bottom right).

Off-road vehicle use along Ningaloo coast

Vehicle traffic passing through the Cape Range National Park from the north to Tantabiddi, increased from 13 940 during 1989-1990, to 30 144 vehicles during 1998-1990. This marked a rise of 42 000 to 84 000 individual visitations (WAPC 2004). The intensification of traffic is causing greater pressure on the existing coastal access network and some areas can no longer support the increased usage. Not satisfied with traditional access areas, visitor often use off-road vehicles to traverse past the

supervised zones and look for more remote locations (Taylor 2001). The presence of four-wheel drive vehicles at Ningaloo is shown in Figure 85.



Figure 85. Four-wheel drive vehicles at Cape Range (left), four-wheel drive vehicle on the beach at Yardie Creek (top right) tracks from off-road vehicles on the beach at Yardie Creek (bottom right).

Inadequate track management risks indiscriminate access to new spots along the coast, as well as the chaotic spread of camping, fishing and snorkelling sites in inappropriate settings. The unplanned expansion of additional tracks and low standard of roads could cause even more detrimental impacts on the environment (WAPC 2004). A strategy to organise sustainable tourism coastal development and guide integrated land use and transport planning along Ningaloo coast has been undertaken through the *Ningaloo Coast Regional Strategy Carnarvon to Exmouth* (WAPC 2004).

Impacts of off-road vehicles on soils

The force of rolling wheels on arid soil can cause soil compaction, which decreases water infiltration and increases runoff, resulting in severe erosion (Webb 1983). Soil stabilizers include macrofloral elements (plants), microfloral elements (lichen, fungal and algal crusts) and inorganic elements (soil crusts) (Webb 1983). When these stabilizing plants are crushed, the susceptibility to wind and water erosion increases, which accelerates decomposition of organic matter, weakens soil stability and causes inorganic surface crusts. These surface crusts increase runoff, inhibit the germination and emergence of seedlings and reduce water penetration, resulting in a harsher environment for plants and animals to survive (Dregne 1983). The degree of loss is dependent on the intensity of use and may vary from site to site. Smaller shrubs are often the first to be damaged or eliminated (Taylor 2001) (Figure 86).

Soil vulnerability to water erosion can be directly related to moisture and organic content and inversely related to clay content. Vulnerability to wind erosion is positively correlated with the degree of sorting and negatively correlated with soil compaction (Van Gool *et al.* 2005). This assessment technique also takes into account the soil's position in relation to surrounding landforms, with vulnerability to water erosion being greater on steep slopes than flat surfaces and vulnerability to wind erosion being greater on crests than in depressions.



Figure 86. Track over semi-arid soil, 1km south of Yardie Creek, Ningaloo.

Impacts of off-road vehicles on vegetation

Hardy plants in the coastal landscape including the dunes can usually withstand natural types of biological and physical harm, including fire, high speed winds, sand blasts, salinity and drought (CALM and MPRA 2005). However, trees and shrubs are the least resilient and suffer widespread degradation from the impact of off-road vehicles (McLachlan and Brown 2006, Groom *et al.* 2007, Defeo *et al.* 2009). Ultimately, continuous traffic flow prevents dune re-vegetation. Research has shown that vehicle traffic over dunes decreases both the total cover and height of vegetation (Rickard *et al.* 1994). The destruction of stabilizing vegetation allows aeolian activity to reduce the dune height, cause erosion blowouts and ultimately decrease the ability of the dune system to endure storm winds and waves (Viles and Spencer 1995, Priskin 2003b). Intense, continued use of a single path over a dune can result in lowering of the dune crests, ultimately causing the dune to split and significantly altering the dune topography (Rickard *et al.* 1994) (Figure 87).



Figure 87. Evidence of track making at Ningaloo in the foredunes and through coastal blowouts.

Management of the Ningaloo coast is shared between the adjacent pastoral land lessees and the Department of Environment and Conservation (DEC), to facilitate access for visitors to and along the coast (WAPC 2004). However, despite the management strategies employed by pastoral stations, considerable degradation of the delicate environment, particularly coastal vegetation, has led to erosion and remobilization of sediment (WAPC 2004). Environmental degradation is linked to the

uncontrolled development of access roads, leading to the proliferation of tracks (Schlacher and Thompson 2008). Further insufficient management of four-wheel drive vehicle access along Ningaloo could cause the erosion of the fore-dune system (CALM and MPRA 2005). Consolidation and supervision of access tracks and camping grounds is necessary to reduce the damage to coastal vegetation and allow degraded areas to recover (CALM and MPRA 2005). If not managed, tracks will increase in density and continue to spread out from inland access points towards the coast (Priskin 2003a).

Hesp and Morrissey (1984) surveyed the northwestern section of the Cape Range Peninsula and found highly sensitive dune vegetation, with exposed sand sheets developing easily and being pushed forward by powerful southerly winds. They cautioned against the removal of dune vegetation as they considered restabilisation of sand sheets and dune blowouts to be difficult, given the local climatic conditions. The same survey also found the adjacent coastal plain potentially vulnerable to flooding from episodic rainfall events such as tropical cyclones. In WA, the risk of fluvial erosion is particularly high in summer, when reduced vegetation cover can result in sediment “flushes” during high rainfall events (Van Gool *et al.* 2005). It is very likely that climate change during the 21st century will increase the frequency and intensity of these events (Intergovernmental Panel on Climate Change (IPCC) 2007), which would amplify the problem of erosion further. If the risk of erosion by wind and water could be determined, management efforts could then be focused on the appropriate means of soil loss prevention.

Off-road vehicles can also spread invasive or noxious plants (Taylor 2001). Exotic plant invasion is evident along the Ningaloo coastline, particularly buffel grass invasion, which is partly the result of disturbance from track making and unregulated camping (Figure 83).

Along many areas of the Ningaloo coastline, visitors can view, or be in very close proximity to, the ocean while travelling along the coastal roads and this also accelerates uncontrolled access to the beach (WAPC 1996) (Figure 88). It is also a challenge to direct visitors to appropriate spots as long stretches of coastline are easily accessible by many tourists (WAPC 1996). Large areas outside the Cape Range National Park, such as south of Yardie Creek are not actively managed and therefore visitors are free to use the area as they please (WAPC 1996).



Figure 88. Tracks observed on saltmarshes nearby Bundegi Coastal Park, Ningaloo.

Impacts of off-road vehicles on wildlife

Most of the impacts of 4WD vehicles on wildlife are due to the motion and sound generated by the vehicles. However sediment displacement by tyres has also been found to have negative effects, for example on lizards (Brattstrom and Bondello 1983). Havlick (2002) showed that wildlife such as birds, small mammals and reptiles are disturbed by four-wheel drive vehicle. Beach buggies are considered to inflict even more damage on sand dune systems than four-wheel drive vehicles due to the limited traction of their rear-wheel tyres, which creates a lot of spin in the sand and excessive sediment displacement (Brattstrom and Bondello 1983). Along the Ningaloo coastline the detrimental effect of buggies on dune systems and the associated wildlife does not appear to be recognised or investigated.

A total of 144 bird species has been recorded on North West Cape, of which one-third are seabirds, shorebirds and waders, both resident and migratory. There are approximately 33 species of seabirds found in the Cape Range National Park, 13 of which are resident and the other 20 are migratory birds or occasional visitors (CALM and MPRA 2005). The main rookeries in the Ningaloo area are found at Mangrove Bay, Mangrove Point, Point Maud and the Mildura wreck site (CALM and MPRA 2005). Other places such as Winderabandi Point are also important bird rookeries. Levels of the use of the coast in the reserves vary considerably. In terms of recreational vehicle and four-wheel drive usage, there is a high level of use around Coral Bay and Point Billy (adjacent to Ningaloo Station) and low use adjacent to Cape Range National Park where driving on the beach is prohibited. Given this diversification of usage and the associated management strategies to control such use, no current major pressures on seabirds, shorebirds and migratory waders in the reserves have been recorded (CALM and MPRA 2005). However, there is discussion for the implementation of spatial controls to offer protection to seabird nesting and roosting areas and increase education and awareness with shoreline users (CALM and MPRA 2005).

Green turtles (*Chelonia mydas*), loggerhead turtles (*Caretta caretta*) and hawksbill turtles (*Eretmochelys imbricata*) inhabit the Ningaloo region for nesting (CALM and MPRA 2005). One of the most significant threats faced by the turtles is the increasing pressure from rapidly growing tourism to the region, which is significantly interfering with turtle nesting along the beaches (CALM and MPRA 2005). Vehicle track making and unregulated camping by visitors, means that turtles are frequently disturbed during nesting, resulting in them abandoning the nest and escaping to the ocean (Hosier *et al.* 1981). The light pollution emitted by car headlights traversing along tracks or from car parks can also disturb nesting turtles and disorientate emerging hatchlings (Hosier *et al.* 1981). Careful consideration of the present road network along Ningaloo's coastline is required, as well as attention to planning of building new coastal roads, which is sensitive to the exposure, these precious coastline communities will endure from the available access routes and subsequent increased visitation.

3.1.3 Remote sensing of soils and vegetation

Application of hyperspectral imagery to soil analysis

Sediment is a product of the slow weathering of solid rock or carbonate reef structures. The separation from its consolidated parent material increases the possibility of its relocation by environmental processes. Despite being removed to an area of differing geology, relocated sediment will retain similar physical and chemical characteristics to the parent material, provided no significant

weathering has occurred (Jenny 1994). It is thus possible to determine the areal extent of dispersal within a specific region by carefully analysing the morphology and composition of all sediment found within that region. The accurate identification of the sediment's spatial distribution is dependant on how accurately the sediment characteristics can be identified.

A variety of soil classification systems have been developed, with each designed for a specific purpose. The Soil Taxonomy system was produced in 1975 for the general interpretation of US soils, followed by a similar worldwide classification in the 1980s called FAO Legend, now known as World Reference Base (Rossiter 2007). Some classification systems such as the Australian Soil Classification consider deposited layers (e.g. alluvial fans) to be phases of the soil layers below if they are less than 0.3 m in thickness (Isbell 1996). Another drawback to existing classification systems is their reliance on vertical soil profile information, which necessitates expensive and time-consuming soil surveys and potentially damaging sample extraction procedures.

In recent years, hyperspectral imagery has been used in terrestrial soil analysis. Asner and Lobell (2000a) found variation in soil reflectance to have a stronger influence on total landscape reflectance than variation in reflectance from vegetation. A Multiple Endmember Spectral Mixture Analysis (MESMA) was used by O'Kin *et al.* (2001) to determine soil types and proportion in arid and semi arid areas with up to 90 % reliability. Shepherd and Walsh (2002) created a method of generating spectral libraries for prediction of soil properties by using multivariate regression to detect correlations between reflectance and soil attributes.

Due to a lack of remote sensing data in the past, there have been few studies of soils on the Ningaloo area. The HyMap survey of 2006, as well as the establishment of the Ningaloo Research Program and the Ningaloo Collaboration Cluster, has lead to a significant number of studies being initiated in recent years. One such study was conducted by D'Andrea (2007), who used a subset of the HyMap data to map vegetation cover and human impacts in the area around Coral Bay and found a correlation between the concentration of invasive buffel grass and the underlying geological unit.

When attempting to record soil properties over a wide area, it is not feasible to rely exclusively on physical sample measurements, therefore, the use of aerial surveying methods must be employed. Remote sensing involves non-invasive measurement of the amount of solar radiation reflected by the Earth's surface at multiple wavelengths of the electromagnetic spectrum. Variations in the measured reflectance of an area of sediment can reveal its salinity, moisture content, mineral and organic matter concentration, texture and surface roughness (Huete 2004). However, commonly used broad channel multispectral sensors such as Landsat TM have insufficient spectral resolution for distinguishing subtle variations in surface reflectance (Asner and Lobell 2000a).

In order to both identify and classify tracks composed of sand, clay and limestone, a remote sensing approach is required that can best discriminate between dry vegetation, bare areas and tracks within the landscape. In arid ecosystems, vegetation cover and condition commonly fluctuate due to large variations in land cover and climate (Asner *et al.* 2000). These changes in dry plant material, leaf litter and bare soils display only discrete variability in the reflectance of their spectral properties in the shortwave spectra (Asner *et al.* 2000, Asner and Lobell 2000b). Therefore, to monitor semi-arid environments, it can be difficult to discriminate such reflectance with broadband, multispectral remote sensing (Hill and Mégier 1994) and hyperspectral imagery offers better opportunities.

The highest spectral resolution remotely sensed data available is hyperspectral imagery. It allows near-continuous measurement up to 2.5 μm (Cocks *et al.* 1998), which facilitates the detection of substances not observable using other forms of remote sensing. The ability to view landscape scale variations in surface properties, while simultaneously observing detailed variations within micro-environments, makes hyperspectral imagery the most suitable means available for detecting patterns of sediment movement and mapping these patterns over large-scale areas.

Application of hyperspectral imagery to vegetation mapping

In arid ecosystems, vegetation cover and condition commonly fluctuate due to large variations in land use and climate (Asner *et al.* 2000). These changes in dry plant material, leaf litter and bare soils display only discrete variability in the reflectance of their spectral properties in the shortwave spectra (Asner and Lobell 2000b). Therefore, to monitor semi-arid environments, it can be difficult to discriminate such reflectance with multispectral remote sensing (Hill and M egier 1994).

Hyperspectral remote sensing provides a good alternative for the characterisation of foliage and bare soils (O’Kin *et al.* 2001). However, applying spectral indices alone, such as the normalized difference vegetation index (NDVI), rarely succeeds in detecting all significant biophysical properties of a semi-arid ecosystem, particularly after regeneration (O’Kin *et al.* 2001). Rather, by combining the automated spectral mixing approach of hyperspectral imagery, using the continuous shortwave spectrum (0.4 μm to 2.5 μm), quantitative estimates for landscape classes can be achieved, as well as assessments of qualitative material (Hill and M egier 1994).

Remote sensing techniques have been widely used to map vegetation that is native or invasive to an environment (Thankappan and Reddy 2004, Schmidt and Skidmore 2003) and vegetation in arid environment, that is woody or halophytic (Asner *et al.* 2000, Lewis 2002).

3.2 Methods

3.2.1 Study area

The study area was located from Red Bluff (24°3'S, 113°26'E) to Exmouth (22°2'S, 113°7'E) along 300 km of the coastline and up to 2 km inland (Figure 89).

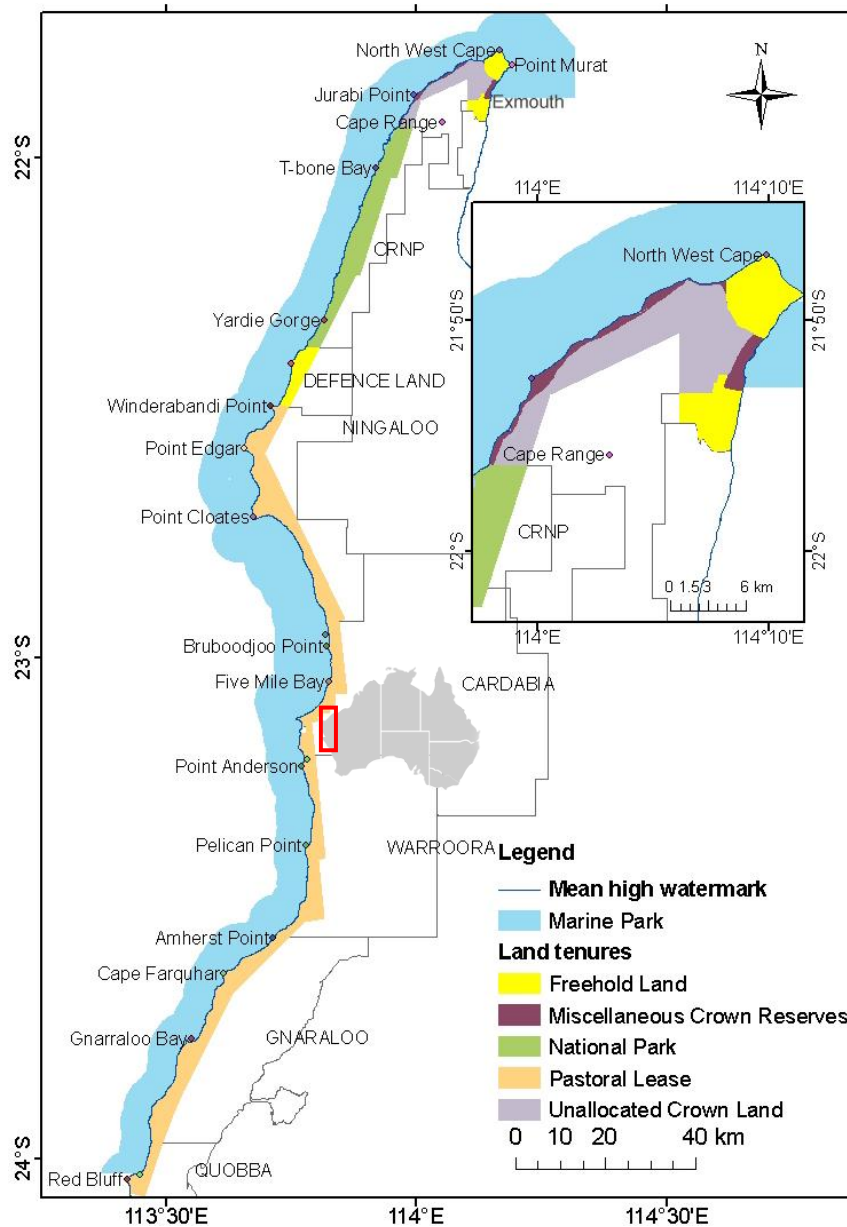


Figure 89. Ningaloo study area and survey extent showing the coastal land tenures and pastoral lease boundaries adjacent to the Ningaloo Marine Park.

3.2.2 Data Processing

Acquisition of HYMAP data was described in an earlier chapter. HyVista carried out the necessary corrections for atmospheric scattering and absorption using HyCorr and delivered the data in band-interleaved by line (.bil) format for use in ENVI. The terrestrial component of the data was filtered with a land mask and corrected for atmospheric effects such as aerosol loading, ozone and column water vapour by Curtin University, using TAFKAA 6S (Gray 2007). As a result, only 109 bands were selected as usable out of the 125 flown by HyMap instrument.

As the data were acquired after prolonged drought in an already arid landscape, for the present study, vegetation was classified into different classes of green only (photosynthetically active) vegetation: *Acacia* spp. dominated, ficus (*Ficus platypoda*), green shrubs in creek lines and gorges, coastal shrubs, mangroves (dominated by *Avicennia marina*, *Rhizophora stylosa*) and tamarisk (not native). In particular, coastal vegetation consisted of a mix of *Acacia spathulifolia*, *Olearia dampieri*, *Thryptomene backeacea*, *Eulalia auera*, *Santalum spicatum*, *Acanthocarpus preissii.*, *Dampiera incana var. incana*, *Salsola tragus*, *Carpobrotus virescens*, *Inidigofera brevidens*, *Dianella revolute var. divaricata* and low herbs and low chenopod shrubs.

Vegetation was first mapped using narrow band indices (ENVI, 2009) (Table 16).

Table 16. The vegetation indices tested in this study for use as vegetation masks in SAM classification (from ENVI 2004). Indices in bold were used for masking vegetation.

Index Category	Vegetation Index
Broadband Greenness	Normalized Difference Vegetation Index
	Simple Ratio Index
	Enhanced Vegetation Index
	Atmospherically Resistant Vegetation Index
	Sum Green Index
Narrowband Greenness	Red Edge Normalized Difference Vegetation Index
	Modified Red Edge Simple Ratio Index
	Modified Red Edge Normalized Difference Vegetation Index
	Vogelmann Red Edge Index 1
	Vogelmann Red Edge Index 2
	Vogelmann Red Edge Index 3
	Red Edge Position Index
Light Use Efficiency	Photochemical Reflectance Index
	Structure Insensitive Pigment Index
	Red Green Ratio Index
Canopy Nitrogen	Normalized Difference Nitrogen Index
Dry or Senescent Carbon	Normalized Difference Lignin Index
	Cellulose Absorption Index
	Plant Senescence Reflectance Index
Leaf Pigments	Carotenoid Reflectance Index 1
	Carotenoid Reflectance Index 2
	Anthocyanin Reflectance Index 1
	Anthocyanin Reflectance Index 2
Canopy Water Content	Water Band Index
	Normalized Difference Water Index
	Moisture Stress Index

In the second step, Spectral Angle Mapper (SAM) using image derived spectra from sites described in the field as unvegetated was run on flightlines, then georeferenced and mosaicked into blocks. As there is quite a variation in vegetation communities from north to south, the final “green” vegetation layer was generalised into six broad classes.

3.2.3 Analysis of the bare sediment component of the landscape

Site descriptions

The field measurements necessary for validation of the hyperspectral data were collected in July 2008. The majority of sampling sites were selected at locations likely to act as sediment sources in future erosion events. These were areas of unconsolidated sediment cover within or adjacent to active or relict drainage channels with potential connectivity to the ocean, as well as exposed aeolian deposits within active dune systems (Figure 90). These areas were located through prior inspection of colour composites images from the HyMap survey. While only Yardie Creek is a permanent source of runoff (CALM and CCWA 2005), the other six major drainage channels surveyed would be the likely suppliers of a large portion of the sediment load received in the Ningaloo Reef lagoon during high rainfall events.

Sub-site locations were selected at various stages of each drainage channel’s longitudinal profile, from the escarpment base to the intertidal zone. Where off-road tracks bisected a site, samples were collected from adjacent areas on both sides of the track. Additional samples were collected opportunistically across a range of surface covers found within the study area (e.g. saltmarsh, alluvial fan, relict dune). The aim of collecting these samples was to represent the full range of sediment types, which could then be compared with sediment classes derived from analysis of the hyperspectral imagery.

Yardie Creek

The first Yardie Creek sample was collected in a narrow stream channel on the north bank of the main Yardie Creek gorge (Figure 91), with the remainder of the samples being collected across an alluvial fan south of the Yardie Creek mouth. The Yardie 2 and 3 sites were located on opposite sides of the main road between Yardie Creek and Coral Bay (Table 17). The north bank was found to be rocky and sparsely vegetated, while the coastal plain further south had more unconsolidated surfaces and denser cover of vegetation.

Osprey Sanctuary Zone

The five Osprey Sanctuary Zone soil samples were collected along a transect from the area adjacent to the sealed main road to the coastal dunes (Figure 92). The Osprey 3 and Osprey 4 subsites were located an equal distance from either side of the unconsolidated Bungarra track. The area contained predominantly unconsolidated sediment with thick shrubland vegetation cover, gently sloping from the crest of the relict dunes to the base of the active dunes in the west (Table 17).

Pilgramunna

The Pilgramunna sampling locations followed the course of the stream channel from the base of the escarpment to the intertidal zone beyond the mouth of the creek (Figure 94), with an additional

sample being collected on the south bank (Pilgramunna 4) for comparison with the streambed sediment. All three subsites located within the stream channel were covered by irregular-shaped limestone cobbles (Table 17). The area was well vegetated, with acacia shrublands in the gorge opening and Spinifex grasslands on the coastal plain.

Bloodwood Creek

The Bloodwood Creek sampling sites were located along the lower course of the stream. A limestone substrate was visible along the stream channel, with a small area of saltmarsh near the coast (Figure 94) (Table 17). The presence of a sandbar separating the mouth of the stream channel from the intertidal zone means that only a combination of a high rainfall event and a storm surge could bring about sediment input into the lagoon. While overall vegetation cover was low, a wide range of vegetation types was observed in the sampled area.

Mandu Creek

The Mandu 1 and 2 samples were collected in the steep Mandu Creek Gorge, and the Mandu 3 and 5 samples being collected in the more gently sloped stream channel on the coastal plain (Figure 94) (Table 17). The Mandu 4 site was an opportunistic sampling of an area of exposed sediment on the coastal plain. The streambed at all sites was covered by a deep, wide layer of rounded limestone cobbles, with sparse vegetation cover in the stream channel itself.

Northern section of Cape Range National Park (Turquoise Bay, Tulki Beach, Trealla Beach and Mangrove Bay)

The northern section of the park was less heavily sampled than the southern section, reflecting the lower density of drainage channels. The Turquoise Bay and Mangrove Bay samples were collected from minor floodways on the coastal plain, a few metres west of the sealed main road in each case (Table 17). The Tulki and Trealla stream channels were sampled on the coastal plain and in the intertidal zone (Figure 95). All streambed sites had a limestone cobble covering. The vegetation cover observed was generally spinifex grassland interspersed with low shrubs.

Tantabiddi Creek and Jurabi Coastal Park

These sites are located outside the Cape Range National Park and the potential for soil erosion through unregulated off-road track-making is thus greater. The wide areas of unconsolidated sediment (Figure 93) and sparse vegetation cover (Table 17) add to the vulnerability of the area to erosion. The Tantabiddi 2 and 3 soil samples were collected adjacent to a small saltmarsh. Large exposed sand sheets and dune blowouts could be seen in the coastal dune fields around the Jurabi site. Despite the shallow stream banks, there was a clear distinction between vegetation cover on the banks and within the creek.

Exmouth Gulf (Bundegi Coastal Park and Exmouth)

Opportunistic sampling was conducted on the eastern side of the Cape Range Peninsula, with a single sample collected from a wide claypan in the Bundegi Coastal Park and a sample collected from a dry stream channel to the north of the town of Exmouth (Figure 90) (Table 17). The density of off-road tracks was observed to be greater in the north-eastern section of the peninsula than in the Cape Range

National Park. Some bank erosion was observed in the Exmouth stream channel. The wide claypans of the Bundegi Coastal Park appeared to be poorly drained. The vegetation cover and underlying substrate north of Exmouth appeared similar to that observed west of the Cape Range.

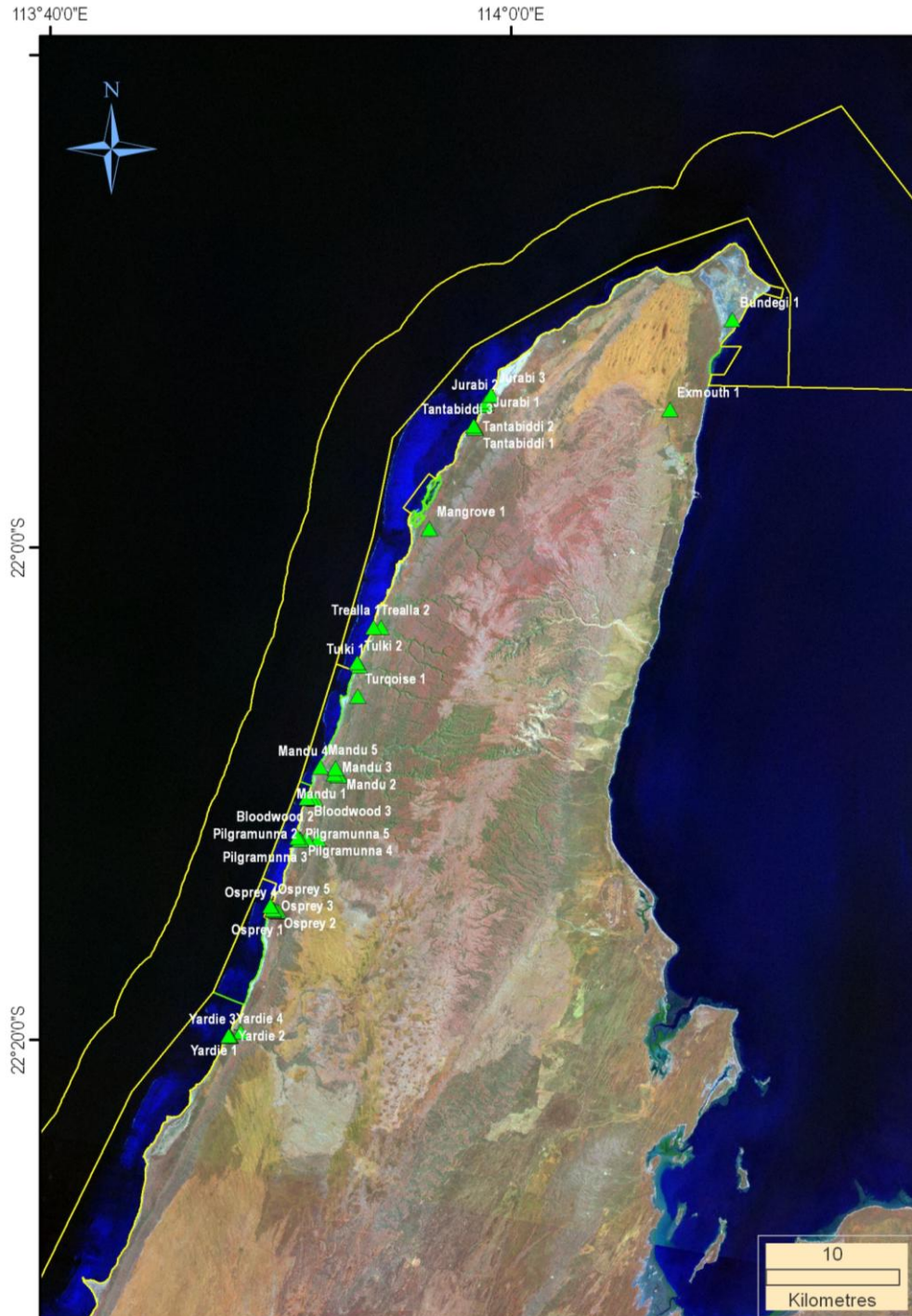


Figure 90. Location of sampling sites (green triangles) for the Cape Range Peninsula soil survey. Yellow lines show the marine park boundaries. Green borders show boundaries of Ningaloo Marine Park sanctuary zones.

Table 17. Site description of field sites for soil and sediment description. Location of all sites is presented in Figure 90.

Site name lat, long (S, E)	Underlying substrate	Nearest road/track	Surrounding landforms	Comments
Yardie Creek 1 -22.3262°, 113.8176°	limestone (pavement)	distant	site in 3 m wide stream channel (steep banks)	sediment between or below rocks only, stream channel enters Yardie Creek
Yardie Creek 2 -22.292°, 113.8102°	limestone (pavement)	10 m west (unconsolidated)	on coastal plain, flat with small limestone outcrops	site surrounded by spinifex and low shrubs.
Yardie Creek 3 -22.329°, 113.8097°	not visible	10 m east (unconsolidated)	on coastal plain. 20 m east of coastal dunes	site surrounded by desert pea, spinifex and low shrubs.
Yardie Creek 4 -22.3287°, 113.8089°	not visible	30 m east (unconsolidated)	near top of coastal dune	site surrounded by desert pea and low shrubs
Osprey 1 -22.2441°, 113.8433°	not visible	10 m north (unconsolidated)	on coastal plain. 20 m east of relict dunes	site surrounded by spinifex and low shrubs
Osprey 2 -22.2473°, 113.8419°	not visible	20 m north (unconsolidated)	top of relict dune, flat	site surrounded by low shrubs
Osprey 3 -22.2431°, 113.8398°	not visible	10 m west	50m west of relict dune, 100m east of coastal dunes	site surrounded by acacia shrubs
Osprey 4 -22.2428°, 113.8393°	not visible	10 m east	roughly equal distance between relict dune and coastal dunes	site surrounded by acacia shrubs
Osprey 5 -22.2403°, 113.8373°	not visible	50 m northeast	undulating dunes, approx. 100 m from shoreline	mostly bare sand, with some low shrubs present
Pilgramunna 1 -22.1946°, 113.8713°	limestone (alluvial fan)	distant	middle of gully, limestone outcrops, steep north bank	site surrounded by spinifex, shrubs and low trees
Pilgramunna 2 -22.1941°, 113.8624°	limestone (alluvial fan)	10 m west (sealed)	culvert with rocky bed	site surrounded by spinifex and low shrubs
Pilgramunna 3 -22.1946°, 113.8581°	limestone (alluvial fan)	50 m north (unconsolidated)	middle of stream channel, shallow banks	low shrubs on north bank, spinifex on south bank, second drainage channel enters from south
Pilgramunna 4 -22.195°, 113.8583°	not visible	100 m north (unconsolidated)	10m south of stream channel. 20 m east of coastal dunes	site surrounded by thick spinifex
Pilgramunna 5 -22.1938°, 113.8563°	limestone (pavement)	20 m (unconsolidated)	intertidal zone (mouth of Pilgramunna).	No surrounding vegetation
Bloodwood 1 -22.1676°, 113.8681°	limestone (pavement)	10 m east (sealed)	Middle of stream bed (roughly 30 m wide).	Site surrounded by spinifex and low shrubs. Soil mostly between rocks.
Bloodwood 2 -22.1670°, 113.8654°	limestone (cobbles)	5 m east (unconsolidated)	Middle of stream bed (10 m wide). Shallow banks.	Marsh vegetation in channel. Spinifex on north bank, buffel grass on south bank.
Bloodwood 3 -22.1670°, 113.8623°	not visible	distant	Low sandbar between end of stream channel and shoreline.	Beach spinifex and salt bushes on top of dunes.
Mandu 1 -22.1513°, 113.8862°	limestone (cobbles)	distant	Middle of stream bed. Smaller gorge opening in southern wall.	Small area of exposed soil. Shrubs present in stream bed and on north bank.

Mandu 2 -22.1513°, 113.8854°	limestone (cobbles)	distant	Middle of channel (10 m wide). Canyon wall on southern side.	Soil under cobbles only. Bed sparsely vegetated. Low shrubs on north bank.
Mandu 3 -22.1505°, 113.8822°	limestone (cobbles)	50 m (unconsolidated)	10 m wide stream channel. Shallow banks.	Soil under cobbles only. Bed sparsely vegetated. Shrubs and low trees on both banks.
Mandu 4 -22.1461°, 113.8827°	limestone (pavement)	distant	On coastal plain. 40 m west of escarpment.	Site surrounded by spinifex and low shrubs.
Mandu 5 -22.1456°, 113.8719°	limestone (cobbles)	100 m south (unconsolidated)	Middle of stream bed (20 m wide).	Soil under cobbles only. Bed sparsely vegetated. Shrubs and spinifex on both banks.
Turquoise 1 -22.0971°, 113.8979°	limestone (pavement)	20 m east (sealed)	On coastal plain. 30 m west of low terrace.	Site surrounded by spinifex and low shrubs. Biological surface cracking and crusting visible.
Tulki 1 -22.0767°, 113.8987°	limestone (alluvial fan)	20 m (unconsolidated)	Narrow stream channel. Roughly 50 m east of dunes.	Site surrounded by buffel grass. Some spinifex and low shrubs
Tulki 2 -22.0746°, 113.897°	not visible	distant	Low sandbar between end of stream channel and shoreline.	Bare sediment
Trealla 1 -22.0503°, 113.9138°	limestone (alluvial fan)	10 m east (sealed)	Middle of stream channel (3 m wide). Steep banks.	Soil between or below rocks only. Low shrubs in channel and on both banks.
Trealla 2 -22.0504°, 113.9084°	not visible	distant	Low sandbar between end of stream channel and shoreline.	Exposed beach sand. Salt bushes and beach spinifex on surrounding dunes.
Mangrove 1 -21.9828°, 113.9477°	limestone (cobbles)	10 m east (sealed)	Middle of stream channel (20 m wide). Low banks.	Soil under cobbles only. Low Shrubs in stream bed and spinifex on both banks.
Tantabiddi 1 -21.914°, 113.9795°	limestone (alluvial fan)	20 m (sealed)	middle of stream channel, shallow banks, approx. 50 m wide.	low shrubs in stream channel, spinifex on both banks
Tantabiddi 2 -21.9143°, 113.9792°	not visible	50 m (sealed)	10 m south of stream channel. 20 m east of coastal dunes	site surrounded by spinifex and some low shrubs
Tantabiddi 3 -21.9128°, 113.9782°	limestone (pavement)	distant	intertidal zone (mouth of Tantabiddi Creek)	site adjacent to boating facility
Jurabi 1 -21.8986°, 113.9868°	not visible	20 m (unconsolidated)	undulating dunes	mostly bare sediment, beach spinifex on some dunes
Jurabi 2 -21.8962°, 113.9869°	not visible	distant	undulating dunes	mostly bare sediment, beach spinifex on some dunes
Jurabi 3 -21.8915°, 113.9906°	not visible	10 m east (unconsolidated)	top of large exposed foredune	bare sediment
Exmouth 1 (-21.8990°, 114.1202°)	limestone (cobbles)	10 m west (sealed)	Middle of stream channel (15 m wide). Steep banks.	Trees along road edge. Streambed sparsely vegetated by shrubs. Spinifex and low trees on both banks.
Bundegi 1 (-21.8372°, 114.1642°)	not visible	5 m northeast	5m from small sand bank	Site surrounded by desiccated samphire vegetation. Some biological crusting visible.

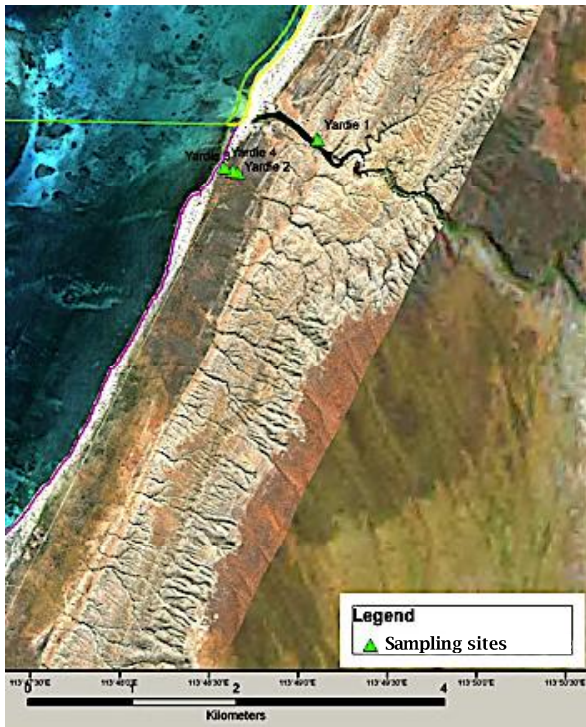


Figure 91. Sampling sites at Yardie Creek and a nearby alluvial fan.



Figure 92. Sampling sites at Osprey Sanctuary Zone, Ningaloo. The unconsolidated former main road can be seen running parallel to the coastline. Current bitumen road is clearly seen in white.

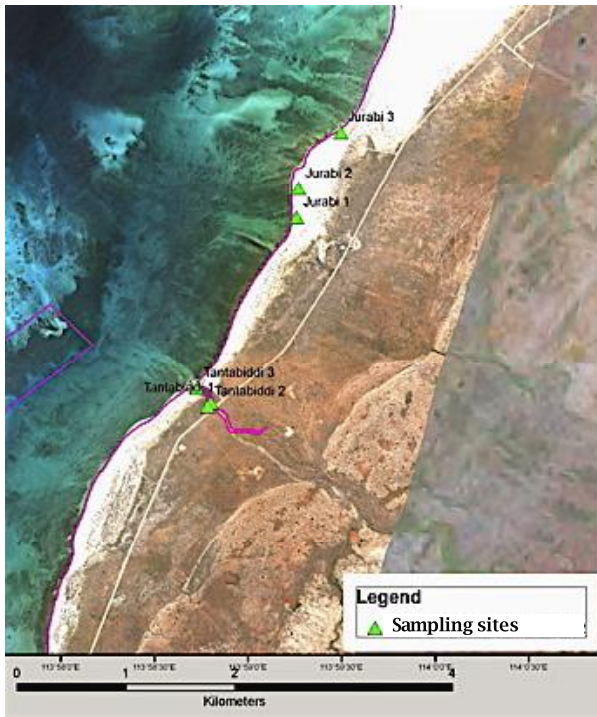


Figure 93. Sampling sites at Tantabiddi Creek and Jurabi Coastal Park.

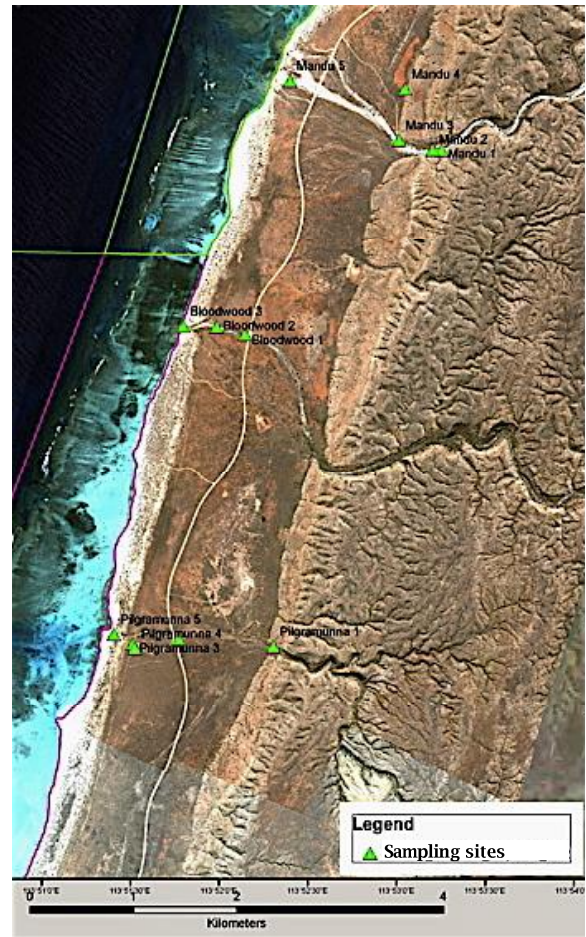


Figure 94. Sampling sites at Pilgramunna, Bloodwood Creek and Mandu Creek. The southern section of Cape Range National Park contains several large gorges carved into the limestone terraces

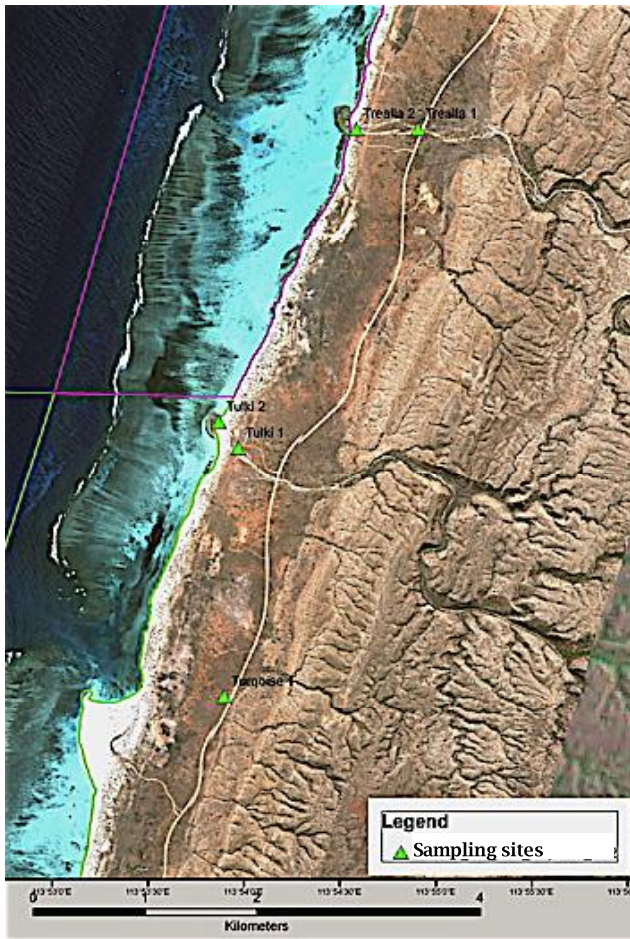


Figure 95. Sampling sites at Turquoise Bay, Tulki Beach and Trealla Beach. The Mangrove Bay site was located further north and is not shown.

3.2.4 Soil analysis

At each site, GPS location and altitude were determined with a Garmin GPSMAP 76CS receiver. Slope gradient was measured with a Suunto PM5 clinometer and aspect was estimated to the nearest of the 16 compass points in areas with slope gradients greater than 5 %. Vegetation cover was recorded in three randomly placed 1 m² quadrats at each sampling location. Within each quadrat, total vegetation cover, litter cover and bare ground were estimated to the nearest 5 %. *In situ* shear strength (N/cm²) of the soil was measured using an Eijkelkamp 06.01.SA hand penetrometer, with five readings taken per site.

Soil sample analysis

The dominant colour of each soil sample was matched in the laboratory with a corresponding colour chip in the Munsell Soil Colour Chart under constant 100 W light source. Soil texture was approximated using the Soil Survey Standard Test Method for particle size analysis (Department of Sustainable Natural Resources 2005). In this method, the changing density of a solution containing the fine (<2 mm diameter) particles of a sample was recorded using a hydrometer (Chemicals & Instruments No.5788, Mumbai, India). The relative proportions of sand (diameter>0.02 mm), silt (diameter between 0.02 mm and 0.002) and clay (diameter <0.002 mm) were identified by plotting particle size (in descending order on a logarithmic abscissa) against the cumulative percentage of suspended soil at the time of each reading. A limitation of the process was the insufficient time allowed for sedimentation of finer particles, which created the need for extrapolation of clay concentration using a regression curve fitted to the measured values.

3.2.5 Spectral analysis of field samples

Sediment samples collected in the field sites were analysed in the laboratory for their spectral properties. The presence of specific substances within a soil sample is indicated by local minima in the spectral profile, which are caused by these substances' increased absorption of radiation at certain wavelengths. The depth of these absorption features indicates the concentration of the associated material within the soil, but can also be affected by grain size (Van der Meer 2004). The presence of heavy metals, such as iron, affects the shape of the entire reflectance curve.

Spectral profiles for each sample were recorded at CSIRO Exploration and Mining (Australian Resources Research Centre) using a field spectrometer (Analytical Spectral Devices (ASD) Fieldspec Pro, Boulder, USA), which has a spectral range of 350–2 500 nm, with a resolution of 1.0 nm. Reflectance measurements were taken on three subsamples from each of the 36 samples, for increased precision of the surface reflectance measurement. Samples were placed in a pistol grip mounted on a tripod and illuminated from below using an artificial light source. After the recording of reflectance values, the mineral composition of each sample was analysed using TSG software, which produced an estimate of the main chemical components within the soil.

3.2.6 Hyperspectral image processing

Vegetation masking

Before any classification of the hyperspectral imagery could be carried out, vegetation cover was masked to isolate areas of bare sediment. Vegetation indices were calculated in ENVI software to generate 27 different indices, each designed to highlight specific vegetation characteristics. These were evaluated for their usefulness by comparing the accuracy with which each vegetation index displayed green or senescent vegetation within the study area. The NDVI (Normalized Difference Vegetation Index) and NDLI (Normalized Difference Lignin Index) were selected as most suitable (Figure 96). The masks were created for each flight line image by selecting all pixels with values below the appropriate threshold values in each index (0.22 for the NDVI and -0.002 for the NDLI).

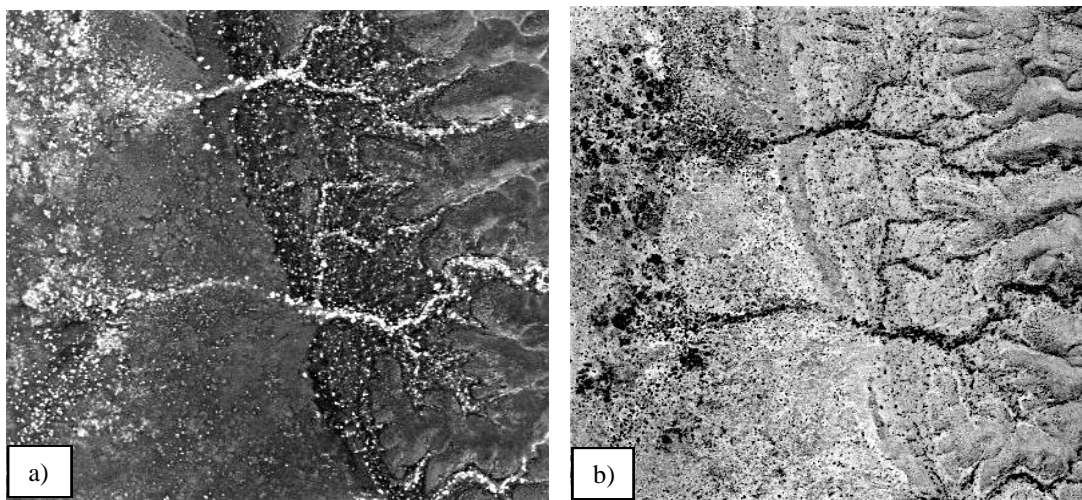


Figure 96. Vegetation indices used to create vegetation masks. All light-coloured pixels in the NDVI (a) indicate areas of high chlorophyll concentration, with values below 0.22 being excluded from further analysis. All light-coloured pixels in the NDLI (b) represent high lignin concentrations, thus indicating areas covered by dry or woody vegetation. NDLI values below -0.002 were also masked, leaving only pixels containing bare surface cover.

Minimum Noise Fraction

The masked hyperspectral imagery was used in the creation of 109-band forward Minimum Noise Fraction (MNF) rotations for each flight line. There is often a high correlation between neighbouring bands of data in datasets with many dimensions, therefore feature extraction techniques are used to reduce unnecessary data volume (De Backer *et al.* 2005). The data used in this study were contained within many wavelengths, thus MNF was used to isolate the main sources of variation and hence reduce processing time. The MNF algorithm removes band-to-band correlation within the data, while isolating the main signal from the noise (ENVI 2004). The plotted eigenvalues produced by the process revealed that twenty bands explained 99% of the total variance in the data. The noise statistics for the MNF were calculated from the entire dataset. RGB image composites of the MNF bands 4, 5 and 6 were used to identify distinct areas

of bare surface cover and later to assess the whether the image classification using Spectral Angle Mapper correctly represented surface types.

Image classification

The Spectral Angle Mapper (SAM) creates a classification based on a small number of reference pixels selected from the original image by the user. The reflectance profiles associated with each reference pixel were grouped in a spectral library according to the subtle differences in the shape of the profiles observed, which corresponded to differences in the surface characteristics of these pixels. The SAM algorithm calculates and compares the difference between the spectral profile of each pixel in the image and the spectral profile of each reference pixel in the spectral library (ENVI 2004). These differences are treated as angles in spectral space, with the number of dimensions used for the comparison being equal to the number of bands in the dataset (ENVI 2004). Each pixel was assigned to the class with the reflectance curve most similar to that pixel's own reflectance curve.

SAM classifications were processed across 109 bands of the terrestrial flight line datasets, with a maximum spectral angle of 0.1 radians. Each class of end-members contained a minimum of three spectra collected from training sites, which were distinct surface type areas revealed through inspection of the MNF-transformed data and through analysis of the spatial variation of measured soil properties. The optimal number of reference spectra for each class was found to be 3-5, since a lesser amount resulted in insufficient mapping accuracy, while a greater amount unnecessarily slowed processing time.

3.2.7 Statistical analysis

A series of Principal Component Analyses (PCA) was performed using The Unscrambler software package. The PCA algorithm rearranges data into a new set of uncorrelated bands, with the first component being aligned in the direction of greatest variation and the remaining bands following in descending order of variance explained (ENVI 2004). Results of the PCA are shown as X-loadings plots, which are scatter plots of the main sources of variance in the data, known as principal components. The loadings score of each sample denotes the difference between the sample's value calculated for the particular principal component and the average value for that principal component. If the sample is plotted on the positive side of the axis, then its value for that component is above average. Closely grouped items are assumed to be correlated with one another.

The samples were first separated into groups according to the geomorphic zones within which the sampling sites were located. These were labelled as 'escarpment', 'plain', 'streambed', 'dunes' and 'intertidal zone'. A PCA was then performed on the mean reflectance curves of the samples located within these zones to determine the main sources of surface variation in the landscape. After completion of the marine and terrestrial SAM classifications, PCAs were calculated on the mean reflectance curves for each class derived from the hyperspectral imagery. In each case, scatter plots of the significant principal components were produced and assessed in relation to the morphological characteristics of the associated spectral profiles to determine the nature of these components.

3.2.8 Other geographic data

For the purpose of this project and due to management differences between the different tenure, the study area was divided according to the land tenure (Figure 89). There were five different types of tenure: pastoral lease, national park, unallocated Crown land, freehold land and coastal park. A summary of the tenure types, their names and controlling bodies is presented in Table 18.

Table 18. List of tenure types, their respective names and the power they are vested in (adapted from CALM and MPRA 2005).

Tenure type	Tenure name	Vested in
Pastoral Lease	Quobba	Pastoralists
	Gnaraloo	
	Warroora	
	Cardabia	
	Ningaloo	
National Park	Cape Range National Park	Conservation Commission of Western Australia
Coastal Park	Jurabi	Shire of Exmouth and
	Bundegi	Executive Director of DEC (jointly)
Freehold Land	Location 44	Department of Defence
	Location 97	
Unallocated Crown Land	Unallocated Crown Land	None

Additional features of the study area included accommodation nodes along the coast. The identification of those was previously undertaken by Smallwood (2010) who identified 81 different sites including backpackers, campsites, caravan parks, chalets/self contained accommodation, hotels, private housing and safari camps.

The last feature of the study area was the mean high water mark. Mean tidal levels are commonly used in both studies and legislative documents, as they provide a static benchmark (Pajak and Leatherman 2002). In the case of the Ningaloo coast, pastoralists are responsible for management of their lands up to 40 m above the high water mark whereas the remaining coastal strip is vested in the Department of Environment and Conservation, the Department of Defence or local shire. For this study, coastal strips of 40 m and 100 m from the mean high water mark were used to analyse the data.

3.2.9 Classification of roads and tracks

The road and track network was extracted from the hyperspectral imagery by image enhancements, hand digitising using ENVI Intelligent digitiser tool and combined with field validation. Data on some existing major roads was provided by the Department of Environment and Conservation. The digitized road network file was further edited in GIS software and classified into major roads, minor roads and tracks. Major roads were defined as constructed roads with sealed bitumen surface and are open for the public access. Minor roads were

constructed roads with a gravel surface. In this context, two-wheel drive vehicles could use minor roads at a low speed. Finally, tracks were defined as unconstructed and unformed roads that were created by off-road vehicles. These tracks were usually spreading from inland access points towards the coast.

3.2.10 Cumulative length of roads/tracks

As previously discussed, the land tenures within the study extent consisted of freehold land, miscellaneous crown reserves, National Park, pastoral lease and unallocated crown land. These land tenure polygons do not extend to the mean high water mark or beyond. In order to analyse the road and tracks data and their relationship to the land tenure, the land tenure polygons were manually adjusted in ArcMap by extending land polygon boundaries seaward, to the mean high water mark line. These modified land tenure polygons therefore have larger area when compared to the original data provided by DEC.

The modified land tenure shape file was modified to exclude areas that were beyond the study area (Figure 89) and the area (km²) for each tenure was calculated. The road network file was intersected with the land tenure shape file to generate a new data with vehicle tracks in different land tenures. Attribute files of land tenure and the road network in different land tenures were generated and further analysed in Microsoft Excel 2003. To calculate the density of roads in all the land tenures within the extent of hyperspectral imagery, the length of each road (major, minor or tracks) was divided by the area of the land tenures (km²) respectively.

3.2.11 Densities of roads/tracks

The extent of the road network along the coast was analysed using a 100 m x 100 m grid. Mean high water mark coastline data were used to generate a buffer in ArcMap 9.3. The 100 m x 100 m grid was generated within that coastal buffer. Cell perimeter and area (in km²) were added to this grid polygon database.

The road network file was intersected with the 100 m x 100 m grid and road length within each grid cell was added to the database. Using the XTools Pro, the length of each road within a grid cell was summed by aggregating the new FID (Feature Identifier, a unique record number). The new aggregated FID was joined with the FID of the 100 m x 100 m grid file. After joining the table, the 100 m x 100 m grid file was used to display the road densities (Figure 97). The road and tracks within the grid cells were classified into four categories according to their cumulative length (Table 19).

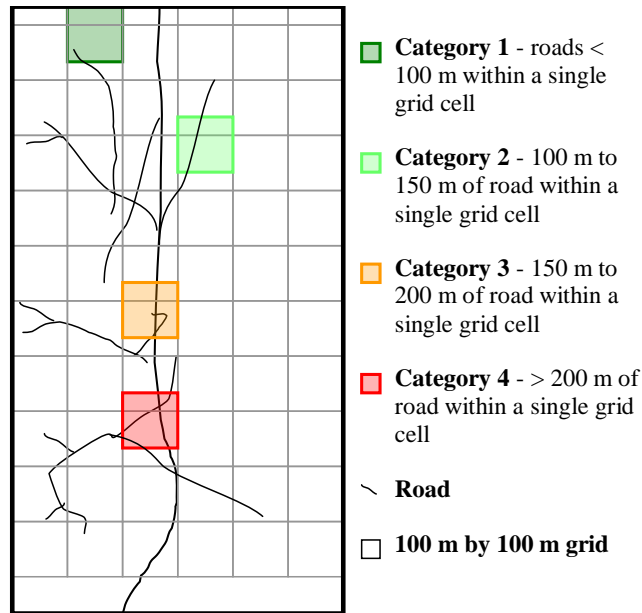


Figure 97. Example of classification of road densities (in metre road per m²) into four categories.

Table 19. Categories of road/tracks used in the Ningaloo coastal strip study.

Category	Cumulative length per grid cell	Density	Comment
1	< 100 m	Low	Short tracks, fan-shaped, spreading from inland toward the coast
2	100 m – 150 m	Medium	Vehicle travel parallel to the coast in south-north direction or vice versa, usually consist of one road within a grid cell
3	150 m – 200 m	High	Consist of parallel roads, road intersection or diversion within a grid cell, roads are closely linked to one another
4	> 200 m	Very high	Roads are heavily used by vehicles, two or usually more roads are created close to one another within a grid cell

Vegetation in track and road buffers

Using ArcMap software, buffers of 5 m and 10 m were created around tracks for the whole study area (Figure 98). These buffers were then intersected with land tenure and previously defined coastal strips. Using ENVI software, the further delimited buffers were added to the vegetation indices mosaics. Turning the buffers into masks allowed limiting maps to specified areas around tracks while showing the vegetation communities at risk. Finally, a post classification tool in ENVI was used to extract summary statistics (text files) for each vegetation community.

The numbers of tracks that provide access to the different sanctuary zones of the Ningaloo Marine Park were calculated as the number of cul-de-sacs leading to the beach. In the case of tracks following the coastline, if both ends were inside the sanctuary zone, two access points were counted (Figure 99). For sanctuary areas not contiguous to the beach but separated by a special purpose (shore-based activities) zone, the number of access tracks for this latter zone was recorded.

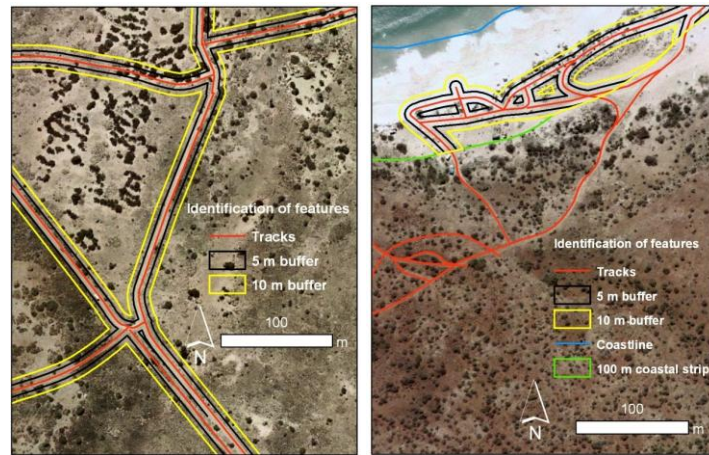


Figure 98. Example of buffers and their connections around tracks (left) and between buffers and the 100 m coastal strip (right) along the Ningaloo coast.



Figure 99. Example of access points (purple circles) along a sanctuary zone bounded by a special-purpose area zone in Ningaloo Marine Park.

3.3 Results

3.3.1 Bare sediment component of the landscape

Soil spectra and field measurements

Despite all samples being taken within a fairly short distances from the shore, there were large differences in general sediment properties as well as resultant spectral measurements from the field samples. Most variation was due to the position in the landscape that is, escarpment, coastal plain, creek, dunes and intertidal zone. In this section, the spectral reflectance and other soil properties of the field samples are described from the southern most sites to the northern most ones.

Yardie Creek

Soil texture and colour varied between the sites and included sand, sandy loam and loamy sand (Table 20). The reflectance curves of samples collected from Yardie 1, 2 and 3 closely resembled each other (Figure 100). The presence of iron oxide minerals resulted in an absorption feature at 900 nm and low reflectance in the blue and green visible wavelengths, which accounted for the reddish colours recorded with the Munsell chart (Figure 108). The red colour of the Yardie 1 – 3 samples compared to Yardie 4 sample correspond to the greater iron content indicated by their spectral profiles. An absorption feature caused by the presence of clay minerals was also evident at 2200 nm, while the minor absorption features at 1400 nm indicate these three samples contain low soil moisture. The sample from Yardie 4 showed no prominent iron and clay features, but had a carbonate absorption feature at 2330 nm and slightly higher moisture content. The higher reflectance in the visible range of this sample corresponds to the lighter Munsell colour. The sample collected from the site with steepest slope gradient, Yardie 1, also had a finer texture than the samples from the other three sites. Yardie 1, on the edge of the escarpment (Figure 91) was the only site with a slope greater than 5 %.

Osprey Sanctuary Zone

The samples collected from the Osprey 2 and 5 sites showed strong carbonate absorption features at 2350 nm (Figure 101), which is consistent with their locations within the dune systems (Figure 92). Samples from the Osprey 1, 3 and 4 sites had less prominent carbonate absorption features. Sites 1-4 had a minor clay absorption feature at 2200 nm. The Osprey 5 sample exhibited higher overall reflectance (in agreement with the lighter Munsell colour) and a higher moisture content than the samples from the four sites further inland. The profile of the sample from Osprey 1 showed iron absorption at 885 nm and in the visible region, which is evident in the change in soil colour between Osprey 1 and Osprey 2 (Figure 100). The texture of the Osprey 1 sample was also found to be finer than the other samples, which were all identified as sand. The Osprey area had the highest vegetation cover overall, with the highest percentage cover at a single site being 86.7 % vegetation cover and 76.7 % leaf litter, observed at Osprey 3 (Table 20). The low shear strength measurements reflected the coarse texture of the soil and the depth of unconsolidated sediment.

Table 20. Field measurements of soils taken at site along the Ningaloo coast.

Site name	Altitude (m)	Slope (%)	Vegetation cover (%)	Leaf litter (%)	Soil colour	Shear strength (N/cm ²)	Soil texture
Yardie 1	15	>5	40	<5	5YR 4/4	N/A	sandy loam
Yardie 2	27	<1	30	40	7.5YR 4/6	N/A	Sand
Yardie 3	16	<1	60	10	5YR 4/6	N/A	loamy sand
Yardie 4	N/A	<5	10	5	10YR 6/4	N/A	Sand
Osprey 1	46	<1	58.3	18.3	5YR 4/6	41.3	sandy loam
Osprey 2	36	<1	30	11.7	8.75YR 6/4	37	Sand
Osprey 3	15	<5	86.7	76.7	10YR 5/6	38	Sand
Osprey 4	6	<1	58.3	50	10YR 5/4	38.4	Sand
Osprey 5	10	varies	43.3	8.3	10YR 7/3	41.2	Sand
Pilgramunna 1	17	<1	50	43.3	7.5YR 4/4	48.5	loamy sand
Pilgramunna 2	18	<5	26.7	18.3	5YR 4/4	41	loamy sand
Pilgramunna 3	1	<1	21.7	1	5YR 6/6	113.9	Sand
Pilgramunna 4	4	<1	55	41.7	5YR 4/6	106.2	loamy sand
Pilgramunna 5	0	<1	0	0	10YR 7/4	N/A	Sand
Tantabiddi 1	0	<1	33.3	25	5YR 4/6	90	sandy loam
Tantabiddi 2	1	<1	75	6.7	7.5YR 4/6	104.4	loamy sand
Tantabiddi 3	N/A	<1	0	0	10YR 6/3	N/A	Sand
Jurabi 1	1	varies	0	0	10YR 7/4	N/A	Sand
Jurabi 2	4	varies	10	0	1.25Y 7/4	N/A	Sand
Jurabi 3	14	<5	0	0	10YR 7/3	N/A	Sand
Mandu 1	13	<5	28.3	15	5YR 4/4	48.2	sandy loam
Mandu 2	19	<1	0	0	7.5YR 6/4	N/A	Sand
Mandu 3	18	<5	0	0	7.5YR 5/4	N/A	Sand
Mandu 4	11	<1	60	40	2.5YR 4/4	N/A	sandy loam
Mandu 5	1	<1	8.3	1.7	7.5YR 5/8	N/A	sand
Bloodwood 1	0	<5	21.7	45	7.5YR 5/6	93.6	sand
Bloodwood 2	0	<1	30	8.3	2.5YR 4/6	105	sandy loam
Bloodwood 3	N/A	<5	0	0	10YR 7/3	N/A	sand
Turquoise 1	17	<5	35	20	5YR 4/4	166.8	loamy sand
Tulki 1	0	<1	40	20	7.5YR 5/4	N/A	loamy sand
Tulki 2	1	<5	0	0	10YR 6/4	N/A	Sand
Trealla 1	0	<5	21.7	3.3	5YR 5/6	N/A	loamy sand
Trealla 2	9	<5	0	0	10YR 8/2	N/A	Sand
Mangrove 1	9	<1	46.7	1.7	5YR 4/4	N/A	sandy clay loam
Bundegi 1	0	<5	73.3	3.3	2.5YR 5/3	20.6	sandy loam
Exmouth 1	7	varies	1.7	1.7	5YR 4/6	N/A	sand

Pilgramunna

Despite Pilgramunna 1 site being the furthest inland (Figure 94), the reflectance curves of Pilgramunna 1, 2 and 4 samples matched each other very closely, with the sample from Pilgramunna 4 showing slightly higher reflectance in the orange and red visible wavelengths as well as the near IR (Figure 101). All three curves show a strong clay absorption feature at 2200 nm and their water absorption features at 1400 nm and 1910 nm indicates low soil moisture. These three samples were also of a finer texture than the Pilgramunna 3 and 5 samples (Table 20). The sample from Pilgramunna 3 matched closely with Pilgramunna 4 site, in the visible and near IR regions, which confirms the identical Munsell colours observed (Figure 100). Both samples

showed a strong iron absorption feature at 850-900 nm. In the SWIR region, the Pilgramunna 3 sample exhibited minor clay, hydrocarbon and carbonate absorption, as well as prominent water absorption features. The high shear strength values for Pilgramunna 3 may have been influenced by the underlying limestone substrate, which does not account for the high recording at Pilgramunna 4.

Of all samples collected, the Pilgramunna 5 sample had the most distinct reflectance curve. Its high reflectance in the visible region matched the light Munsell colour, while the deep absorption features at 1440 nm and 1900 nm indicate high soil moisture (explained by its location in the intertidal zone). It showed no noticeable iron, clay or carbonate features, instead had a prominent hydrocarbon absorption feature at 1790 nm and minor absorption features at 680 nm, 970 nm and 1180 nm.

Bloodwood Creek

The sample from Bloodwood 2 had the most prominent iron absorption features of all samples collected (Figure 101), which was consistent with the dark red Munsell colour observed (Figure 100, Table 20). Shear strength was relatively high at Bloodwood 2 site as a result of soil compaction from the nearby road crossing. The sample's reflectance curve also indicated the presence of clay, which explained the finer soil texture recorded and the shear strength and vegetation cover which were higher than those of the upstream site. The spectral profile of the Bloodwood 1 sample exhibited iron, clay and carbonate absorption features at 880 nm, 2210 nm and 2330 nm, respectively. The lighter colouration of the sample from Bloodwood 3 was caused by higher reflectance in the visible and near IR regions and the curve showed a carbonate absorption feature at 2330 nm. Both the Bloodwood 2 and the Bloodwood 3 samples had prominent water absorption features in their spectral profiles.

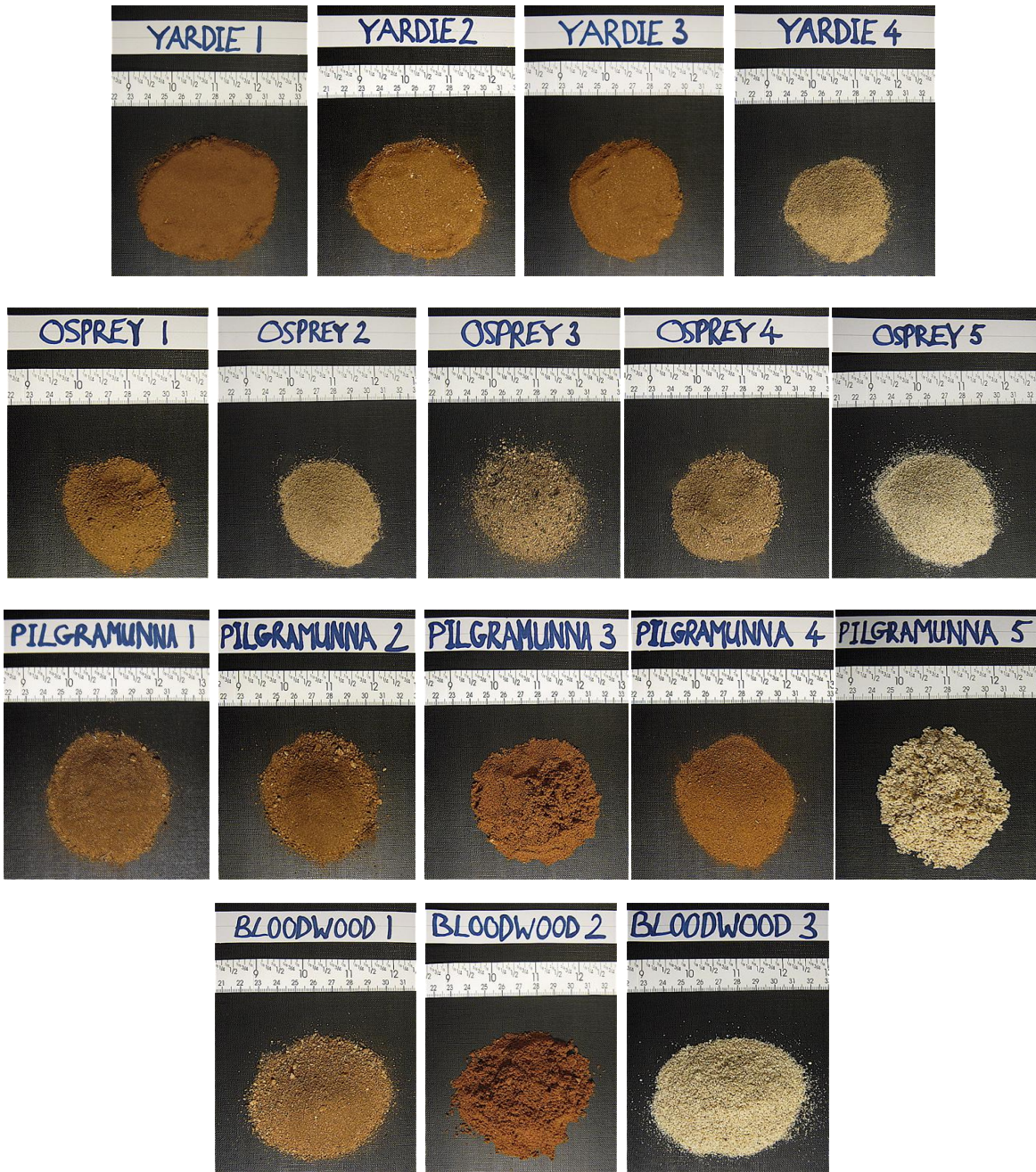


Figure 100. Photographs of soil samples from Yardie Creek (top row), the Osprey Sanctuary Zone (2nd row, Pilgramunna (3rd row) and Bloodwood Creek (bottom row).

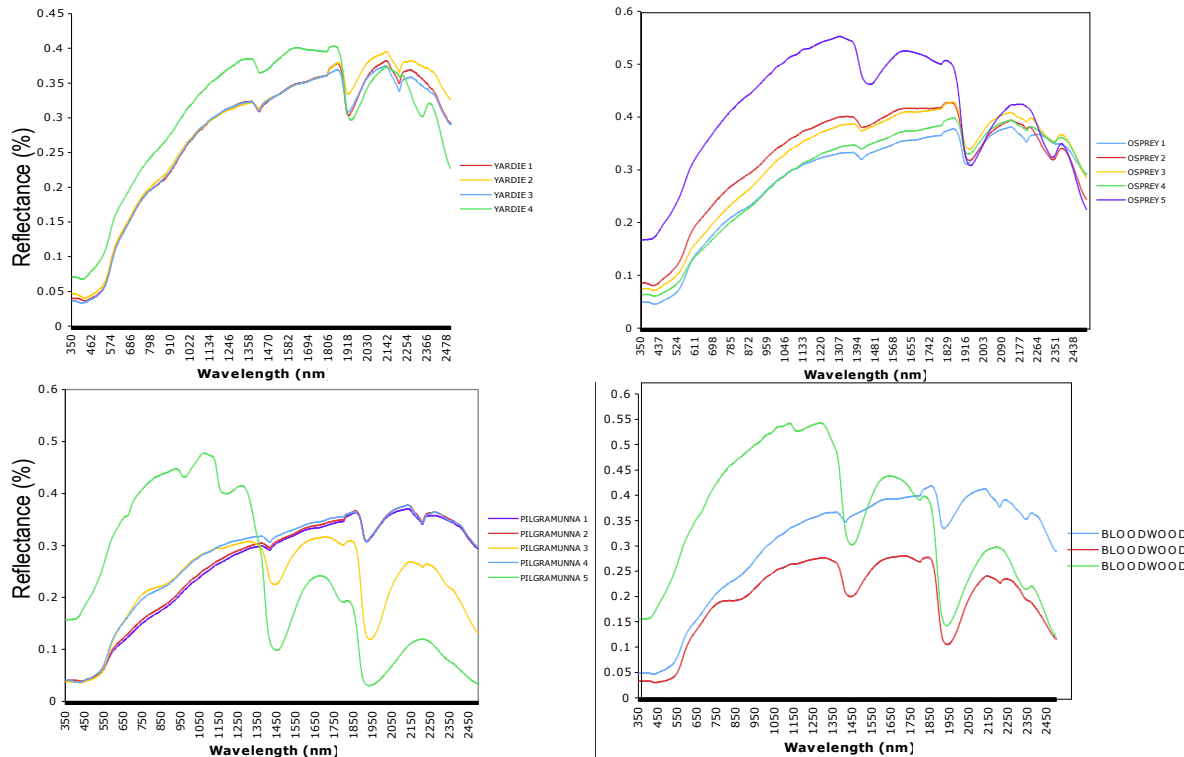


Figure 101. Average reflectance curves of three replicate soil measurements for each sample collected near Yardie Creek (top left), Osprey (top right), Pilgramunna (bottom left) and Bloodwood Creek (bottom right). Note the differences in the scales for the vertical scale.

Mandu Creek

All reflectance curves showed iron oxide absorption features in both the visible region and at 900 nm (Figure 103). These features were most prominent in the samples from Mandu 1 and 4, in agreement with the reddish Munsell colours observed (Figure 102 and Table 20). There was a minor clay absorption feature at 2200 nm on all five curves and a carbonate absorption feature at 2360 nm on the profiles of the samples collected at Mandu 2, 3 and 5. Higher vegetation and leaf litter cover were recorded at Mandu 1 (furthest inland, in the gorge) and 4 (edge of the escarpment) (Figure 94), with samples from these sites also characterised by finer soil texture. The Mandu 4 sample's reflectance curve showed a more prominent clay absorption feature and also indicated a lower moisture content than the sites within the streambed. Steeper slope gradients were recorded at the escarpment sites (Table 20).

Tantabiddi Creek

The samples collected within the creek (Tantabiddi 1 and 3) (Figure 93) showed higher soil moisture than the sample from the southern bank (Tantabiddi 2). The Tantabiddi 1 and 2 samples showed absorption features attributable to iron oxide minerals at 850 nm and in the visible region (Figure 103), with the Tantabiddi 2 sample also showing a clay absorption feature at 2210 nm.

Despite the indication from the spectral profiles that the Tantabiddi 2 sample contained a higher clay concentration than the other two samples, its soil texture was determined as being less fine than that of the Tantabiddi 1 sample. The sample from Tantabiddi 3 exhibited higher reflectance in the visible region, which corresponds to the lighter Munsell colour (Figure 102, Table 20). The sample also showed higher reflectance in the IR wavelengths up to 1400 nm, with a carbonate absorption feature at 2340 nm. Higher values of shear strength and vegetation cover were recorded on the south bank of the creek than in the streambed.

Jurabi Coastal Park

The reflectance curves of all three dune-based samples (Figure 93) showed the same morphological structure (Figure 103), with carbonate and water absorption features of approximately the same magnitude. Only slight variations can be seen and the similarities are confirmed by the closely aligned reflectance spectra. The high reflectance in the visible region corresponds to the light Munsell colours recorded (Figure 102 and Table 20). The overall reflectance of the Jurabi 2 sample was slightly lower than that of the samples from the two foredune sites. Since the location of the sites was a dune, vegetation and leaf litter cover were minimal, slope was undulating, soil texture was sand and shear strength was not recorded.

Northern section of Cape Range National Park

The reflectance curves of the samples from the inland sites (Turquoise 1, Mangrove 1, Tulki 1 and Trealla 1) showed prominent iron oxide absorption features in the visible region and at 880 nm (Figure 103) as a clay absorption feature at 2210 nm. Finer soil texture and moderate vegetation cover were also recorded at these sites (Table 20). The Tulki 1 sample also showed a minor carbonate absorption feature at 2340 nm, with the Trealla 1 sample showing a deeper trough at the same wavelength. The low reflectance of the Turquoise 1 and Mangrove 1 samples in the blue and green wavelengths account for their darker red Munsell colour (Figure 102). The samples from the two intertidal sites (Tulki 2 and Trealla 2, Figure 95) exhibited high reflectance in the visible and near IR regions, with prominent carbonate, water and OH⁻ absorption features. Despite their close geographic proximity (Figure 90), there was a clear difference in the spectral reflectance at these two sites. Shear strength could not be recorded due to the hard limestone cobble substrate. Soil texture was finer in this area compared to other sites.

Exmouth Gulf

The spectral profile of the Bundegi sample showed very low overall reflectance due to the high soil moisture and organic matter concentration in the sample (Figure 103). The Exmouth sample's reflectance curve showed prominent iron oxide absorption features in the blue and green regions and at 880 nm, with a prominent clay absorption feature at 2210 nm. These features matched with its orange-red colour and finer texture (Figure 102 and Table 20). The low shear strength recorded at Bundegi 1 site was due to the high soil moisture at that site.

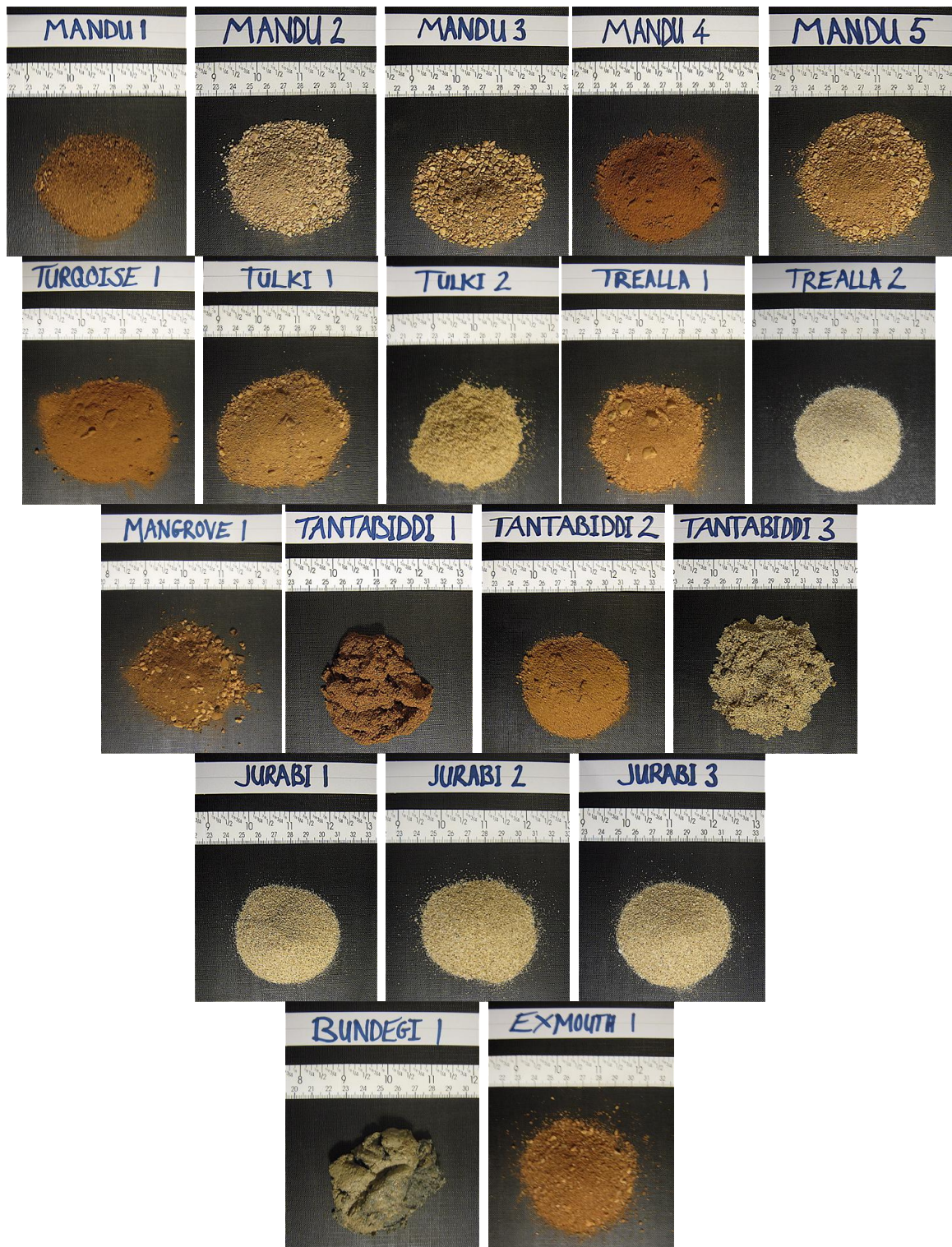


Figure 102. Photographs of soil samples from Yardie Creek (top row), the Osprey Sanctuary Zone (2nd row, Pilgramunna (3rd row) and Bloodwood Creek (bottom row).

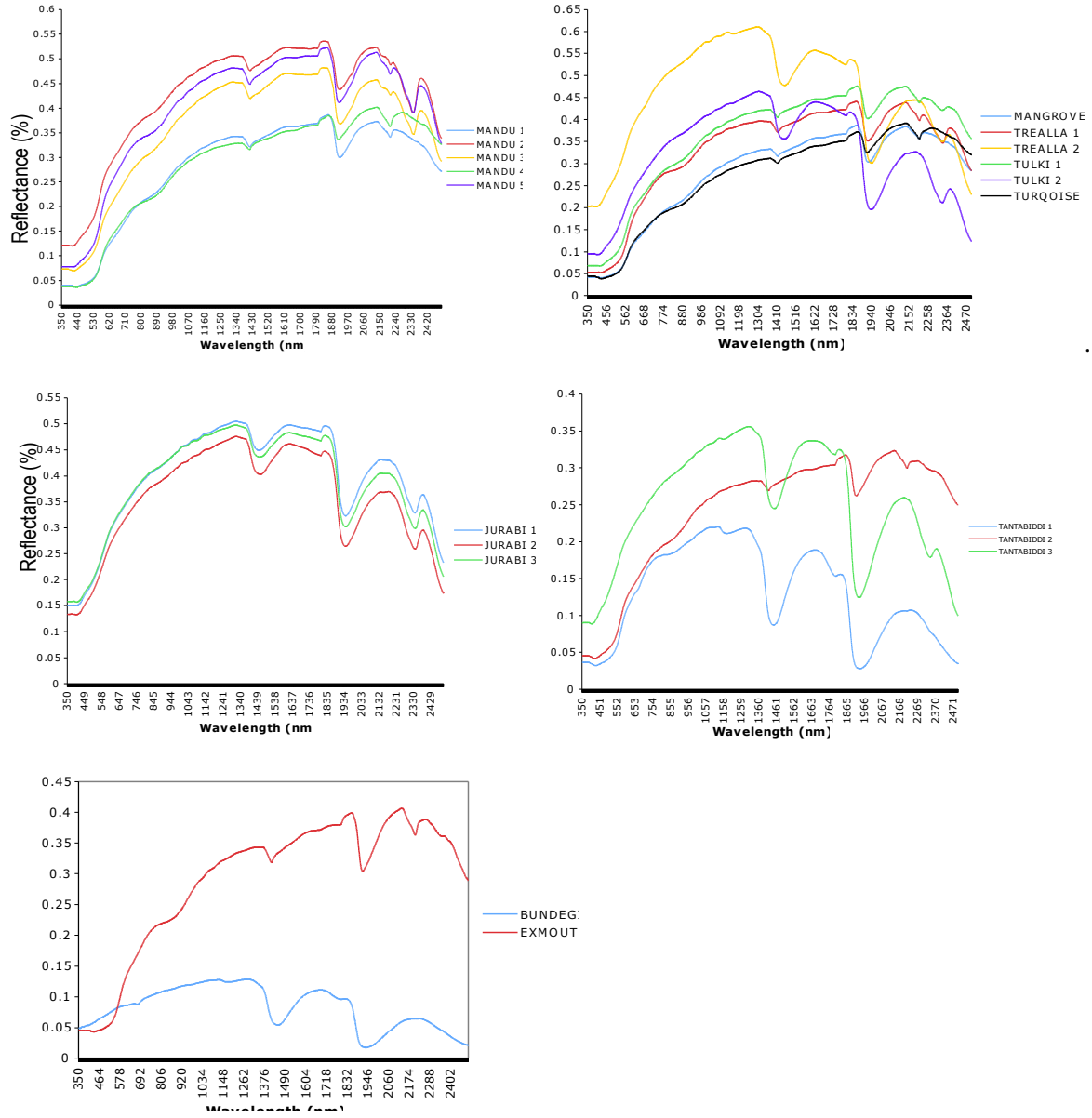


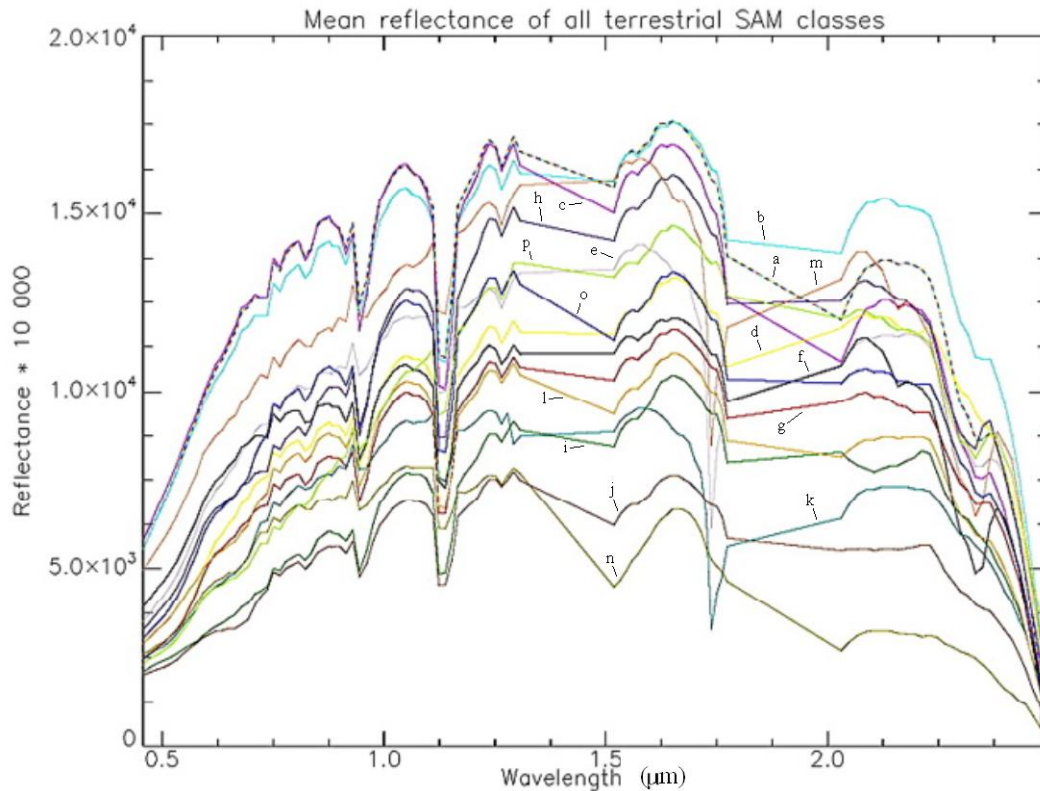
Figure 103. Average reflectance curves of three replicate soil measurements for each sample soil collected at Mandu (top left), Trealla, Tulki and Turquoise Bay (top left), Jurabi (middle left), Tantabiddi (middle right) and around Exmouth Gulf at Bundegi and Exmouth (bottom left).

3.3.2 Spectral Angle Mapper Classifications

The detailed sediment classification presented here included only the flightlines coinciding with locations where soil samples were collected. A total of 16 bare surface types were identified (Table 21) (Figure 104), with attention on classes representing unconsolidated sediments. Class labels were based on geological units from the 1:250 000 map series, or the dominant surface material for classes not represented in the map series. The colour representing each surface type is shown by the labels in Figure 105. Due to subtle variations in the general shape of reflectance curves in each flight line, certain classes represented different surface properties in different data blocks. The geological units mapped by each class in selected data blocks are shown in Table 21. All data blocks were classified using this approach but only three data blocks are presented here.

Table 21. The 16 terrestrial surface types identified through SAM classification of the HyMap hyperspectral data and the corresponding geological unit(s) in the 1:250 000 geological map series (Van de Graaf *et al.* 1980, 1982). In some cases, multiple classes were associated with a single geological unit, such as the five classes occupying the same area as Qs. Example presented here is for the three northern data blocks G, H and K.

SAM Class	Main attributes	Geological units mapped in hyperspectral data set		
		Block G	Block H	Block K
1. Exmouth sandstone	Carbonate-rich quartzose calcarenite	Qxm (Milyering Member) and Qxn (Muiron Member)	Qxn (Muiron Member)	Not present
2. Alluvium	Dark, partly calcreted mixed sediments with high clay content	Cza (Alluvium)	Cza (Alluvium) and Tp (Pilgramunna Formation)	Cza (Alluvium)
3. Sandplains	Pleistocene corallgal and aeolian deposits with moderate clay content	Qbt (Tantabiddi Member) and Qe (Dune and sandplain deposits)	Qbt (Tantabiddi Member)	Qe (Dune and sandplain deposits) and Czc (colluvium)
4. Streambeds	Carbonate-rich limestone cobbles	N/A	N/A	N/A
5. Beach sand and foredunes	Bright quartzose calcarenite with moderate carbonate content	Qs (Coastal-dune and beach deposits)	Qs (Coastal-dune and beach deposits)	Qs (Coastal-dune and beach deposits) and Qt (supratidal flat deposits)
6. Supratidal sand flats	Saline calcareous clay, silt and sand with low moisture content	Qs (Coastal-dune and beach deposits)	Qt (supratidal flat deposits)	Qt (supratidal flat deposits) and Czp (Claypan and dune deposits)
7. Moist beach sand	Bright quartzose calcarenite with moderate carbonate content and high moisture content	Qs (Coastal-dune and beach deposits)	Qs (Coastal-dune and beach deposits)	Qt (supratidal flat deposits)
8. Bundera calcarenite and limestone terraces	Reddish-coloured Pleistocene and Miocene sediments of marine origin, with low moisture content	Tk (Tulki Limestone), Qbj (Jurabi Member) and Qbt (Tantabiddi Member)	Qbj (Jurabi Member), Qbt (Tantabiddi Member) and Tv (Vlaming Sandstone)	Qb (Bundera calcarenite), Qbt (Tantabiddi Member), Qe (Dune and sandplain deposits), Tt (Trealla limestone) and Czc (colluvium)
9. Cape Range Plateaux	Higher altitude quartzose deposits	Qe (Dune and sandplain deposits)	Not present	Tp (Pilgramunna Formation)
10. Secondary dunes (south)	Transition between Tantabiddi Member and beach sediment	Qs (Coastal-dune and beach deposits) and Qbt (Tantabiddi Member)	Not present	Not present
11. Secondary dunes (north)	High soil moisture and low carbonate content	Not present	Qs (Coastal-dune and beach deposits) and Qt (supratidal flat deposits)	Qs (Coastal-dune and beach deposits) and Czp (Claypan and dune deposits)
12. Miocene calcarenite	Iron-rich quartzose calcarenite with high moisture content	Tv (Vlaming Sandstone) and Qbt (Tantabiddi Member)	Tv (Vlaming Sandstone) and Tp (Pilgramunna Formation)	Not present
13. Limestone and sandstone conglomerates	Bright sedimentary deposits	Not present	Tk (Tulki Limestone), and Qxm (Milyering Member)	Czc (colluvium)
14. Carbonate-rich limestone	Visually dark substrate with high iron and carbonate content	Not present	Tk (Tulki Limestone)	Not present
15. Claypans	High iron content, high soil moisture, low reflectance in SWIR region	Not present	Qw (Intertidal flats and mangrove swamps)	Czp (Claypan and dune deposits)
16. Bitumen	Road surface	n.a	n.a.	n.a.



- a) Beachsand and Foredues
- b) Supratidal sand flats
- c) Moist beachsand
- d) Sandplains
- e) Secondary dunes (north)
- f) Bitumen
- g) Bundera Calcarenite and limestone terraces
- h) Exmouth Sandstone
- i) Alluvium
- j) Miocene Calcarenite
- k) Limestone and sandstone conglomerates
- l) Secondary dunes (south)
- m) Streambeds
- n) Claypans
- o) Cape Range Plateaux
- p) Carbonate-rich limestone

Figure 104. Example of the mean reflectance spectra and representative colours of each of the 16 surface types identified. The beach sand and foredues class are shown in white in the SAM images, but represented by the dashed curve in this plot. Deep carbonate (2.3 μm) and iron (0.75-0.95 μm) absorption features can be seen in some classes.

Block G

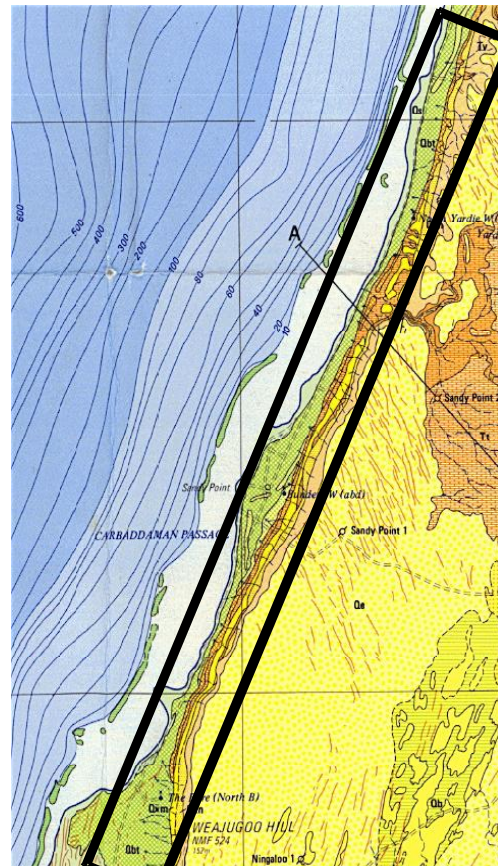
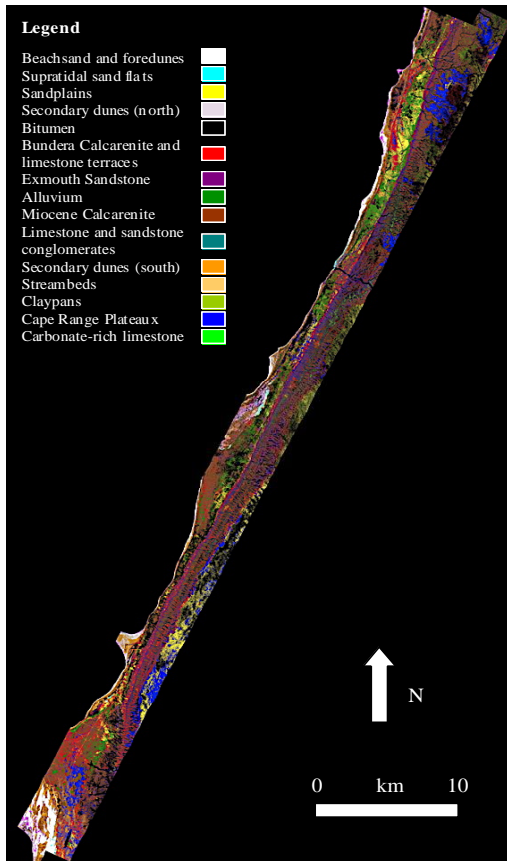
The area covered by Block G (Yardie and Osprey sites) featured wide terraces of marine origin, with sand plains on the plateaux to the east and along the coastal belt to the west (Figure 105). In the northern section of the data block these terraces were generally classified as Miocene calcarenite, with the Bundera calcarenite and limestone terraces class being the dominant surface cover in the south and the Exmouth Sandstone class being the most common surface type around Yardie Creek Gorge. At the southern edge of the block, a large coastal dunefield could be seen, aligned in the direction of the prevailing southerly wind (Figure 105). The area within the black rectangle matches the area occupied by Block G. Spatial variation of surface types closely matches the major landscape features such as dunefields, coastal plain, escarpment and plateau. A degree of overlap between SAM classes is visible, with pixels in the area corresponding to Qbt being assigned to classes representing Qe (e.g. Cape Range Plateau) and single classes representing multiple terraces (e.g. the Miocene calcarenite class). Another inconsistency between the classified image and the geological map is that several of the alluvial fans clearly identifiable in the hyperspectral imagery but not on the geological map.

Block H

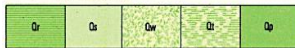
Most of the field sites were contained within this data block. The area within block H featured a narrow coastal plain, which widened towards the north. This area was generally represented by the sandplains and alluvium classes, with the exception of the southern edge which was categorized as Bundera calcarenite and limestone terraces (Figure 106). The escarpment was dominated by the limestone and sandstone conglomerates surface type in the north and the Miocene calcarenite class in the south. East of the escarpment, carbonate-rich limestone was the most commonly assigned label. The coastal dunefield at Jurabi was found to consist of five distinct sediment types. The limestone terraces are well represented, however the separation between classes is less accurate on the coastal plain. As in block G, some alluvial fans shown in the SAM classification do not appear in the geological map (e.g. Bloodwood Creek) (Figure 106).

Block K

The two flightlines shown here for the Block K classification covered the eastern escarpment and the northeast edge of the Cape Range Peninsula. They contained two sites: Bundegi and Exmouth. The escarpment was mostly categorized as Bundera calcarenite and limestone terraces, while the north-eastern headlands were dominated by the claypans surface type (Figure 107). The large expanse of relict aeolian deposits was determined to be sandplains. The claypans and relict dunefields at the northern end of the peninsula are well represented, as is the escarpment west of Exmouth. One inconsistency between the images is the classification of relict dunefield areas as the Bundera calcarenite and limestone terraces class (Figure 107).



REFERENCE



- Qr Ningaloo Reef – living coral reef
- Qs Beaches and coastal dunes – quartzose calcarenite
- Qw Intertidal flats and mangrove swamps – calcareous clay, silt and sand
- Qt Supratidal flats – calcareous clay, silt and sand with authigenic gypsum and salt
- Qp Claypans – poorly sorted clay, silt, sand and minor pebbles

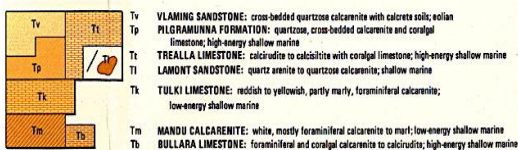
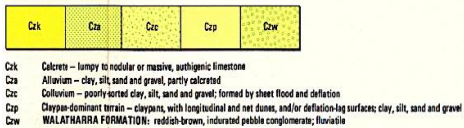
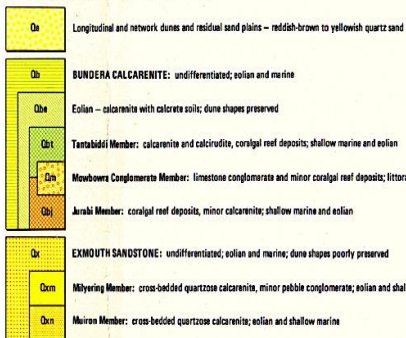


Figure 105. Results of the SAM classification of Block G (left) and subset of the 1:250 000 geological map series (right) (Van de Graaff *et al.* 1980; 1982), shown with key (bottom left).

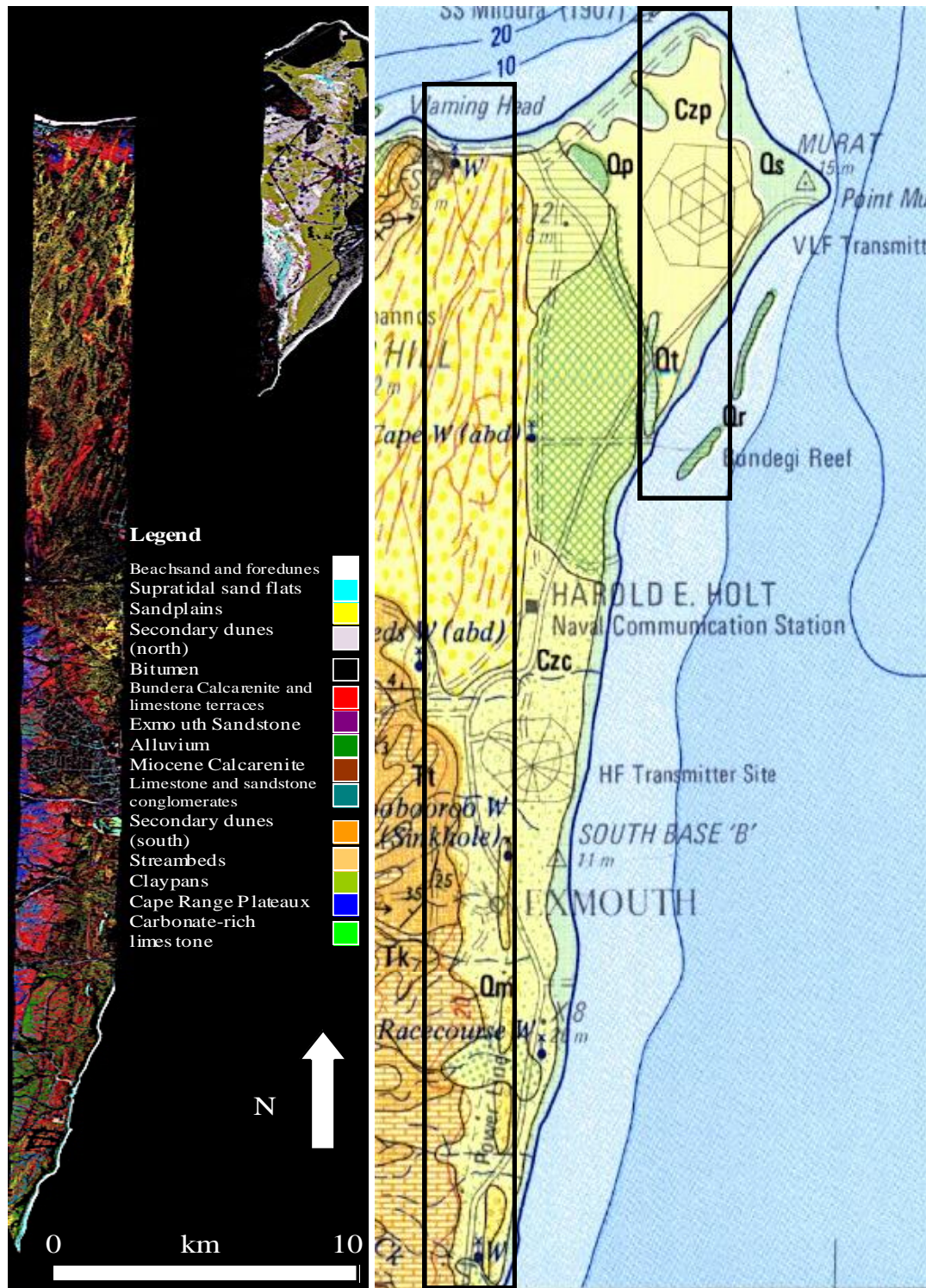


Figure 107. Results of the SAM classification for Block K in the northern part of the Cape Range and Exmouth Peninsula (left) and subset of the 1:250 000 geological map series matching the area of Block K (right) (see key in Figure 105 for geological unit labels) Black rectangles on the right panel illustrate position of the flightlines in the hyperspectral imagery.

3.3.3 Principal Component Analysis

Field spectra PCA

The five geomorphic zones of field sites were escarpment, coastal plain, creek, dunes and intertidal zone. The PCA of the field sample reflectance spectra showed clear separation of the average spectral profile of all samples in each zone (Figure 108). Sediments in the intertidal zones had overall the highest reflectance and those from the escarpment and coastal plain, the lowest. The first two principal components were found to explain 99 % of total variance. PC1 (78 %) is most likely the mean reflectance of each curve, while PC2 (21 %) is most likely the moisture content of the sample (Figure 109).

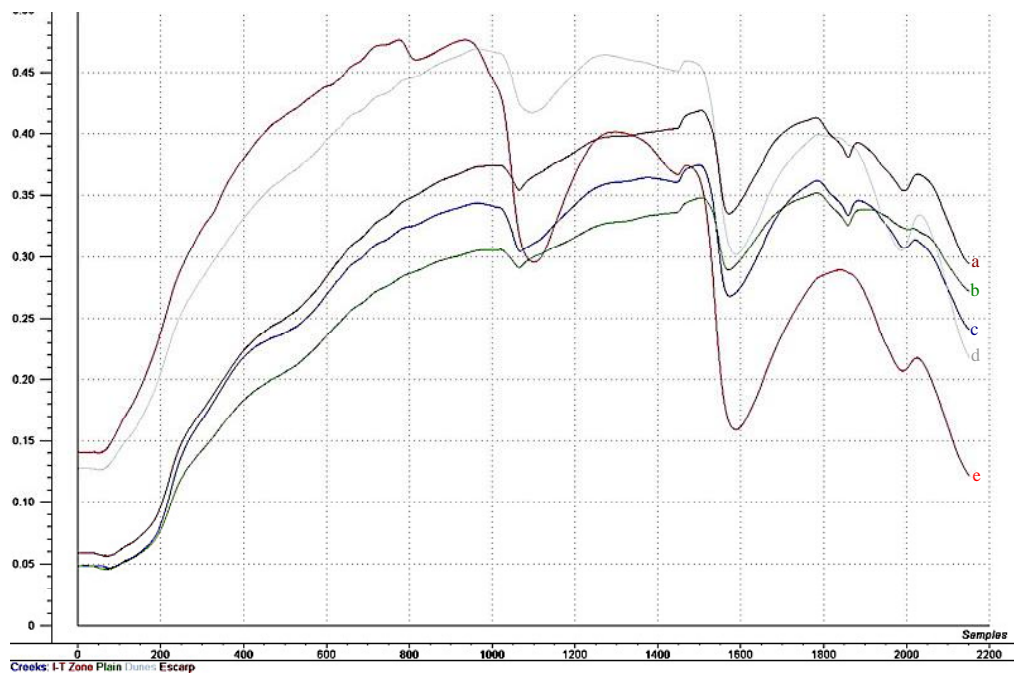


Figure 108. Mean reflectance of all samples located within each geomorphic zone. a) escarpment; b) coastal plain; c) creek; d) dunes; e) intertidal zone.

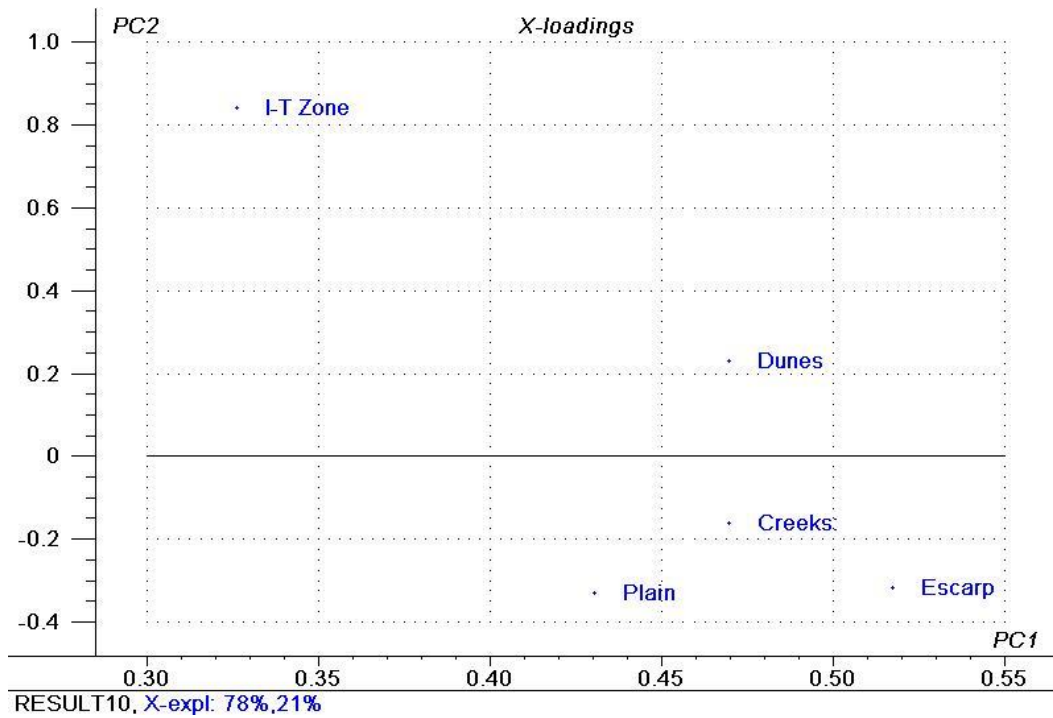


Figure 109. PC1 of the field spectra PCA plotted against PC2. The main sources of variance were judged to be mean reflectance and soil moisture.

PCA of image derived spectra

In order to determine the degree of separability possible between spectra of the field samples (Figure 108), a PCA analysis was applied to the spectra derived from the image data. The PC1 (90 %) was judged to represent mean reflectance, which would not affect the SAM classification due to the spectral angle mapping technique involved (Figure 110). The most likely source of PC2 (6 %) was considered to be the variation in the shape of reflectance profiles created by differences in moisture content, with the largest difference being between the shape of the claypan profile and the carbonate-rich limestone profile. The distribution of classes within the scatter plot indicates two groups within which surfaces share similar characteristics. The two main sources of variance within the SAM class spectra were judged to be mean reflectance and profile shape, which is influenced by soil moisture. This means the darkest and wettest surface type was the claypans class. The first grouping (a) contained surfaces with high average reflectance and high moisture content and were found exclusively in coastal areas. The second grouping (b) contained three escarpment surfaces and the alluvium class, all with low moisture content.

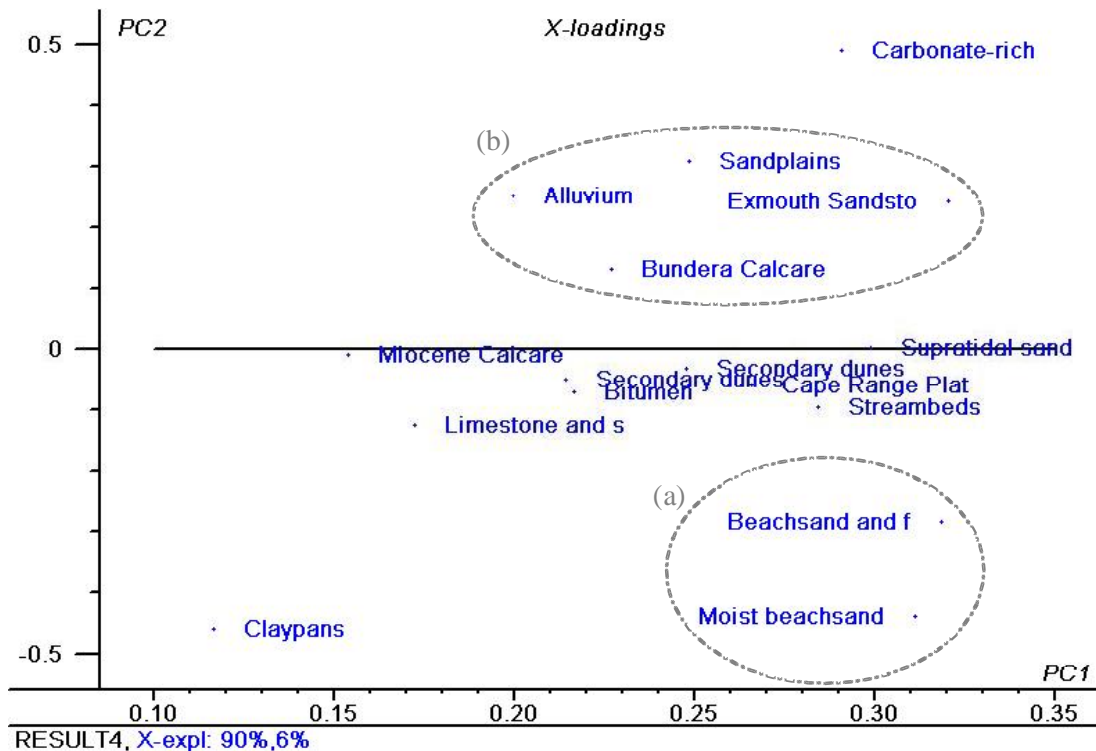


Figure 110. PCA plot of image derived reflectance spectra retrieved from locations corresponding to the field sites. Groupings found were bright coastal sediments with high moisture content (a) and bright inland sediments with low moisture content (b).

3.3.4 Vegetation cover

Vegetation Indices

A total of 27 vegetation indices were compared with respect to their abilities to isolate and thus mask out vegetation from the imagery (Table 16). The NDVI, a broadband greenness index, is a robust indicator of chlorophyll absorption and hence the presence of green vegetation (ENVI 2004). The NDLI is a senescent carbon index, which highlights areas of high lignin concentration indicative of woody vegetation (ENVI 2004). Thus used together, the NDVI and NDLI indices effectively removed the signal from both green and dry vegetation.

Green vegetation cover

There was a distinct difference in vegetation cover from south to the north of the whole study area along the 300m coastline, with majority of live shrubs and trees mapped being found in the northern part. Total area mapped for vegetation cover was 6 556km². Live shrubs and trees along the coast made up between 0.29% to 6.5% of the area, with the median of 1.0%. Shrubs and trees were mostly confined to drainage channels and two patches of mangroves, one small one along Yardie Creek and the second, larger one in the Mangrove Sanctuary.

Table 22. Summary of area (hectares) of live shrubs and trees along the coastal strip of Ningaloo, aggregated to five information classes for all data blocks. (Except for Murion Islands).

Cover type (ha)	Blk A	Blk B	Blk C	Blk D	Blk E	Blk F	Blk G	Blk H	Blk I	Blk K	Total
Acacia dominated	309.9	727.6	282.2	187.7	175.3	255.3	1061.5	1015.5	722.7	1253.1	5990.8
Ficus	23.4	179.0	8.5	1.3	0.1	0.6	151.7	463.2	19.5	23.8	871.0
Mixed shrubs in drainage systems	56.7	275.1	57.3	7.5	3.8	4.0	43.4	77.6	12.6	80.0	618.1
Coastal shrubs	3.4	3.1	0.9	7.5	1.5	3.8	2.2	4.3	158.8	276.0	461.4
Mangrove			0.0				0.2	17.4			17.7
Saltmarsh with sparse mangrove								12.6			12.6
Tamarisk	0.6	0.5	0.3	1.0	0.0						2.4
Total vegetation	394.0	1185.4	349.1	204.9	180.7	263.7	1259.0	1590.5	913.7	1632.9	7974.0
Percentage of vegetation the area mapped (%)	0.8	2.1	0.8	0.3	0.3	0.3	1.0	1.4	6.5	5.9	0.0

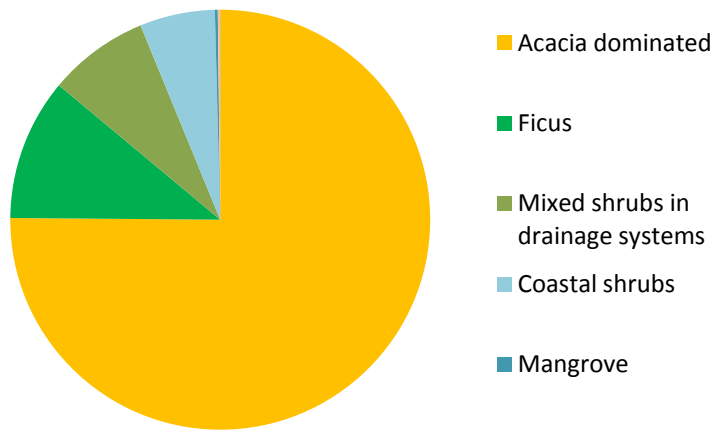


Figure 111. Overview of the green shrubs and trees cover within the Ningaloo coastal study area.

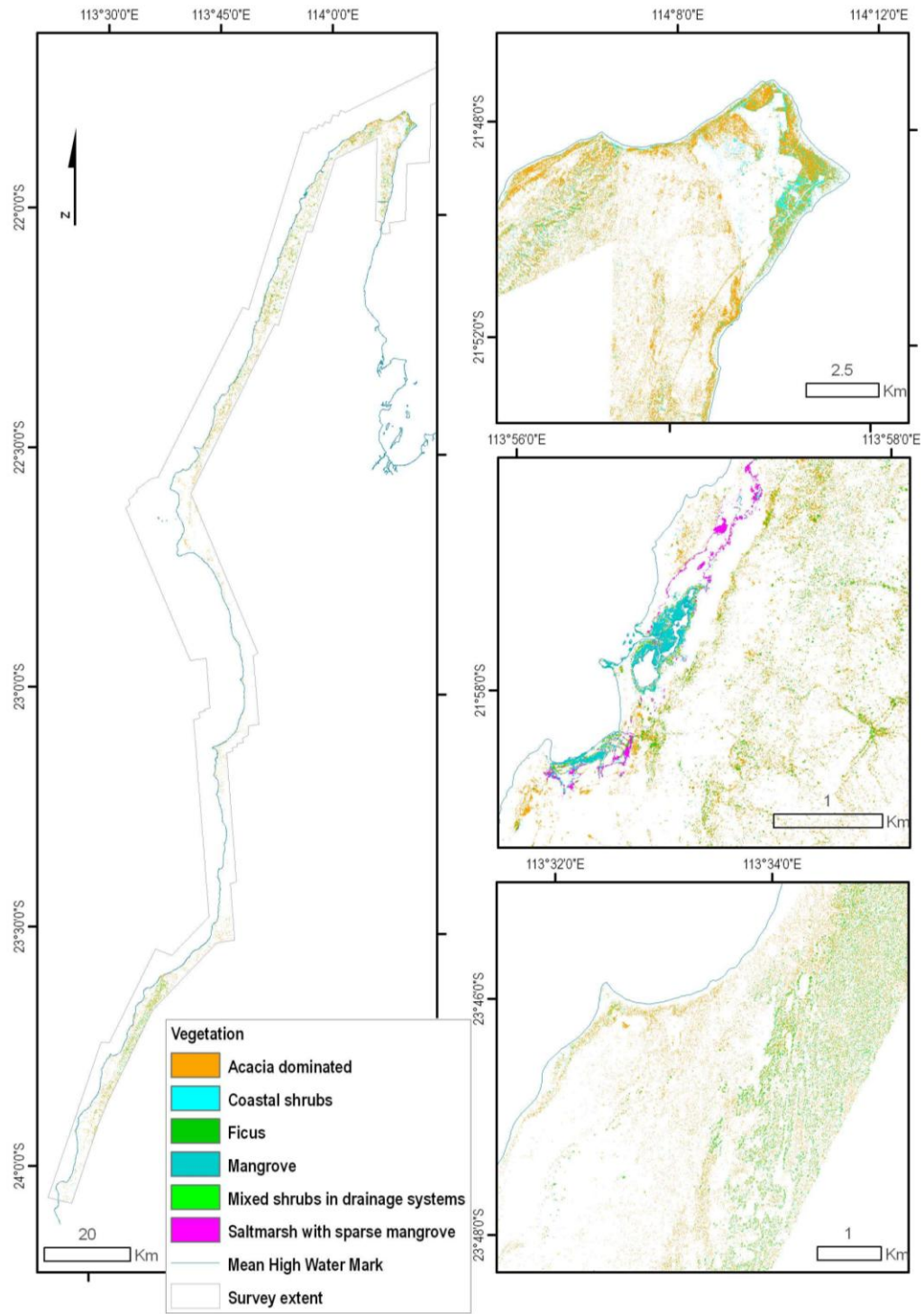


Figure 112. Overview of the green shrub and tree cover of the coastal areas adjacent to the Ningaloo coast. Inset maps are for the northern area of the Cape Range (top), Mangrove Bay (middle) and Gnaraloo Bay (bottom).

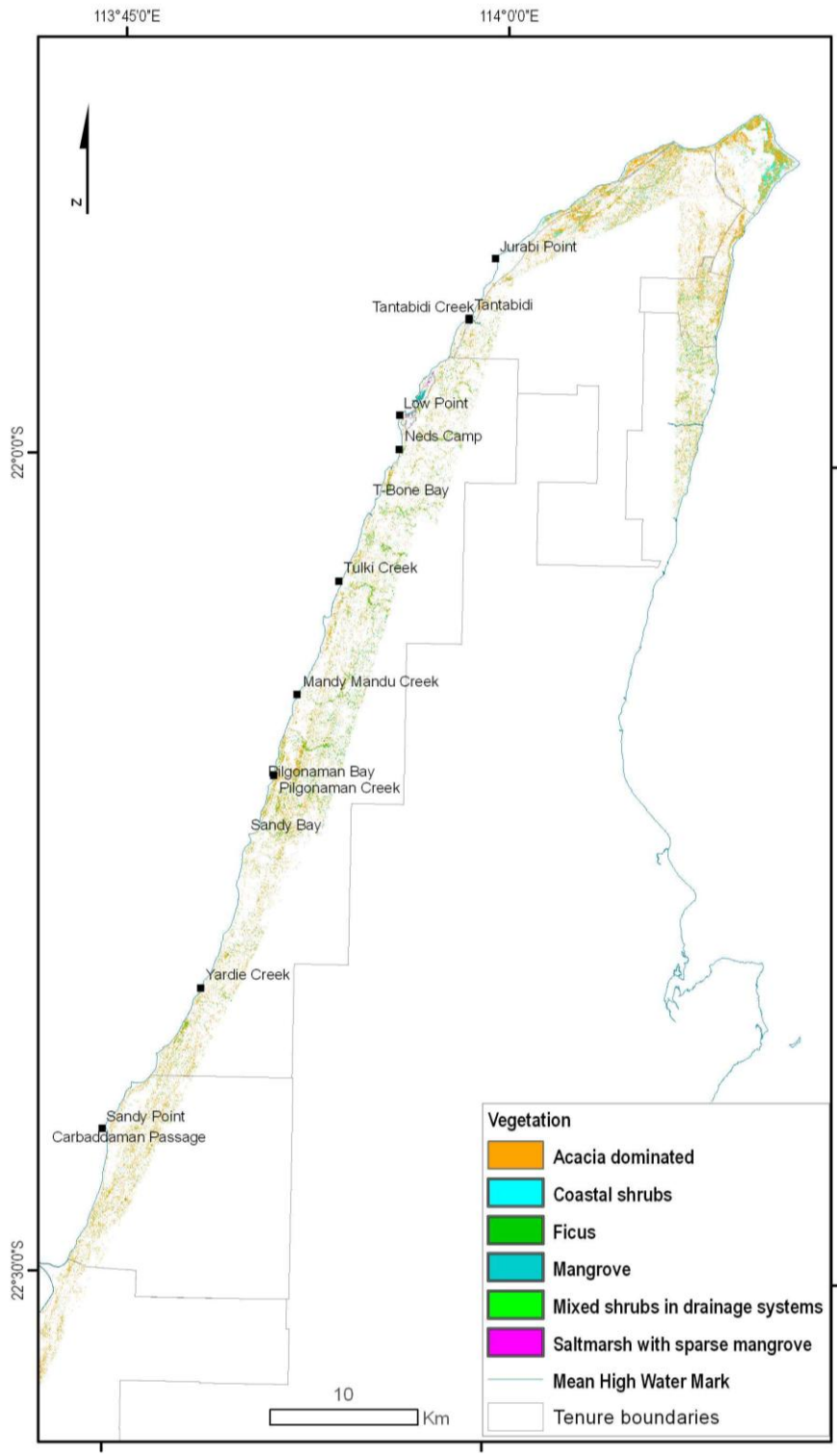


Figure 113. Overview of the green shrub and tree cover of the northern areas along the Ningaloo coast.

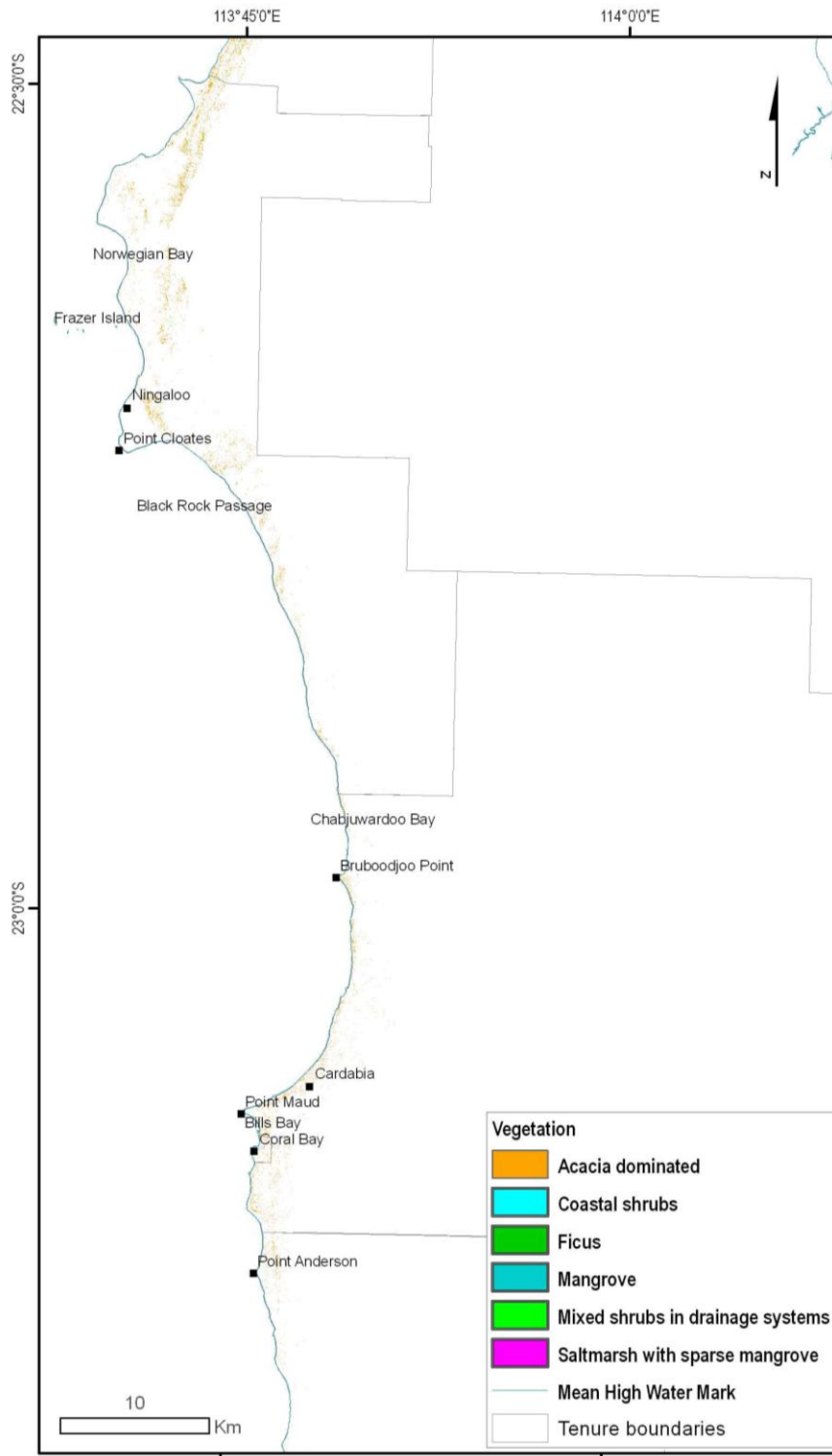


Figure 114. Overview of the green shrub and tree cover of the central section of along the Ningaloo coast.

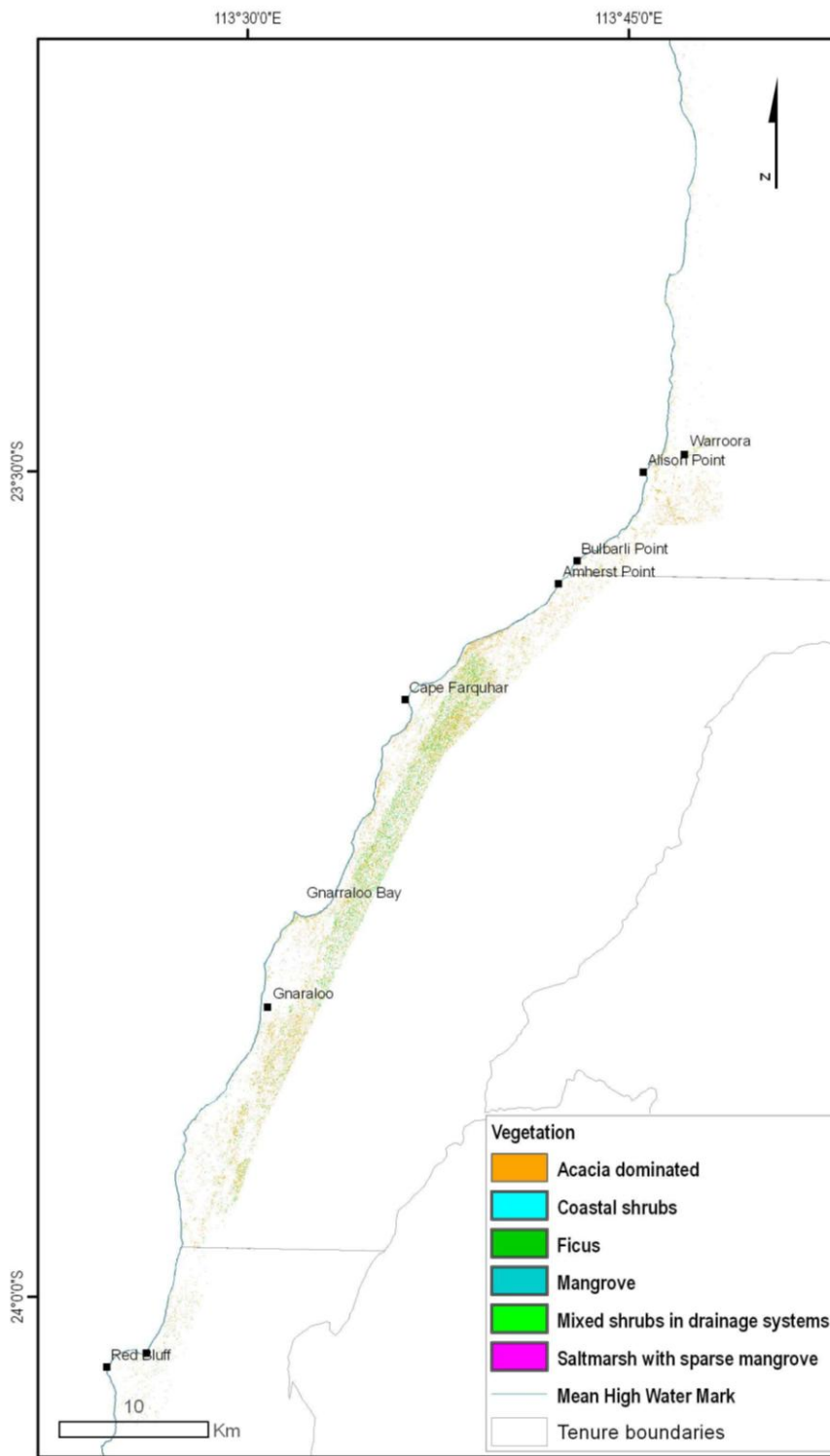


Figure 115. Overview of the green shrub and tree cover of the southern section of the Ningaloo coast.

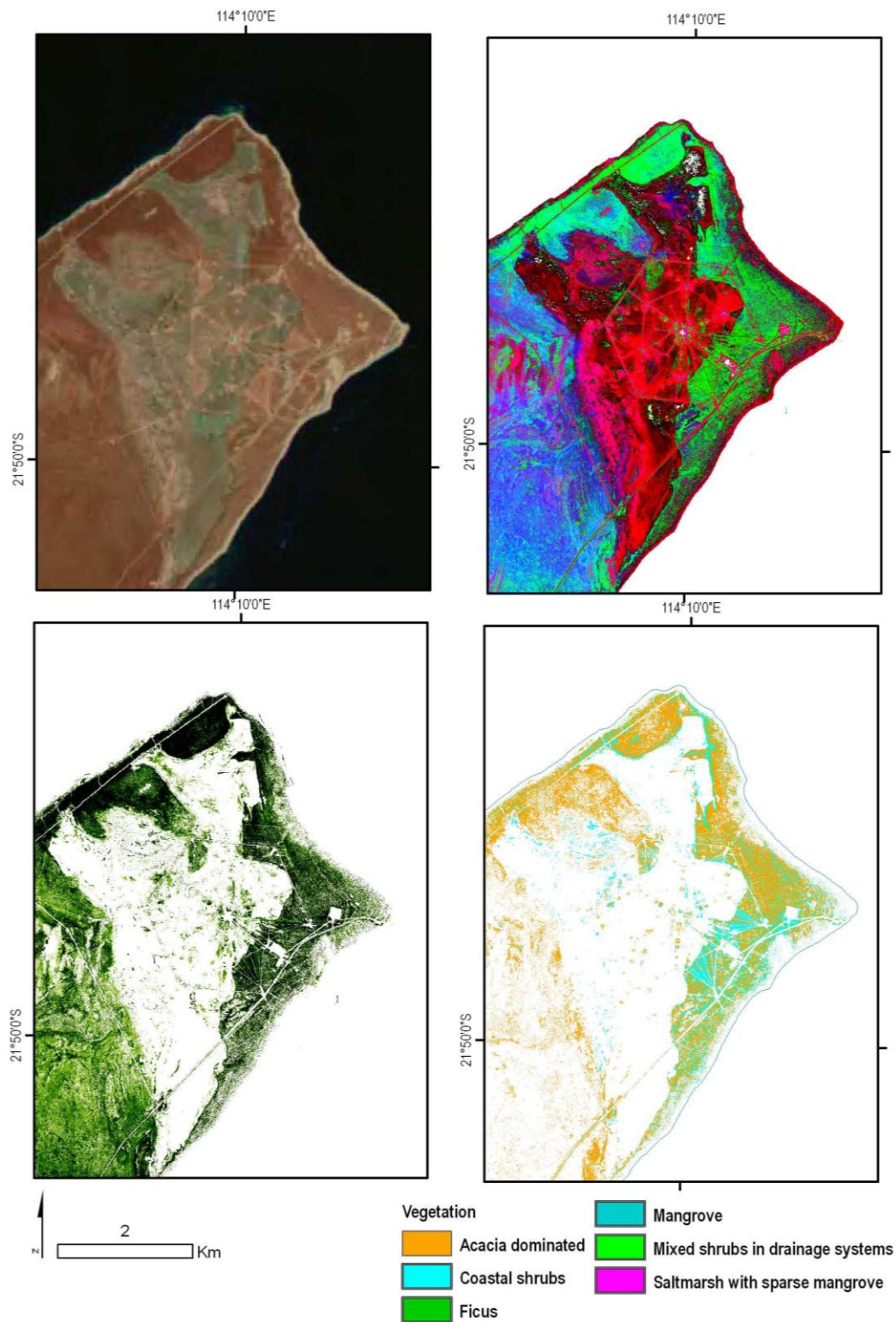


Figure 116. Example of the vegetation cover maps for the northern part of the North West Cape (top left-near normal colour image), top right is a composite of three vegetation indices highlighting bare areas (in red), relatively densely vegetated areas (green) and sparse vegetation in senescent state (blue). Bottom right image depicts vegetation index data and bottom right image illustrates the extent of the green shrub cover.

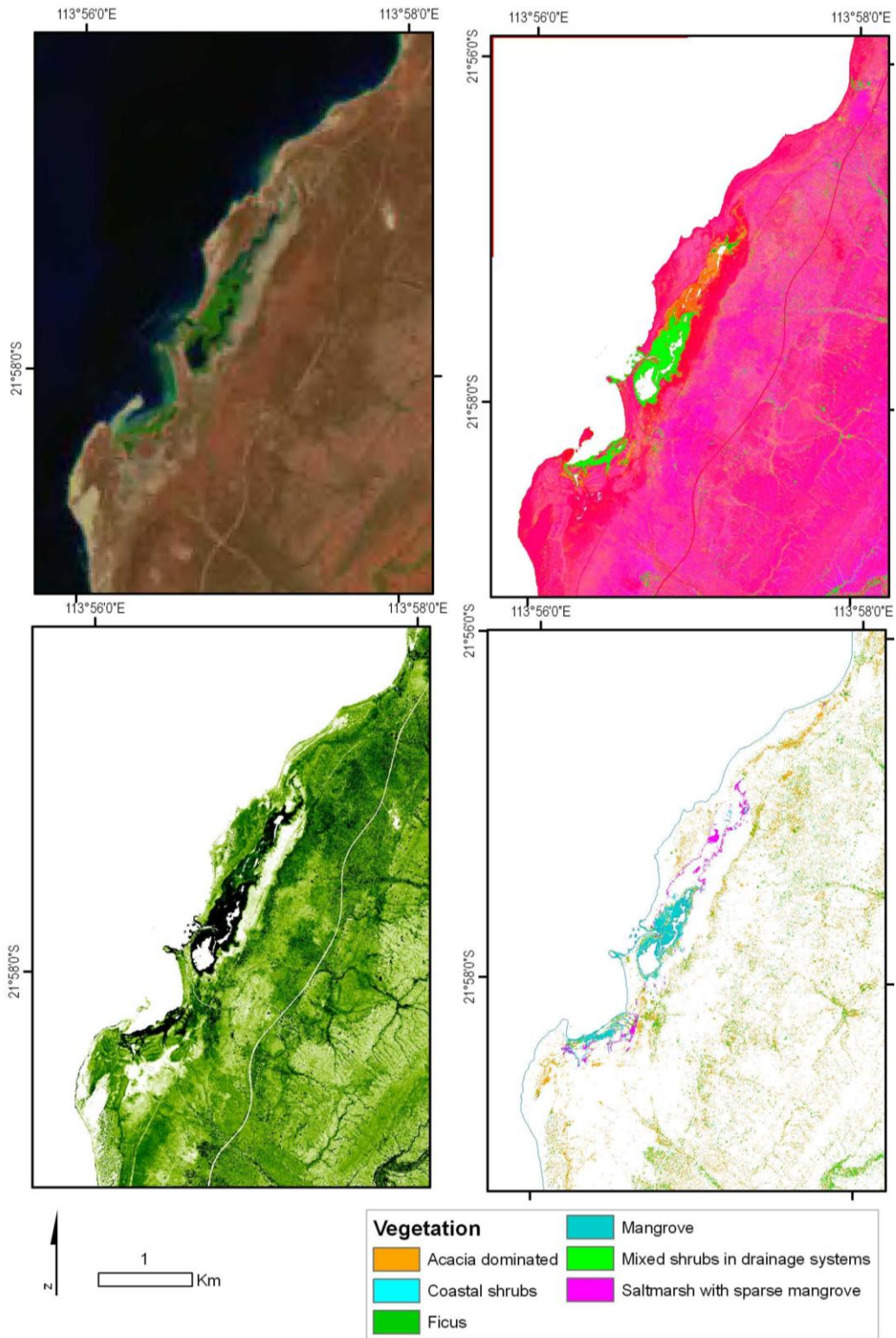


Figure 117. Example of the vegetation cover maps for the Mangrove Bay region (top left- near normal colour image), top right is a composite of three vegetation indices highlighting bare areas (in red), relatively densely vegetated areas (green) and sparse vegetation in senescent state (blue). Bottom right image depicts vegetation index data and bottom right image illustrates the extent of the green shrub cover.

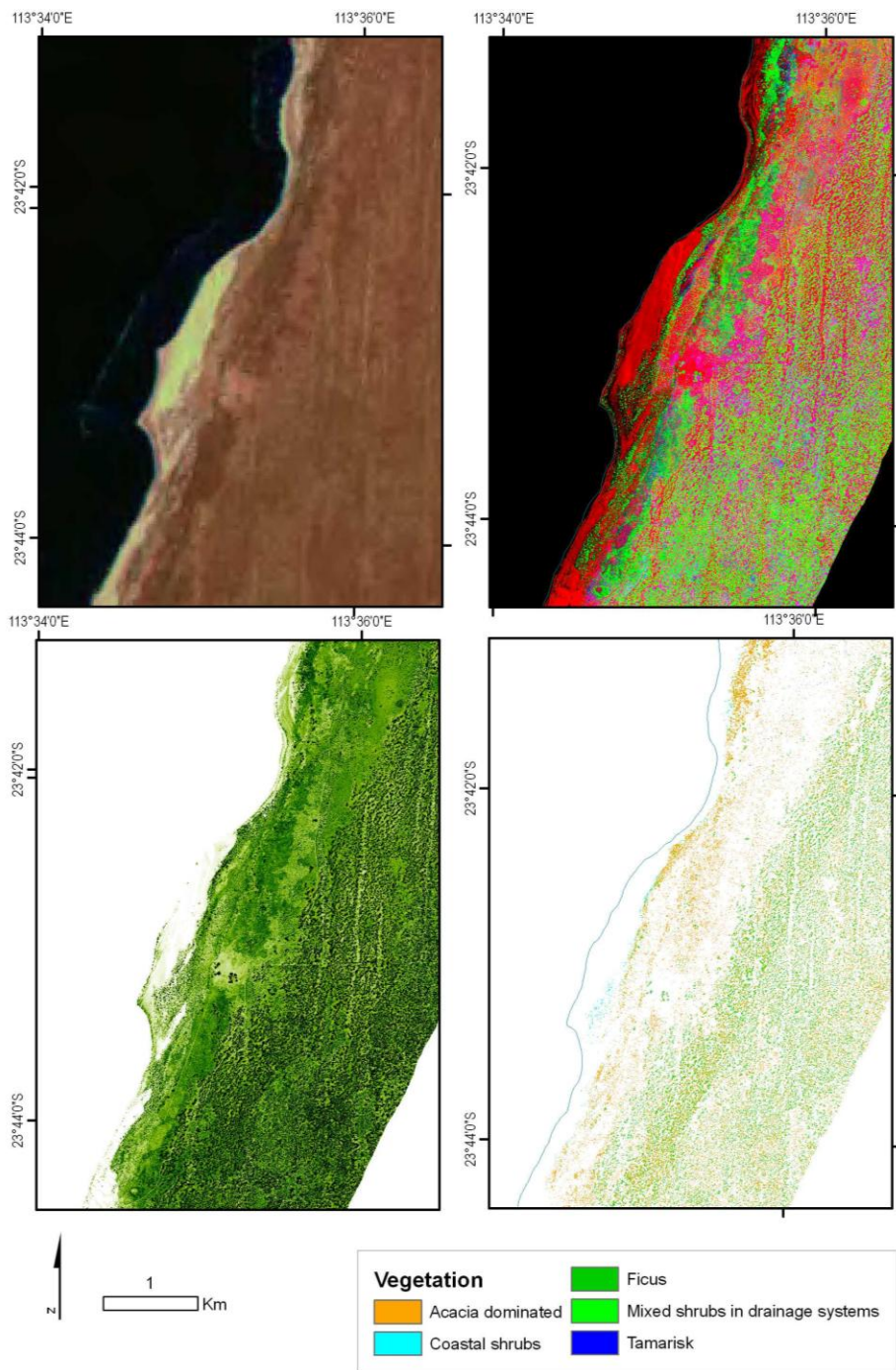


Figure 118. Example of the vegetation cover maps for the southern part of the Ningaloo coast (top left-near normal colour image), top right is a composite of three vegetation indices highlighting bare areas (in red), relatively densely vegetated areas (green) and sparse vegetation in senescent state (blue). Bottom right image depicts vegetation index data and bottom right image illustrates the extent of the green shrub cover.

3.3.5 Lengths and densities of roads and tracks

Pastoral leases and the Cape Range National Park comprised the greatest proportion of the study area and areas for each type of land tenure are shown in Table 23.

Table 23. Total area of (km²) in different land tenures within the Ningaloo study area.

Category	Miscellaneous crown land	National Park	Freehold land	Unallocated crown land	Pastoral Lease	Total
Total area (km ²)	16.5	102.0	56.7	39.1	399.2	613.5

The road network along the southern and northern Ningaloo coast is shown in Figure 119 and Figure 120. The cumulative distance of roads/tracks in different land tenures shows that the pastoral leases had the highest number of total roads and tracks (847.5 km), followed by freehold land (115.9 km) (Table 24).

Table 24. Total cumulative length (km) of major roads, minor roads and tracks adjacent to the Ningaloo Marine Park.

Category	Misc. crown reserve	Unallocated crown land	National Park	Freehold land	Pastoral lease	Total
Major	11.4	22.5	50.7	15.9	4.2	104.7
Minor	9.3	1.2	23.4	7.0	41.0	81.9
Tracks	32.0	51.4	29.1	93.0	802.3	1007.8
Total roads (km)	52.7	75.1	103.2	115.9	847.5	1194.4

The total cumulative distance of roads/tracks in different land tenures is also related to the area of the land under investigation. The highest density of major roads was found in miscellaneous crown reserve with 1.0 km/km² and the lowest was in pastoral leases (0.1 km/km²) (Table 25). As for minor roads, the highest density of was also found in miscellaneous crown reserve and the lowest was in unallocated crown land. The highest density of tracks was found in pastoral leases (9.7 km/km²) and the lowest track density was found in Cape Range National Park (Table 25).

Table 25. Density of roads (major, minor and track) in different land tenures (km road per km² area) adjacent to the Ningaloo Marine Park.

Category	National Park	Unallocated Crown Land	Freehold Land	Miscellaneous Crown Reserve	Pastoral Lease
Major	0.5	0.6	0.6	1.0	0.1
Minor	0.2	0.0	0.2	2.6	0.6
Track	0.3	1.3	3.3	3.6	9.7
Total	1.0	1.9	4.1	7.2	10.4

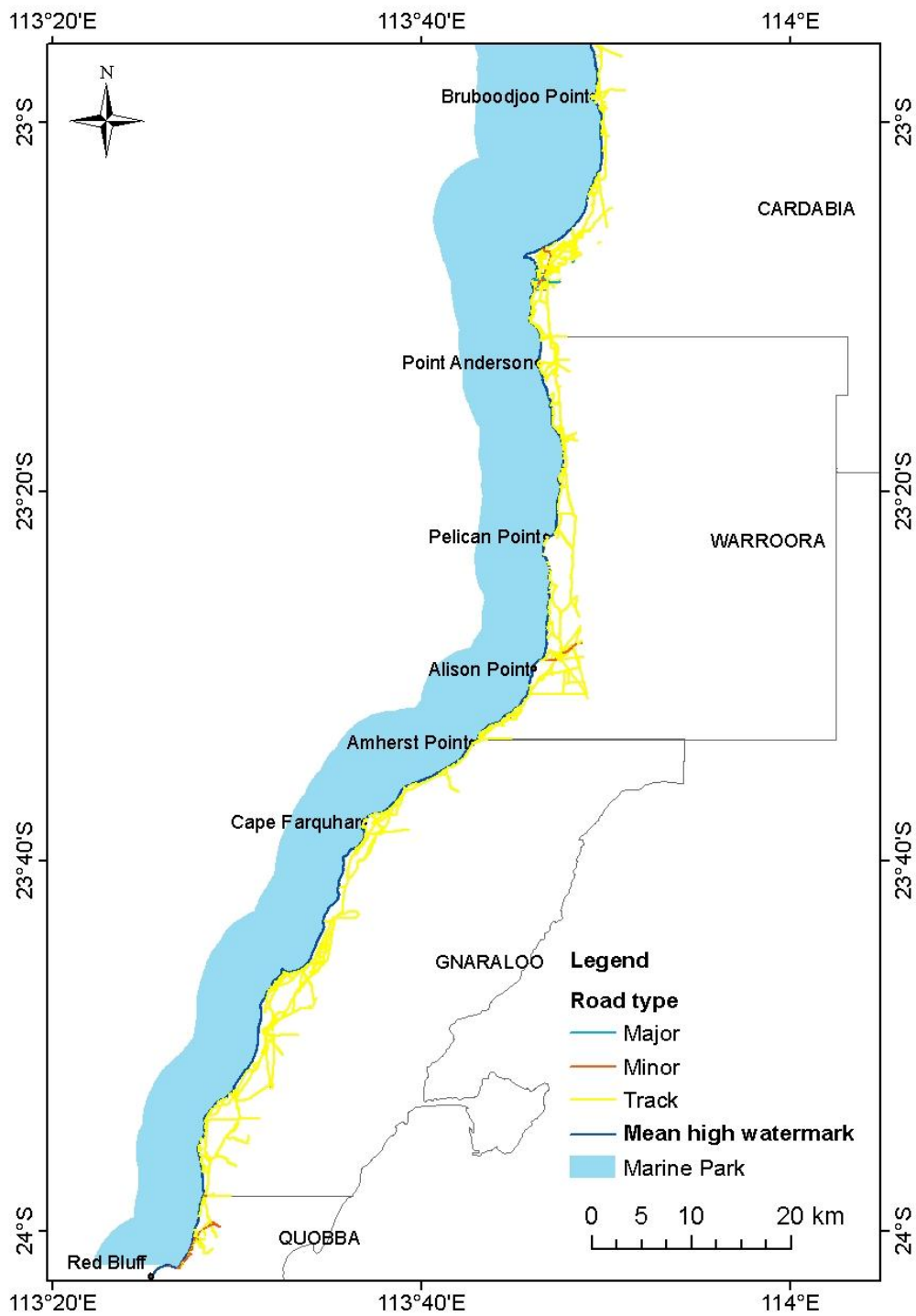


Figure 119. The road and track network along the southern coast adjacent to Ningaloo Marine Park from Red Bluff to Bruboodjoo Point.

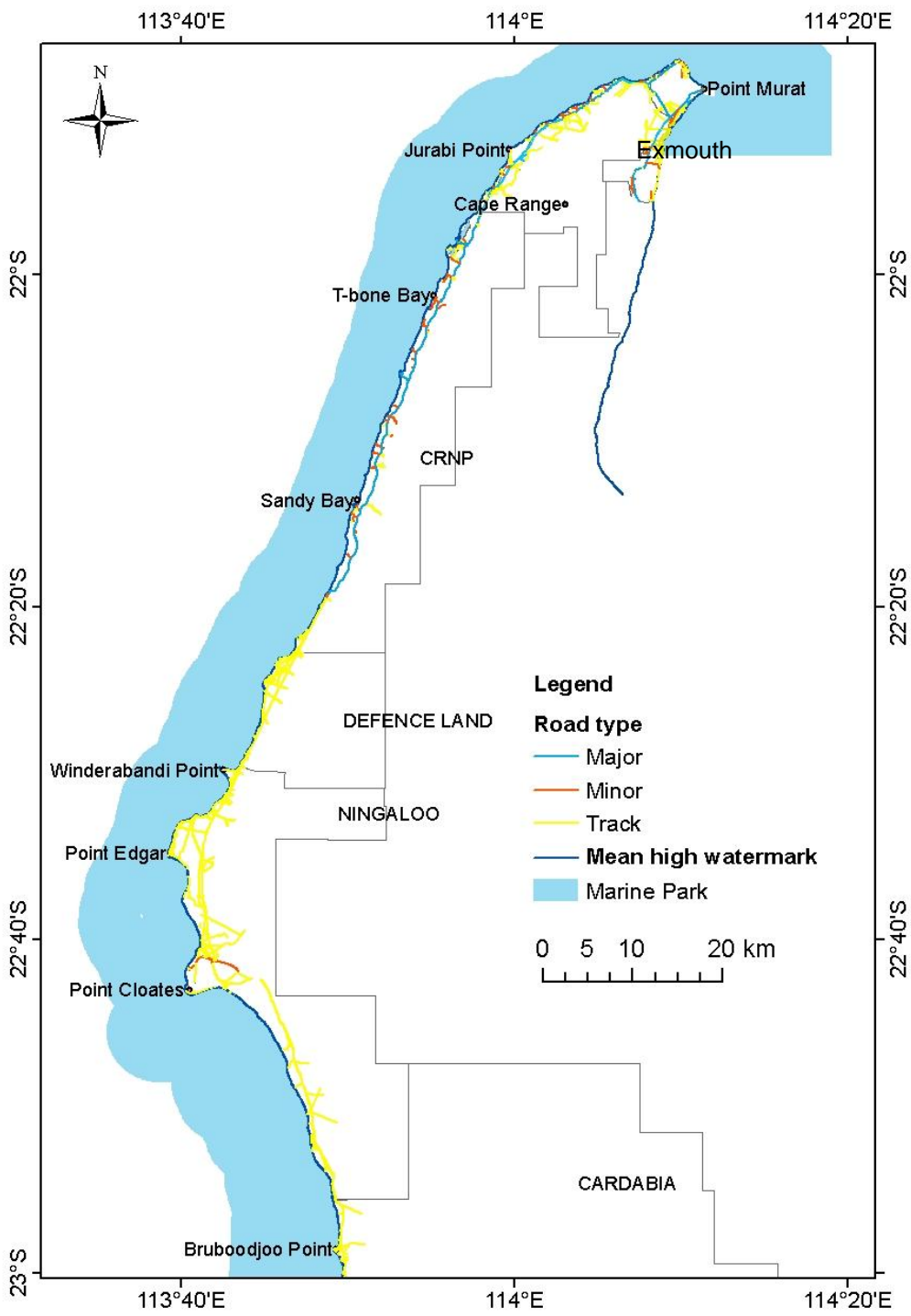


Figure 120. The road and track network along the southern coast adjacent to Ningaloo Marine Park from Bruboodjoo Point to Exmouth.

3.3.6 Cumulative length and densities of roads/tracks in pastoral stations

The cumulative distance of roads/tracks in different pastoral stations (Table 26) showed that Gnaraloo station had the greatest length number of total roads and tracks (239.4 km), followed by Ningaloo station (213.7 km) (Table 26).

Table 26. Total cumulative length of major roads, minor roads and tracks (km) in the pastoral stations adjacent to the Ningaloo Marine Park.

Pastoral Station	Major roads (km)	Minor roads (km)	Tracks (km)	Total (km)
Ningaloo	0.0	3.4	210.3	213.7
Cardabia	4.2	7.0	169.1	180.3
Warroora	0.0	2.3	168.8	171.1
Gnaraloo	0.0	17.5	221.9	239.4
Quobba	0.0	10.8	32.1	42.9

The total road and track density for the pastoral stations is shown in Table 27. Cardabia Station had the highest total road density (3.1 km/km²) and Quobba station has the lowest densities of roads/tracks (1.1 km/km²).

Table 27. Density of roads (major, minor and tracks) in the pastoral stations (km of road per km² area) adjacent to the Ningaloo Marine Park.

Pastoral Station	Major roads (km/km ²)	Minor roads (km/km ²)	Tracks (km/km ²)	Total (km/km ²)
Ningaloo	0.0	0.0	1.8	1.9
Cardabia	0.1	0.1	2.9	3.1
Warroora	0.0	0.0	2.1	2.1
Gnaraloo	0.0	0.2	2.1	2.3
Quobba	0.0	0.3	0.8	1.1

High densities of roads/tracks were found at a range of locations along the coast. Between Red Bluff Camp and 3 Mile Camp were six locations with high densities of road (Figure 121) including areas at Red Bluff Camp and 3 Mile Camp. On Gnaraloo station there were areas with high density of road and track with four of these around Gnaraloo Bay, one at Gnaraloo homestead and one at 3 Mile Camp (Figure 122). Between Cape Farquhar and Amherst Point there was a low density of roads/tracks with no area of high density except south of Cape Farquhar (Figure 123). From Amherst Point to Warroora there were five locations with high density of roads/tracks, particularly near the camp sites and around Warroora homestead (Figure 124). Along the northern extent of Warroora station, two adjacent areas with high density of roads were located around 14 Mile camping area (Figure 125).

On Cardabia station, north of Point Anderson there were seven locations with high density of roads that were located around Coral Bay and Cardabia homestead (Figure 126) with a few grid cells that had > 500 m per grid cell. In the northern part of Cardabia station there was a high density of road/tracks around the camping area at Bruboodjoo Point (Figure 127). In the southern part of Ningaloo station, high densities of roads/tracks were located at six locations (Figure 128). On Ningaloo station there was a vast network of tracks north of the homestead

around the sheds and shearers' quarters (Figure 129). On the northern part of Ningaloo station there were many areas of high track density especially at camp sites around Lefroy Bay and Winderbandi Point (Figure 130). At three locations within the land managed by the Department of Defence, south of Cape Range National Park, there were high densities of tracks. Tracks were associated with camping areas around Sandy Point and Kangaroo Flats (Figure 130 and Figure 131).

In Cape Range National Park, between Yardie Creek and Ned's Camp there were no distinct locations with high density of roads (Figure 132 and Figure 133). However, along the sealed road extending south to Yardie Creek there were several tracks to the west, servicing camping sites. In the northern Cape Range National Park and in the Jurabi Coastal Park, there were two locations with high density of tracks, namely Low Point and Jurabi Point (Figure 133). Note that the main sealed road between Yardie Creek and Exmouth traverses the region. Between Jurabi Point and North West Cape, there were no distinct locations with high density of roads (Figure 134) although the main road from Exmouth to Yardie Creek traverses the area. Around the North West Cape, there were five locations with high density of roads (Figure 135) near Point Murat and Bundegi. Around the town of Exmouth there were six locations with high density of roads (Figure 136). They were along the coast around the residential and industrial areas of the town.

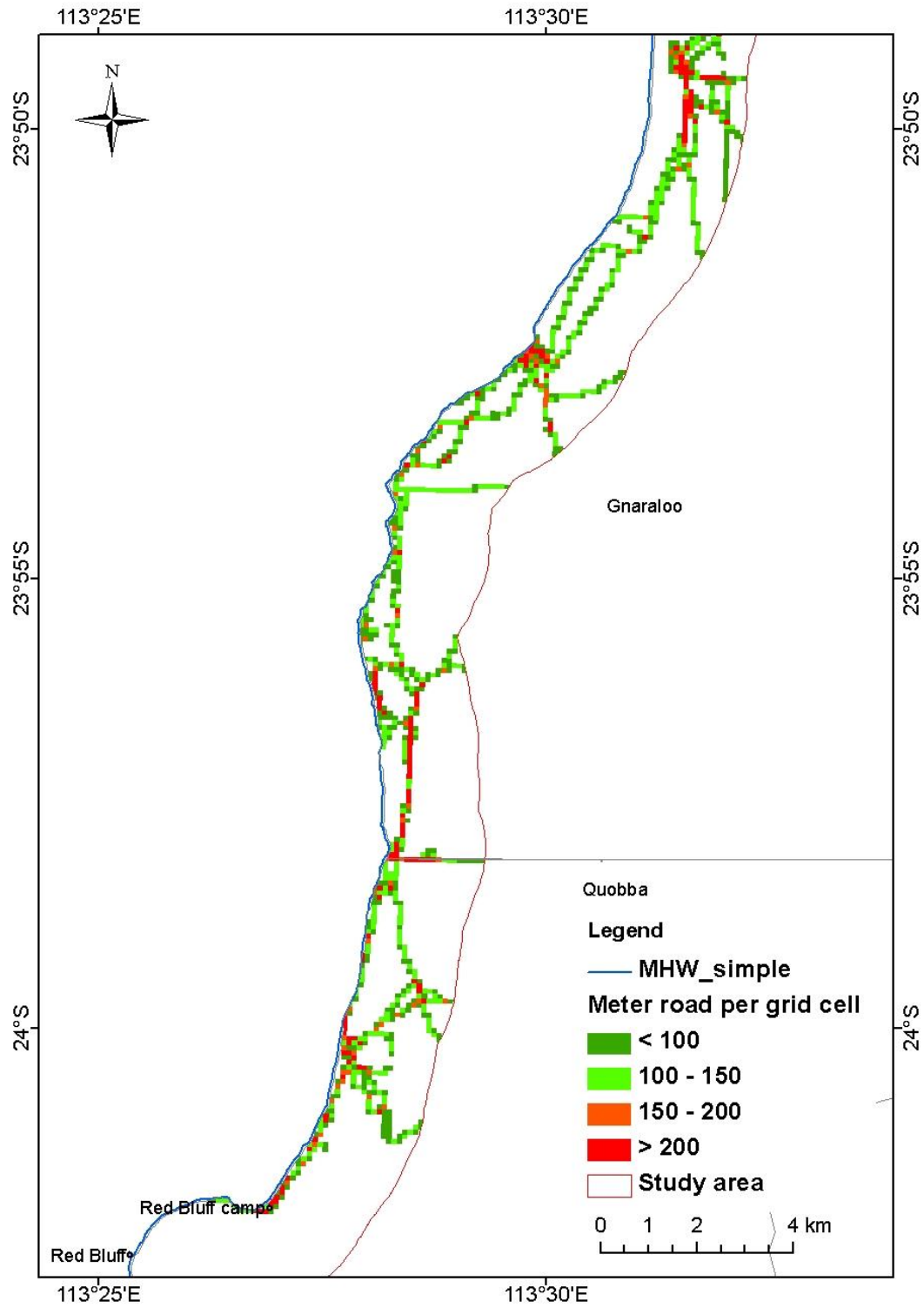


Figure 121. Road and track density on Quobba and Gnaraloo stations highlighting the six areas with density greater than 200 m per 100 m x 100 m grid cell.

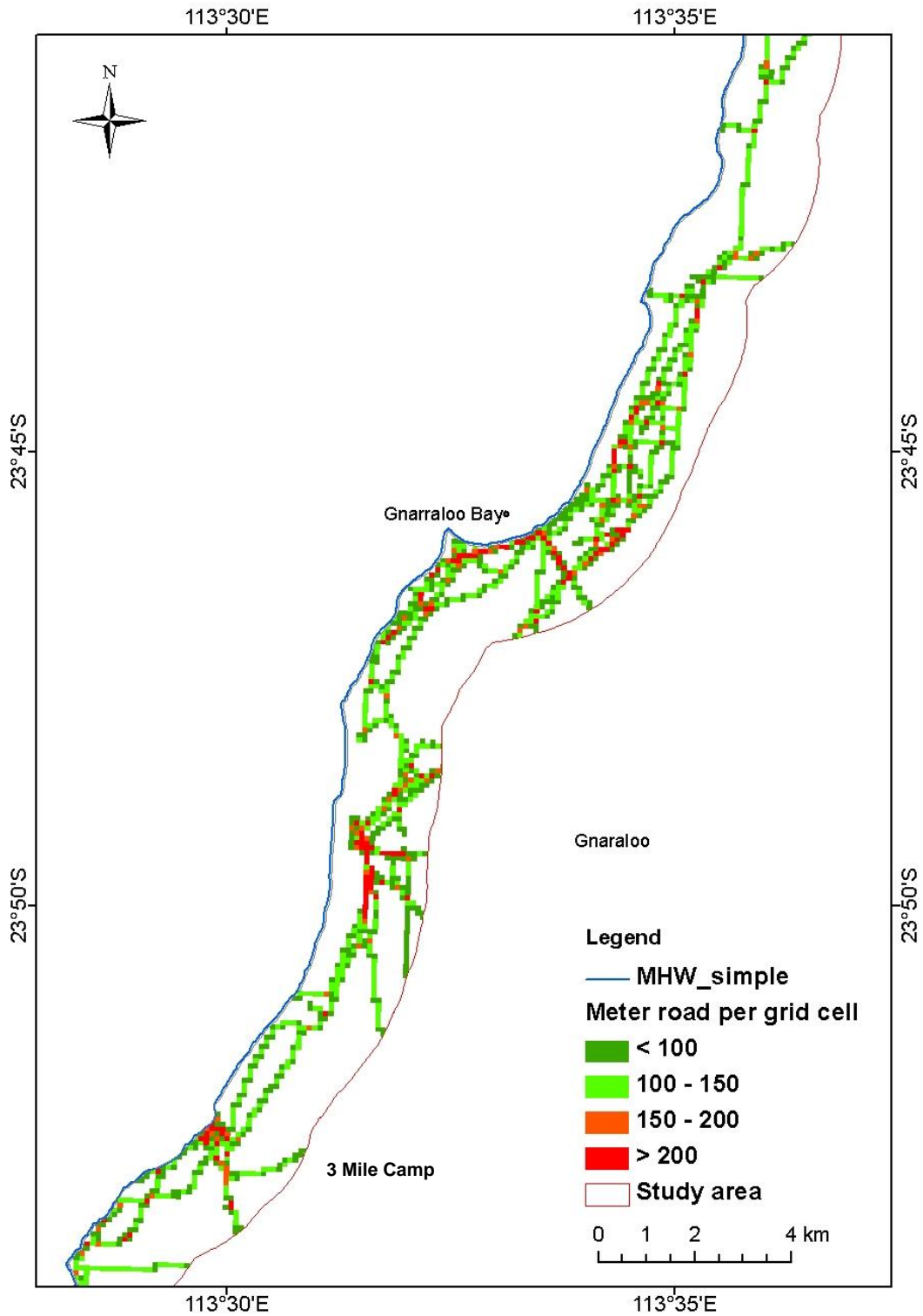


Figure 122. Road and track density between 3 Mile Camp and Gnaraloo Bay highlighting six areas with density greater than 200 m per 100 m x 100 m grid cell.

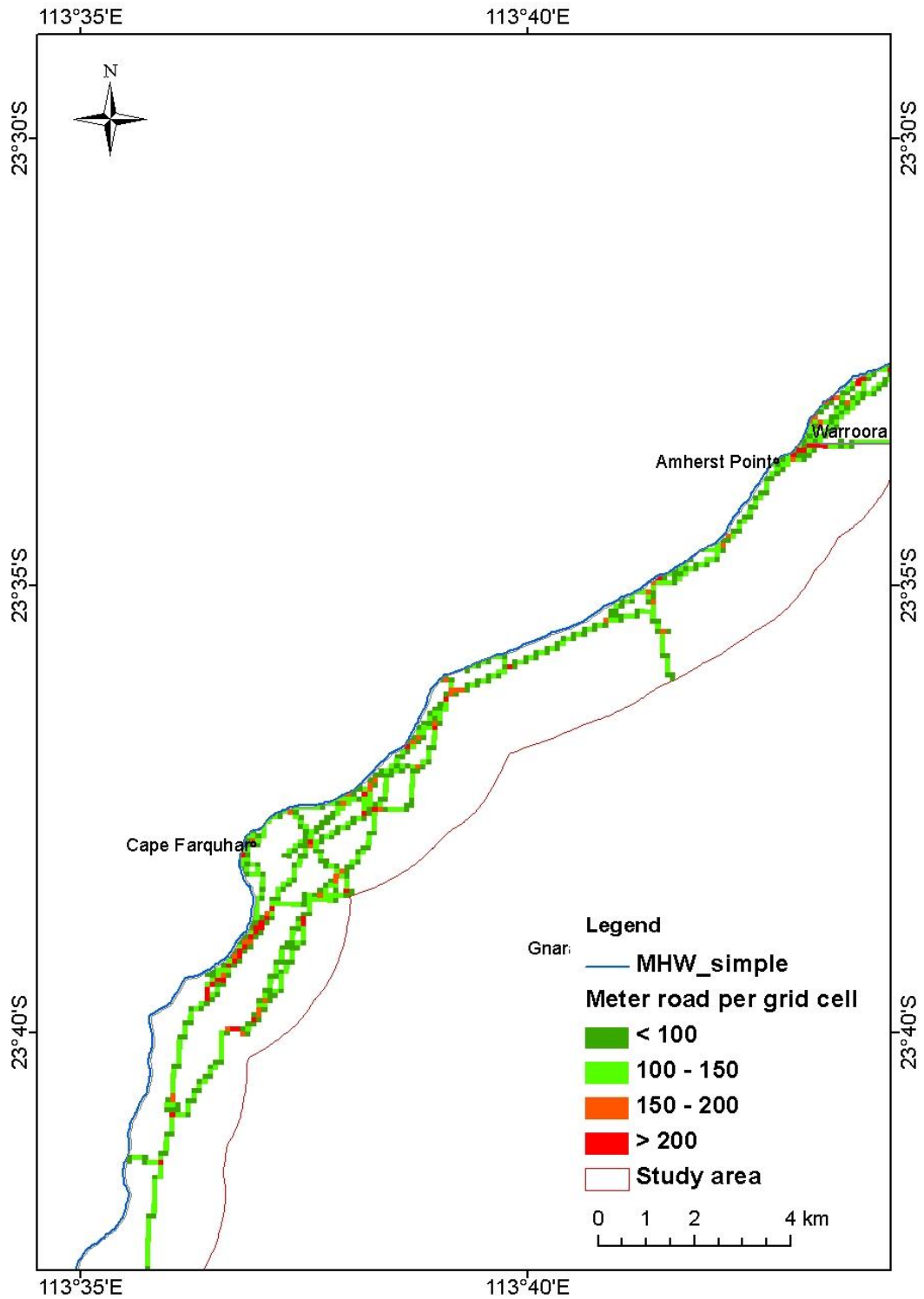


Figure 123. Roads/tracks density between Cape Farquhar to Amherst Point with one area showing high density on the southern extent of Cape Farquhar.

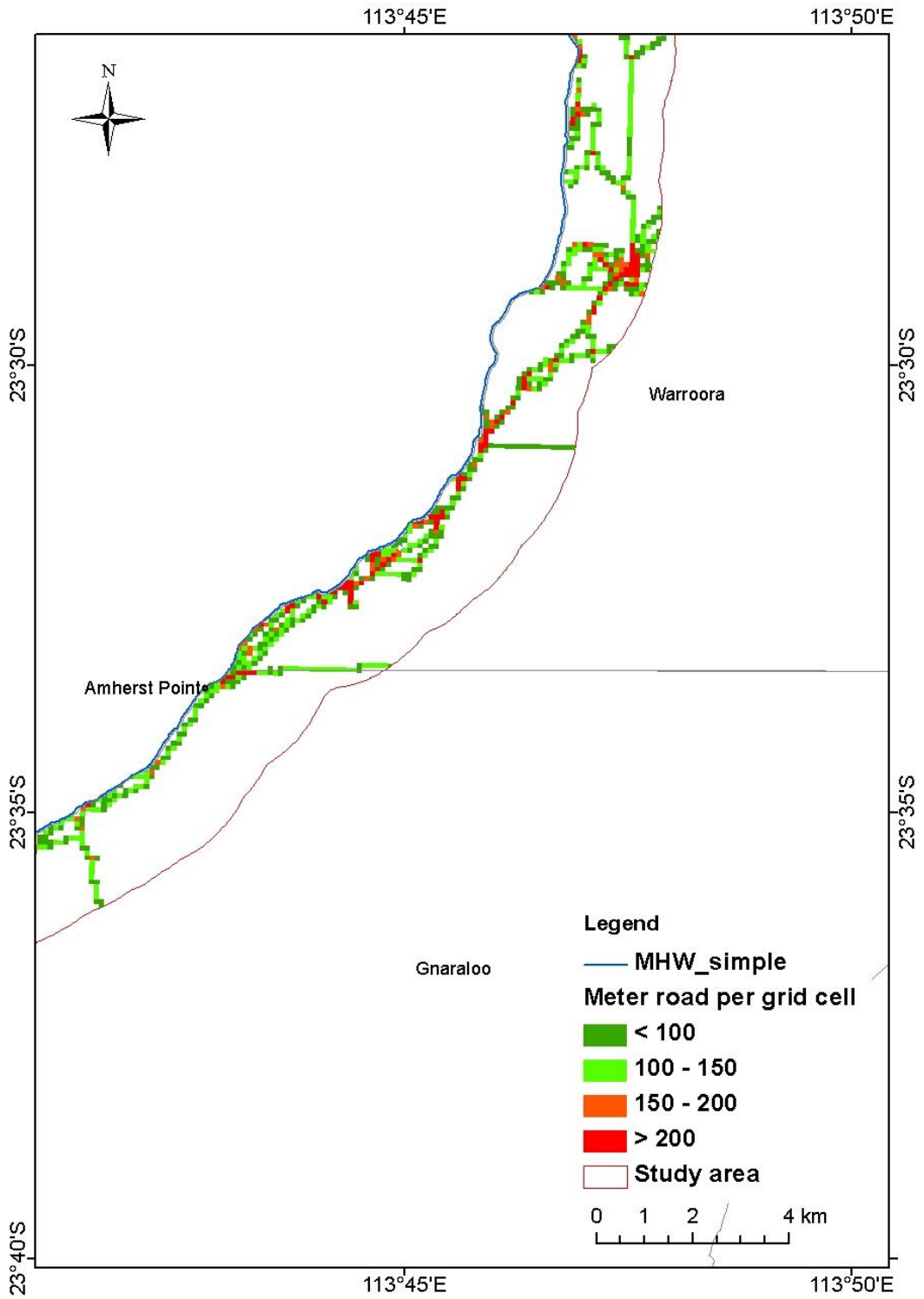


Figure 124. Road/track density between Amherst Point and Warroora homestead indicating five areas with high density of tracks.

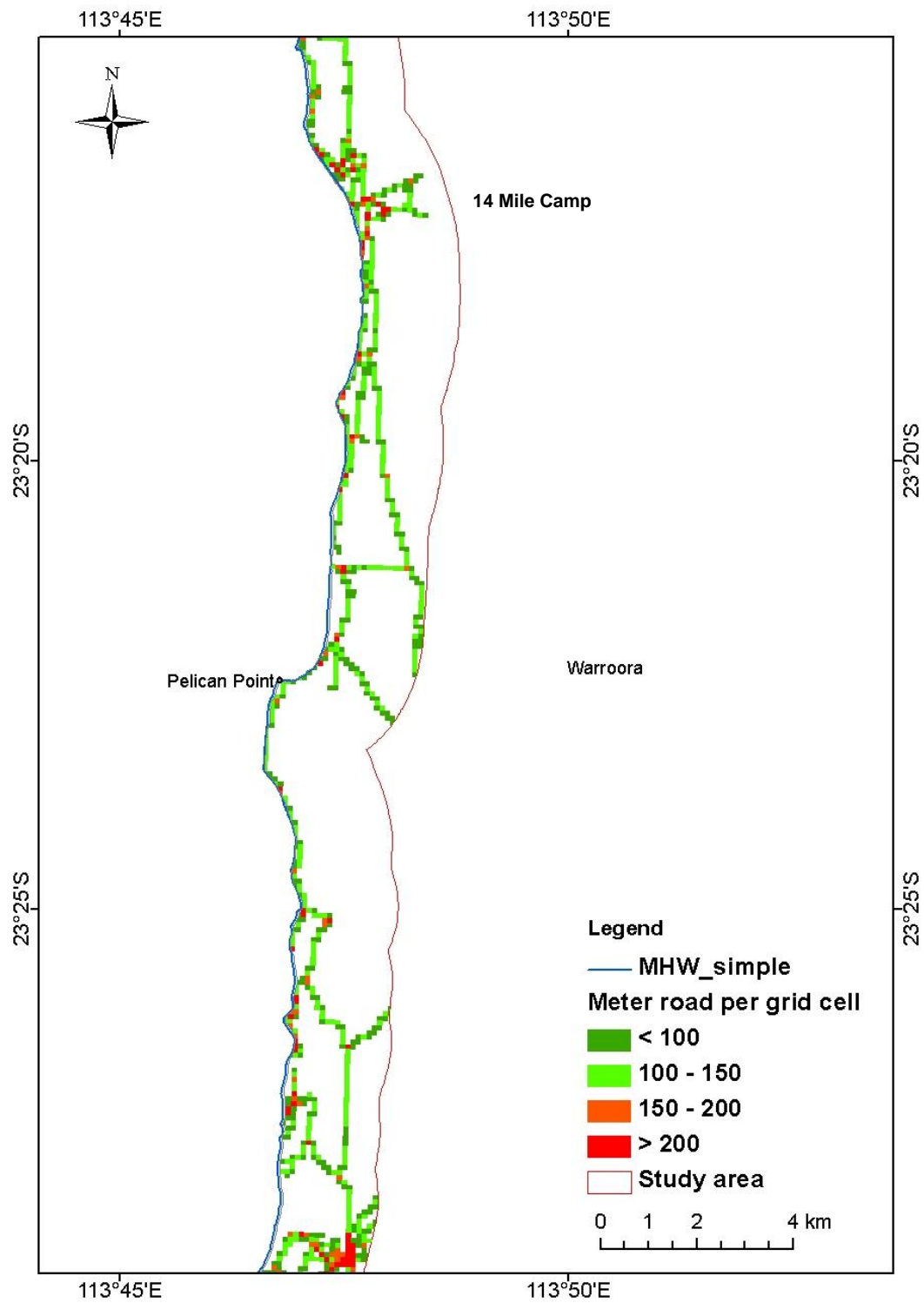


Figure 125. Road/track density on the Northern part of Warroora station showing high density of tracks around the 14 Mile Camp site.

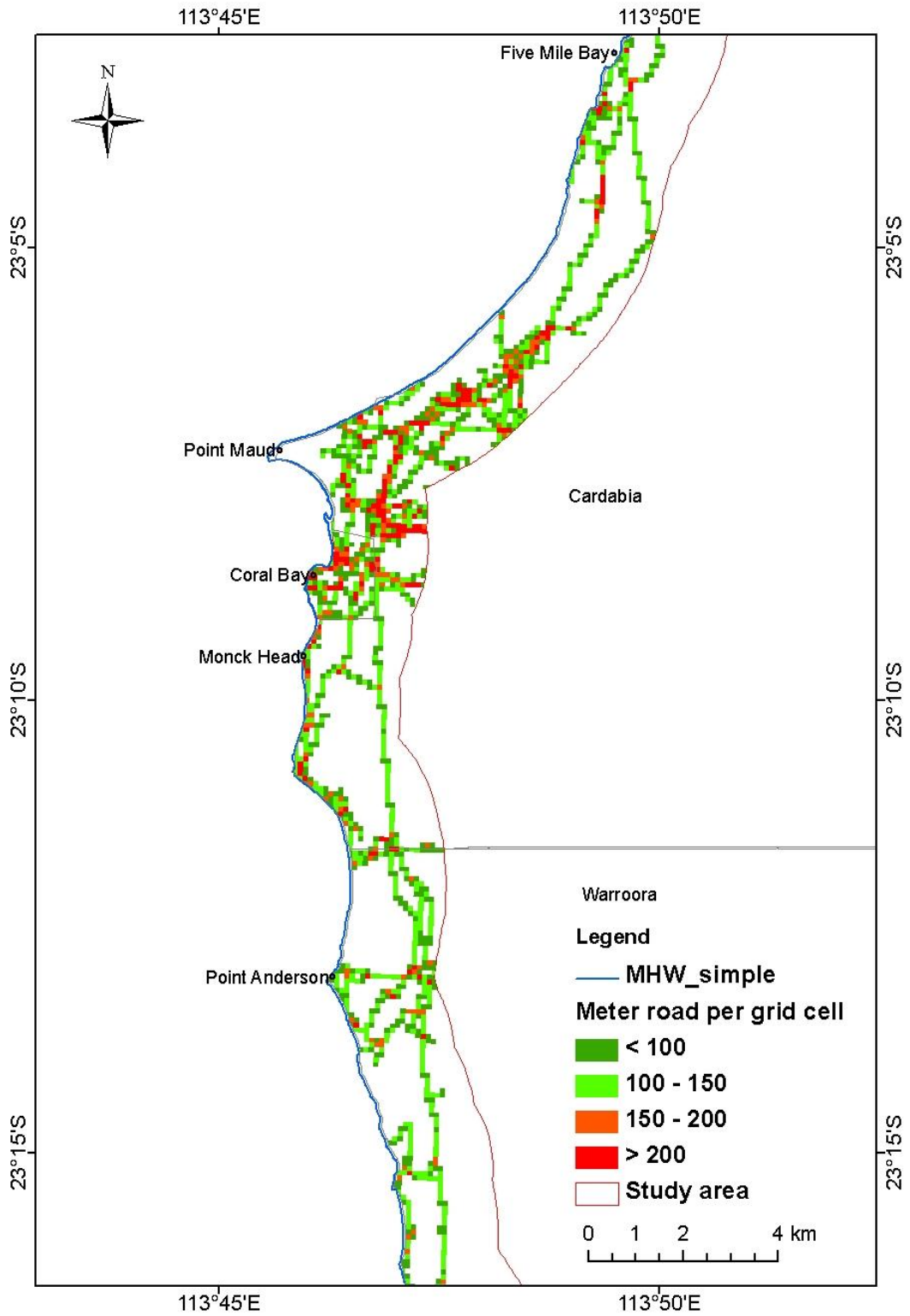


Figure 126. Road and track density on the southern part of Cardabia station showing high density of tracks around Coral Bay.

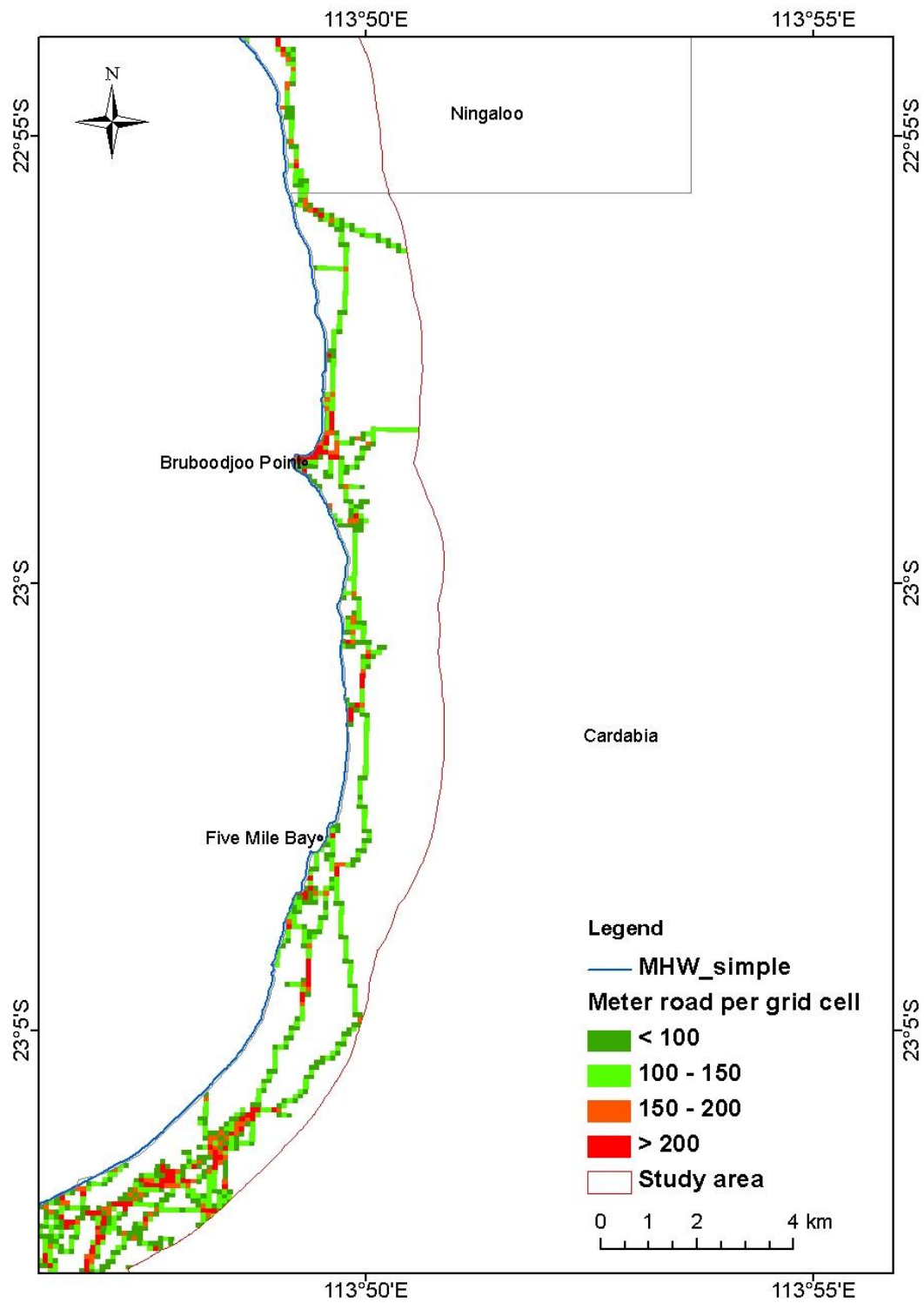


Figure 127. Road and track density on the northern extent of Cardabia station with high density around Bruboodjoo Point.

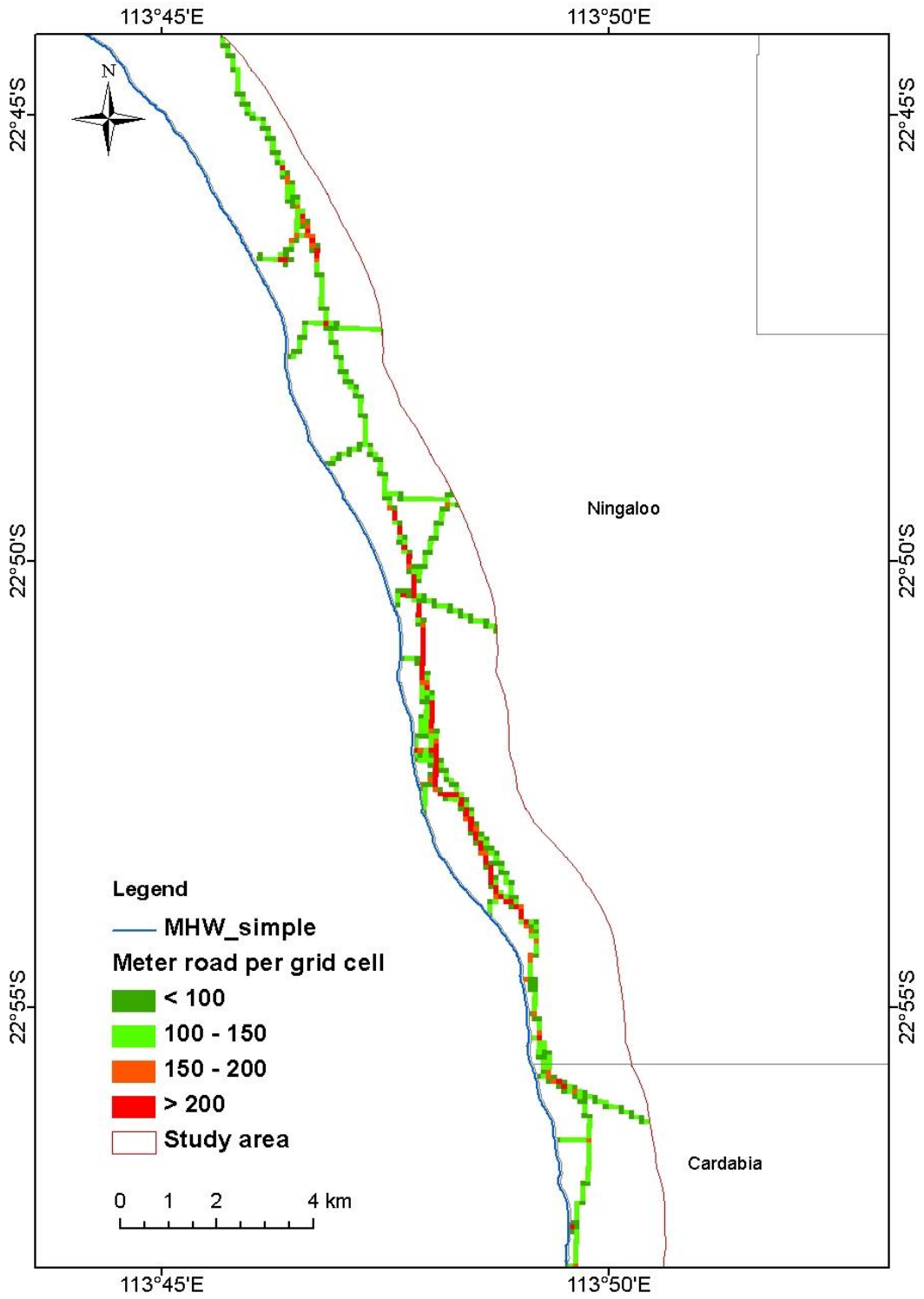


Figure 128. Southern part of Ningaloo station indicating six areas with high road and track density.

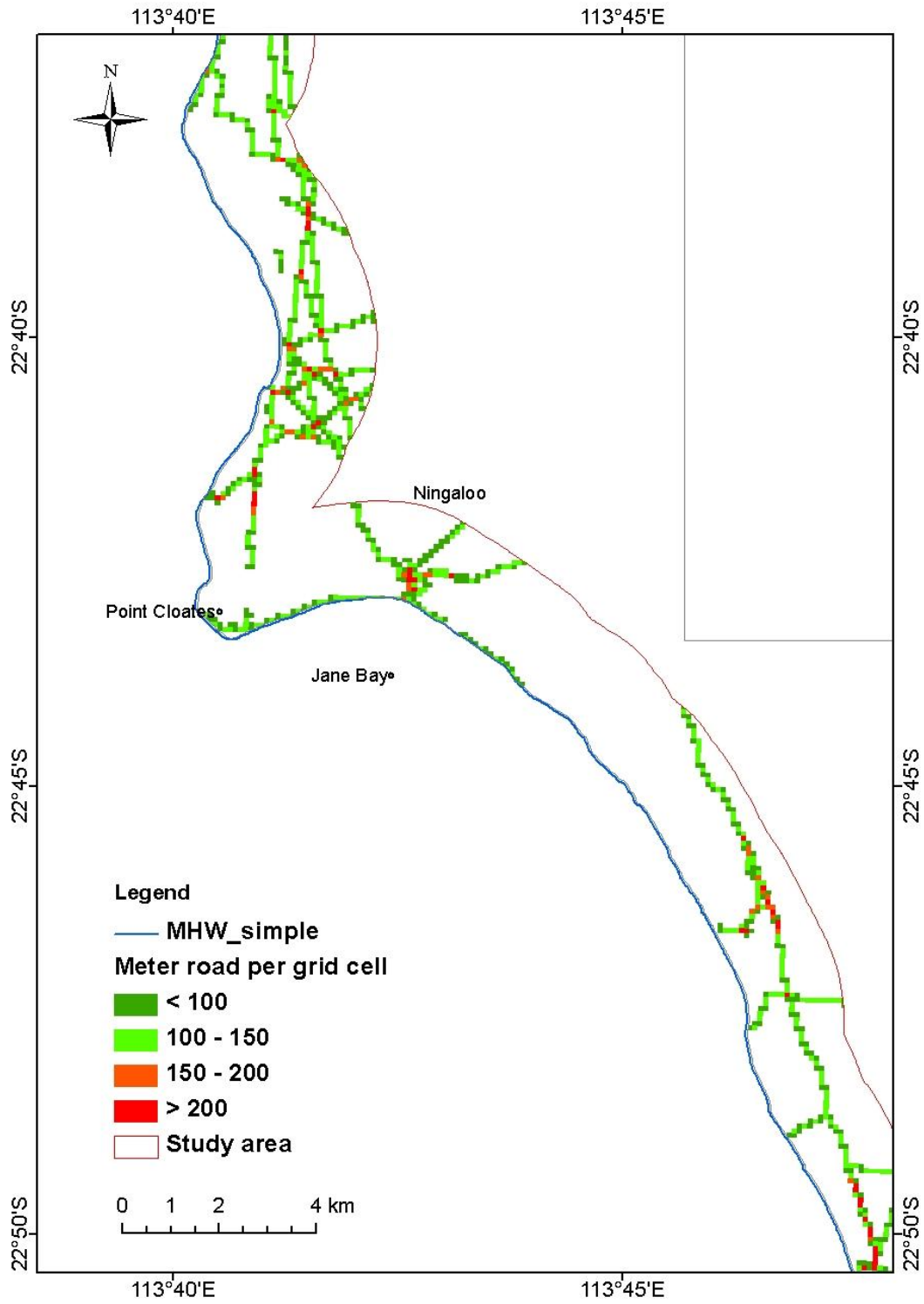


Figure 129. Road/track density on the central part of Ningaloo station showing locations of high density.

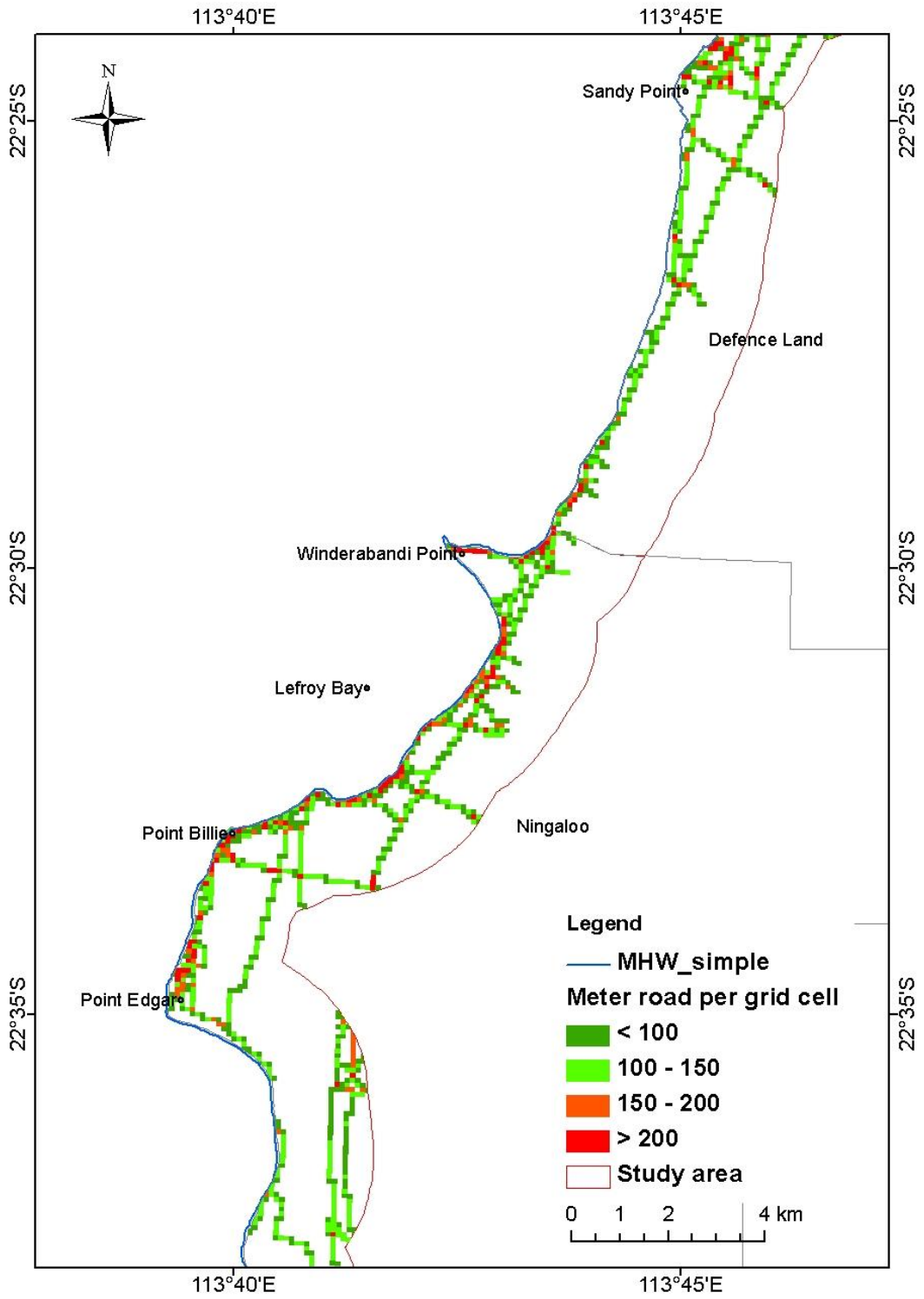


Figure 130. Road/track density for the northern part of Ningaloo station showing the high density areas in camping areas at Lefroy Bay and Winderabandi Point.

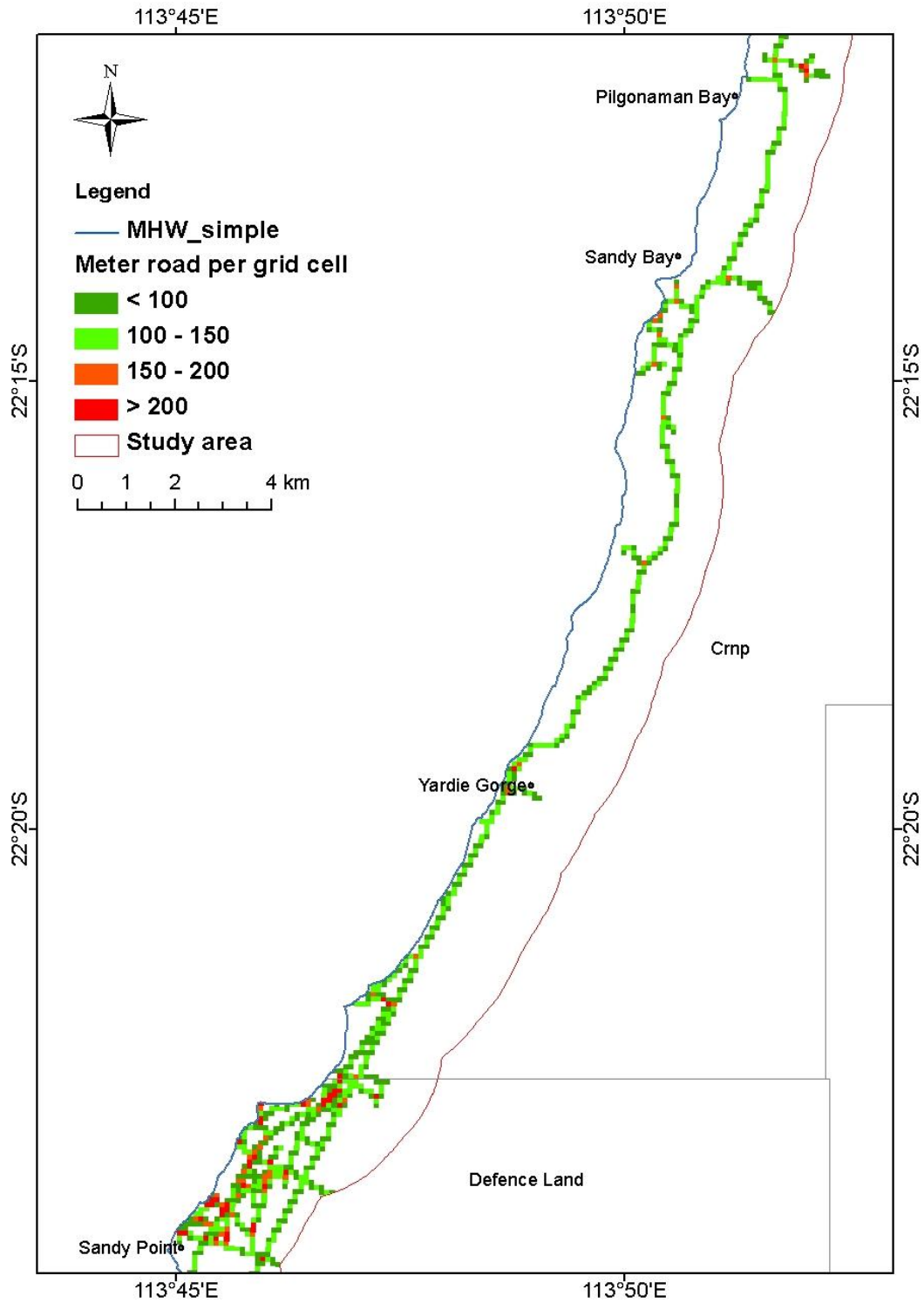


Figure 131. Road/track density in the Department of Defence Land and southern part of Cape Range National Park showing high density of tracks in camping areas north of Sandy Point.

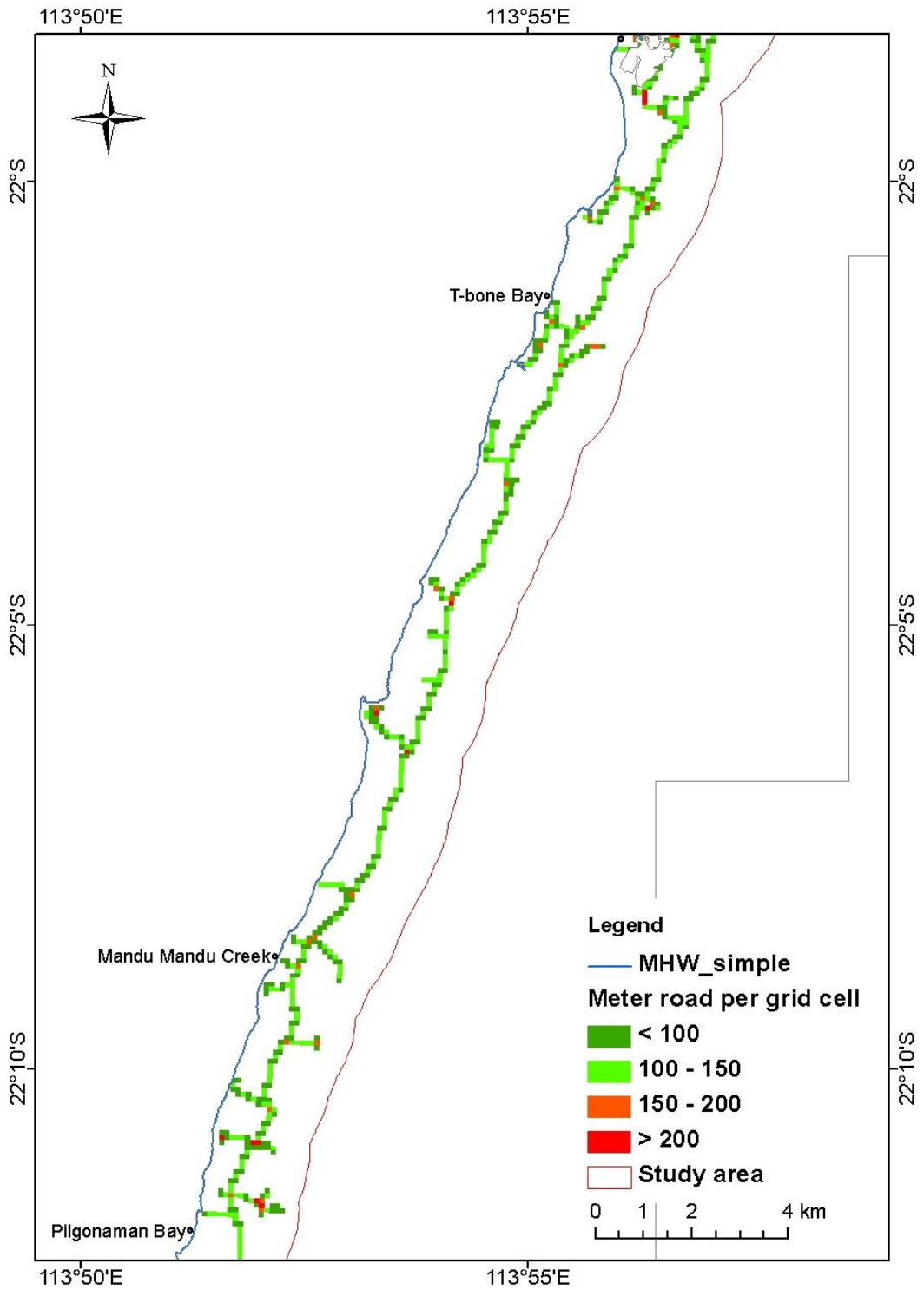


Figure 132. Road/track density in Cape Range National Park. Note the sealed main access route and tracks servicing formal DEC camping sites.

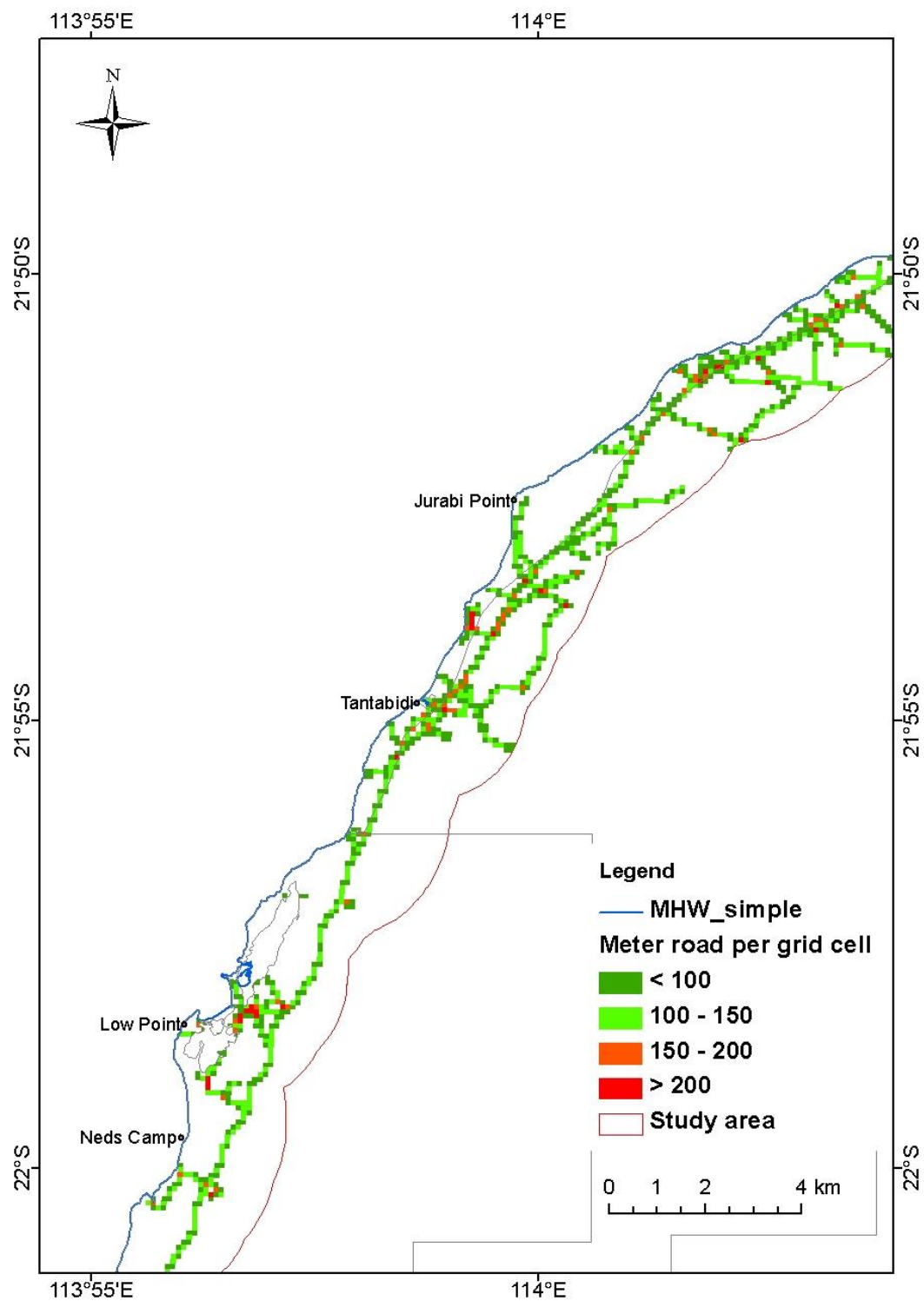


Figure 133. Road/track density near northern extent of Cape Range National Park showing high density around Low Point and South of Jurabi Point.

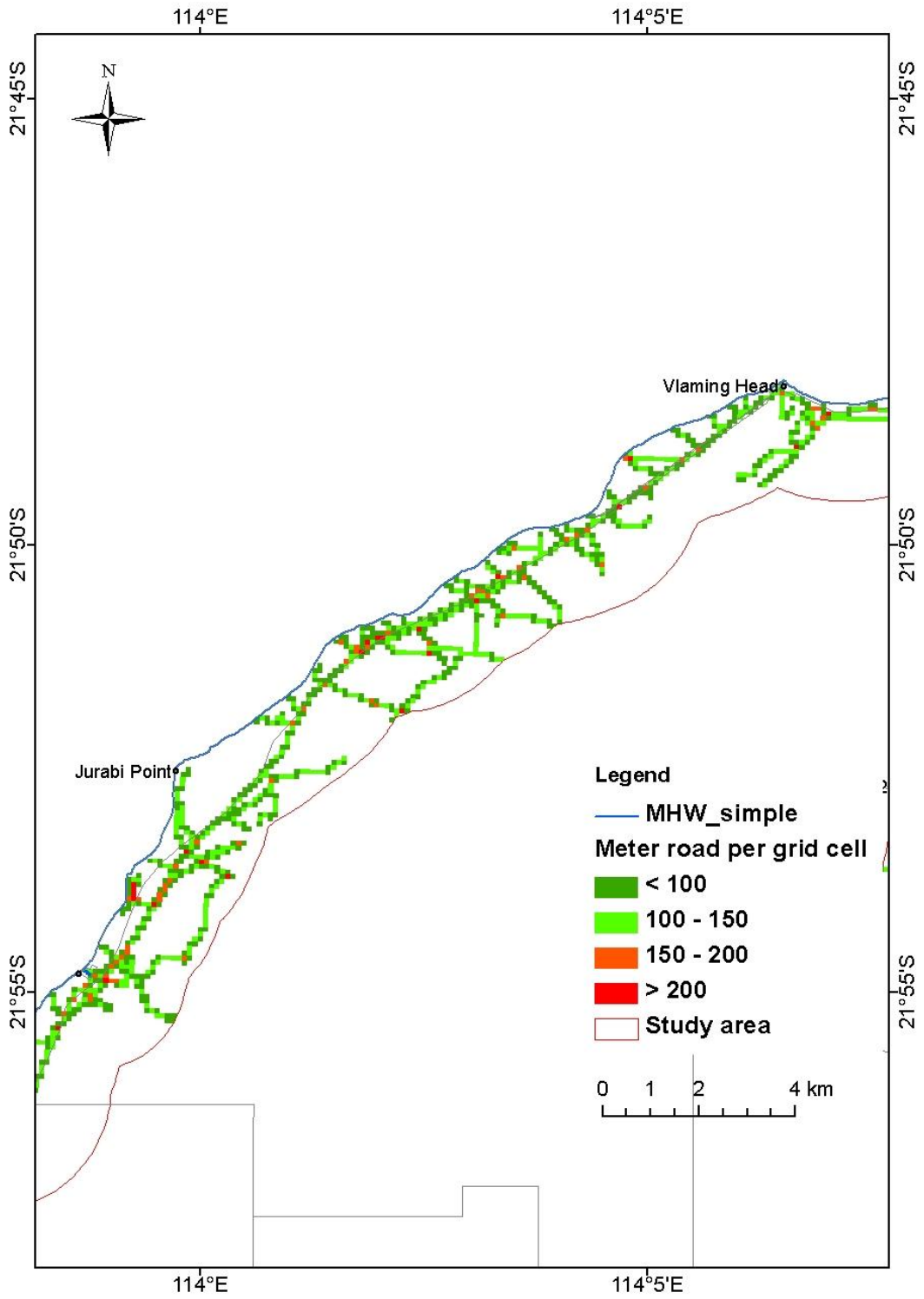


Figure 134. Road/track density between Jurabi Point and North West Cape. Note that the major road from Exmouth to Yardie Creek traverses the region.

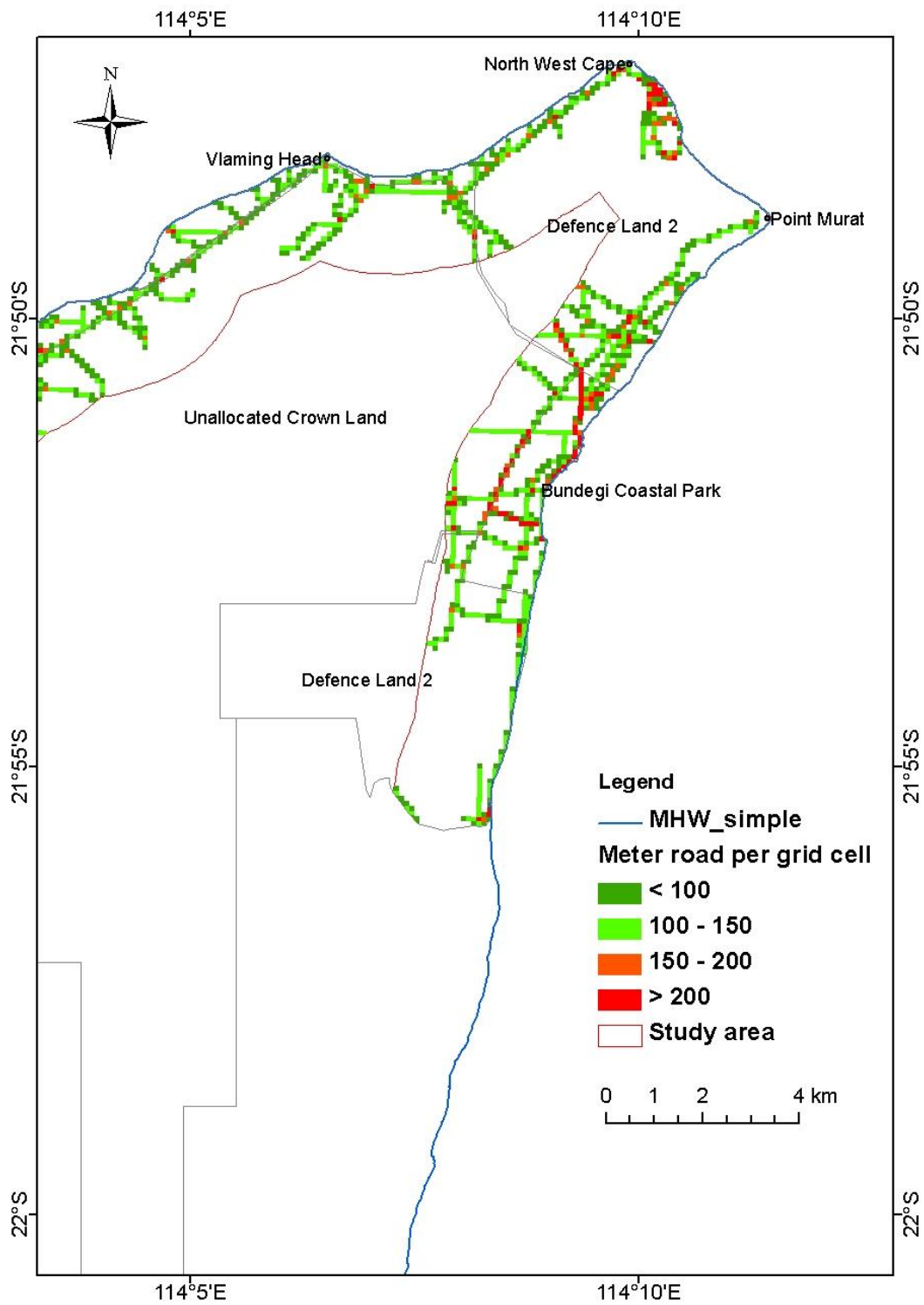


Figure 135. Road/track density around North West Cape showing high density in the Bundegi Coastal Park.

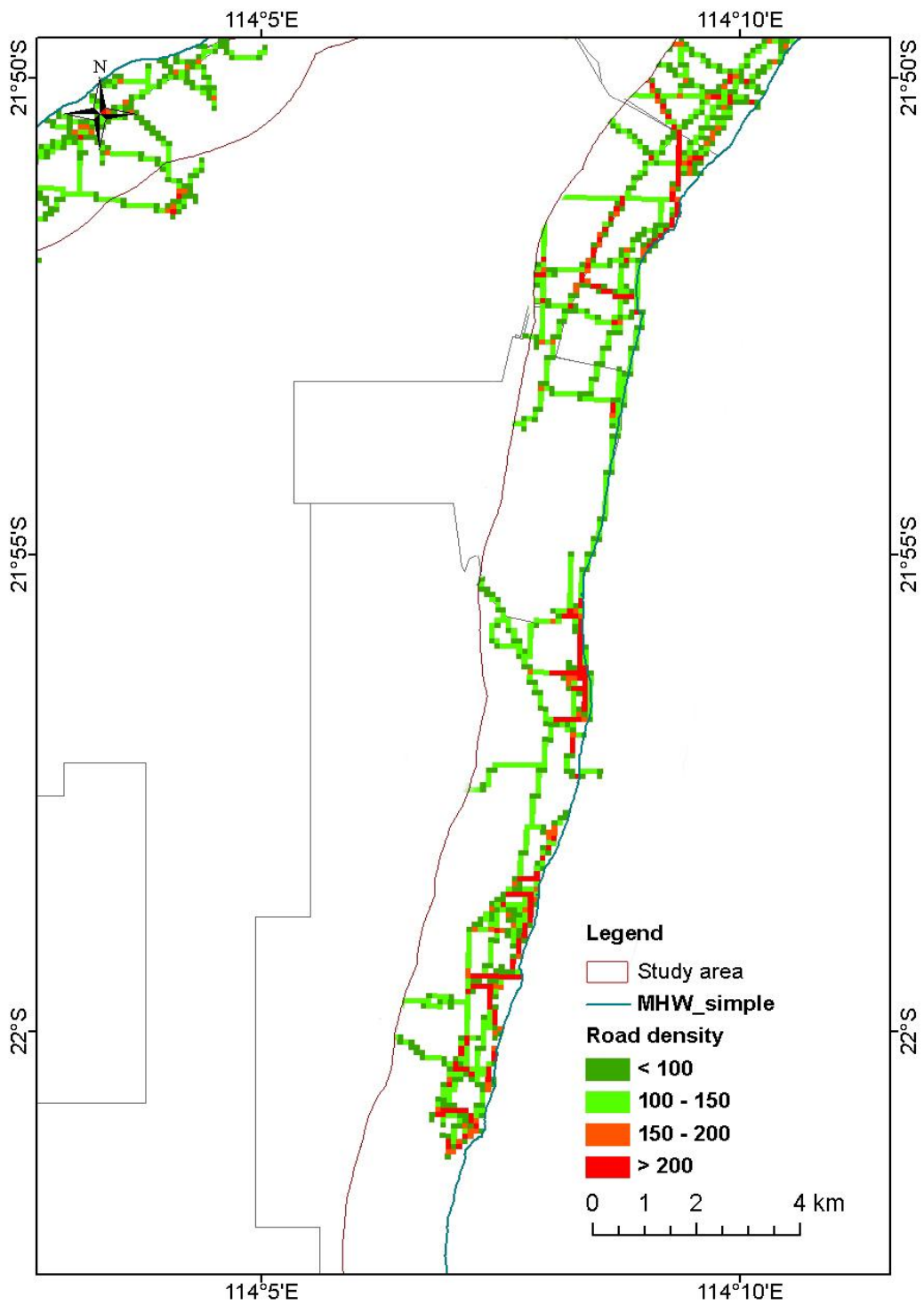


Figure 136. Road/track densities around the town of Exmouth showing high densities in the residential and commercial areas.

3.3.7 Land tenure and vegetation

The largest tenure areas in the study area are Gnaraloo and Cape Range National Park (CRNP). Even though the percentage of vegetation at risk within 5 m or 10 m of tracks is the lowest at Gnaraloo and CRNP, the vegetated area within buffers is important. On the other hand, the Northwest Cape Peninsula (Coastal Parks of Bundegi and Jurabi, Defence Land and unallocated Crown land) along with Warroora and Cardabia have a higher percentage of vegetation within buffers of tracks compared to other land tenures (Table 28). In addition, the percentage of ‘other’ groundcover (bare soil, saltmarshes or senescent grass or shrubs) significantly decreases (p -value<0.01) according to the type of land tenure (pastoral lease vs. other types) and latitude (Figure 137).

Table 28. Vegetated areas in hectares within 5 m and 10 m of tracks and their representative vegetated areas within land tenures.

Land tenure	Vegetated area (ha) within coastal buffers		Percentage of total area vegetated		Total vegetated area within land tenure (ha)
	5 m	10 m	5 m buffer	10 m buffer	
<i>Bundegi Coastal Park</i>	4.83	8.51	5.05%	8.90%	95.65
<i>Defence Land 44</i>	12.85	24.91	1.74%	3.36%	740.27
<i>Jurabi Coastal Park</i>	3.53	7.94	1.69%	3.81%	208.53
<i>Unallocated Crown Land</i>	21.51	43.40	1.68%	3.40%	1277.18
<i>Cape Range National Park</i>	9.41	22.72	0.38%	0.92%	2470.09
<i>Defence Land 97</i>	3.97	9.91	0.85%	2.13%	465.01
<i>Ningaloo</i>	3.01	6.74	0.66%	1.48%	454.80
<i>Cardabia</i>	5.63	11.83	3.01%	6.33%	187.02
<i>Warroora</i>	4.42	8.81	1.94%	3.88%	227.26
<i>Gnaraloo</i>	14.28	35.77	0.77%	1.93%	1851.67
<i>Quobba</i>	0.65	1.35	1.05%	2.18%	62.07
Total	84.09	181.89	1.05%	2.26%	8039.55

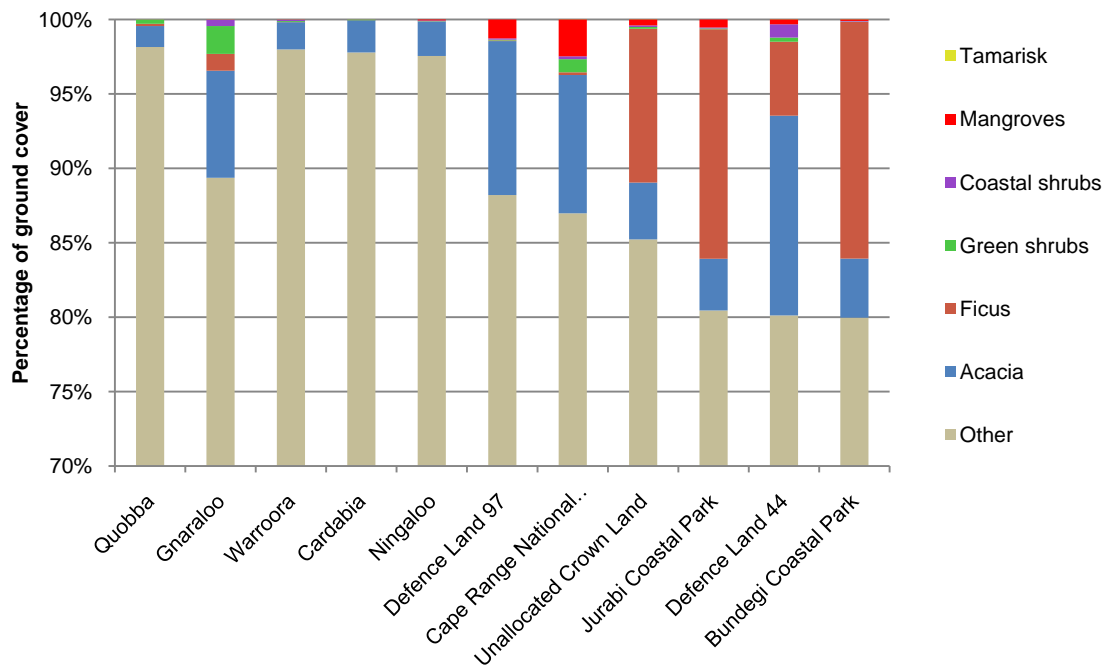


Figure 137. Percentage of different vegetation communities or 'other' ground cover in different land tenures. The scale for percentage ground cover ranges from 70 % to 100 % and the land tenures are sorted according to their locations with the most southern one on the left and the furthest away on the right.

The network of tracks in Quobba pastoral station is not very dense and mainly *Acacia* dominated shrub communities are at risk within 5 m or 10 m of tracks (Figure 138). At Gnaraloo station even though the amount of tracks is greater than at Quobba, the total quantity of *Acacia* sp., *Ficus* sp., other green and coastal shrubs present along the tracks only represented <2 % of the area covered by vegetation (Table 28). At Warroora, Cardabia and Ningaloo pastoral stations, *Acacia* dominated communities and other green shrubs were also the main vegetation communities impacted (Figure 139). Of all pastoral stations, Warroora and Cardabia stations had the highest percentage of green shrub vegetation within the 5 or 10 m buffers for pastoral stations (Table 28).

Defence Land is the most southern land parcel within the study area where mangroves occur. Mangroves and *Acacia* sp. are the communities more likely to be impacted by 4WD at Ningaloo, Defence Land and CRNP.

Around the North West Cape (Figure 143), 4WD vehicles impact mainly on *Ficus* and *Acacia* sp. The percentage of vegetated area within buffers compared to the total of vegetated area was also high, especially in Bundegi Coastal Park (Table 28). Furthermore, within the Defence Land, shrubs and mangroves may also be impacted.

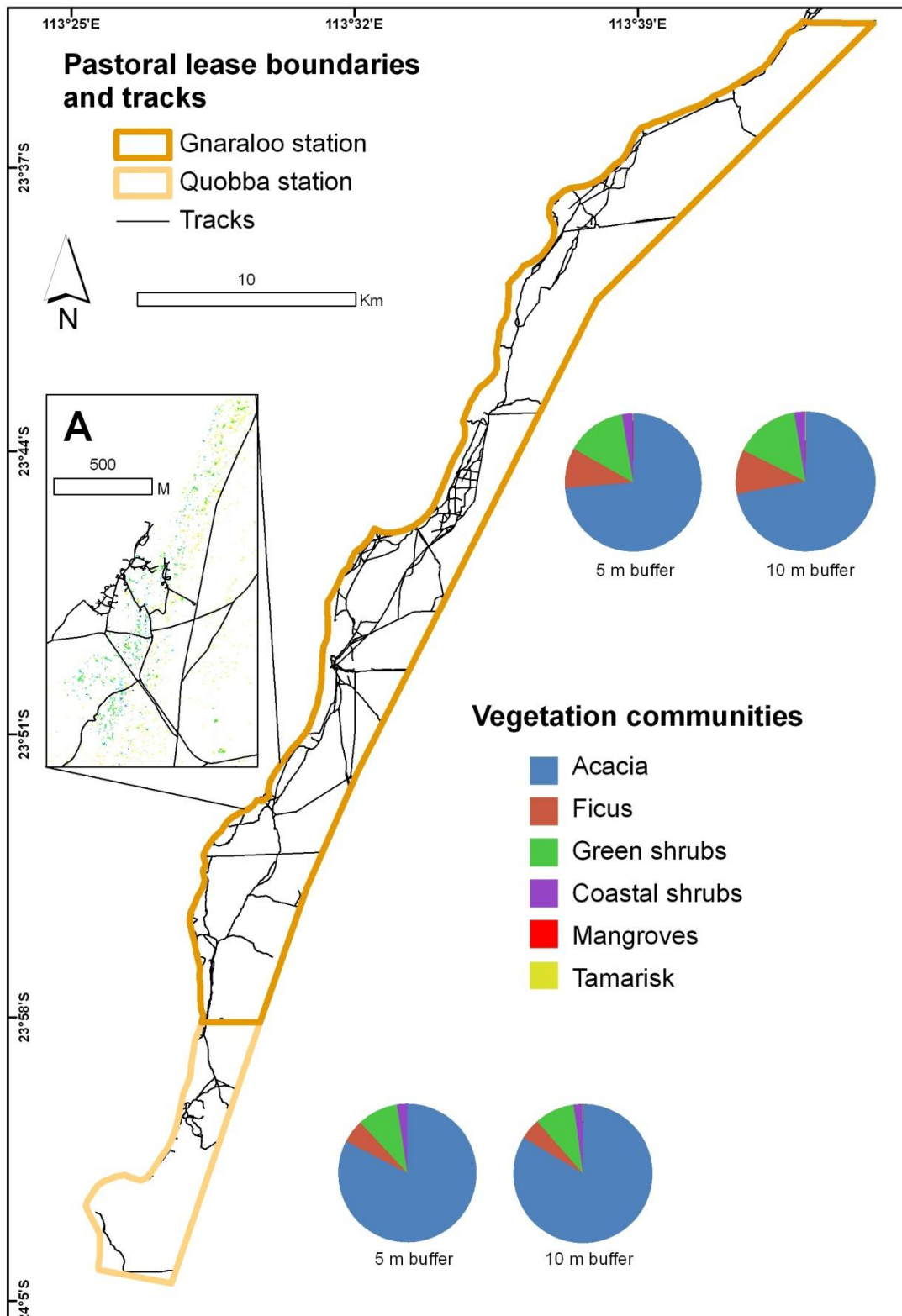


Figure 138. Vegetation communities at risk within 5 m and 10 m of tracks in the study subset Quobba and Gnaraloo pastoral stations. Inset A shows an example of coastal tracks around 3 Mile Camp with surrounding mosaic vegetation indices. The colours of vegetation classes do not correspond to vegetation communities.

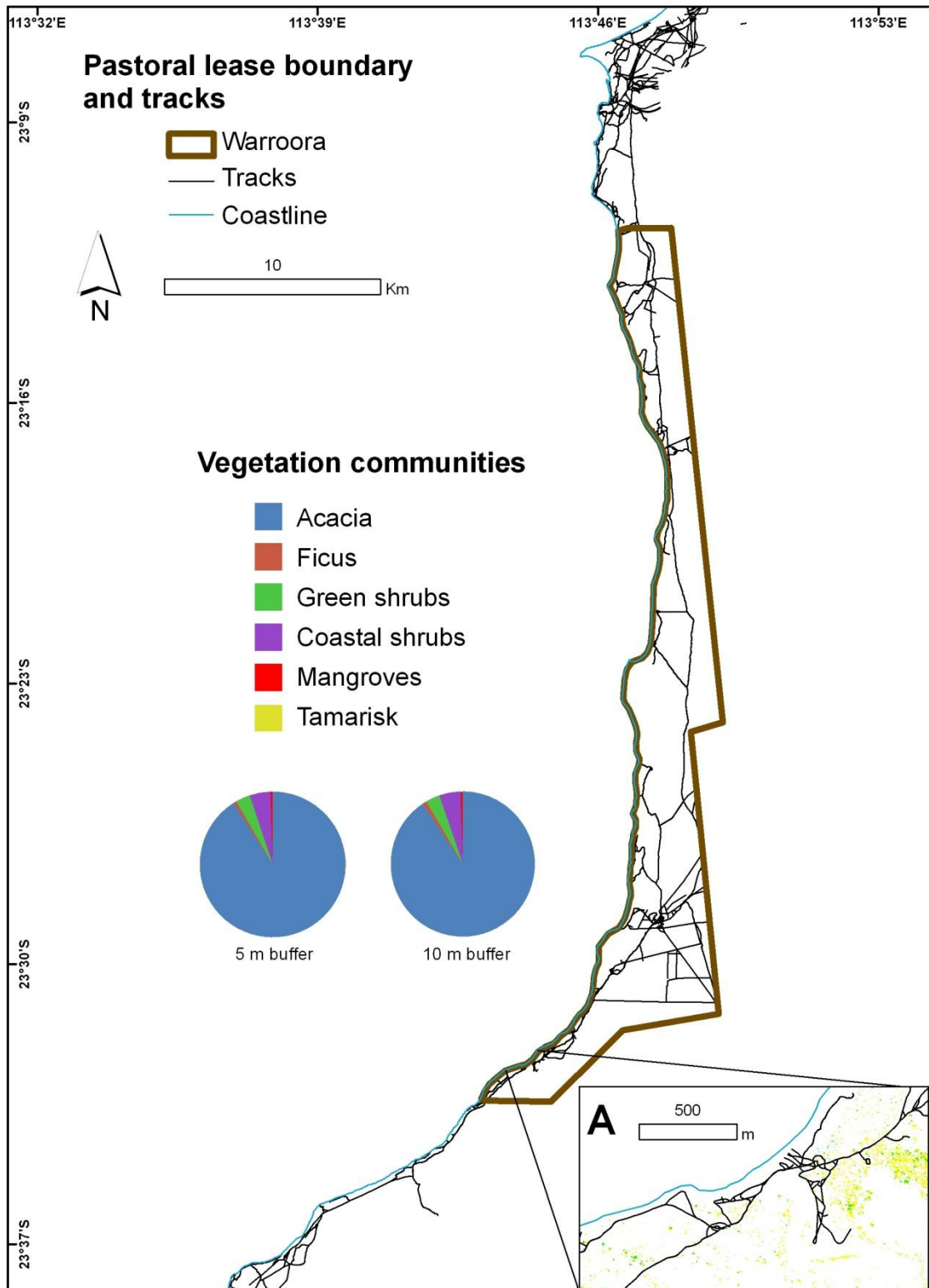


Figure 139. Vegetation communities at risk within 5 m and 10 m of tracks in the study subset of Warroora pastoral station. Inset A shows an example of coastal tracks with surrounding mosaic vegetation indices. The colors of vegetation classes do not correspond to vegetation communities.

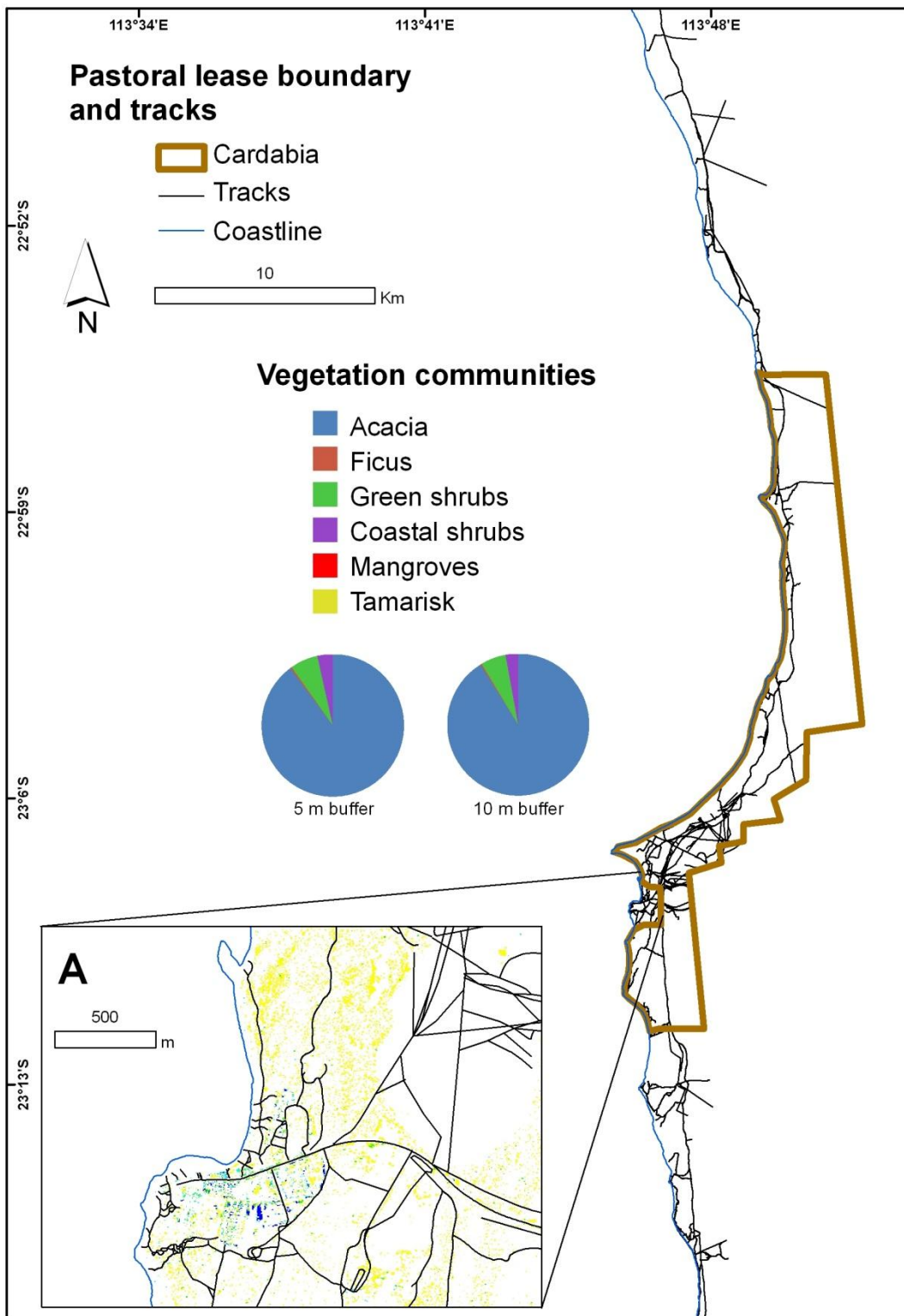


Figure 140. Vegetation communities at risk within 5 m and 10 m of tracks in the study subset of Cardabia pastoral station. Inset A shows the network of tracks around Coral Bay with surrounding mosaic vegetation indices. The colors of vegetation classes do not correspond to vegetation communities.

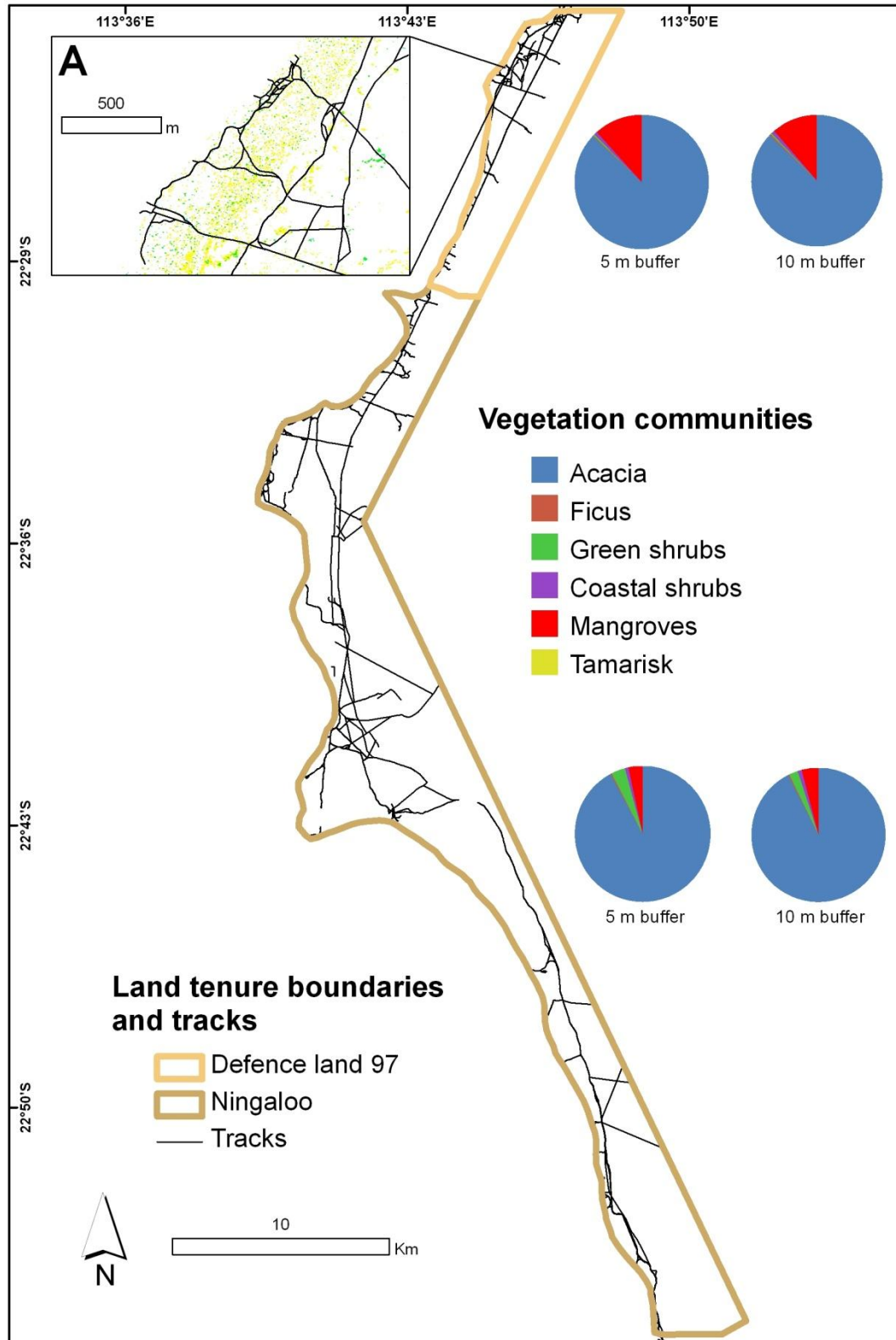


Figure 141. Vegetation communities at risk within 5 m and 10 m of tracks in the study subset of Ningaloo pastoral station and Defence land 97. Inset A shows the coastal network of tracks along the Ningaloo Yardie Creek Rd within the Defence Land 97 with surrounding mosaic vegetation indices. The colors of vegetation classes do not correspond to vegetation communities.

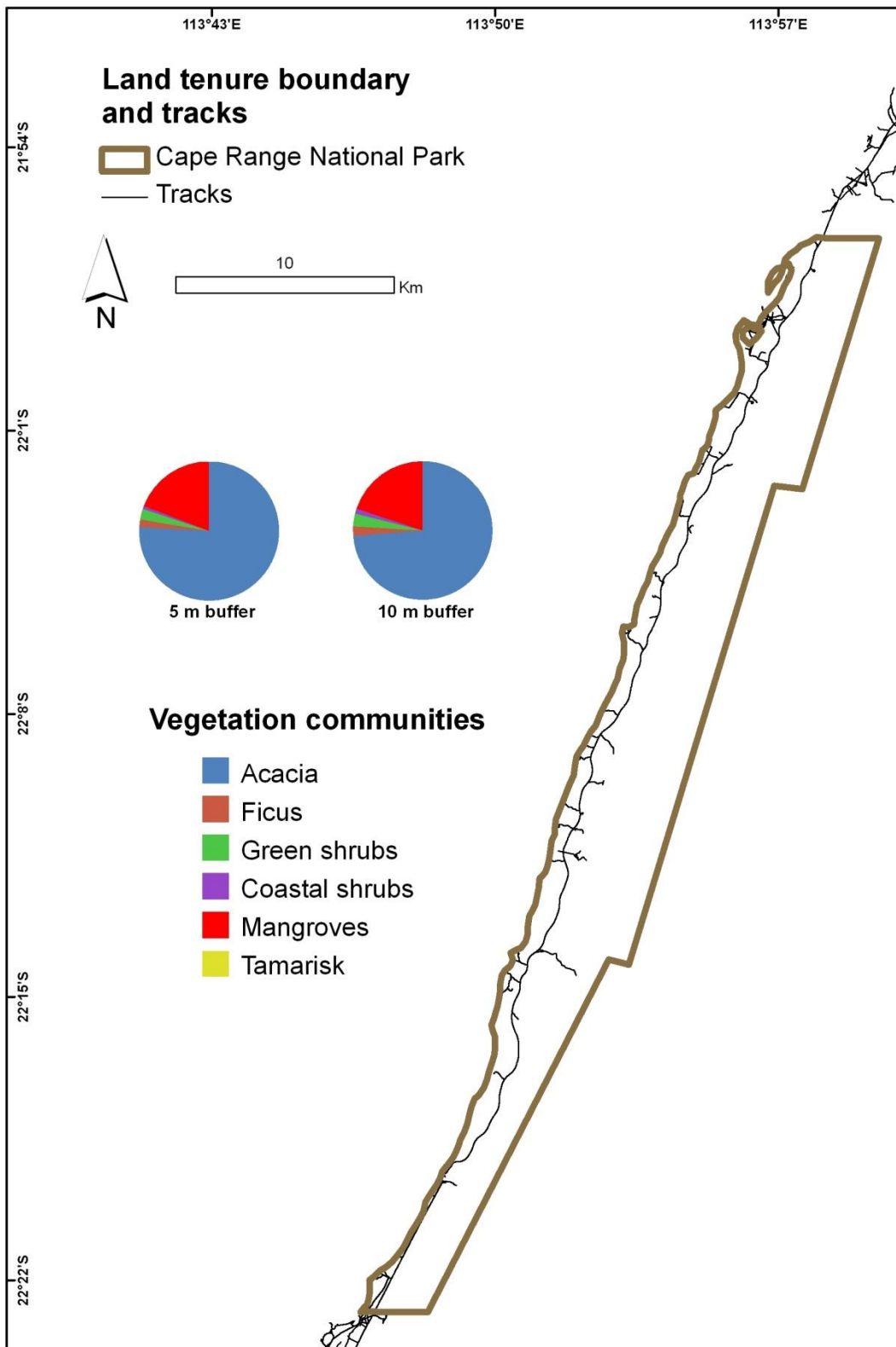


Figure 142. Vegetation communities at risk within 5 m and 10 m of tracks in the study subset of Cape Range National Park.

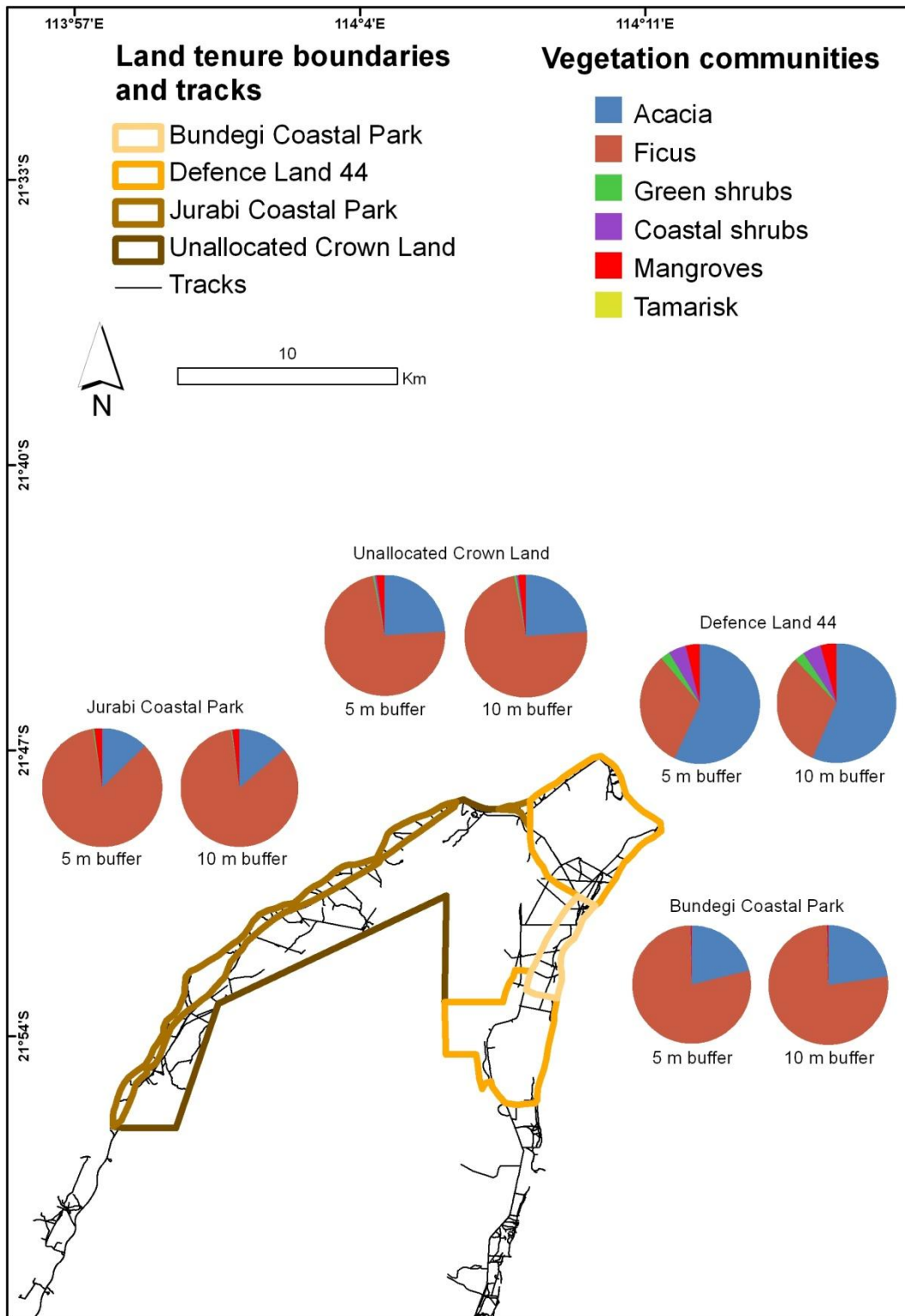


Figure 143. Vegetation communities at risk within 5 m and 10 m of tracks in the study subset of the North West Cape peninsula.

3.3.8 Vegetation around accommodation nodes

Acacia sp. characterises the majority of vegetation communities at risk around accommodation nodes (Figure 144). Moreover, it has to be noted that while *Ficus* sp., green and coastal shrubs account for less than 10 % of those communities at risk, mangroves represent a slightly greater share.

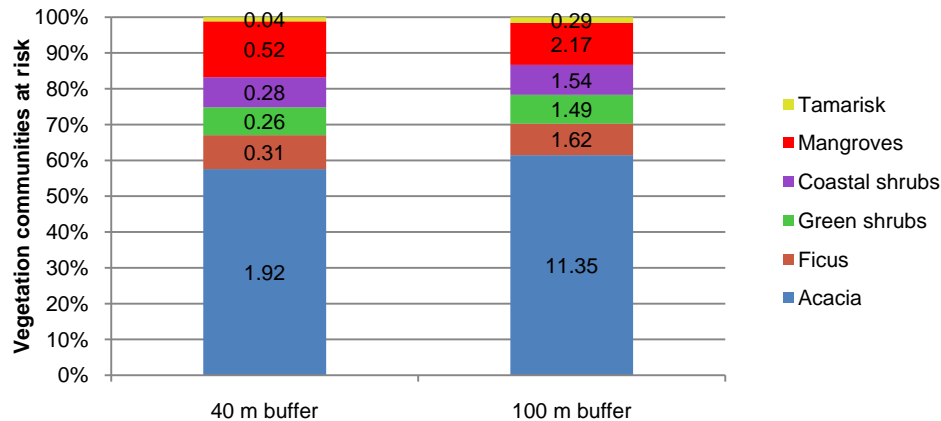


Figure 144. Percentage of green shrub and tree vegetation communities at risk within a 40 m and 100 m radius from the 81 accommodation nodes identified along the Ningaloo Coastal Region. The figures represent the area (ha) covered by the vegetation communities.

3.3.9 Vegetation in coastal strip and adjacent to sanctuary zones

The proportion of *Ficus* sp. at risk increased with greater distance from the shore. However, *Acacia* sp. still represented more than 60 % of the vegetation likely to be impacted by 4WD vehicles along the coastal strip (Figure 145). Furthermore, the network of tracks provides access to sanctuary zones of the Ningaloo Marine Park. The highest number of access tracks occurred adjacent to Winderabandi Sanctuary zone with 66 access points (Figure 146). Maud Sanctuary, (north of Coral Bay), Pelican and Cape Farquhar Sanctuary zones also had a high number of access tracks relative to the distance of coastline adjacent to the zone. Tantabiddi Sanctuary did not have any terrestrial access as it is located offshore while off-road drivers have not extended the track network further than the car park situated 500 m north of Lakeside Sanctuary zone.

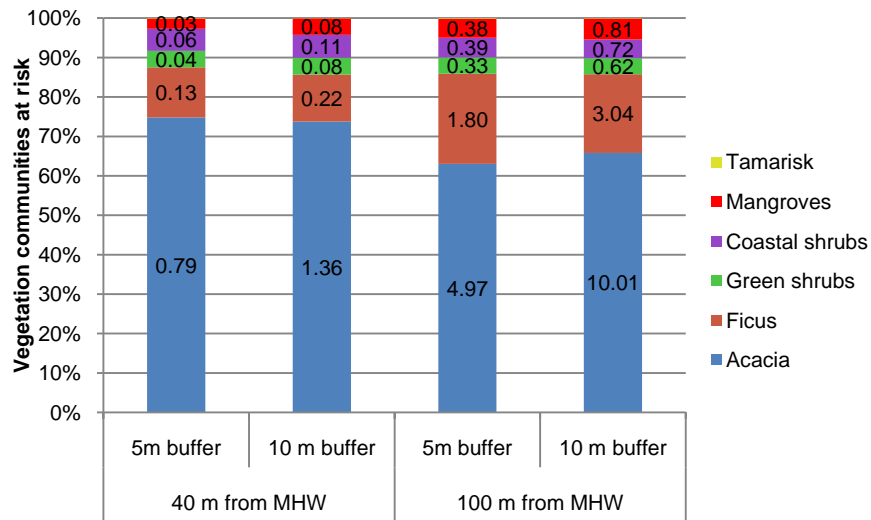


Figure 145. Percentage of green shrub and tree communities within 5 m and 10 m from tracks and located 40 m and 100 m inland from the Mean High Water mark (MHW). The figures represent the area (ha) covered by the vegetation communities.

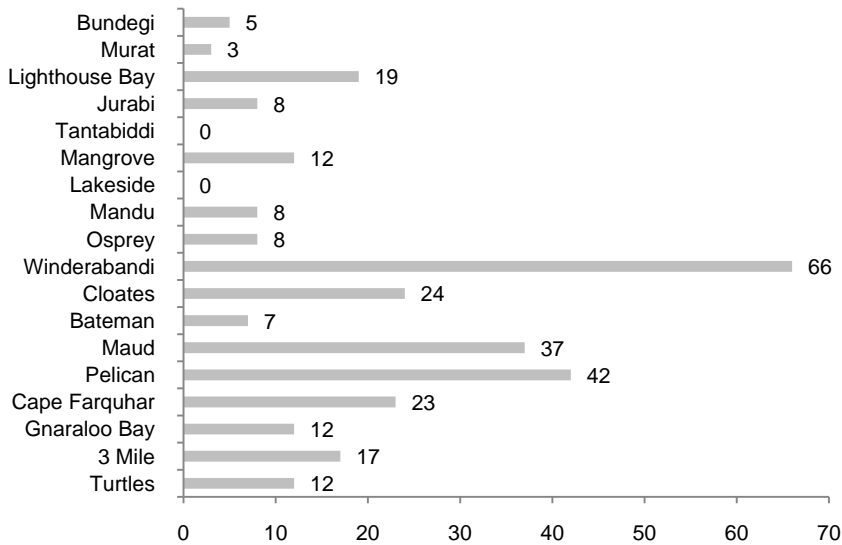


Figure 146. Number of access tracks to sanctuary zones or special purpose areas leading to sanctuary zones within the Ningaloo Marine Park.

3.4 Discussion

The information extracted from the reflectance spectra of the soil samples compared favourably with field-measured variables such as soil colour and soil texture. For example, samples with deep clay absorption features in their spectral profiles generally had fine soil texture, while samples with high iron content were matched with reddish Munsell colours. There was good separability between the sixteen terrestrial classes, with sediment properties and geomorphic features providing the means for distinguishing between surface types. The spatial distribution of surface types was not entirely consistent across the three data blocks, with certain classes representing different geological units in each data block. PCA allowed the detection of two main sediment groupings, based on iron-content and moisture content, respectively.

3.4.1 Sources of variance within field measurements

Measured soil properties

Sandy soils are considered to be more sensitive to recreational disturbance than other soil texture types (Priskin 2003) and the particle size analysis conducted in this study determined that sand was the main component of all samples collected. Samples from sites located on or near the escarpment contained slightly higher clay concentrations than samples from coastal sites. Samples collected at sites located on alluvial fans tended to have finer soil texture than samples collected at sites located on aeolian deposits, while the samples with the finest soil texture were taken from sites in saltmarsh communities. High clay content anomalies were found at sites where an external source was present, two examples of which were the unsealed road crossing at Bloodwood 2 and the tributary gorge opening at Mandu 1.

No obvious correlations were found between surface shear strength and location within the landscape, however, the highest shear strengths were recorded for loamy sands. Using the negative correlation determined by Van Gool *et al.* (2005), these areas are therefore less vulnerable to wind erosion than areas displaying other soil texture types. The higher shear strength values at sites within stream channels could have been influenced by the limestone cobble substrate found at the majority of these locations. Soil colour can be influenced by the presence of iron-bearing minerals and some examples of this included the samples collected at Yardie 1-3, Pilgramunna 2, Tantabiddi 1, Mandu 1 and 4, Bloodwood 2, Turquoise 1 and Exmouth 1. The high iron content detected in the samples from these sites is in agreement with the noticeable iron absorption features in their reflectance spectra, however, the Tulki 1 and Trealla 1 samples did not exhibit a reddish colouration despite the deep iron absorption features observed. This could be due to grain size, since particles of certain iron-bearing minerals become paler in colour as size decreases (Ramanaidou and Wells 2008).

PCA determined these sources of variation to be less significant than mean reflectance and soil moisture. This is in agreement with the studies conducted by Holden and LeDrew (1998) as well as Ustin *et al.* (1998), which found mean reflectance to be the main source of variance. The high contribution of soil moisture was most likely due to the omission of the air-drying procedure from sample preparation.

Biological factors

The cover of vegetation and leaf litter was found to be highest on the coastal plain, with the similar values recorded for escarpment sites and streambed sites reflecting the similar sampling locations chosen in these areas. Coastal dunes were sparsely vegetated in comparison to inland areas, with a lower proportion of leaf litter covering the sediment. The presence of soil crusting at the Turquoise Bay and Bundegi Sanctuary Zone sites could be causing decreased hydraulic conductivity at these sites, which increases the risk of soil erosion (Moore and Singer 1990).

3.4.2 Discrimination of sediment types

The degree of separation between reference spectra used in the terrestrial SAM classification was sufficient for the purpose of mapping the broad surface type categories found in the study area. There was some overlap between classes with similar reflectance properties, such as the overlap which led to areas of the coastal dunes being classified as escarpment surface types and *vice versa*. Overlaps between SAM classes were noted by Shrestha *et al.* (2005) who concluded that no single representative curve exists for a soil type, since many factors influence the shape of a reflectance curve. Mean reflectance, the main source of variance as determined by the PCA, is not a means of discrimination used by the SAM algorithm.

3.4.3 Distribution patterns within sediment classifications

Terrestrial sediment classification

There are multiple factors influencing sediment distribution in an area. The deposition of sediment along a drainage profile follows a three-stage process. The first sediments to be deposited are the poorly sorted coarse grains (often at the base of steep slopes), followed by the deposition of fine-grained sediment on the flood plain and finally the deposition of silt and clay in estuaries and deltas (Reineck and Singh 1980). Evidence of these stages can be seen in the SAM classifications, with rocky colluvium found close to the escarpment, particularly in Block K. The finer alluvial sediments were seen spread further out across wide areas of the coastal plain, with properties distinct from the underlying substrate. The deposits of the third stage were more difficult to detect due to the convergence of many differing sediment types near the land-ocean interface. However, the detailed classifications showed fine-grained sediments in intertidal flats and claypans.

In the southern section of the study area, the SAM mapped the deep drainage channels through which the sediments from the upper terraces are transported to the coastal plains. In the northern section these channels were less common. As identified by Hesp and Morrissey (1984), wind appears to be an influential means of sediment transport in these northern areas. Breshears *et al.* (2003) argue that wind is a far more erosive agent than water in dry shrubland areas and a more efficient means of sediment transport over any land surface. There is a strong prevailing wind from the south across the Cape Range Peninsula (Sanderson 2000) and this can be seen from the orientation of several active dune systems in the region (D'Andrea 2007). In the SAM classifications, these systems were shown to consist of multiple surface types with differing physical and chemical properties.

Assessment of erosion risk from sediment classification

Positive correlation between moisture content and vulnerability to fluvial erosion is well known (Van Gool *et al.* 2005) and negative correlation between clay content and erosion risk, the groupings identified in the PCA of terrestrial surface types suggest that the sediments with the carbonate-rich limestone class (Figure 110) and low moisture content, are least vulnerable to erosion. Two of these surface types, alluvium and sandplains, were also the sediments with deepest clay absorption features.

Bare areas composed of sediments with low clay content could be the areas at greatest risk of erosion. Samples from these areas (intertidal zone and coastal dunes) had mostly sandy soil textures and the sites from which these samples were collected contained the lowest density of vegetation and leaf litter cover. The slope gradients at these sites were also steeper and more variable relative to sites in other zones. Considering that this is the area where off-road tracks are most commonly created (D'Andrea 2007), the spatial distribution of these sediments as mapped by this study could be useful for future soil conservation efforts.

Comparison of the results from the PCA of soil sample spectra and the PCA of reference spectra from the hyperspectral imagery provides an understanding of how closely the surface property variation within the classified images matches the variation in soil properties measured on the ground. Both analyses found average reflectance to be the main source of variance, with the soil moisture content being another important factor. Direct comparison between average reflectance spectra from the two datasets shows slightly higher clay content in the field soil samples, with carbonate absorption features being roughly in agreement. The discrepancy between the 3.5 m pixel resolution of the hyperspectral data and the much finer spatial resolution of the field spectrometer could explain some of the inconsistencies. A spectral unmixing algorithm could be used to calculate the proportion of pixel cover attributed to each surface type in the SAM classifications.

Some shortcomings in onsite data collection included the absence of measurements for subsurface soil characteristics, as well as the unsuitability of the hand penetrometer for use on soils overlying rocky substrates, such as limestone cobbles. In this study, it was assumed that the moisture content of sediments (and spectral therefore some spectral properties) remained unchanged from the levels observed in the April 2006 HyMap survey. However, in reality these levels are likely to fluctuate over time. This means that soil erodibility may be greater following periods of high rainfall. A further limitation was the discrepancy between the spatial and spectral resolution of the hyperspectral data and the soil sample data, which had the potential to add uncertainty to the results.

3.4.4 Tracks and roads

This study has shown that remote sensing, especially hyperspectral imagery and GIS were useful for this analysis. The existing roads/tracks in the area could be easily classified into different road categories such major, minor and track. Categorization of road class helped to identify the presence or absence of roads/tracks in an area and analysis could be done on individual road class. As there is limited empirical research into the impacts of coastal tourism and recreation in Western Australia, this study has successfully ascertained the levels of off-road vehicle tracks at Ningaloo. This study has given an overall picture of the road and track

networks in the Ningaloo coastal region. Quantification of cumulative road lengths and road density in the area also provided analytical information on the existing roads/tracks. Factors such as land tenure, camp sites, fishing spots and accommodation were observed to be correlated with the high road and track density seen in certain areas, for example, Coral Bay.

Tracks on some beaches were not mapped as they were not detectable in the imagery. Beach traffic is becoming more common and it is a major environmental issue. Several studies have shown that beach traffic kills is responsible for loss of beach fauna (invertebrates, birds, turtles) (Moss and McPhee 2006; Schlacher, Dugan *et al.* 2007; Schlacher, Richardson *et al.* 2008a).

In certain areas, roads/tracks were closed to the public and could only be accessed by the pastoralists. These tracks were not excluded in the analysis and certain tracks were actually farm tracks and not for recreation such as Gnarlou station. It was also challenging to differentiate between tracks and minor roads as tracks that are frequently travelled by off-road vehicles can become an established road, making road and track classification difficult.

Densities of roads and tracks along the coast

According to Northcote and Macbeth (2008), road infrastructure in the region is relatively underdeveloped. Nevertheless, the measured cumulative length and densities of roads/tracks in the region were high in certain areas such as the pastoral stations and miscellaneous crown reserves. This limited coastal access and high demand for coastal tourism and recreation activities have contributed to the high use of off-road vehicles in the area. The chaotic labyrinth of tracks, particularly at Coral Bay and on the pastoral stations, indicates that four-wheel driving has become an uncontrolled activity in the region.

Cape Range National Park had the lowest road and track densities. This is due to the clear control and management of the Park by the Department of Environment and Conservation. Access to beach is provided at certain sites in Cape Range National Park for recreational activities such as small boat launching, swimming or picnics. The use of quad-bikes, ATVs (all terrain vehicles) and dune buggies are not permitted within the national park which also explains why roads and tracks were very organized in the park. With a good management system, the quality of access in the Park has steadily improved over the years (CALM and CCWA 2005).

Better roads were also available in Cape Range National Park for vehicles and a sealed road extends from the northern park boundary to Yardie Creek. Yardie Creek itself also forms a natural barrier between the north and south coastal parts of the Park where only four-wheel drive can cross the sandbar at the creek mouth when the river level is low. This natural barrier has indirectly helped to minimize the number of vehicles accessing the Park from the south. Currently, the only access across the range within the existing national park is the Learmonth to Sandy Bay four-wheel drive track and permission is required from the managers of Exmouth Gulf Station in order to gain access to the part of the track. These factors contribute to the explanation for the low road and track densities in Cape Range National Park.

In contrast, pastoral leases have the highest roads/track densities (10.4 km/km²). All pastoral leases in Western Australia are administered by the Pastoral Lands Board of Western Australia (PLBWA). These stations are leased to different private owners for the purpose of livestock

grazing on native vegetation and thus the tracks found in the pastoral stations could be also used for pastoral activities.

Off-road vehicles became common after World War Two and they are important elements for travel and recreation. By the end of the 1950s and 1960s, most Western Australian farmers owned a four-wheel drive. It was reported by Priskin (2003a) that farmers use off-road vehicles to explore the coast during weekends for recreational purposes. Today, most coastal areas in these stations are widely used for tourism and outback activities. This can be seen through the location of camping sites in the coastal areas to accommodate the demand for tourism and recreation. Areas such as Red Bluff Camp, 3 Mile Camp, Gnaraloo homestead, Warroora homestead, 14 Mile Camp, Coral Bay, Bruboodjoo Point, Winderabandi Point were some of the hot spots for tourism and recreation activities shown in this study. Track densities were high in these areas. In many instances, off-road drivers are likely to create new tracks rather than to go over old tracks that had blown out and potential 'bog' sites. This may explain the relative high numbers of four-wheel drive tracks in pastoral stations. Smallwood *et al.* (2011) who undertook a year-long, intensive aerial survey of human use of the marine park, reported highest number of vehicles and camps during the peak tourist season, and were observed even during off-season along the entire length of the Ningaloo coast. These observations concur with finding in this study of high density of tracks along the coast.

Jurabi and Bundegi Coastal Parks were classified as miscellaneous crown reserves. The total roads/tracks density for both parks were about 7.2 km/km² and was the second highest road and track density after pastoral leases. Jurabi and Bundegi Coastal Parks are jointly vested in the Shire of Exmouth and Department of Environment and Conservation. Due to its close proximity to Exmouth, these places are often visited by tourists and locals. In addition, there were major roads such as Murat Road and Yardie Creek Road that links Exmouth with Jurabi and Bundegi Coastal Park and further down to Cape Range National Park. These major roads provide access to both four-wheel drive and two-wheel drive vehicles to the parks. Even though 22 tracks within the Jurabi Coastal Park were closed and were replaced by nine formed gravel roads, many informal tracks still remain (Shire of Exmouth and DEC 1999). There is a need to restrict off-road vehicle to access authorized roads/tracks only and maintain the road and track to a standard suitable for visitor use and recreation (Shire of Exmouth and DEC 1999). Closed tracks need to be revegetated in order to minimize the impact of track-making by off-road vehicles.

For unallocated crown land and freehold land, the roads/tracks densities were lower compared to pastoral leases. Unallocated crown land is located between Jurabi and Bundegi Coastal Parks. Due to distance away from the coast and beaches, visitors appear to prefer the park nearby. In addition, most camp sites, fishing spots and tourist attraction nodes are located along the coast.

There are a few Freehold lands located in the Ningaloo region. One is situated between Cape Range National Park and Ningaloo stations and the other two are located on the eastern side of the Cape. These lands are used by the Australian Department of Defence for military and training purposes. In certain areas, these lands are fenced off from the public.

Impacts of tracks

It is inevitable that impacts on the environment are caused by different activities, of which tourism is one. Trampling by off-road vehicles has been reported to be harmful to the coastal environment in other locations (Lonsdale and Lane 1994, Priskin 2003a, Priskin 2003b, Moss and McPhee 2006, Schlacher, Schlacher and Thompson 2007, Schlacher and Morrison 2008, Schlacher and Thompson 2008, Schlacher *et al.* 2008b). Off-road vehicles can impact on large areas in just a single trip (Godfrey and Godfrey 1980, Liddle 1997). The first few passes of a vehicle are sufficient to cause significant damage to vegetation, soil compaction, dune destruction, erosion, killing of terrestrial animals, habitat loss, introduction of new diseases and weeds and disruption of nesting birds and turtles. In general, the overall impact on the environments is expected to increase with increased use. From many studies done on trampling and off-road driving, the impacts of off-road vehicles on the Ningaloo region could be considerable.

The physical impact of off-road vehicle tracks is similar to those of human-induced trampling (Cole 1993). Studies by Kutiel *et al.* (1999) and Kutiel (2002) indicated that the area impacted by human trampling can extend as far as 6 m from tracks. With this, a total of 1 008 km of tracks can impact approximately 503 ha of land and a total of 82 km of minor roads can impact 82 ha of land at Ningaloo. Moreover, off-road vehicles were reported to exert greater impacts than human-induced trampling (Cole 1993, Priskin 2003a). Kutiel *et al.* (1999) also showed that dispersed low use trails have a high potential to adversely affect larger areas than high use trails. Whether this is the same for four-wheel drive tracks at Ningaloo, remains to be examined.

At Ningaloo, many of the low use tracks are 'blind' tracks and after being driven over several times, they become established tracks. Vegetation may not be able to recover due to the continuous trampling and crushing by off-road vehicles. For example, in Gnaraloo station, old farm tracks that were redundant can still be seen in the aerial imagery of the region. Ningaloo is an arid region and vegetation does not grow or recover easily after being crushed by heavy vehicles so tracks will remain for many years. Resulting soil erosion could impact not only the land but also the adjacent marine environment.

If terrestrial soil erosion causes sediment deposition within a reef system to increase beyond natural levels, fatal coral smothering can occur, as well as impacts such as the interruption of natural biological cycles and a reduction in the rate of photosynthetic activity through increased turbidity (Rogers 1990). Corals can also suffer due to the energetic expense of sediment shedding and the potential release of toxic sulfides caused by the smothering of benthic organisms (Richmond *et al.* 2007; Rogers 1990). A single instance of abnormally high sediment deposition is capable of producing recurring damage due to resuspension in sufficiently powerful swell conditions (Richmond *et al.* 2007). While no severe sedimentation has thus far been recorded at Ningaloo Reef, its close proximity to a large landmass makes it particularly vulnerable to the effects of any land use changes that may occur.

Track-making can be serious issue in the region (Priskin 2001; Priskin 2003a) and a similar study by Priskin (2003b) in the Central Coast Region of WA perceived four-wheel driving to be the most harmful land-based and nature-based activity. This can be the same for the coastal strip for the pastoral leases. An environmental assessment involving biotic indicators may have a more in-depth view of levels of destruction. However, such assessments are limited by cost,

time, data availability and resources and may not be the practical or applicable approach for a large area such as Ningaloo.

There is a need for more research in recreational impacts on coastal environment (Sun and Walsh 1998; Priskin 2003a; Schlacher and Thompson 2008). A standard protocol and procedures for measuring recreation and tourism impacts is needed. As DEC has indicated that off-road vehicle related activities in the area are part of the management issues, tracks densities can be used as indicators of impacts. If a sustainable management system is implemented, the existing impacts may be mitigated, because tracks will not increase if the use of off-road vehicles is being restricted and rehabilitation can take place. However, to implement such system can be difficult and costly. Dune rehabilitation processes will take years and given the nature of climate and coastal processes in the region, this can be very challenging.

While a sound management plan is yet to be produced, a temporary solution to this is to have off-road vehicle use limited to the existing areas impacted by off-road vehicles and visitors deterred from making new tracks through an education program.

Further increases in tourism and recreation pose a continued threat to development of sustainable nature-based tourism in Ningaloo. The need for open space and opportunities for off-road vehicle activities have to be accommodated through strategic planning and management. However, sound management can only be implemented by understanding the relationship between recreation use, and the environment's natural carrying capacities. As the Ningaloo region becomes more accessible, coupled with the increase of the Western Australia population, the region may not be suitable for off-road vehicle oriented activities without damaging the quality of its natural resources.

By 2015, the coastal strip inland from the high water mark is expected to be excised from the current pastoral leases and handed over to the Department of Environment and Conservation (DEC) for management.

3.5 Conclusion

Distinct landcover types at Ningaloo were classified based on variations in surface properties observed in remotely sensed hyperspectral imagery. Sixteen terrestrial surface types and eight marine sediment types were identified, with comparison of their spatial distribution indicating lagoon areas downwind from coastal dunefields to be at greatest risk of sedimentation. Assessment of the effectiveness of the classification technique indicates accurate representation of geological units and a good approximation of variations in measured surface properties.

More knowledge is needed concerning the mechanisms of erosion, transport, and deposition of sediment in the Cape Range area. The soil attributes recorded in this study could then be used to determine soil erodibility constants used in the erosion models, which could then be used to calculate the volume of sediment eroded from areas containing specific surface types. Other approaches to the discrimination of soil properties might include derivative analysis or band-ratio analysis, since absorption features are not necessarily the main sources of variance between reflectance profiles.

The measurement of off-road vehicle tracks provided an indication of direct impacts caused by coastal tourism and recreation. In pastoral leases, 802 km of off-road vehicle tracks were measured compared to 29 km in Cape Range National Park. Road and track density was also high in pastoral leases when compared to Cape Range National Park. With the average size of an off-road vehicles track being 5 m wide, by conservative estimate, land in the Ningaloo region needing revegetation due to off-road vehicle track use is about 503 ha. These results may be useful for resource managers and local government authorities to define levels of acceptable change on the coast as a result of tourism and recreation, or in planning budgets for dune restoration and revegetation.

REFERENCES

- Ahmad, W. and Neil, D.T., 1994. An evaluation of Landsat Thematic Mapper (TM) digital data for discriminating coral reef zonation: Heron Reef (GBR). *International Journal of Remote Sensing*, 15, 2583-2597.
- Allen, A.D. 1993. Outline of the geology and hydrogeology of Cape Range, Carnarvon Basin, Western Australia. In: *The biogeography of Cape Range Western Australia*. Proceedings, Ed. Humphreys, W.F., Western Australian Museum, Perth pp. 25-38.
- Alongi, D. M., Tirendi, F. and Goldrick, A. 1996. Organic matter oxidation and sediment chemistry in mixed terrigenous-carbonate sands of Ningaloo Reef, Western Australia. *Marine Chemistry* 54 (1996): 203-219.
- Alongi, D.M., Tirendi, F. and Clough, B.F. 2000. Below-ground decomposition of organic matter in forests of the mangroves *Rhizophora stylosa* and *Avicennia marina* along the arid coast of Western Australia. *Aquatic Botany* 68: 97-122.
- Andréfouët, S., Claereboudt, M., Matsakis, P.J., Pageá S. and Dufour, P. 2001. Typology of atoll rims in Tuamotu Archipelago (French Polynesia) at landscape scale using SPOT HRV images. *International Journal of Remote Sensing*, 22(6):987-1004.
- Andréfouët, S. and Payri C. 2001. Scaling-up carbon and carbonate metabolism in coral reefs using in situ and remote sensing data. *Coral Reefs* 19:259–269.
- Asner, G. P. and Lobell, G. B. 2000. A biogeophysical approach for automated variability of arid ecosystems. *Remote Sensing of Environment* 74:69–84.
- Asner, G. P., Wessman, A. C., Bateson, C. A. and Privette, J. L. 2000. Impact of tissue, canopy, and landscape factors on the hyperspectral reflectance. *Remote Sensing of Environment*, 1:69-84.
- Asner, G.P. and Lobell, D.B. 2000. A biogeophysical approach for automated SWIR unmixing of soils and vegetation. *Remote Sensing of Environment* 74: 99-112.
- Bancroft, K.P. and Sheridan, M.W., 2000. The major marine habitats of Ningaloo Marine Park and the proposed southern extension. Report: MMS/PI/NMP&NSE-26/2000. Marine Conservation Branch, Department of Conservation and Land Management, Perth, WA, 35p.
- Barott, K., Smith, J., Dinsdale, E., Hatay, M., Sandin, S. and Rohwer, F. 2009. Hyperspectral and physiological analyses of coral-algal interactions. *PloS ONE* 4(11): e8043. doi:10.1371/journal.pone.0008043.
- Brattstrom, B.H. & Bondello, M.C. 1983. Effects of off-road vehicle noise on desert vertebrates. 167-206 in: Webb R. H. & Wilshire H. G. (eds.). *Environmental effects of offroad vehicles: Impacts and management in arid regions*. Springer-Verlag, New York.
- Beard, J.S. 1975. Pilbarra 1:1 000 000 *Vegetation Series. Explanatory Notes to Sheet 5. Vegetation Survey of Western Australia*. University of Western Australia Press, Nedlands WA.

- Beard, J.S. 1990. *Plant life of Western Australia*. Kangaroo Press, Kenthurst, NSW, pp.319.
- Benfield, S. L., Guzman, H. M., Mair, J. M. and Young, J. A. T. 2007. Mapping the distribution of coral reefs and associated sublittoral habitats in Pacific Panama: a comparison of optical satellite sensors and classification methodologies. *International Journal of Remote Sensing*, 28(22):5047-5070.
- Boulton, A. J., Humphreys, W. F. and Eberhard, S. M. 2003. Imperilled subsurface waters in Australia: Biodiversity, threatening processes and conservation. *Aquatic Ecosystem Health & Management* 6(1):41–54.
- Bour, W., Dupont, S. and Joannot, P., 1996. Establishing a “spot” thematic neo-channel for the study of hard-of-access lagoon environments: Example of application on the growth areas of the new Caledonian Reefs. *Geocarto International*, 11(1): 29-39.
- Breshears, D. D., Whicker, J. J., Johansen, M. P. and Pinder III, J. E. 2003. Wind and water erosion and transport in semi-arid shrubland, grassland and forest ecosystems: quantifying dominance of horizontal wind-driven transport. *Earth Surface Processes and Landforms* 28:1189–1209.
- Bryant, D., Burke, L., McManus, J and Spalding, M. 1998. *Reefs at risk. A map based indicator of threats to the world's coral reefs*. World Resources Institute, 57pp.
- Bureau of Meteorology. 2011. Bureau of Meteorology Weather Station Data. Retrieved on the 8 May 2011 from <http://www.bom.gov.au>.
- Call, K. A., Hardy, J. T. Wallin, D. O. 2003. Coral reef habitat discrimination using multivariate spectral analysis and satellite remote sensing. *International Journal of Remote Sensing*. 24(13): 2627-2639.
- CALM and MPRA. 2005. *Management plan for the Ningaloo Marine Park and Muiron Islands Marine Management Area 2005-2015*. Management plan no. 52. Perth: Department of Conservation and Land Management and Marine Parks and Reserves Authority, Perth, Western Australia.
- Cassata, L. and Collins, L.B. 2008. Coral reef communities, habitats, and substrates in and near sanctuary zones of Ningaloo Marine Park. *Journal of Coastal Research* 24(1): 139-151.
- Cocks, T., Janssen, R., Stewart, A., Wilson, S. I. and Shields, T. 1998. The HYMAP™ airborne hyperspectral sensor: the system, calibration and performance. *Proceedings of the 1st EARSEL Workshop on Imaging Spectroscopy, University of Zurich*.
- Cole, D. N. 1993. Minimizing conflict between recreation and nature conservation. In: *Ecology of greenways: design and function of linear conservation areas*, edited by Smith DS and Hallmund PC. University of Minnesota Press, Minneapolis, USA.105-122.
- Collins, L.B., Zhu, Z.R., Wyrwoll, K-H. and Eisenhauer, A., 2003. Late quaternary structure and development of the northern Ningaloo Reef, Australia. *Sedimentary Geology*, 159, 81-94.
- Commonwealth of Australia. 2002. Ningaloo Marine Park (Commonwealth Waters) Management Plan. Environment Australia, Canberra.

REFERENCES

- Congalton, R.G. and Green K., (2008). *Assessing the accuracy of remotely sensed data*. CRC Press Inc, 183p.
- D'Andrea, L. 2007. Using hyperspectral imagery to map vegetation condition and ground cover of the coastal area at Coral Bay, WA. MSc Thesis, Murdoch University, Perth. 67p.
- Dalleau, M., Andréfouët, S., Wabnitz, C.C., Payri, C., Wantiez, L., Pichon, M., Friedman, K., Vigliola, L. and Benzoni, F. 2010. Use of Habitats as Surrogates of Biodiversity for Efficient Coral Reef Conservation Planning in Pacific Ocean Islands. *Conservation Biology*, 24(2): 541–552.
- De Backer, S., Kempeneers, P., Debruyne, W. and Scheunders, P. 2005. A band selection technique for spectral classification. *Geoscience and Remote Sensing Letters* 2(3): 319-323.
- Defeo, O., McLachlan, A., Schoeman, D.S., Schlacher, T.A., Dugan, J., Jones, A., Lastra, M. and Scapini, F. 2009. Threats to sandy beach ecosystems: A review. *Estuarine, Coastal and Shelf Science* 81: 1-12.
- Demetriades-Shah, T.H., Steven, M.D. and Clark J.A. (1990). High resolution derivative spectra in remote sensing. *Remote Sensing of Environment* 33: 55–64.
- Department for Planning and Infrastructure. 2004. Ningaloo coast regional strategy Carnarvon to Exmouth. Western Australia Planning Commission, Perth. 204p.
- Department of Conservation and Land Management. 1987. *Cape Range National Park Management Plan No. 8 1987-1997*. Perth: Department of Environment and Conservation.
- Department of Conservation and Land Management (CALM). 2005. Cape Range National Park Management Plan. : Department of Environment and Conservation.
- Department of Conservation and Land Management. 2004. Management plan for Cape Range National Park and proposed public conservation land additions: Issues paper, 32p.
- Department of Environment, Water, Heritage and Arts (DEWHA), 2010. *Ningaloo coast, World Heritage nomination*, Commonwealth of Australia, 240p.
- Department of Sustainable Natural Resources. 2005. *Soil survey standard test method: Particle size analysis*. NSW (www.environment.nsw.gov.au/resources/soils/testmethods/psa.pdf).
- Dregne, H.E. 1983. Soil and soil formation in arid regions. pp.15-30 in: Webb R. H. & Wilshire H.G. (eds.). *Environmental effects of off-road vehicles: Impacts and management in arid regions*. Springer-Verlag, New York.
- Dustan, P., Dobson, E., Nelson, G. 2001. Landsat Thematic Mapper: detection of shifts in community composition of coral reefs. *Conservation Biology*, 15(4): 892-902.
- ENVI User's Guide, version 4.7 (2009), ITT Visual Information Solutions.
- Erickson, R., George, A.S., Marchant, N.G. and Morcombe, M.K. 1993. *Flowers and plants of Western Australia*, AH&AW Reed Pty Ltd. 231p.

- Federal Geographic Data Committee (FGDC), 2010. Coastal and marine ecological classification standard, version 3.1 (accessed 15 Feb 2011), http://www.cmeccatalogue.org/docs/CMECS_doc.pdf.
- Federal Chamber of Automotive Industries (2011), online access <http://www.fc.ai.com.au/>
- Godfrey, P. J. and Godfrey, M. M. 1980. Ecological effects of off-road vehicles on Cape Cod. *Oceanus* 23 (4):56-66.
- Gopal, S. and Woodcock, C. 1994. Theory and methods for accuracy assessment of thematic maps using fuzzy sets. *Photogrammetric Engineering and Remote Sensing*, 60(2): 191-188.
- Gray, M. A. 2007. *Hymap Ningaloo Corrected Reflectance Dataset Report*. Curtin University of Technology, Bentley Western Australia.
- Green, E. P., Mumby, P. J. Edwards, A. J. and Clarke, C. D. 2000. *Remote sensing handbook for tropical coastal management*. Paris, United Nations Educational. 316p.
- Groom, J.D., McKinney, L.B., Ball, L.C. and Winchell, C.S. 2007. Quantifying off-highway vehicle impacts on density and survival of a threatened dune-endemic plant. *Biological Conservation* 135: 119-134.
- Harvey, N. and Caton, B. 2003. *Coastal management in Australia*. Melbourne: Oxford University Press. 342pp.
- Harvey, M., Kobryn, H.T., Beckley, L.E., Heege, T., Hausknecht, P. and Pinnel, N. 2007. Mapping the shallow marine benthic habitats of Rottnest Island, Western Australia. Proceedings of the 3rd workshop for remote sensing of the coastal zone: from inland to marine waters, 7 – 9th June 2007, Bolzano, Italy. http://las.physik.uni-oldenburg.de/projekte/earsel/3rd_CZ_workshop/WSCoastalZone_2007_programme.htm
- Harvey, M.J. 2009. Development of techniques to classify marine benthic habitats using hyperspectral imagery in oligotrophic, temperate waters. PhD thesis, Murdoch University, Perth, Western Australia, 280p.
- Hedley, J.D. and Mumby, P.J. 2002. Biological and remote sensing perspectives of pigmentation in coral reef organisms. *Advanced Marine Biology* 43: 277-317.
- Hedley, J.D., Mumby, P.J., Joyce, K.E. and Phinn, S.R. 2004. Spectral unmixing of coral benthos under ideal conditions. *Coral Reefs* 23: 60-73.
- Heege, T. and Fischer, J. 2000. Sunlitter correction in remote sensing imaging spectrometry. SPIE Ocean Optics XV Conference, Monaco, October 16-20.
- Heege, T., Bogner, A., Häse, C., Albert, A., Pinnel, N. and Zimmermann, S. 2003. Mapping aquatic systems with a physically based process chain. Proc. 3rd EARSeL Workshop on Imaging Spectroscopy, Herrsching, 13-16 May 2003. Edited by M. Habermeyer, A. Müller, S. Holzwarth. pp. 415-422.

REFERENCES

- Heege, T. and Fischer, J. 2004. Mapping of water constituents in Lake Constance using multispectral airborne scanner data and a physically based processing scheme. *Canadian Journal of Remote Sensing* 30 (1): 77-86.
- Hesp, P. A. 1986. Ningaloo Marine Park: terrestrial geomorphology and potential development sites. Macquarie University, Sydney.
- Hesp, P. A. and J.G. Morrissey. 1984. A resource survey of the coastal lands from Vlaming Head to Tantabiddi Well: West Cape Range Region. Resource Management Technical Report No. 24.
- Hill, J. and Mégier J. 1994. *Imaging spectrometry, a tool for environmental observations*. Kluwer Academic Publishers, Dordrecht, Boston pp.328.
- Hochberg, E. J. and Atkinson, M. J. 2000. Spectral discrimination of coral reef benthic communities. *Coral Reefs*, 19: 164– 171.
- Hochberg, E. J. and Atkinson, M. J. 2003. Capabilities of remote sensors to classify coral, algae, and sand as pure and mixed spectra. *Remote Sensing of Environment*, 85:174– 189.
- Hochberg, E. J., Atkinson, M. J. and Andréfouët, S. 2003. Spectral reflectance of coral reef bottom-types worldwide and implications for coral reef remote sensing. *Remote Sensing of Environment* 85:159–173.
- Holden, H. and LeDrew, E. 1998. Spectral discrimination of healthy and non-healthy corals based on cluster analysis, principal components analysis, and derivative spectroscopy. *Remote Sensing of Environment* 65: 217-224.
- Holden, H. and LeDrew, E. 1999. Hyperspectral identification of coral reef features. *International Journal of Remote Sensing* 20:2545–2563.
- Holthus, P.F. and Maragos, J.E. 1995. Marine ecosystem classification for the tropical island Pacific. In: *Marine and Coastal Biodiversity in the Tropical Island Pacific Region*, edited by J.E. Maragos, M.N.A. Peterson, L.G. Eldredge, J.E. Bardach and H.F. Takeuchi (Honolulu: East-West Center), pp. 239–278.
- Hosier, P. E., Kochhar, M. and Thayer, V. 1981. Off-road vehicle and pedestrian track effects on the sea approach of hatchling loggerhead turtles. *Environmental Conservation* 8:158–161.
- House of Representatives Standing Committee on Environment and Conservation. 1977. *Off-road Vehicles: impact on the Australian Environment*. Australian Government Publishing Service, Canberra, Australia.
- Huete, A. 2004. Remote sensing of soils and soil processes. In *Remote Sensing for Natural Resource Management and Environmental Monitoring*, 3rd Edition. ed. S. L. Ustin, 3-52. Hoboken, New Jersey: John Wiley & Sons.
- HyVista Corporation. 2006. *HyMap Data acquisition report for the Australian Institute of Marine Science*. North Ryde, NSW.
- Intergovernmental Panel on Climate Change (IPCC). 2007. *Climate Change 2007: Synthesis Report*. Geneva, Switzerland.

- Isbell, R. F. 1996. *The Australian soil classification*. CSIRO Publishing. Collingwood, Victoria.
- Jenny, H. 1994 (Originally published in 1941). *Factors of Soil Formation: A System of Quantitative Pedology*. New York: Dover Publications.
- Joyce, K. and Phinn, S. 2003. Hyperspectral analysis of chlorophyll content and photosynthetic capacity of coral reef substrates. *Limnology and Oceanography*, 48(1):489-496.
- Kay, R., Elio, I., Panizza, V. and Donaldson, B. 1997. Reforming coastal management in Western Australia. *Ocean and Coastal Management* 35(1): 1-29.
- Keighery, G. and Gibson, N. 1993. Biogeography and composition of the flora of the Cape Range peninsula, Western Australia. In: *The biogeography of Cape Range Western Australia*. Proceedings, Ed. Humphreys, W.F., Western Australian Museum, Perth pp. 52-85.
- Kendall, M. S. and Miller, T. J. 2008. The influence of thematic and spatial resolution on maps of a coral reef ecosystem. *Marine Geodesy* 31:75-102.
- Kuchler, D. 1986, Geomorphological nomenclature: reef cover and zonation on the Great Barrier Reef (Townsville: Great Barrier Reef Marine Park Authority Technical Memorandum 8).
- Kutiel, P. 2002. Effect of experimental trampling and off-road motorcycle traffic on soil and vegetation of stabilized coastal dunes, Israel. *Environmental Conservation* 27 (1):14-23.
- Kutiel, P., Zhevelev, H. and Harrison, R. 1999. Effect of recreational impacts on soil and vegetation of stabilized coastal dunes in the Sharon Park, Israel. *Ocean Coastal Management* 42 (12):1041-1060.
- Lewis, M. 2002. Spectral characterisation of Australia arid zone plants. *Canadian Journal of Remote Sensing*, 28(2) 219-230.
- Liddle, M. 1997. *Recreation ecology: the ecological impact of outdoor recreation and ecotourism*: Kluwer Academic Publishers.638p.
- Lidz, B.H. Reich, C.D., Peterson, R.L. and Shinn, E.A. 2006. New maps, New information: coral reefs of the Florida Keys. *Journal of Coastal Research*, 22(2):260:282.
- Lillesand, T. M., Kiefer, R.W. and Chipman, J.W. 2008. *Remote sensing and image interpretation*. 6th ed. John Wiley & Sons Inc. 756p.
- Long, S.C. 2007. Disturbance and recovery of coral communities in Bill's Bay, Ningaloo Marine Park: Field survey 16-23 October 2006. Technical and Data Report MBI-2007/05. Marine Science Program, Department of Environment and Conservation, Perth, Western Australia.
- Lonsdale, W. M. and Lane, A. M. 1994. Tourist vehicles as vectors of weed seeds in Kakadu National Park, northern Australia. *Biological Conservation* 69 (3):277-283.
- McLachlan, A. and Brown, A.C. 2006. *The ecology of sandy shores*. 2nd ed. Academic Press, Burlington, Massachusetts 373p.
- Mather, P. M. 1999. *Computer processing of remotely-sensed images*, 2nd ed. Wiley, New York, 292p.

REFERENCES

- McCarthy, A. R. 2009. Mapping coral reef biodiversity, surrogacy at two levels. Honours Thesis, University of Queensland, 50p.
- McCoy, R.M. 2005. *Field methods in remote sensing*. The Guilford Press, New York, 159p.
- Mishra, D. R., Narumalani, S., Rundquist, D., Lawson, M. and Perk, R. 2007. Enhancing the detection and classification of coral reef and associated benthic habitats: A hyperspectral remote sensing approach, *Journal of Geophysical Research*. 112, C08014,doi:10.1029/2006JC003892.
- Moore, D. C. and Singer, M. J. 1990. Crust formation effects on soil erosion processes. *Soil Science Society of America Journal* 54: 1117–1123.
- Moss, D. and McPhee, D. P. 2006. The impacts of recreational four-wheel driving on the abundance of the ghost crab (*Ocypode cordimanus*) on a subtropical sandy beach in SE Queensland. *Coastal Management* 34 (1):133-140.
- Mumby, P.J., Skirving, W. Strong, A.E., Hardy, J.T., LeDrew, E., Hochberg, E.J., Stumpf, R.P. and David, L.T. 2004. Remote sensing of coral reefs and their physical environment. *Marine Pollution Bulletin*, 48(3-4): 219-228.
- Northcote, J. and Macbeth, J. 2008. A preliminary investigation of effects on visitation patterns and human usage. In: *Socio-economic impacts of sanctuary zone changes in Ningaloo Marine Park*. Perth CRC for Sustainable Tourism.1-98.
- O’Kin, G. S., Roberts, D. A., Murray, B. and O’Kin, W. J. 2001. Practical limits on hyperspectral vegetation discrimination in arid and semi-arid environments. *Remote Sensing of Environment* 77: 212-225.
- Oksanen, J., Kindt, R., Legendre, P., O’Hara, B., Simpson, G. L., Solymos, P., Stevens, H. and Wagner, H. 2009: vegan: Community Ecology Package. R package version 1.16-32. <http://vegan.r-forge-project.org>
- Pachauri, R.K. and Reisinger, A. 2007. *Climate Change 2007: Synthesis Report*. Cambridge, UK: Intergovernmental Panel on Climate Change.
- Page, C., Coleman, G., Ninio, R. and Osborne, K. 2001. Surveys of benthic reef communities using underwater video. Long-term Monitoring of the Great Barrier Reef. Standard Operational Procedure Number 7. Australian Institute of Marine Science, Townsville.
- Pajak, M.J. and Leatherman, S. 2002. The high water line as shoreline indicator. *Journal of Coastal Research* 18(2): 329-337.
- Palandro, D. A., Andréfouët, S., Hu, C. Hallock, P. Müller-Karger, Frank E., Dustan, P., Callahan, M. K., Kranenburg, C. and Beaver, C. R., 2008. Quantification of two decades of shallow-water coral reef habitat decline in the Florida Keys National Marine Sanctuary using Landsat data (1984-2002). *Remote Sensing of Environment*. 112(8):3388-3399.

- Payne, A.L., Curry, P.J. and Spencer, G.F. 1980. *An inventory and condition survey of rangelands in the Carnarvon Basin, Western Australia*. Technical Bulletin No 73. Western Australian Department of Agriculture.
- Priskin, J. 2001. Assessment of natural resources for nature-based tourism: the case of the Central Coast Region of Western Australia. *Tourism Management* 22 (6):637.
- Priskin, J. 2003a. Physical impacts of four-wheel drive related tourism and recreation in a semi-arid, natural coastal environment. *Ocean & Coastal Management* 46 (1-2):127.
- Priskin, J. 2003b. Tourist perceptions of degradation caused by coastal nature-based recreation. *Environmental Management* 32 (2):189-204.
- R Development Core Team (2008). R: A language and environment for statistical computing. R Foundation for Statistical Computing, Vienna, Austria. ISBN 3-900051-07-0, URL <http://www.R-project.org>
- Ramanaidou, E. and Wells, M. 2008. Chapter 5: Mineralogical and microchemical methods for the characterization of high-grade banded iron formation-derived iron ore. Society of Economic Geologists. *SEG Reviews* 15: 129-156
- Reineck, H. E. and Singh, I. B. 1980. *Depositional Sedimentary Environments*, Second, Revised and Updated Edition. Berlin, Heidelberg, New York: Springer-Verlag.
- Richmond, R. H., Rongo, T., Golbuu, Y., Victor, S., Idechong, N., Davis, G., Kostka, W., Neth, L., Hamnett, M. and Wolanski, E. 2007. Watersheds and coral reefs: conservation science, policy, and implementation. *Bioscience* 57: 598-607.
- Rickard, C.A., McLachlan, A. and Kerley, G.I.H. 1994. The effects of vehicular and pedestrian traffic on dune vegetation in South Africa. *Ocean and Coastal Management* 23: 225-247.
- Rogers, C. S. 1990. Responses of coral reefs and reef organisms to sedimentation. *Marine ecology progress series* 62: 185-202.
- Roelfsema, C.M., Dennison, W.C. and Phinn, S.R. 2002. Spatial distribution of benthic microalgae on coral reefs determined by remote sensing. *Coral Reefs*, 21(3): p264-274.
- Rossiter, D. G. 2007. *Compendium of On-Line Soil Survey Information*. International Institute for Geo-information Science & Earth Observation. [online: http://www.itc.nl/personal/rossiter/research/rsrch_ss.html]
- Rouillard, D. 2008. The use of hyperspectral imagery in mapping marine and terrestrial sediment distribution on the Cape Range peninsula. MSc Thesis, Murdoch University, Perth. 103p.
- Sanderson, P. G. 2000. A comparison of reef-protected environments in Western Australia: the Central West and Ningaloo coasts. *Earth Surface Processes and Landforms* 25 (2000): 397-419.
- Schlacher, T. A., Dugan, J., Schoeman, D. S., Lastra, M., Jones, A., Scapini, F., McLachlan, A. and Defeo, O. 2007. Sandy beaches at the brink. *Diversity and Distributions* 13 (5):556-560.

REFERENCES

- Schlacher, T. A. and Morrison, J. M. 2008. Beach disturbance caused by off-road vehicles (ORVs) on sandy shores: Relationship with traffic volumes and a new method to quantify impacts using image-based data acquisition and analysis. *Marine Pollution Bulletin* 56 (9):1646-1649.
- Schlacher, T. A., Richardson, D. and McLean, I. 2008. Impacts of off-road vehicles (ORVs) on macrobenthic assemblages on sandy beaches. *Environmental Management* 41 (6):878-892.
- Schlacher, T. A. and Thompson, L. M. C. 2007. Exposure of fauna to off-road vehicle (ORV) traffic on sandy beaches. *Coastal Management* 35 (5):567-583.
- Schlacher, T. A. and Thompson, L. M. C. 2008. Physical impacts caused by off-road vehicles to sandy beaches: spatial quantification of car tracks on an Australian Barrier Island. *Journal of Coastal Research* 24 (2B):234-242.
- Schlacher, T. A. and Thompson, L. M. C. 2009. Changes to dunes caused by 4WD vehicle tracks in beach camping areas of Fraser Island. Paper read at 2nd Queensland Coastal Conference, at Gold Coast.
- Schlacher, T. A., Thompson, L. M. C. and Walker, S. J. 2008b. Mortalities caused by off-road vehicles (ORVs) to a key member of sandy beach assemblages, the surf clam *Donax deltoides*. *Hydrobiologia* 610 (1):345-350.
- Schlacher, T.A., Thompson, L.M.C. and Price, S. 2007. Vehicles versus conservation of invertebrates on sandy beaches: quantifying direct mortalities inflicted by off-road vehicles (ORVs) on ghost crabs. *Marine Ecology* 28: 354-367.
- Schmidt, K. S. and Skidmore, A. K. 2003. Spectral discrimination of vegetation types in a coastal wetland. *Remote Sensing of Environment* 85:92-108.
- Shepherd, K. D., and M. G. Walsh. 2002. Development of reflectance spectral libraries for characterization of soil properties. *Soil Science Society of America Journal* 66: 988-998.
- Short, A. 1999. *Handbook of beach and shoreface morphodynamics*. John Wiley, Chechester, New York, p379.
- Short, A. and Woodroffe, C.D. 2009. *The coast of Australia*. Cambridge University Press, 288pp.
- Schweizer, D., Armstrong, R. A. and Posada, J., 2005. Remote sensing characterization of benthic habitats and submerged vegetation biomass in Los Roques Archipelago National Park, Venezuela. *International Journal of Remote Sensing*, 26(12):2657-2667.
- Settle, J.J. and Drake, N.A. 1993. Linear mixing and the estimation of ground cover proportions. *International Journal of Remote Sensing* 14:1159-1177.
- Shepherd, K. D. and Walsh, M. G. 2002. Development of reflectance spectral libraries for characterization of soil properties. *Soil Science Society of America Journal* 66: 988-998.
- Shire of Exmouth and DEC. 1999. Management Plan for Jurabi and Bundegi Coastal Parks, and Muiron Islands 1999-2009. Management Plan No.43. National Parks and Nature Conservation Authority. Perth.1-24.

- Shrestha D. P., Margate D. E., Van der Meer, F. and Anh, H. V. 2005. Analysis and classification of hyperspectral data for mapping land degradation: an application in southern Spain. *International Journal of Applied Earth Observation and Geoinformation* 7: 85–96.
- Smallwood, C.B. 2010. *Spatial patterns of human usage in the Ningaloo Marine Park*. PhD Thesis, Murdoch University, School of Environmental Science, Murdoch, Western Australia.
- Smallwood, C.B., Beckley, L.E., Moore, S.A. and Kobryn, H.T., 2011. Assessing patterns of recreational use in large marine parks: A case study from Ningaloo Marine Park, Australia. *Ocean & Coastal Management*. 54: 330-340.
- Spalding, M.D., Ravilious, C. and Green E.P. 2001. *World Atlas of Coral Reefs*. Berkeley, Calif. ; London : University of California Press, 424pp.
- Stephens, C.F., Louchard, E. M., Reid, P. R. and Maffione, R. A. 2003. Effects of microalgal communities on reflectance spectra of carbonate sediments in subtidal optically shallow marine environments. *Limnology and Oceanography* 48 (1, part 2): 535-546.
- Sun, D. and Walsh, D. 1998. Review of studies on environmental impacts of recreation and tourism in Australia. *Journal of Environmental Management* 53 (4):323-338.
- Taylor, R.B. 2001. The Effects of Off-Road Vehicles on Ecosystems, Texas Parks and Wildlife, Austin Texas. Accessed 10 May 2008.
www.tpwd.state.tx.us/publications/pwdpubs/media/pwd_rp_t3200_1081.pdf
- Thankappan, M. and Reddy, S. 2004. Evaluation of MODIS data for vegetation classification. 12th Australasian Remote Sensing Conference. The Remote Sensing and Photogrammetry Commission of the Social Sciences Institute, 18-22 October, Perth Australia, 176-185.
- Thompson, L. M. C. 2008. Physical damage to coastal dunes and ecological impacts caused by vehicle tracks associated with beach camping on sandy shores: a case study from Fraser Island, Australia. *Journal of Coastal Conservation* 12 (2):67-82.
- Tille, P. 2006. Soil-landscapes of Western Australia's rangelands and arid interior. Resource Management Technical Report 313. Department of Agriculture and Food, Perth.
- UNEP/IUCN 1988. *Coral Reefs of the World*. Vol 2: Indian Ocean,, Red Sea and Gulf. UNEP Regional Seas Directories and Bibliographies. IUCN, Gland, Switzerland and Cambridge, UK./UNEP, Nairobi, Kenya, 389 pp.
- Ustin, S.L., Roberts, D.A., Pinzon, J., Jacquemond, S., Gardner, M., Sheer, G., Castañeda, C. M. and Palacios-Orueta, A. 1998. Estimating canopy water content of chaparral shrubs using optical methods. *Remote Sensing of Environment* 65: 280-291.
- Van de Graaff, W. J. E., Denman, P. D. and Hocking, R. M. 1982. 1:250 000 Geological Series-Explanatory Notes. Onslow. Western Australia. Perth, WA.
- Van de Graaff, W. J. E., Denman, P. D., Hocking, R. M. and Baxter, J. L. 1980. 1:250 000 Geological Series-Explanatory Notes. Yanrey-Ningaloo. Western Australia. Perth, WA.

REFERENCES

- Van der Meer, F. 2004. Analysis of spectral absorption features in hyperspectral imagery. *International Journal of Applied Earth Observation and Geoinformation* 5: 55–68.
- Vanderstraete, T., Goossens, R., Ghabour, T. K. 2006. The use of multi-temporal Landsat images for the change detection of the coastal zone near Hurghada, Egypt. *International Journal of Remote Sensing*. 27(17):3645-3655.
- Van Gool, D., Tille, P. and Moore, G. 2005. Resource Management Technical Report 298. Land evaluation standards for land resource mapping: assessing land qualities and determining land capability in south-western Australia. 3rd ed. Department of Agriculture, Western Australia, 141p.
- Venables, W. N. and Ripley, B. D. 2002. *Modern Applied Statistics with S*. Fourth Edition. Springer, New York.
- Viles, H. and Spencer, T. 1995. *Coastal problems. Geomorphology, ecology and society at the coast*. Oxford University Press, New York, p350.
- Wabnitz, C.C., Andréfouët, S. Torres-Pulliza, D., Müller-Karger, F. E., Kramer, P. A., 2008. Regional-scale seagrass habitat mapping in the Wider Caribbean region using Landsat sensors: Applications to conservation and ecology. *Remote Sensing of Environment*. 112(8):3455-3467.
- Wajon, E. 2008. *Colour guide to spring wildflowers of Western Australia*. Part 4. Exmouth and the Pilbara. Wajon Publishing Company, Winthrop, WA, p120.
- Webb, R.H. 1983. Compaction of desert soils by off-road vehicles. Pp.51-79 in: Webb, R.H. & Wilshire H. G. (eds.). *Environmental effects of off-road vehicles: Impacts and management in arid regions*. Springer-Verlag, New York.
- Wee Beng Huat, S. 2009. *Extent and density of roads and tracks along the Ningaloo coastline, North West Australia*. MSc Thesis, Murdoch University, Perth Western Australia, 61p.
- Western Australian Planning Commission. 1996. *Gascoyne Coast, Regional Strategy*. Perth: Western Australia Planning Commission.
- Western Australian Planning Commission. 2004. *Ningaloo Coast Regional Strategy Carnarvon to Exmouth*. Perth: Western Australia Planning Commission.
- Wood, D. S. 2003. Tourism on the Carnarvon-Ningaloo Coast Between Quobba Station and Exmouth and its Implications for Sustainability of the coast. Prepared for the Western Australian Planning Commission. Curtin University of Technology, Perth.
- Wood, D. and Dowling, R. 2002. Tourism surveys in North West Cape region 1989-2002. A summary prepared for the Department for Planning and Infrastructure. Curtin University of Technology and Edith Cowan University, Perth, Western Australia.
- Wood, D. and Glasson, J. 2005. Giving the environment a voice: the transformational potential of valuing tourism in sensitive natural environments: the case of the Ningaloo Coastal Region, Western Australia. *Planning, Practice & Research* 20(4): 391–407.

- Wyrwoll, K.-H., Kendrick, G.W. and Long, J.A. 1993. The geomorphology and Late Cenozoic geomorphological evolution of the Cape Range – Exmouth Gulf region. In: *The biogeography of Cape Range Western Australia*. Proceedings, Ed. Humphreys, W.F., Western Australian Museum, Perth pp. 1-23.
- Zainal, A.J.M., Dalby, D.H. and Robinson, I.S. 1993. Monitoring marine ecological changes on the east coast of Bahrain with Landsat TM, *Photogrammetric Engineering and Remote Sensing* 59(3):415-421.
- Zharikov, Y., Skilleter, G.A. Loneragan, N.R., Taranto, T. and Cameron, B.E. 2005. Mapping and characterising subtropical estuarine landscapes using aerial photography and GIS for potential application in wildlife conservation and management. *Biological Conservation*, 125: p87–100.
- Zhu, A. 1997. A similarity model for representing soil spatial information. *Geoderma* 77 (1997) 217-242.

APPENDIX A

HyMap survey report

HyMap Data Acquisition Report

May 2006

for the *Australian Institute of Marine Science*



Australian Government



**AUSTRALIAN INSTITUTE
OF MARINE SCIENCE**

Survey area covers 67 flight lines over the Ningaloo Marine Park, NW-WA

Data acquisition sponsored by:



Petroleum Division

1. PROJECT OVERVIEW

HyVista Corporation was contracted by AIMS to acquire hyperspectral data over the Ningaloo Marina Park area NW-WA, Australia. A total of 67 HyMap image strips were acquired, within 11 individual Blocks, between the 20th of April 2006 and the 2nd of May. The HyMap data products that have been delivered are radiance, reflectance and geocorrected data. The following report contains information on sensor specifications, survey site parameters, flight logs, image mosaics and HyVista data product information.

2. ACQUISITION SUMMARY

Site Name(s) : Block A to Block K; in total 67 individual flight lines totaling about 3350 km ² @ 3.5m pixel size
Location : Ningaloo Reef Marine Park, NW-WA , Australia
Date of Acquisition : 21 st April 2006 – 2 nd of May 2006
Company / Organization : AIMS
Contact : Andrew Heyward – a.heyward@aims.gov.au
HVC Contact : Peter Cocks – pac@hyvista.com

HyMap Survey Summary:

The aircraft HyVista used for the airborne survey was provided by Australian Aerial Surveys – the HyMap was installed in Bankstown, NSW left there on the 19th of April and ferried across to Learmonth (Exmouth), where it was based for the entire survey until leaving on the 3rd of May. The survey was carried out by pilot Stuart Criddle – AAS, operator Mike Hornibrook – HyVista and QC and project manager Peter Hausknecht – HyVista. The flight planning was done by Peter Cocks – HyVista.

The data acquisition (DA) was conducted in individual blocks – each HyMap data block was acquired in one sortie – and whenever possible HyVista tried to fly more than one block in one day. Due to survey time restrictions Block F was acquired on two different days to allow for optimal sun angles. The figure on the following page shows the Ningaloo marine park outline together with color coded bathymetry lines and the flight pattern planned for the Ningaloo HyMap survey. The textbox to the right shows the number of lines contained in each block, the optimal survey time based on the survey direction, number of minutes for DA in normal conditions and the line direction towards north.

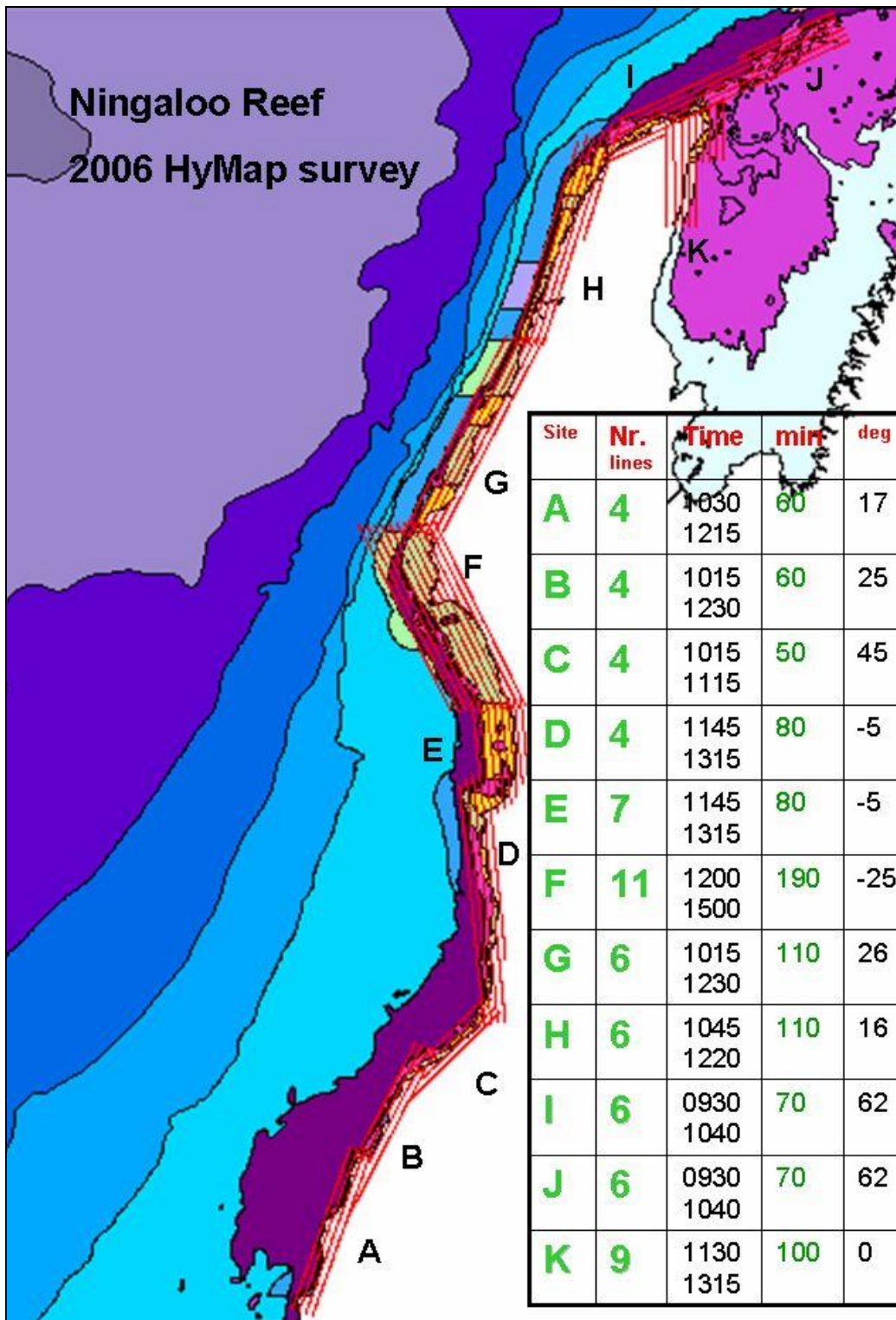


Figure 1 Ningaloo – HyMap survey plan

The HyMap survey was planned to cover the water areas to the 20m bathymetry line (light purple) – two blocks (G & F) cover it all the way to the 50m line (dark purple). The survey was also extended to cover the Muiron Islands and the land area past Exmouth town. The area covered total 3400 square kilometers collected at 3.5m pixel size.

3. HYMAP™ AIRBORNE IMAGING SENSOR

The HyMap sensor is an airborne imaging system that is used for earth resources remote sensing. It records a digital image of the earth's sunlit surface underneath the aircraft but unlike standard aerial cameras, the HyMap records images in a large number of wavelengths. In essence, the HyMap is an airborne spectrometer and like spectrometers used in analytical chemistry, it can detect and identify materials by the spectral features contained in the recorded data.

The HyMap records an image of the earth's surface by using a rotating scan mirror which allows the image to build line by line as the aircraft flies forward. The reflected sunlight collected by the scan mirror is then dispersed into different wavelengths by four spectrometers in the system. The spectral and image information from the spectrometers is digitized and recorded on tape.

The HyMap sensor utilizes four 32-element detector arrays (1 Si, 3 liquid-nitrogen cooled InSb) to provide 126 spectral channels covering the 450nm to 2500nm spectral range over a 512 pixel swath.

To minimize distortion induced in the image by aircraft pitch, roll and yaw motions, the HyMap is mounted in a gyro-stabilized platform (Zeiss SM2000). While the platform minimizes the effects of aircraft motion, small image distortions remain. These residual motions are monitored with a 3 axis gyro, 3 axis accelerometer system (IMU – inertial monitoring unit). The system currently used with the HyMap is a Boeing C-MIGITS II.

Associated with the actual HyMap optical system is an electronics sub-system which is rack mounted in the aircraft. This electronics sub-system provides the sensor with power and contains a computer system that controls the data acquisition process. There is a touch screen monitor used by the operator to set data acquisition parameters, start and stop recording, view the image as it is being acquired and review various engineering status indicators (power, temperature etc).

The HyMap system has been designed to operate in aircraft that have standard aerial photo-ports. The angular width of the recorded image is 61.3 degrees or about 2.3 km when operating 2000m above ground level. Typically, the spatial resolution achieved with the HyMap is in the range 3 to 10 m. For the Ningaloo survey (3.5 m pixel size) the average survey altitude was about 1400m – 1500m above ground with a swath width of 1.8 km.

The general technical specifications of the HyMap system are given in the tables below:

Typical Operational Parameters	
Platform	Light, twin engine aircraft e.g. Cessna 404, unpressurised
Altitudes	2000 – 5000 m AGL
Ground Speeds	110 – 180 kts

Spatial Configuration	
IFOV	2.5 mr along track 2.0 mr across track
FOV	61.3 degrees (512 pixels)
Swath	2.3 km at 5m IFOV (along track) 4.6 km at 10m IFOV (along track)

Typical Spectral Configuration			
<i>Module</i>	<i>Spectral range</i>	<i>Bandwidth across module</i>	<i>Average spectral sampling interval</i>
VIS	0.45 – 0.89 μm	15 – 16 nm	15 nm
NIR	0.89 – 1.35 μm	15 – 16 nm	15 nm
SWIR1	1.40 – 1.80 μm	15 – 16 nm	13 nm
SWIR2	1.95 – 2.48 μm	18 – 20 nm	17 nm

The following figures show the HyMap and associated electronics installed in a light, twin-engine aircraft.



4. SURVEY PLANNING AND SPECIFICATIONS

HyVista Corporation established in consultation with the client an optimum survey plan designed to deliver a combination of spatial resolution and survey efficiency.

For survey operations and flight logistics and planning, HyVista utilizes two integrated software and hardware packages.

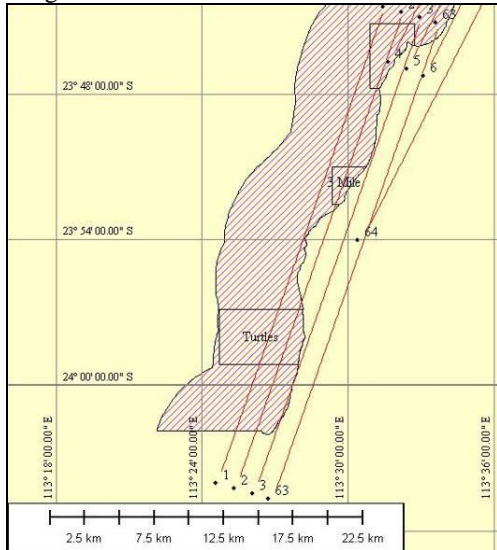
The first is FliteMap (Jeppesen - www.jeppesen.com) which is a high resolution moving map and flight planning application. Using HyVista proprietary software, flight line information is plotted as user waypoints and entered to the FliteMap database. This information then can be used to plan day to day flight logistics and flight logging and reporting. Another important feature of Flitemap is the ability to log the GPS signal from the HyMap system while in flight. A GPS signal is transmitted from the HyMap system via the Omnistar 3000LR DGPS as RTCM. This signal is recorded every second and plotted on the Flitemap display and can also be saved for archiving and reporting purposes to easily and quickly show terrain coverage and target acquisition completion.

The second and most important survey operation software/hardware package is Eztrack Aerial Survey System (TRACK'AIR – www.trackair.com). The system is a combination of specially developed software and hardware tools integrated to streamline airborne survey operations. The system consists of an equipment kit and the TRACKER planning and reporting software. This includes the TECI (Tracker External Camera Interface), snapSHOT software running on a laptop, a panel display for pilot viewing and a complementary cross track indicator (CTI) for the pilot. The Eztrack is a complete Aerial Survey System which starts at the planning stages of a survey mission. Utilizing snapXYZ and snapPLAN a survey area consisting of flight lines can be planned in minutes from any waypoint or polygon coordinates. Flight lines are stored in a database system making it easy to archive and report survey missions. Tracker also accepts many different projections and datum information, making it easy to use with different client needs. Actual flight operation utilizes the Eztrack hardware and snapSHOT software. The Eztrack receives a GPS signal transmitted from the HyMap system via the Omnistar 3000LR DGPS as RTCM. This increases the accuracy of flight line operations.

4.1 PLANNING REPORT

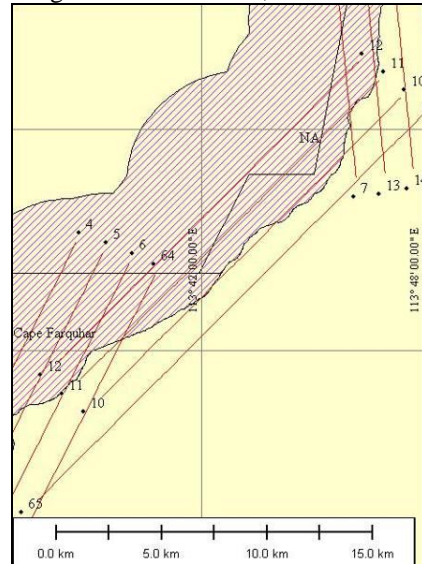
Site Name : "Block A"

Flying height asl: 1400 m
 Course: 017°/197°
 Length: 38 km – 4 lines



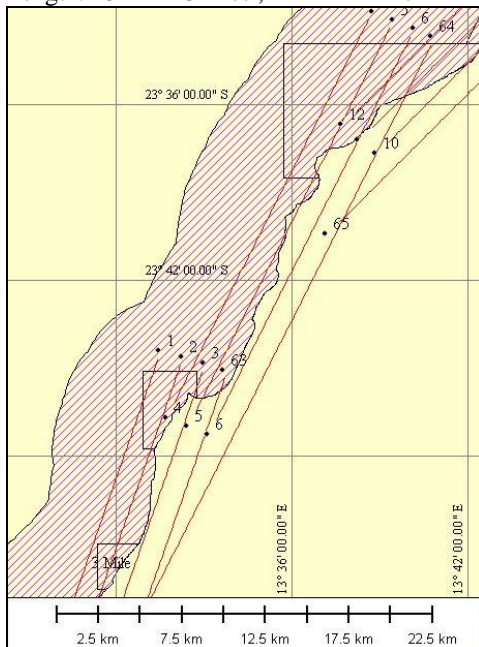
Site Name : "Block C"

Flying height asl: 1400 m
 Course: 45°/225°
 Length: 22 km – 3 lines ; 27 km – 1 line



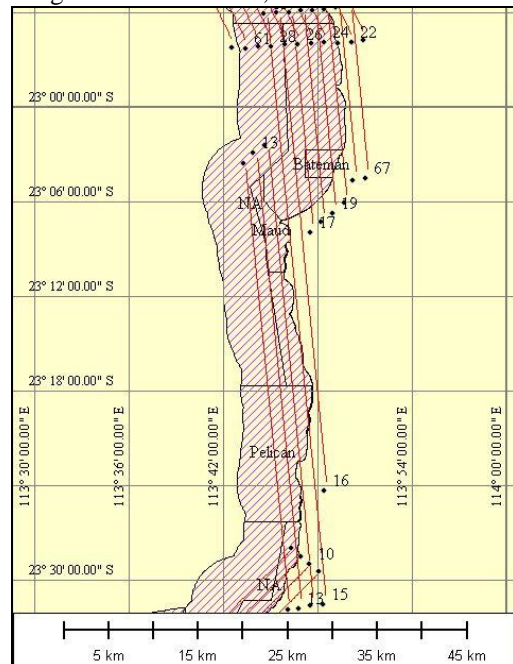
Site Name : "Block B"

Flying height asl: 1400 m
 Course: 025°/205°
 Length: 28 km – 3 lines ; 42 km – 1 line



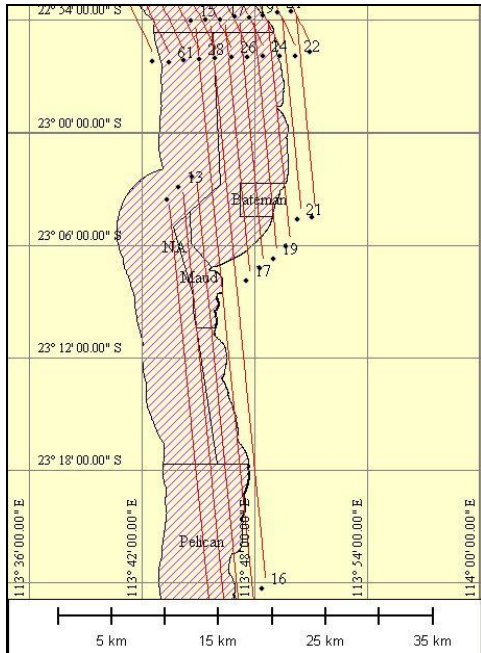
Site Name : "Block D"

Flying height asl: 1400 m
 Course: -5°/175°
 Length: 52 km – 3 lines ; 68 km – 1 line



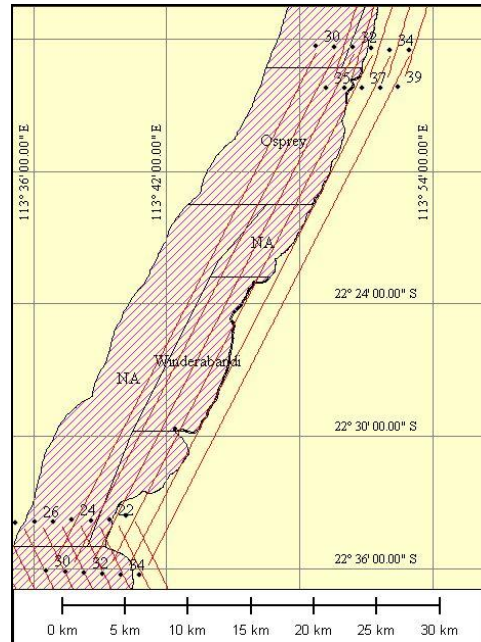
Site Name : “Block E”

Flying height asl: 1400 m
 Course: -5°/175°
 Length: 21km – 2 lines ; 24 km – 4 lines ;
 55 km – 1 line



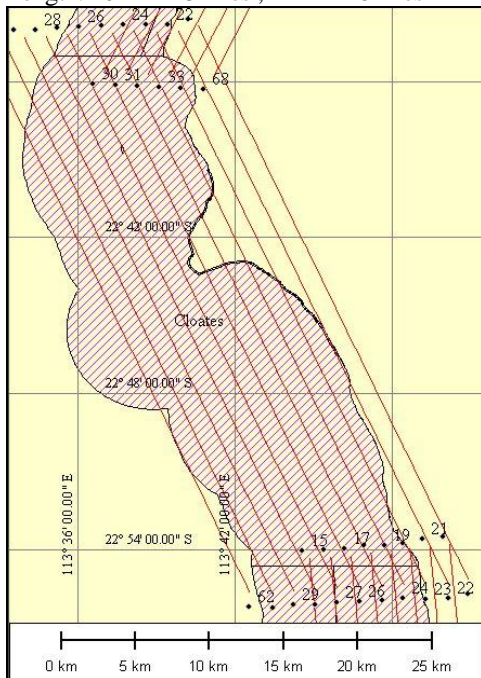
Site Name : “Block G”

Flying height asl: 1400 m
 Course: 26°/206°
 Length: 50 km – 6 lines



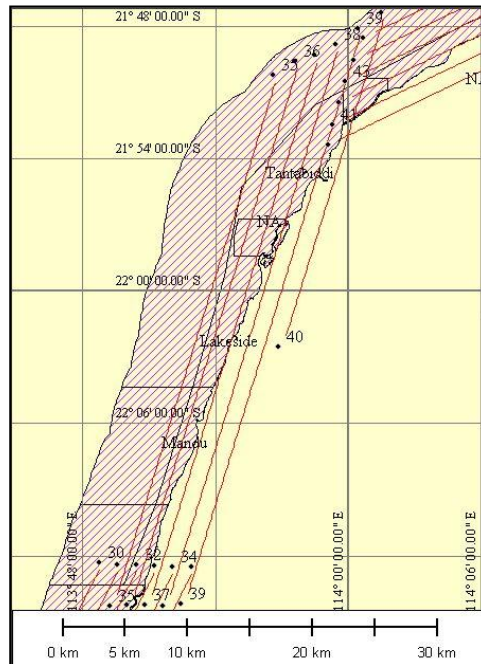
Site Name : “Block F ”

Flying height asl: 1400 m
 Course: -25°/155°
 Length: 40 km – 3 lines ; 44 km – 8 lines



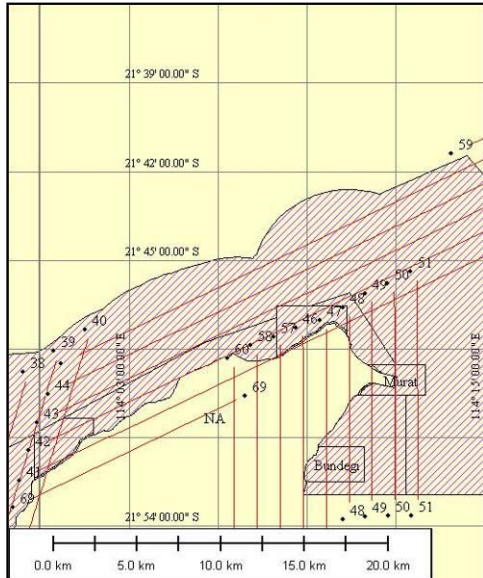
Site Name : “Block H”

Flying height asl: 1400 m
 Course: 16°/196°
 Length: 47 km – 5 lines ; 28 km – 1 line



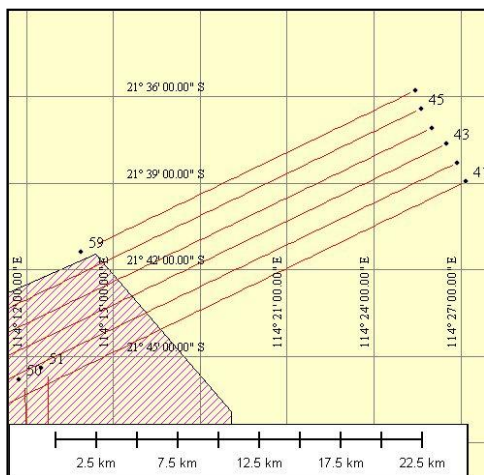
Site Name : "Block I"

Flying height asl: 1400 m
Course: 62°/242°
Length: 24-28 km – 5 lines ; 15 km – 1 line



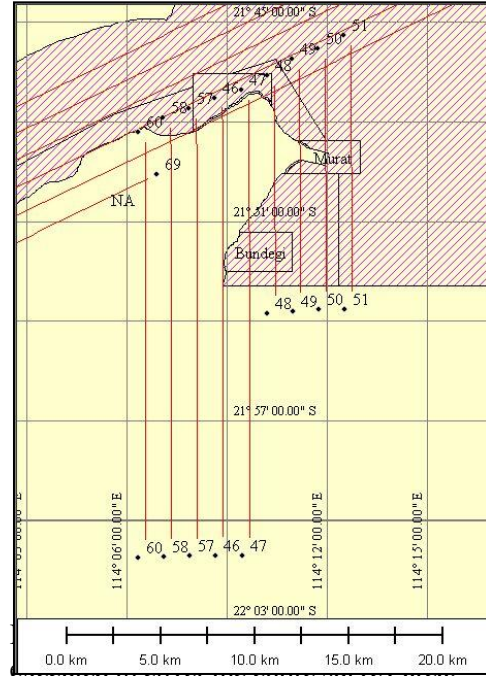
Site Name : "Block J"

Flying height asl: 1400 m
Course: 62°/242°
Length: 28 km – 5 lines ; 21 km – 1 line



Site Name : "Block K"

Flying height asl: 1400 m
Course: 0°/180°
Length: 25 km – 5 lines ; 14 km – 4 lines



5. HYMAP DATA PRODUCTS

The data processing and data products that HyVista Corporation delivered is radiance calibrated data (at sensor), atmospheric correction (to apparent reflectance) and geometric correction information. All data are delivered as ENVI™ compatible files and are delivered on Maxtor external hard disk (300GB).

In operation, the HyMap sensor records 128 spectral bands of data. However, the delivered data contains 125 bands because two bands (band 1 and 32 of the VIS module and band 1 of the NIR module) are deleted during the pre-processing steps.

Spectral and radiometric calibration of the HyMap sensor was accomplished prior to the survey and this information was used to allow the conversion of the raw DN counts to radiance values in $\mu\text{W}/\text{cm}^2 \text{ nm sr}$.

Atmospheric correction (spectral processing to remove the effects of atmospheric absorptions and scattering) was performed using the HyCorr software package. HyCorr is a program for converting raw, “near-raw” or radiance HYMAP images to apparent surface reflectance. HyCorr offers two levels of processing. The simpler level is essentially compatible with ATREM3 processing. The more advanced level consists of an ATREM pass followed by an EFFORT polishing pass to remove systematic ATREM errors.

Geometric correction algorithms were used to correct the hyperspectral data. The HyMap system is mounted on a Zeiss SM2000 gyro-stabilized platform that provides 5 degrees of pitch and roll correction and 8 degrees of yaw correction. High quality DGPS integrated with a Boeing CMIGITS II GPS/INS inertial monitoring unit was used to provide sensor pointing data to precisely geocode the raw data. Geometric correction factors are provided to convert the data to map coordinates and provide GIS ready, map-based products.

Listed below is a summary of the pre-processing stages.

Radiance	<i>Radiometric Calibration Date Calibration File Software Version</i>	1 st April 2006 Calibration_hymap2_01april06.txt 1.9
Reflectance	<i>Software Aerosol Model Atmospheric Model Total Ozone Visibility H2O vapor modeling EFFORT correction</i>	HyCorr v2 Continental Mid Latitude Summer 0.34 (atm-cm) 75 km Rock, soil & minerals YES
Geocorrection	<i>Software Digital Elevation Model</i>	HyGeo v1.6 SRTM not used – default 1m

Below is listed the files that are delivered followed by a complete description of each.

Radiance Data Files

“filename”_rad.bil – HyMap image data, 126 channels x 512 pixels x N lines (BIL format).
“filename”_rad.hdr – associated ENVI header file.
“filename”_q.img – single band (VIS ch25) quicklook image (BSQ format). **image will be flipped*
“filename”_q.hdr – associated ENVI header file.
“filename”_mask.bsq – masking output file (BSQ format).
“filename”_mask.hdr – associated ENVI header file.
“filename”_c.cal – internal lamp data, 128 channels x 10 pixels.
“filename”_c.hdr – associated ENVI header file.
“filename”_d.drk – dark current data, 128 channels x 10 pixels.
“filename”_d.hdr – associated ENVI header file.
“filename”.JPG – composite true colour (3 band RGB) image in JPG format.

Reflectance Data Files

“filename”_ref.bil – HyMap image data, 125 channels x 512 pixels x N lines (BIL format).
“filename”_ref.hdr – associated ENVI header file.
“filename”_h2o.bil – water vapour band image.
“filename”_h2o.hdr – associated ENVI header file.
“filename”_eff_gain_sli – HyCorr EFFORT gain spectral library.
“filename”_eff_gain_sli.hdr – associated ENVI header file.
“filename”_eff_model_sli – HyCorr EFFORT model spectral library.
“filename”_eff_model_sli.hdr – associated ENVI header file.
“filename”_eff_raw_sli – HyCorr EFFORT final calibration spectral library.
“filename”_eff_raw_sli.hdr – associated ENVI header file.

Geocorrection Data Files

“filename”_geo.img – 3 band colour (RGB) geocoded “quicklook” image.
“filename”_geo.hdr – associated ENVI header file.
“filename”_geo.ers – associated ER-MAPPER header file.
“filename”_glt.bsq – Geographic Lookup Table file.
“filename”_glt.hdr – associated ENVI header file.
“filename”_igm.bil – Input Geometry file.
“filename”_igm.hdr – associated ENVI header file.
“filename”.gps – HyMap navigation file.
“filename”_ephemeris.txt – Aircraft ephemeris data for each scan line.
“filename”_report.txt – summary of the geocorrection parameters.

5.1 Radiance Data Files

“filename”_rad.bil

This file is the 126 band, 512 pixel wide image in BIL format that has been converted to physical units of radiance (strictly, the measurement is “at sensor radiance”). The data is in $\mu\text{W}/\text{cm}^2 \text{ nm sr}$.

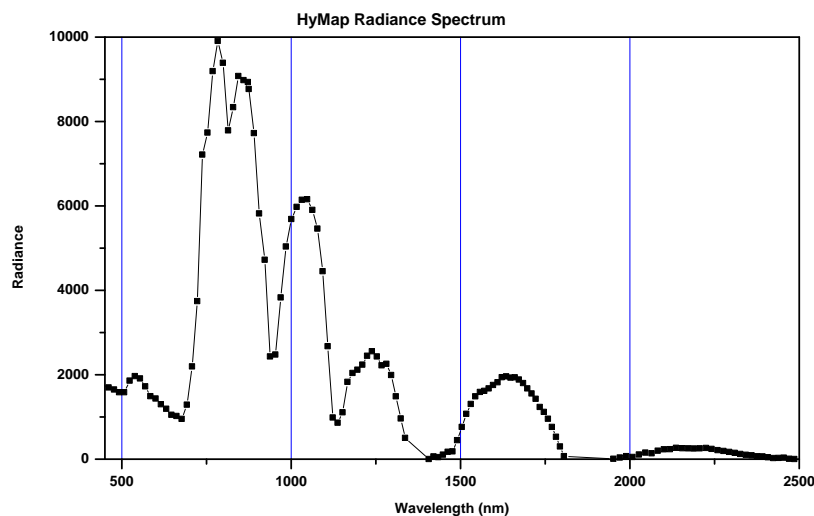
The in-flight recorded DN (digital numbers) have been corrected for dark current/electronic offsets and converted to radiance using laboratory radiometric calibration information and in-flight measurements of the on-board calibration lamp.

Typically the file will be labelled as “filename”_rad.bil or “filename”_radiance.bil to further indicate that the data is in radiance units.

The preferred data format is a two byte, integer format and the data is rescaled to preserve dynamic range, especially in the SWIR range. This rescaling involves multiplying bands 1 – 62 by 1000 and bands 63 – 126 by 4000.

The wavelength and bandwidth (in nanometres) information is imbedded in the ENVI header file (*.hdr).

A typical radiance spectrum (over a vegetated scene) is shown below.



The HyMap sensor has 4 spectrometers (VIS, NIR, SWIR1 and SWIR2), each producing 32 spectral bands of imagery. The VIS and NIR provide contiguous sampling across the 900 nm region. In fact, the spectrometers are set up to provide a slight overlap in the long wavelength region of the VIS spectrometer and the short wavelength region of the NIR spectrometer.

Image data is written in band order from the VIS to the NIR to the SWIR1 to the SWIR2 spectrometer and this leads to the bands being in wavelength order except at the VIS – NIR overlap.

Typically, band 30 (the last band of the VIS spectrometer) of the radiance data will have a wavelength larger than band 31 (the first band of the NIR spectrometer).

When radiance spectra are plotted as a Z-profile in ENVI, the line of the plot is connected to the data points in band order, not wavelength order. This can give a “strange” appearance to the plot in the VIS-NIR overlap region.

“filename”_q.img

This file is a single band image in BSQ format. The file is used to provide a “quicklook” at the HyMap image. The image has the same dimensions as the radiance file but will be displayed in a mirrored orientation as it has been derived from the “raw” HyMap data. Therefore the image is displayed “as it is recorded on the HyMap system”. The band used is from VIS ch25.

“filename”_mask.bsq

This file is the masking output file. The file has the same dimensions as a 1-band image with byte formatting. A 1 value in a pixel represents a valid pixel while a 0 in the pixel represents an invalid mapped pixel in the radiance file. The masking process also sets pixels between 0 and the MinDN value back to zero, thus removing any negative radiance values that may have been generated due to very low signal bands with noise levels of greater than 1DN standard deviation. The file is imported by ENVI and used for masking corrupt pixels during data analysis.

“filename”_c.cal

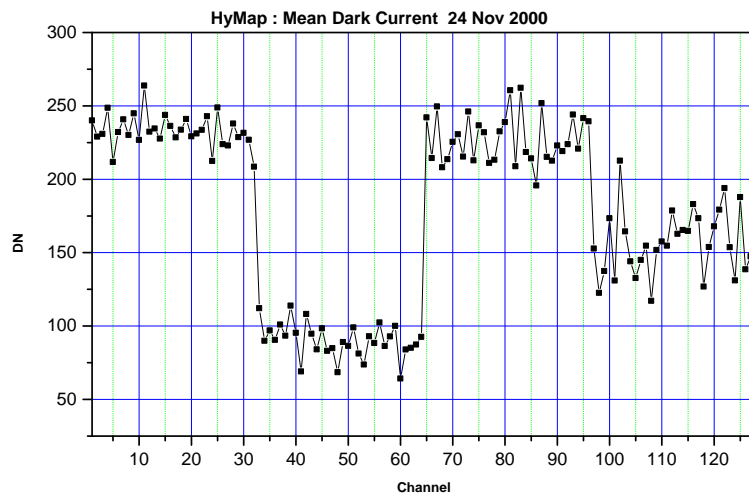
During image acquisition, the HyMap sensor measures the on-board calibration lamp, acquiring a 10 pixel wide “image” after alternate image scan lines. This data is in DN and is used by HyVista Corp. during the radiometric pre-processing. The data in this file are not dark current/offset corrected. Typically, this file will be delivered in the HyMap 128 channel mode. (NOTE: in the 126 band radiance data, bands 1 and 32 have been deleted)

To most users, this file is of little value and has some properties that require additional information from HyVista Corp for a complete understanding.

“filename”_d.drk

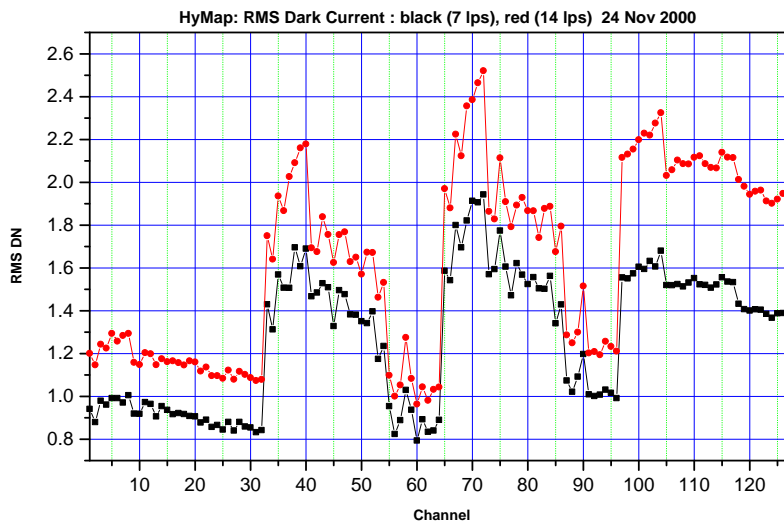
During image acquisition, the HyMap sensor measures detector dark currents and offsets, acquiring a 10 pixel wide “image” after alternate image scan lines. The data is in DN and can be used to examine the dark current statistics. Typically, this file will be delivered in the HyMap 128 channel mode. (NOTE: in the 126 band radiance data, bands 1 and 32 have been deleted)

A typical mean dark current spectrum is shown below where data from the 4 spectrometers can be easily recognised.



Typical dark current noise (in rms DN) is shown in the following figure. Again the 4 spectrometer data can be easily recognised. Note that the details of both the mean and rms dark currents will be dependent of which detector array is installed at the time of the survey and on the electronic gains set during the laboratory calibration.

Note also that the rms dark current noise is dependent on the scan line acquisition rate. The higher the line rate, the higher the rms noise.



“filename”.JPG

This file is a 3-band colour image of the imported data. It is displayed as RGB as R-VISch18, G-VISch10, B-VISch4. It is radiance corrected and gaussian stretched to provide the best quality picture and is provided in the common JPG image format.

5.2 Reflectance Data Files

HyVista Corporation produces reflectance data files from the software HYCORR. HYCORR is a program for converting radiance HYMAP images to apparent surface reflectance. It offers two levels of processing. The simpler level is essentially compatible with ATREM3 processing. The more advanced level consists of an ATREM pass followed by an EFFORT polishing pass to remove systematic ATREM errors. EFFORT processing has been used on this dataset and the derived files are explained below.

“filename”_ref.bil

This is the main reflectance product. It is an ENVI file-pair with the same dimensions as the input image. It is also a BIL short-integer image and has been scaled by 10,000. (reflectance*10000.) Wavelength is displayed as um.

“filename”_h2o.bil

This file is the water-vapour band image. This gives the amount of water vapour modelled for each pixel. It has the same #samples and #lines as the input image but only 1 band. It is a short-integer image. It has (water vapour in atm-cm) * 1000.

“filename”_eff_gain_sli

This file is the HyCorr EFFORT gain spectral library. It is the EFFORT gain and error in finding the gain: It is in ENVI spectral library format.

“filename”_eff_model_sli

This file is the HyCorr EFFORT model spectral library. It is in ENVI spectral library format.

“filename”_eff_raw_sli

This file is the HyCorr EFFORT final calibration spectral library. It is in ENVI spectral library format.

5.3 Geocorrection Data Files

HyVista Corporation uses proprietary software for geo-correcting hyperspectral images collected by the HyMap airborne hyperspectral scanner. The software uses HyMap sensor position and orientation data collected at the same time as the image to calculate the position of each pixel in the image. The software uses this position information to map input image pixel values onto a geo-referenced grid of output image pixels.

The geocorrection software also makes use of a Digital Elevation Model (or DEM) of the geographic region containing the imagery.

The geocorrection software produces an "_igm" input geometry file, a "_glt" geometry lookup table file and, finally, the geo-corrected output image. All geocoded products are in the UTM projection and WGS84 datum. These files are explained in detail as follows.

"filename"_geo.img

Typically a 3 band colour (RGB) geocoded "quicklook" image. Bands used to derive the "true colour" image are R-ch15, G-ch9, B-ch3. When geocoded flight lines are mosaiced together, make sure to set the background value to ignore to -99. The null pixels around the images have this value. The "quicklook" image is produced with an associated ENVI header file and also produced with an associated ER-MAPPER header file. (*"filename"_geo.ers*)

"filename"_glt.bsq

The geometric lookup table file represents much of the important information that is created in the geo-correction process. The "_glt" file contains the information about which original pixel occupies which output pixel in the final product. Additionally, it is sign-coded to indicate if a certain output pixel is "real" or a nearest-neighbor in-fill pixel. The "_glt" file is a geo-corrected product, with a fixed pixel size projected into a rotated UTM system. The pixel size, scene elevation, UTM zone number, and rotation angle information is reported in an associated ASCII header file. The "_glt" file is two-byte integer binary data in a BIL format. The two bands of the "_glt" file refer to original sample number and original line number, respectively. The sign of the value indicates whether the pixel is an actual image pixel, located at its proper position indicated by a positive value) or a nearest-neighbor in-fill pixel placed to fill an under-sampled image gap (indicated by a negative value). A zero value signifies that no input pixel corresponds to this output pixel.

The importance of the "_glt" image and its role in identifying image gaps and in-fill pixels must be stressed, especially for studies involving small targets. The geometric lookup table file can be used to geo-correct any band or derived product through a simple lookup table procedure.

"filename"_igm.bil

Input geometry file that denotes the UTM Easting and Northing values derived by the geo-correction process for each original image pixel. The first band contains UTM Easting values in meters and the second band contains UTM Northing values in meters for each original pixel. The input geometry file has the same spatial size as the raw HyMap imagery. The file is double precision, binary data in a BIL format. The pixel size, and UTM zone number information are given in an associated ASCII header file. The input geometry file itself is not geo-corrected, but does contain the geo-location information for each original raw pixel.

"filename".gps

This file is the HyMap navigation file. The *.gps files is a multi-column ASCII file that is derived from the *.log file by HyVista Corp. proprietary software. The program “unpacks” the *.log file, synchronizes times and generates an output which is indexed by scan line number. Not all possible parameters are supplied to a client; again it depends on the specifics of the survey contract. The table below shows the total list of possible output parameters.

Parameter	Example	Description	Comment
CMIGITS Time	419819098.2	Internal CMIGITS time in microseconds	Of no interest or value to end user
Pitch	0.85741807	IMU output Decimal degrees	
Roll	1.14817758	IMU output Decimal degrees	
Heading	-67.36104012	IMU output Decimal degrees	
Lat	39.9147011	DGPS output Decimal degrees (neg = Sth)	
Long	-116.3251269	DGPS output Decimal degrees (0 to 180 E, 0 to -180 W)	
Alt	4754.163811	DGPS output Metres above MSL	
UTC Time	61606.1032/5/10/2000	DGPS output Time of day in seconds /day/month/year	61606.1032= 17 Hrs,6 Min,46.1 Seconds
Grnd Spd	81.97301031	DGPS output Metres per second	
True Track	293.4184839	DGPS output Decimal degrees (0 to 360)	
DGPS	1	DGPS status 1 = DGPS being received 0 = no DGPS received	
Satellites	5	Number of satellites being received	
Line Num.	1	Image scan line number	
VME time	344844473	Internal computer tick time in microseconds	Of no interest or value to end user

All of the above timing, position and pointing information has been referenced to the **end** of the image scan line.

The parameters are derived as follows.

Once per second, the DGPS receiver generates an interrupt signal. At the time of this interrupt, the system records the VME time (referred to as tick time) and the CMIGITS time, both in microseconds. The DGPS receiver then sends UTC time, lat, long, altitude etc to the system referenced to the time of the interrupt signal.

At the end of each image scan line, VME time is recorded. The CMIGITS sends pitch, roll and heading information to the system at a 10 Hz rate and time tagged with CMIGITS time.

The program uses the CMIGITS and VME tick times to synchronize (and interpolate) the other parameters, including UTC time, to the time corresponding to the end of a scan line.

One question that might arise is “if the time is referenced to the end of the image scan line, what positional difference occurs from the centre pixel of the scan line to the end pixel?”

In the following table, the relationship between scan rate (lines per second) and along track positional difference between middle and end pixel is shown.

Line Rate (lines per second)	Time period per scan line (pixel 1 to pixel 512) in milliseconds	Difference (centre to last pixel) at 100 Kts	Difference (centre to last pixel) at 120 Kts	Difference (centre to last pixel) at 140 Kts
8	42.6	1.05 m	1.3 m	1.5 m
10	34.1	1.35 m	1.0 m	1.2 m
12	28.4	0.7 m	0.85 m	1.0 m
14	24.3	0.6 m	0.75 m	0.85 m
16	21.3	0.55 m	0.65 m	0.75 m

Thus it can be seen that unless positional information and/or geo-correction is being attempted at the metre or less precision, that the fact that the timing information generated is referenced to the end of the scan line rather than the centre contributes minimal error. The differences are smaller than the positional information derived from the DGPS and smaller than the accuracy of the IMU pointing information when traced to actual ground positions.

“filename”_ephemeris.txt

Aircraft ephemeris information for each scan line. The file contains: line number, UTM X meters), UTM Y (meters), altitude (meters), pitch (degrees), roll (degrees), and heading (degrees).

“filename”_report.txt

This file contains a summary of data used and generated by the geo-correction process.

6. Project Execution

Survey progress – Data acquisition and conditions from survey diary:

- Wed. 19th: Aircraft (with HyMap and operator) leaves Sydney (a/noon) makes it to Broken Hill
Thu. 20th: Aircraft only makes it to Newman – very strong head winds
Fri. 21st: Aircraft arriving at 10 am – unloading / filling with LN2 / test flights over Airstrip and coral spawning – HyMap data looks good.
Sat. 22nd: Decision on starting the survey – high winds 13/18 knots 5% Cirrus in the sky Block I survey first starting at 9:30, Block K next
Sun 23rd: Winds even stronger – no cirrus, but forecast has not changed - decision to fly. Block J survey starting at 9:30, Block H next – decision to abort by operator – crosswinds reaching 30 knots – white caps will make data analysis difficult. Lots of white caps on survey block J – borderline to re-fly
Mon 24th: Wind has died down (10 knots) – no cirrus – looks like an ideal survey day. Block H starting at 10:40, 1st part of block F (6 lines). All o.k. - however line 27 cannot be read from tape – will be re-flown with part 2 of block F.
Tue. 25th: Wind stronger again 15-20 (white caps in gulf, but N. Reef seems better) – they are borderline – but perfect blue sky. Consultation with teams in coral bay - decision to and start Block G at 10:15, try rest of Block F + re-flight of line 27 – just in case; had to abandon block F cumuli moving in the survey area.
Wed 26th: Pilots rest day
Thu. 27th: pickup LN2 from Karratha – too far to drive 620 km one way - not enough LN2 to try rest of Block F - weather conditions good
Fri 28th: Weather conditions almost perfect: Wind is now 10-15 knots, perfect blue skies – however swell is 2m and creates strong draft in Reef channels (= > sediments is stirred) Block C, D & F-2 acquired, repeat of line F-27 just in case
Sat 29th: Weather as the day before – we attempt Block A, B & E – data quality not so good due to very strong turbulences – can be used but if possible we re-fly.
Sun 30th: Weather as before – swell still high decide on repeating Block J (Muiron Islands). Data acquired but does not look much better – almost as many white caps as in 1st attempt – otherwise good.
Mon 1st: Weather still good – we re-fly a Block A, B & E
Tue 2nd: Aircraft leaves Exmouth to Perth for maintenance – back to Sydney a few days later.

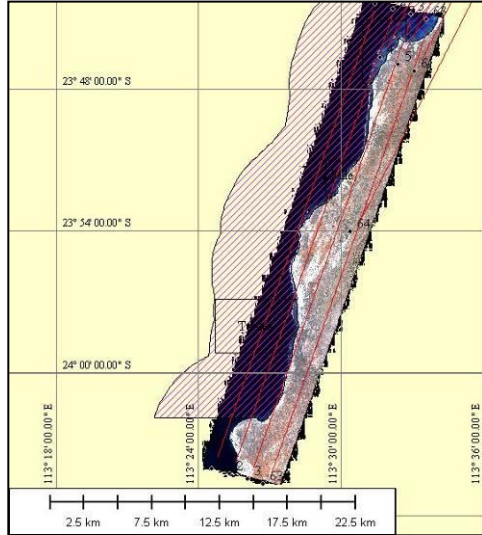
The different blocks have approximately the following sizes based on survey shape file outlines: Block A: ~ 230 sqkm, Block B: ~ 220 sqkm, Block C:~ 140 sqkm, Block D:~ 350 sqkm, Block E:~ 260 sqkm, Block F:~ 650 sqkm, Block G:~ 420 sqkm, Block H:~ 410 sqkm, Block I:~ 210 sqkm, Block J:~ 240 sqkm, Block K:~ 270 sqkm and total: 3400 sqkm

The pixel size for the survey was nominated to be acquired at a size of 3.5 m – due to difference in ground speed of the aircraft the actual pixel size may not be perfectly 3.5 during data acquisition – however during pre-processing all the geo located files are re-sampled to a 3.5 m pixel size and spacing.

During a number of days of the survey and especially the last three days, the aircraft encountered extreme mechanical turbulence due to shear zones occurring at the flight altitudes over the land water boundary. This long term exposure to extreme vibration affected the liquid nitrogen cooled detector assembly (some internal structural parts were shaken loose) and resulted in some signal artifacts being introduced into the imagery. Most affected was the NIR spectrometer module. The VIS module, from which most of the reef mapping results will be derived, was unaffected

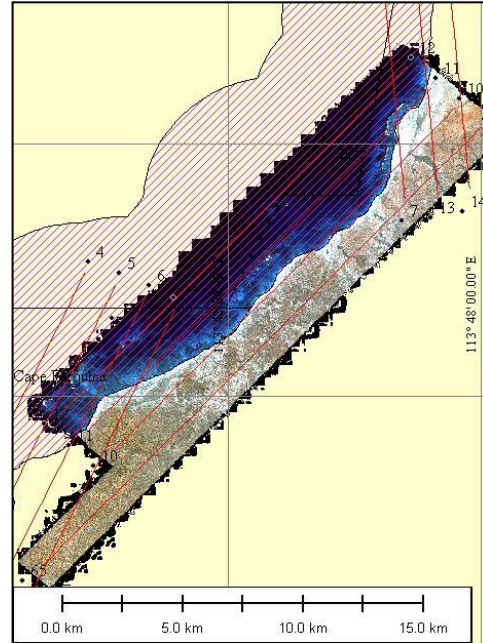
Site Name : “Block A”

Flying height asl: 1400 m
Course: 017°/197°, ~230 sqkm
Length: 38 km – 4 lines



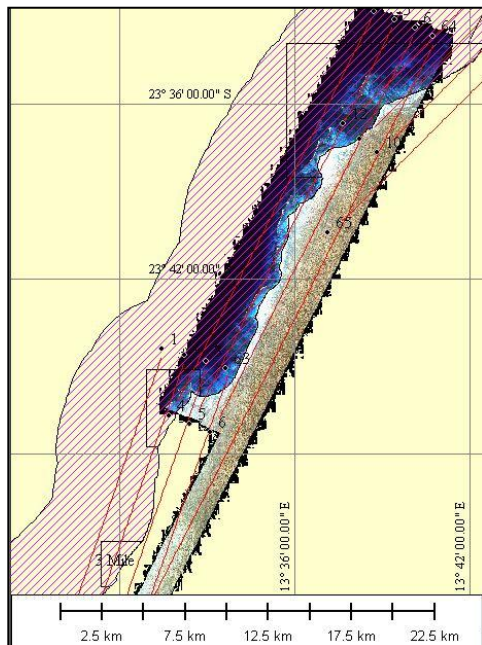
Site Name : “Block C”

Flying height asl: 1400 m
Course: 45°/225°, ~ 140 sqkm
Length: 22 km – 3 lines ; 27 km – 1 line



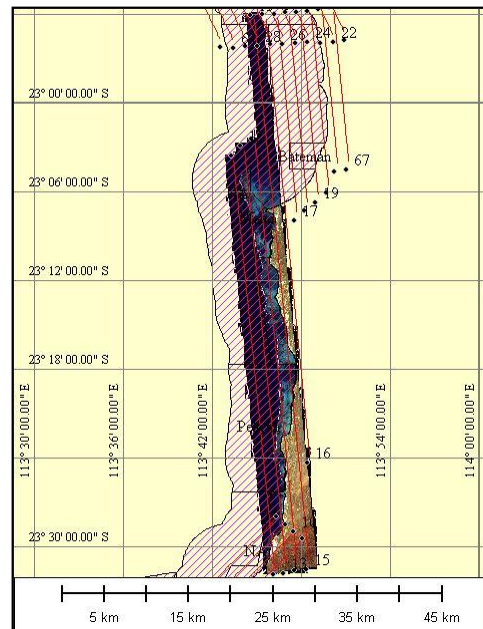
Site Name : “Block B1”

Flying height asl: 1400 m
Course: 025°/205°, ~ 220 sqkm
Length: 28 km – 3 lines ; 42 km – 1 line



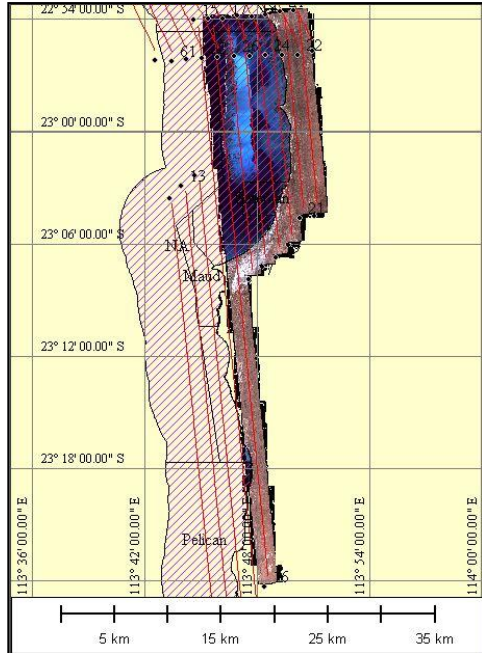
Site Name : “Block D”

Flying height asl: 1400 m
Course: -5°/175°, ~ 350 sqkm
Length: 52 km – 3 lines ; 68 km – 1 line



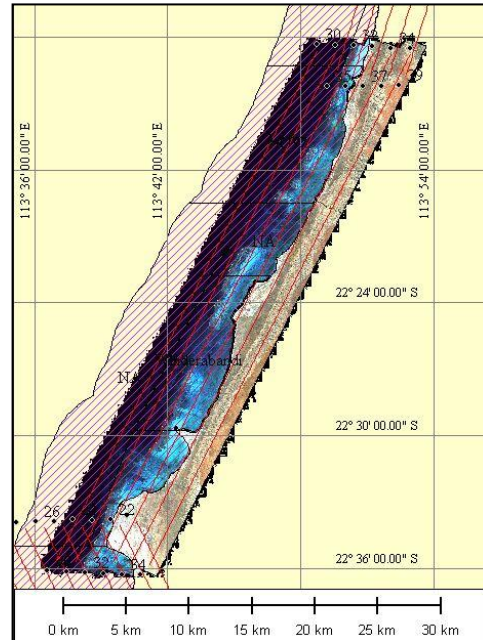
Site Name : "Block E"

Flying height asl: 1400 m
 Course: -5°/175°, ~ 260 sqkm
 Length: 21km – 2 lines ; 24 km – 4 lines ;
 55 km – 1 line



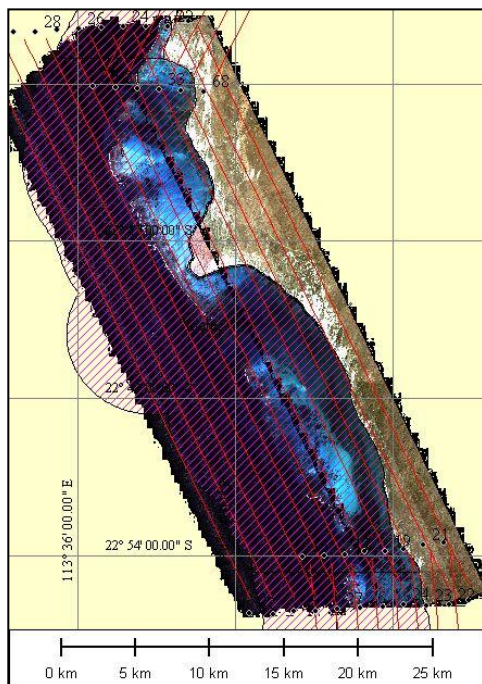
Site Name : "Block G"

Flying height asl: 1400 m
 Course: 26°/206°, ~ 420 sqkm
 Length: 50 km – 6 lines



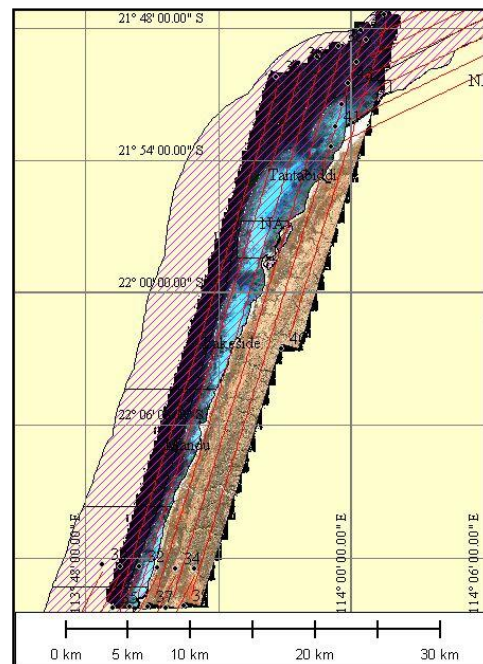
Site Name : "Block F"

Flying height asl: 1400 m
 Course: -25°/155°, ~ 650 sqkm
 Length: 40 km – 3 lines ; 44 km – 8 lines



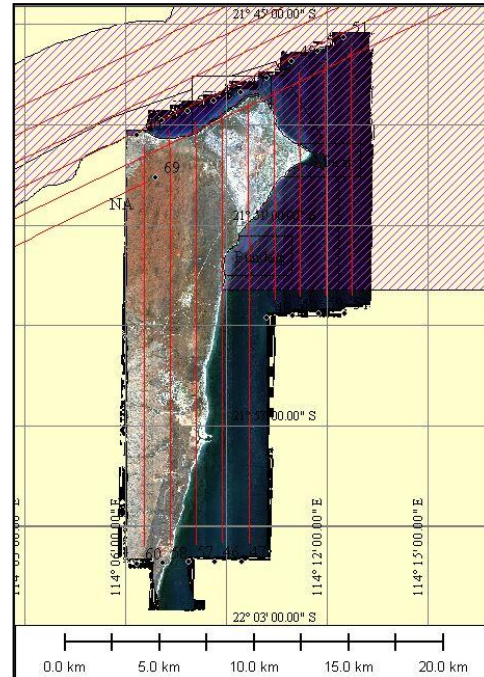
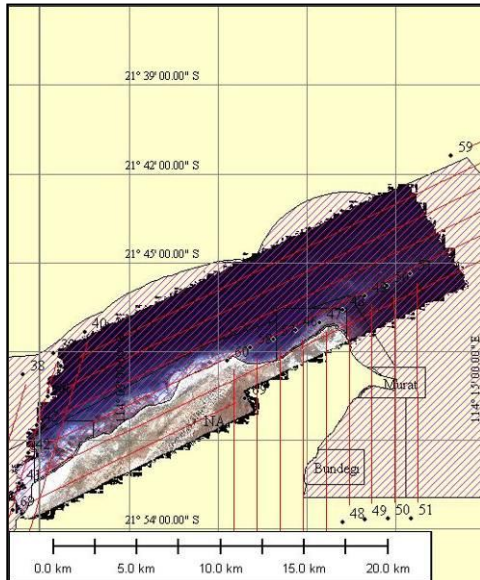
Site Name : "Block H"

Flying height asl: 1400 m
 Course: 16°/196°, ~ 410 sqkm
 Length: 47 km – 5 lines ; 28 km – 1 line



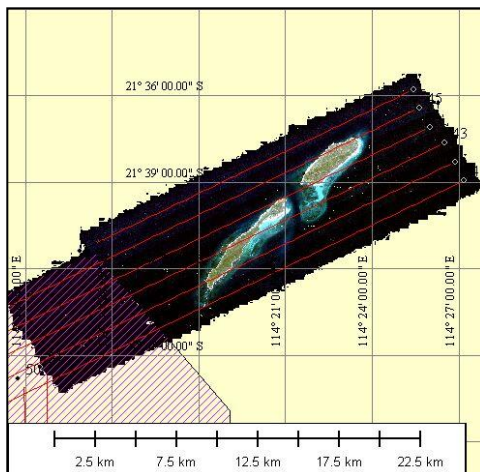
Site Name : “Block I”

Flying height asl: 1400 m
Course: 62°/242° , ~ 210 sqkm
Length: 24-28 km – 5 lines ; 15 km – 1 line



Site Name : “Block J”

Flying height asl: 1400 m
Course: 62°/242° , ~ 240 sqkm
Length: 28 km – 5 lines ; 21 km – 1 line



Site Name : “Block K”

Flying height asl: 1400 m
Course: 0°/180° , ~ 270 sqkm
Length: 25 km – 5 lines ; 14 km – 4 lines

In total 67 flight lines were acquired in 11 blocks to cover the entire survey area.

Individual Survey Lines : Center coordinates every 500 lines extracted from *.igm file:

Block A: Ningaloo_20060501

File: blk_a_04_igm.bil (WGS-84
Z49SOUTH) - 10448 lines

749116 7335307
749661 7337046
750270 7338820
750874 7340565
751458 7342268
752027 7344009
752626 7345701
753194 7347398
753758 7349076
754358 7350743
754900 7352386
755470 7354019
756019 7355673
756607 7357351
757186 7359010
757786 7360840
758405 7362597
759010 7364353
759607 7366125
760213 7367884
760811 7369658
761328 7371274

File blk_a_03_igm.bil (WGS-84
Z49SOUTH) - 10283 lines

760021 7371469
759393 7369644
758749 7367816
758153 7366069
757552 7364263
756915 7362459
756320 7360695
755704 7358904
755103 7357114
754490 7355318
753871 7353518
753252 7351727
752658 7349951
752047 7348162
751449 7346438
750853 7344708
750278 7342989
749692 7341260
749067 7339531
748489 7337785
747882 7336006
747632 7334917

File blk_a_02_igm.bil (WGS-84
Z49SOUTH) - 10529 lines

746495 7336204
747090 7337851
747661 7339598
748262 7341303
748853 7342987
749428 7344720

750016 7346451
750617 7348183
751197 7349893
751781 7351617
752362 7353327
752965 7355022
753547 7356725
754119 7358401
754683 7360102
755282 7361810
755856 7363513
756445 7365242
757025 7366946
757599 7368655
758174 7370371
758746 7372108
758786 7372201

File blk_a_01_igm.bil (WGS-84
Z49SOUTH) - 10482 lines

757479 7372312
756850 7370613
756286 7368905
755696 7367197
755117 7365479
754524 7363737
753917 7361990
753331 7360276
752735 7358560
752166 7356844
751578 7355166
751014 7353435
750403 7351746
749819 7350026
749217 7348277
748632 7346544
748050 7344816
747455 7343090
746851 7341364
746291 7339644
745702 7337941
745156 7336292

Block B: Ningaloo_20060501

File blk_b_08_igm.bil (WGS-84
Z49SOUTH) - 11968 lines

755631 7354750
756384 7356315
757130 7357844
757905 7359408
758664 7360975
759428 7362536
760180 7364087
760927 7365621
761688 7367185
762445 7368715
763208 7370265
763959 7371854

764738	7373410	764041	7381030
765487	7374985	763164	7379209
766278	7376559	762256	7377378
767064	7378180	761367	7375585
767818	7379738	760517	7373804
768569	7381260	759646	7372050
769332	7382819	758766	7370308
770062	7384354	757959	7368564
770835	7385909	757844	7368300
771584	7387451		
772331	7389003		
773081	7390548		
773825	7392009		

Block C: Ningaloo_20060428

File blk_c_12_igm.bil (WGS-84
Z49SOUTH) - 7830 lines

767555	7379797
768807	7381121
770063	7382419
771286	7383713
772521	7384998
773732	7386295
774945	7387533
776120	7388796
777309	7390023
778463	7391262
779639	7392472
780860	7393718
782047	7394975
783241	7396196
784410	7397456
785585	7398703
786380	7399511

File blk_b_07_igm.bil (WGS-84
Z49SOUTH) - 6996 lines

772578	7392454
771718	7390673
770853	7388897
769971	7387088
769081	7385297
768206	7383495
767326	7381671
766434	7379858
765535	7378054
764644	7376221
763782	7374432
762883	7372640
762029	7370820
761145	7369005
760276	7367232

File blk_b_06_igm.bil (WGS-84
Z49SOUTH) - 7834 lines

759093	7367863
759863	7369419
760622	7371018
761395	7372569
762189	7374179
762954	7375769
763735	7377344
764508	7378947
765281	7380543
766085	7382134
766839	7383731
767631	7385358
768426	7386953
769205	7388576
769986	7390196
770814	7391810
771343	7392887

File blk_c_11_igm.bil (WGS-84
Z49SOUTH) - 5724 lines

785374	7400374
784020	7398932
782672	7397530
781330	7396128
780009	7394752
778703	7393378
777393	7392009
776095	7390668
774830	7389321
773571	7388006
772335	7386695
771050	7385390
770506	7384776

File blk_c_10_igm.bil (WGS-84
Z49SOUTH) - 6290 lines

769548	7385727
770789	7387038
772030	7388352
773245	7389595
774458	7390844
775641	7392097
776830	7393349
778022	7394605
779158	7395797
780310	7397015
781463	7398201

File blk_b_05_igm.bil (WGS-84
Z49SOUTH) - 7072 lines

770145	7393560
769314	7391810
768434	7390057
767562	7388249
766692	7386460
765806	7384671
764934	7382860

782610 7399387
783758 7400593
784424 7401321

781787 7464651
781763 7465049

File blk_c_09_igm.bil (WGS-84
Z49SOUTH) - 5632 lines

783440 7402219
782145 7400841
780816 7399450
779494 7398102
778247 7396763
776926 7395382
775609 7393993
774268 7392621
772931 7391210
771542 7389777
770190 7388355
768829 7386925
768473 7386526

File blk_d_15_igm.bil (WGS-84
Z49SOUTH) - 15291 lines

781638 7449463
781747 7447637
781908 7445747
782043 7443901
782162 7442054
782293 7440210
782436 7438309
782585 7436436
782702 7434611
782850 7432839
782963 7431080
783082 7429329
783213 7427558
783347 7425808
783476 7424053
783575 7422352
783730 7420654
783823 7419055
783950 7417465
784071 7415819
784191 7414116
784314 7412376
784429 7410631
784565 7408900
784682 7407154
784807 7405380
784938 7403623
785073 7401862
785190 7400084
785308 7398323
785438 7396565
785517 7395568

Block D: Ningaloo_20060428

File blk_d_16_igm.bil (WGS-84
Z49SOUTH) - 18613 lines

786900 7395848
786749 7397746
786615 7399528
786503 7401355
786352 7403173
786220 7405014
786095 7406807
785957 7408639
785809 7410527
785664 7412347
785544 7414166
785403 7415949
785286 7417771
785131 7419621
784997 7421506
784863 7423383
784715 7425269
784591 7427143
784445 7429041
784303 7430960
784179 7432849
784008 7434832
783876 7436742
783755 7438648
783598 7440539
783457 7442428
783328 7444244
783163 7446155
783040 7448018
782905 7449941
782753 7451769
782619 7453652
782480 7455512
782345 7457364
782219 7459241
782098 7461032
781949 7462842

File blk_d_14_igm.bil (WGS-84
Z49SOUTH) - 14247 lines

784216 7395518
784074 7397463
783929 7399352
783798 7401266
783643 7403110
783515 7404983
783402 7406839
783248 7408716
783128 7410585
782984 7412466
782834 7414311
782707 7416207
782556 7418103
782443 7419993
782304 7421839
782167 7423704
782018 7425566
781899 7427441
781750 7429226
781630 7431056
781486 7432870

781360	7434725	File blk_e_22_igm.bil (WGS-84
781233	7436570	Z49SOUTH) - 4986 lines
781101	7438457	789714 7465520
780962	7440348	789850 7463454
780812	7442228	789998 7461458
780663	7444088	790133 7459462
780549	7445972	790284 7457499
780400	7447873	790415 7455532
780333	7448771	790572 7453498
		790709 7451473
File blk_d_13_igm.bil (WGS-84		790855 7449478
Z49SOUTH) - 14249 lines		791000 7447434
779097 7447377		791184 7445586
779246 7445608		
779361 7443863	File blk_e_21_igm.bil (WGS-84	
779484 7442077	Z49SOUTH) - 5714 lines	
779610 7440318	790064 7443026	
779752 7438531	789897 7445141	
779850 7436742	789724 7447162	
780021 7434952	789605 7449095	
780136 7433129	789429 7451142	
780269 7431303	789277 7453169	
780411 7429478	789137 7455176	
780537 7427649	788988 7457164	
780683 7425823	788855 7459147	
780811 7423971	788688 7461123	
780937 7422133	788546 7463100	
781075 7420266	788403 7465123	
781195 7418377	788322 7466022	
781340 7416525		
781474 7414674	File blk_e_20_igm.bil (WGS-84	
781616 7412822	Z49SOUTH) - 5958 lines	
781752 7410946	787176 7465095	
781876 7409096	787301 7463112	
782008 7407250	787447 7461078	
782165 7405377	787574 7459115	
782291 7403522	787729 7457120	
782417 7401698	787896 7455160	
782567 7399832	788017 7453221	
782692 7397947	788158 7451219	
782821 7396099	788298 7449223	
782899 7395185	788429 7447232	
	788577 7445303	
	788713 7443378	
	788855 7441623	
Block E: Ningaloo_20060501		
File blk_e_23_igm.bil (WGS-84	File blk_e_19_igm.bil (WGS-84	
Z49SOUTH) - 5314 lines	Z49SOUTH) - 6427 lines	
792436 7445766	787519 7440773	
792257 7447834	787422 7442517	
792124 7449807	787295 7444363	
791980 7451625	787165 7446253	
791855 7453411	787023 7448178	
791699 7455208	786865 7450126	
791592 7456988	786744 7451982	
791442 7458898	786617 7453924	
791338 7460743	786471 7455862	
791206 7462567	786335 7457776	
791053 7464435	786182 7459755	
790948 7465618	786075 7461697	
	785935 7463600	

785811	7465256	783777	7465224
		782983	7467128
File blk_e_18_igm.bil (WGS-84		782165	7469042
Z49SOUTH) - 5849 lines		781347	7470943
784525	7464990	780519	7472862
784653	7463078	779728	7474767
784808	7461162	778874	7476660
784935	7459292	778092	7478537
785091	7457424	777280	7480450
785204	7455558	776463	7482319
785343	7453641	775643	7484183
785474	7451832	774891	7486047
785614	7450019	774097	7487914
785725	7448200	773271	7489791
785869	7446337	772505	7491615
786007	7444447	771730	7493427
786133	7442658	770960	7495221
786262	7440844	770200	7496975
786337	7439609	769460	7498759
		768675	7500540
File blk_e_17_igm.bil (WGS-84		767909	7502281
Z49SOUTH) - 15184 lines		767900	7502303
787229	7409188		
787061	7411109	File blk_f_28_igm.bil (WGS-84	
786931	7413051	Z49SOUTH) - 12303 lines	
786758	7415176	766848	7501361
786635	7416986	767540	7499723
786500	7418850	768244	7498100
786375	7420645	768941	7496447
786231	7422440	769670	7494785
786119	7424219	770353	7493164
785979	7425959	771069	7491464
785870	7427776	771783	7489813
785719	7429691	772499	7488143
785567	7431478	773207	7486496
785461	7433307	773904	7484874
785325	7435234	774591	7483214
785203	7437081	775286	7481597
785064	7438937	776004	7479946
784884	7440795	776714	7478296
784780	7442665	777403	7476671
784664	7444475	778114	7475058
784526	7446288	778802	7473415
784394	7448141	779485	7471809
784248	7449990	780162	7470206
784115	7451829	780863	7468611
783993	7453651	781539	7466995
783857	7455395	782225	7465380
783724	7457215	782929	7463769
783599	7459041	783599	7462186
783469	7460886	783992	7461196
783347	7462703		
783197	7464542	File blk_f_27_igm.bil (WGS-84	
783137	7465203	Z49SOUTH) - 10694 lines	
		782401	7461355
		781696	7463115
		780923	7464928
Block F: 1 - Ningaloo_20060424		780159	7466684
File blk_f_29_igm.bil (WGS-84		779422	7468445
Z49SOUTH) - 11007 lines		778680	7470252
785356	7461541	777898	7472029
784601	7463343		

777102	7473886	768488	7487143
776288	7475699	767718	7488955
775517	7477545	766947	7490720
774731	7479437	766165	7492535
773929	7481286	765406	7494352
773155	7483148	764638	7496154
772327	7484996	763865	7497943
771541	7486875	763722	7498249
770736	7488762		
769935	7490649		
769149	7492473	File blk_f_24_igm.bil (WGS-84	
768361	7494290	Z49SOUTH) - 9896 lines	
767573	7496149	763025	7496585
766790	7497959	763855	7494694
765983	7499869	764636	7492795
765685	7500598	765469	7490892
		766302	7488976
		767069	7487144
		767875	7485304
File blk_f_26_igm.bil (WGS-84		768634	7483517
Z49SOUTH) - 11846 lines		769386	7481740
764753	7499320	770134	7479959
765483	7497657	770945	7478167
766178	7496024	771687	7476421
766880	7494391	772413	7474649
767597	7492751	773185	7472922
768300	7491116	773916	7471182
768981	7489506	774671	7469393
769664	7487873	775416	7467669
770374	7486283	776189	7465921
771062	7484661	776923	7464167
771758	7483053	777680	7462440
772431	7481427	778280	7461005
773136	7479791		
773832	7478184		
774539	7476575		
775226	7474961		
775901	7473391	Block F: 2 Ningaloo_20060428	
776557	7471810	File blk_f_34_igm.bil (WGS-84	
777253	7470234	Z49SOUTH) - 12824 lines	
777920	7468635	775032	7502790
778624	7467055	775723	7501153
779269	7465477	776417	7499523
779939	7463962	777110	7497892
780594	7462418	777813	7496284
781073	7461346	778494	7494685
		779167	7493122
		779826	7491564
File blk_f_25_igm.bil (WGS-84		780495	7489978
Z49SOUTH) - 10084 lines		781183	7488404
779680	7461194	781883	7486769
778852	7463092	782560	7485176
778010	7465037	783244	7483568
777152	7466970	783936	7481957
776322	7468939	784614	7480366
775519	7470798	785286	7478779
774748	7472631	785961	7477203
773946	7474436	786657	7475582
773188	7476233	787339	7473988
772399	7478040	788013	7472421
771629	7479855	788700	7470816
770819	7481695	789376	7469252
770057	7483513	790029	7467687
769273	7485335	790740	7466092

791416	7464476	File blk_f_31_igm.bil (WGS-84
792064	7462916	Z49SOUTH) - - 12821 lines
792523	7461928	770751 7502524
		771477 7500856
File blk_f_33_igm.bil (WGS-84		772218 7499179
Z49SOUTH) - 11430 lines		772915 7497525
791209 7461660		773617 7495904
790323 7463639		774314 7494276
789536 7465422		774987 7492676
788797 7467208		775673 7491101
788018 7469009		776337 7489513
787258 7470772		777020 7487935
786508 7472554		777720 7486328
785752 7474325		778410 7484710
784974 7476137		779077 7483134
784207 7477951		779752 7481561
783444 7479682		780404 7480019
782697 7481466		781088 7478422
781934 7483229		781788 7476814
781144 7485089		782474 7475206
780350 7486962		783179 7473553
779563 7488775		783861 7471940
778803 7490552		784523 7470367
778034 7492309		785224 7468730
777281 7494070		785900 7467160
776546 7495829		786589 7465572
775789 7497573		787237 7464060
775057 7499309		787899 7462527
774300 7501063		788289 7461528
773654 7502589		
		File blk_f_30_igm.bil (WGS-84
File blk_f_32_igm.bil (WGS-84		Z49SOUTH) - 11594 lines
Z49SOUTH) - 12050 lines		786771 7461619
772194 7502503		786051 7463358
772939 7500803		785297 7465125
773681 7499085		784528 7466891
774395 7497386		783814 7468624
775131 7495693		783054 7470395
775876 7493950		782273 7472191
776611 7492207		781509 7473973
777371 7490467		780738 7475762
778100 7488776		779964 7477557
778816 7487088		779214 7479320
779535 7485389		778449 7481107
780274 7483706		777702 7482914
780997 7481992		776924 7484706
781730 7480283		776169 7486450
782450 7478578		775394 7488235
783207 7476866		774623 7490044
783941 7475138		773880 7491812
784671 7473400		773129 7493594
785400 7471715		772350 7495359
786103 7470057		771610 7497100
786838 7468368		770844 7498886
787557 7466706		770118 7500634
788253 7465028		769344 7502334
788970 7463348		769207 7502663
789727 7461637		
789788 7461479		

Block G:

File blk_g_40_igm.bil (WGS-84
Z49SOUTH) - 12144 lines

775938	7498110
776847	7499963
777754	7501775
778656	7503587
779557	7505398
780431	7507169
781316	7508978
782224	7510787
783146	7512602
784032	7514406
784921	7516166
785783	7517923
786654	7519639
787518	7521351
788374	7523143
789261	7524892
790148	7526685
791034	7528483
791918	7530283
792823	7532114
793724	7533890
794625	7535738
795540	7537527
796432	7539347
797303	7541156
797593	7541650

File blk_g_39_igm.bil (WGS-84
Z49SOUTH) - 14708 lines

795937	7541343
795192	7539797
794429	7538248
793630	7536683
792870	7535120
792110	7533617
791415	7532192
790689	7530757
789988	7529309
789281	7527848
788527	7526365
787798	7524896
787070	7523459
786349	7522026
785623	7520546
784902	7519087
784176	7517654
783460	7516187
782746	7514734
782030	7513327
781310	7511889
780596	7510443
779866	7508998
779144	7507535
778419	7506094
777689	7504609
776927	7503085
776178	7501604
775406	7500051

774695	7498550
774407	7497970

File blk_g_38_igm.bil (WGS-84
Z49SOUTH) - 12287 lines

773041	7498272
773943	7500078
774826	7501849
775726	7503589
776576	7505374
777448	7507140
778318	7508872
779179	7510593
780009	7512314
780866	7514009
781710	7515724
782606	7517468
783461	7519215
784358	7520976
785218	7522680
786058	7524399
786918	7526153
787796	7527902
788672	7529682
789549	7531472
790476	7533311
791398	7535182
792310	7537017
793244	7538858
794156	7540695
794661	7541772

File blk_g_37_igm.bil (WGS-84
Z49SOUTH) - 13856 lines

793153	7541622
792366	7540052
791614	7538540
790832	7536959
790054	7535417
789297	7533900
788525	7532326
787764	7530793
786991	7529257
786232	7527743
785482	7526191
784703	7524657
783946	7523107
783174	7521576
782403	7520022
781644	7518465
780857	7516903
780069	7515352
779304	7513745
778503	7512183
777714	7510618
776924	7509019
776157	7507471
775356	7505872
774546	7504239
773753	7502610
772922	7500957

772131	7499377	769214	7499466
771520	7498201	768605	7498290

File blk_g_36_igm.bil (WGS-84
Z49SOUTH) - 12290 lines

770215	7498482
771069	7500223
771941	7501980
772818	7503759
773705	7505541
774602	7507341
775509	7509138
776409	7510897
777282	7512685
778176	7514502
779074	7516348
779988	7518127
780873	7519926
781755	7521694
782643	7523475
783544	7525218
784392	7526992
785246	7528727
786131	7530467
786983	7532202
787871	7533942
788718	7535701
789590	7537393
790446	7539132
791280	7540859
791780	7541872

File blk_g_35_igm.bil (WGS-84
Z49SOUTH) - 13872 lines

790253	7541798
789475	7540222
788676	7538651
787920	7537069
787150	7535560
786412	7534036
785619	7532529
784906	7531013
784133	7529518
783393	7527992
782625	7526485
781858	7524949
781115	7523446
780345	7521891
779567	7520323
778784	7518734
778001	7517171
777229	7515594
776439	7514061
775654	7512479
774889	7510886
774090	7509280
773255	7507647
772447	7505993
771626	7504333
770802	7502708
769976	7501084

Block H: Ningaloo_20060424

File blk_h_46_igm.bil (WGS-84
Z50SOUTH) - 7311 lines

192731	7587542
192252	7585677
191746	7583827
191262	7581951
190730	7580044
190235	7578163
189708	7576236
189211	7574331
188710	7572423
188187	7570497
187693	7568581
187179	7566676
186695	7564755
186158	7562844
185662	7560919
185341	7559733

File blk_h_45_igm.bil (WGS-84
Z49SOUTH) - 12052 lines

796658	7538538
797238	7540497
797849	7542450
798447	7544434
799076	7546405
799691	7548361
800301	7550324
800891	7552332
801483	7554302
802125	7556317
802748	7558344
803366	7560365
803997	7562341
804616	7564355
805217	7566360
805847	7568348
806452	7570365
807070	7572366
807694	7574358
808302	7576359
808925	7578345
809510	7580320
810115	7582323
810731	7584300
811368	7586277
811451	7586471

File blk_h_44_igm.bil (WGS-84
Z49SOUTH) - 124112 lines

809478	7584888
808990	7583072
808396	7581223
807829	7579398
807276	7577512
806705	7575655

File blk_i_51_igm.bil (WGS-84	198879	7588129
Z49SOUTH) - 7341 lines	200587	7589020
809018 7578211	202218	7589910
810722 7579067	203876	7590831
812436 7579915	205537	7591736
814158 7580772	207236	7592625
815923 7581621	208939	7593520
817657 7582488	210601	7594453
819444 7583370	211961	7595145
821223 7584215		
822962 7585067	File blk_i_47_igm.bil (WGS-84	
824685 7585945	Z50SOUTH) - 5995 lines	
826436 7586812	211278	7596348
828148 7587646	209510	7595427
829911 7588514	207826	7594487
831632 7589359	206117	7593549
833398 7590207	204424	7592656
834591 7590791	202752	7591759
	201093	7590836
File blk_i_50_igm.bil (WGS-84	199449	7589946
Z49SOUTH) - 7145 lines	197823	7589050
809849 7580195	196176	7588203
811493 7580989	194553	7587315
813143 7581774	192912	7586414
814805 7582593	191278	7585522
816475 7583409		
818161 7584236		
819847 7585085		
821551 7585899	Block J: Ningaloo_20060423	
823283 7586746	File blk_j_58_igm.bil (WGS-84	
824963 7587584	Z50SOUTH) - 17321 lines	
826688 7588424	212150	7590698
828400 7589279	213870	7591635
830115 7590129	215591	7592575
831759 7590923	217315	7593495
833428 7591730	219040	7594458
833906 7591938	220716	7595358
	222422	7596273
File blk_i_49_igm.bil (WGS-84	224136	7597174
Z50SOUTH) - 6444 lines	225792	7598095
212633 7594062	227463	7598990
210861 7593114	229165	7599918
209098 7592159	230876	7600836
207315 7591207	232573	7601748
205551 7590253	234275	7602648
203795 7589283	235963	7603594
202036 7588331	237058	7604177
200284 7587409		
198539 7586476	File blk_j_57_igm.bil (WGS-84	
196801 7585494	Z50SOUTH) - 6954 lines	
195078 7584592	236300	7605261
193353 7583650	234472	7604305
191642 7582712	232651	7603313
190106 7581900	230822	7602318
File blk_i_48_igm.bil (WGS-84	228975	7601330
Z50SOUTH) - 6402 lines	227234	7600391
190798 7583758	225460	7599426
192374 7584621	223673	7598466
193995 7585504	221886	7597489
195608 7586356	220090	7596529
197258 7587233	218317	7595566
	216571	7594622

214786	7593680	File blk_j_53_igm.bil (WGS-84
212994	7592703	Z50SOUTH) - 5364 lines
211383	7591787	233575 7609803
		231740 7608804
File blk_j_56_igm.bil (WGS-84		229923 7607819
Z50SOUTH) - 7600 lines		228130 7606864
210785 7593095		226321 7605886
212422 7593909		224479 7604880
214038 7594798		222653 7603873
215665 7595687		220792 7602884
217300 7596556		218967 7601881
218913 7597429		217116 7600905
220553 7598318		215307 7599928
222207 7599197		213951 7599189
223854 7600098		
225515 7600979		
227153 7601856		
228805 7602773		
230430 7603633		
232068 7604540		
233744 7605412		
235374 7606329		
235706 7606518		
		Block K: Ningaloo_20060422
File blk_j_55_igm.bil (WGS-84		File blk_k_67_igm.bil (WGS-84
Z50SOUTH) - 6992 lines		Z50SOUTH) - 3545 lines
234985 7607587		211976 7576844
233242 7606681		211906 7578851
231437 7605700		211868 7580851
229672 7604717		211842 7582899
227878 7603780		211797 7584938
226093 7602785		211738 7587012
224317 7601833		211693 7589056
222540 7600867		211643 7591157
220753 7599916		211647 7591750
218975 7598974		
217213 7598015		File blk_k_66_igm.bil (WGS-84
215413 7597048		Z50SOUTH) - 3544 lines
213592 7596050		210344 7590663
211798 7595072		210365 7588713
210025 7594142		210413 7586729
		210467 7584748
		210516 7582704
		210547 7580740
		210579 7578737
		210626 7576737
		210640 7576569
		File blk_k_65_igm.bil (WGS-84
		Z50SOUTH) - 3497 lines
File blk_j_54_igm.bil (WGS-84		209276 7576500
Z50SOUTH) - 7477 lines		209246 7578492
209442 7595346		209214 7580403
211102 7596255		209163 7582383
212766 7597164		209121 7584384
214422 7598058		209062 7586373
216076 7598941		209031 7588366
217726 7599822		209005 7590399
219406 7600740		
221082 7601635		
222743 7602548		
224425 7603455		
226062 7604321		
227718 7605253		
229379 7606109		
231005 7606995		
232672 7607893		
234233 7608776		
		File blk_k_64_igm.bil (WGS-84
		Z50SOUTH) - 3282 lines
		207752 7589283
		207781 7587305
		207836 7585329
		207884 7583365
		207932 7581364
		207954 7579394
		207987 7577432
		207993 7576299

File blk_k_63_igm.bil (WGS-84	203884	7580307
Z50SOUTH) - 6551 lines	203842	7582225
206951 7562889	203780	7584213
206911 7564796	203757	7586143
206872 7566767	203730	7587510
206811 7568715	File blk_k_60_igm.bil (WGS-84	
206773 7570677	Z50SOUTH) - 6998 lines	
206729 7572617	202366	7586815
206693 7574572	202442	7584855
206660 7576515	202506	7582923
206622 7578453	202548	7580981
206576 7580416	202568	7579021
206542 7582342	202623	7577079
206491 7584349	202639	7575136
206489 7586318	202700	7573189
206429 7588294	202728	7571246
206428 7588497	202766	7569317
File blk_k_62_igm.bil (WGS-84	202801	7567381
Z50SOUTH) - 6463 lines	202838	7565488
205064 7587972	202879	7563584
205102 7586033	202920	7561682
205156 7584094	203215	7559814
205196 7582151	File blk_k_59_igm.bil (WGS-84	
205249 7580215	Z50SOUTH) - 6070 lines	
205277 7578247	201570	7562629
205303 7576274	201533	7564565
205333 7574337	201468	7566507
205359 7572387	201429	7568469
205424 7570423	201418	7570404
205480 7568486	201389	7572316
205501 7566531	201355	7574294
205534 7564582	201282	7576248
205578 7562788	201270	7578168
File blk_k_61_igm.bil (WGS-84	201219	7580152
Z50SOUTH) - 6354 lines	201159	7582064
204220 7562781	201112	7583956
204171 7564695	201080	7585858
204134 7566619	201065	7586136
204097 7568577		
204064 7570517		
204035 7572469		
203960 7574424		
203933 7576358		
203916 7578331		

Survey Summary:

Block	Date of Acq.	Lines / Block	total	Survey Line Nr.	Nr. of lines	Approx. Area in sqkm 0.006272	Area block in sqkm	Area from shape file in sqkm
A	1-May	4	4	1	10482	65.743104	261.8058	230
				2	10529	66.037888		
				3	10283	64.494976		
				4	10448	65.529856		
B	28-Apr	4	8	5	7072	44.355584	212.4326	220
				6	7834	49.134848		
				7	6996	43.878912		
C	28-Apr	4	12	8	11968	75.063296	159.7854	140
				9	5632	35.323904		
				10	6290	39.45088		
				11	5724	35.900928		
D	28-Apr	4	16	12	7830	49.10976	391.3728	350
				13	14249	89.369728		
				14	14247	89.357184		
E	28-Apr	7	23	15	15291	95.905152	310.0375	260
				16	18613	116.740736		
				17	15184	95.234048		
				18	5849	36.684928		
				19	6427	40.310144		
				20	5958	37.368576		
				21	5714	35.838208		
F	24-Apr	11	34	22	4986	31.272192	796.8136	650
				23	5314	33.329408		
				24	9896	62.067712		
				25	10084	63.246848		
				26	11846	74.298112		
				27	10694	70.171136		
				28	12303	77.164416		
				29	11007	69.035904		
				30	11594	72.717568		
				31	12821	80.413312		
				32	12050	75.5776		
G	28-Apr	6	40	33	11430	71.68896	496.4727	420
				34	12824	80.432128		
				35	13872	87.005184		
				36	12290	77.08288		
				37	13856	86.904832		
				38	12287	77.064064		
H	22-Apr	6	46	39	14708	92.248576	421.039	410
				40	12144	76.167168		
				41	11356	71.224832		
				42	12272	76.969984		
				43	11728	73.558016		
				44	12411	77.841792		
I	22-Apr	6	48	45	12052	75.590144	40.153344	
				46	7311	45.854592		
				47	5995	37.60064		
				48	6402	40.153344		

				49	6444	40.416768		
				50	7145	44.81344		
				51	7341	46.042752		
			52	52	3658	22.942976	231.9692	210
J	23-Apr	6		53	5364	33.643008		
				54	7477	46.895744		
				55	6992	43.853824		
				56	7600	47.6672		
				57	6954	43.615488		
			58	58	7321	45.917312	261.5925	240
K	22-Apr	9		59	6070	38.07104		
				60	6998	43.891456		
				61	6354	39.852288		
				62	6463	40.535936		
				63	6551	41.087872		
				64	3282	20.584704		
				65	3497	21.933184		
				66	3544	22.227968		
			67	67	3645	22.86144	291.0458	270
Total				67	611347	3834.368384	3834.368	3400
	Estim.	overlap	-10%			383.4368384		
Final							3450.931	3400

7. DATA DELIVERY INFORMATION

All HyMap data will be delivered on Maxtor external hard discs with USB2 and fire wire connectivity. Each block will have its own subdirectory holding the respective flight lines, also with a subdirectory each.

Site Name *line Name*

... ..

Block H:

...

Block I:

Blk_I_48

**geocorrection
radiance
reflectance**

Blk_I_49

... ..

Blk_I_50

... ..

Block J:

... ..

Directory List

For each line exists a base directory relating to the relevant flight line. Each base directory contains sub-directories for *radiance*, *geocorrection* and *reflectance* products. Some of the higher level products will be delivered at a later stage - they should be copied into a common structure on the receiving 'hard disc' for easier processing.

An example for the files on the hard disc is listed below – all full print out is beyond the scope of this document.

Generated on 2006-06-15 14:51:20 by Directory Lister v0.8.1

```
-----
h:\ (0)                                0 ---c
-----
<Block_A>                               <DIR> 2006-06-15 09:00 ----
<Block_B>                               <DIR> 2006-06-13 10:44 ----
<Block_C>                               <DIR> 2006-06-15 14:12 ----
<Block_D>                               <DIR> 2006-06-15 13:55 ----
<Block_E>                               <DIR> 2006-06-15 14:23 ----
<Block_F-1>                             <DIR> 2006-06-15 08:50 ----
<Block_F-2>                             <DIR> 2006-06-15 14:01 ----
<Block_G>                               <DIR> 2006-06-15 09:03 ----
<Block_I>                               <DIR> 2006-06-15 14:47 ----
<Block_H>                               <DIR> 2006-06-15 14:47 ----
<Block_J>                               <DIR> 2006-06-15 09:06 ----
<Block_K>                               <DIR> 2006-06-15 09:00 ----
<RECYCLER>                             <DIR> 2006-06-15 08:36 --hs-
<System Volume Information>             <DIR> 2006-06-13 10:36 --hs-
-----
h:\Block_A\ (1)                        12 274 808 095 2006-06-15 09:00 ----
-----
<blk_A_01>                              <DIR> 2006-06-15 14:05 ----
<blk_A_02>                              <DIR> 2006-06-15 14:05 ----
<blk_A_03>                              <DIR> 2006-06-15 14:05 ----
<blk_A_04>                              <DIR> 2006-06-15 14:05 ----
<geospec_reports>                      <DIR> 2006-06-13 10:47 ----
<gs_mosaic>                            <DIR> 2006-06-13 10:46 ----
flight_path.dat                          1 794 2006-05-29 16:41 -a---
-----
h:\Block_A\blk_A_01\ (0)                3 053 904 830 2006-06-15 14:05 ----
-----
<gs_geocorrection>                     <DIR> 2006-06-13 10:59 ----
<radiance>                             <DIR> 2006-06-13 10:59 ----
<reflectance>                           <DIR> 2006-06-13 10:57 ----
-----
h:\Block_A\blk_A_01\gs_geocorrection\ (11) 315 387 687 2006-06-13 10:59 ----
-----
blk_a_01_igm.bil                         64 401 408 2006-06-08 10:42 -a---
blk_a_01_glt.bsq                         166 529 016 2006-06-08 10:42 -a---
blk_a_01_geo.ers                          771 2006-06-08 10:43 -a---
blk_a_01_geo.hdr                          252 2006-06-08 10:43 -a---
blk_a_01_glt.hdr                          255 2006-06-08 10:42 -a---
blk_a_01_igm.hdr                           303 2006-06-08 10:42 -a---
blk_a_01_geo.img                           83 264 508 2006-06-08 10:43 -a---
```

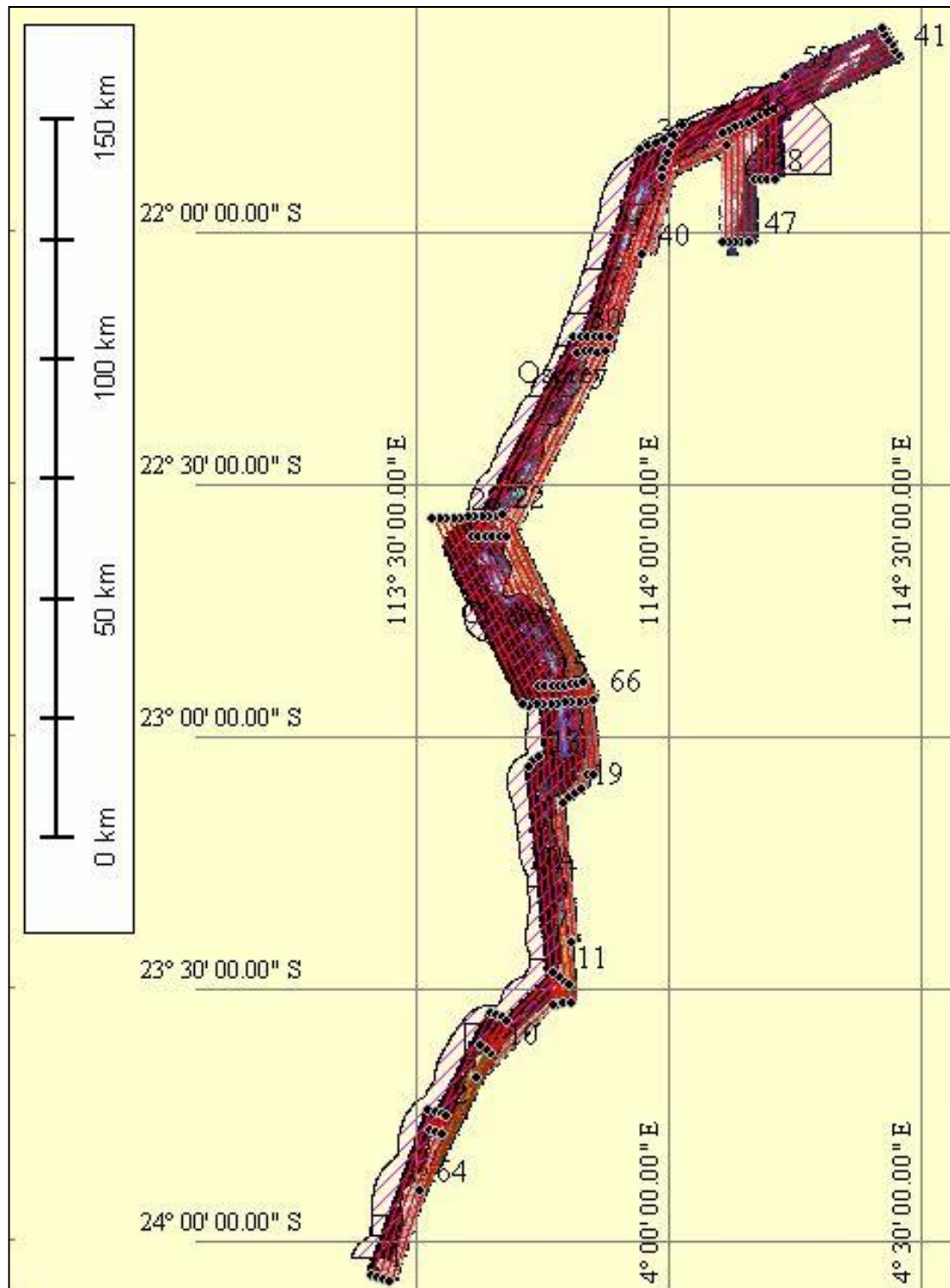
```

blk_a_01.ini                391 2006-06-08 10:39 -a---
blk_a_01_geo.lim           100 851 2006-06-08 10:43 -a---
blk_a_01_ephemeris.txt     1 086 128 2006-06-08 10:39 -a---
blk_a_01_report.txt        3 804 2006-06-08 10:43 -a---
-----
h:\Block_A\blk_A_01\radiance\ (11)      1 384 992 192 2006-06-13 10:59 -----
-----
blk_A_01_rad.bil           1 341 696 000 2006-05-04 11:08 -a---
blk_A_01_mask.bsq         5 366 784 2006-05-04 11:08 -a---
.....
.....
-----
h:\Block_B\ (1)                10 082 583 405 2006-06-13 10:44 -----
-----
<blk_B_05>                   <DIR> 2006-06-15 09:00 -----
<blk_B_06>                   <DIR> 2006-06-15 09:00 -----
<blk_B_07>                   <DIR> 2006-06-15 09:00 -----
<blk_B_08>                   <DIR> 2006-06-15 09:00 -----
<geospec_reports>          <DIR> 2006-06-13 10:36 -----
<gs_mosaic>                <DIR> 2006-06-13 10:36 -----
flight_path.dat            1 506 2006-05-29 16:42 -a---
-----
h:\Block_B\blk_B_05\ (0)       2 068 536 546 2006-06-15 09:00 -----
-----
<gs_geocorrection>         <DIR> 2006-06-13 10:46 -----
<radiance>                 <DIR> 2006-06-13 10:46 -----
<reflectance>              <DIR> 2006-06-13 10:45 -----
-----
h:\Block_B\blk_B_05\gs_geocorrection\ (12)  220 496 062 2006-06-13 10:46 -----
-----
blk_b_05_igm.bil           43 450 368 2006-06-08 12:07 -a---
blk_b_05_glt.bsq          117 485 056 2006-06-08 12:08 -a---
blk_b_05_geo.cfg           493 2006-06-08 12:18 -a---
blk_b_05_geo.ers           772 2006-06-08 12:08 -a---
blk_b_05_geo.hdr           253 2006-06-08 12:08 -a---
blk_b_05_glt.hdr           256 2006-06-08 12:08 -a---
blk_b_05_igm.hdr           302 2006-06-08 12:07 -a---
blk_b_05_geo.img           58 742 528 2006-06-08 12:08 -a---
blk_b_05.ini               392 2006-06-08 12:05 -a---
blk_b_05_geo.lim           71 628 2006-06-08 12:08 -a---
blk_b_05_ephemeris.txt     740 128 2006-06-08 12:05 -a---

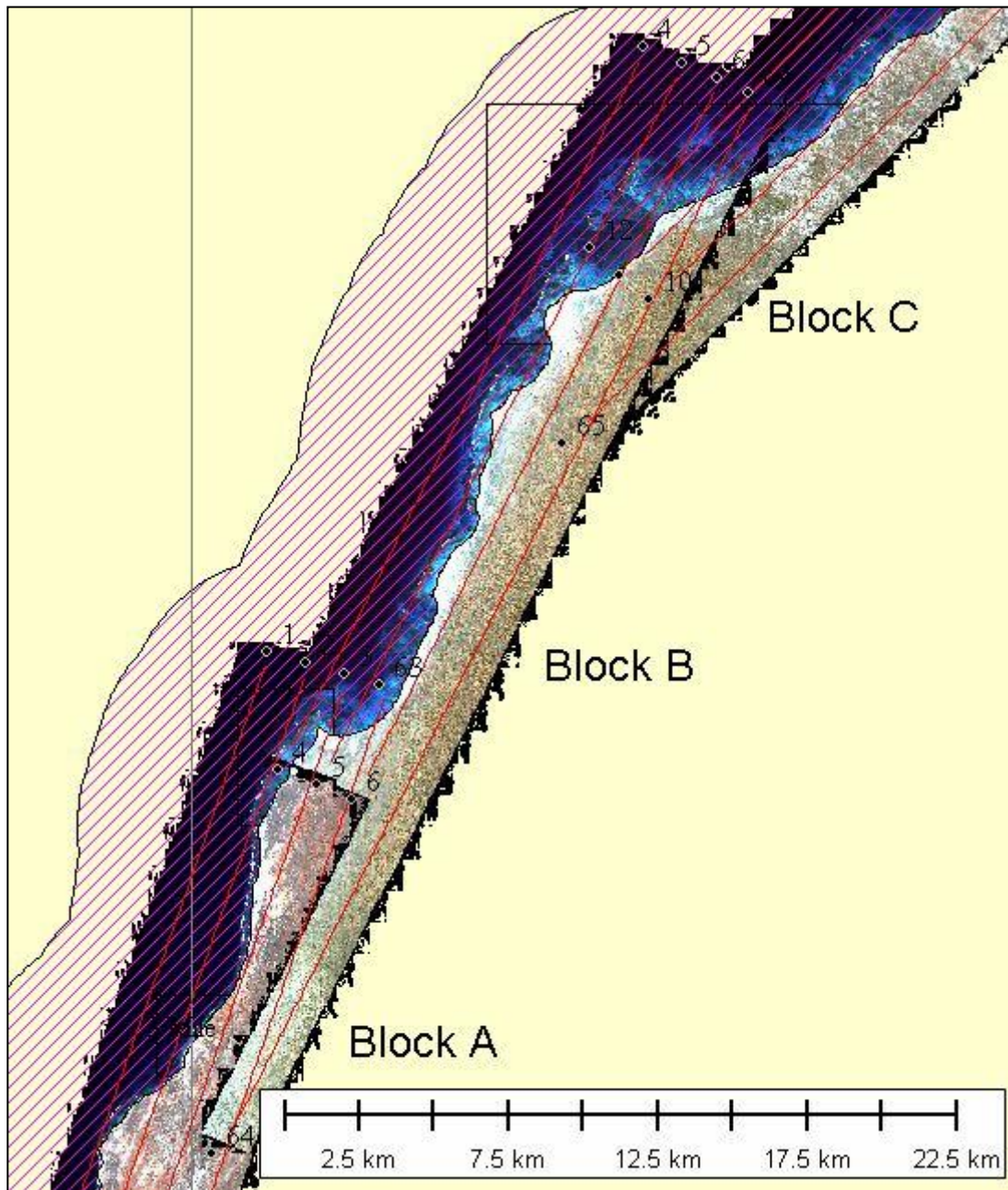
```

8. ANNEXES

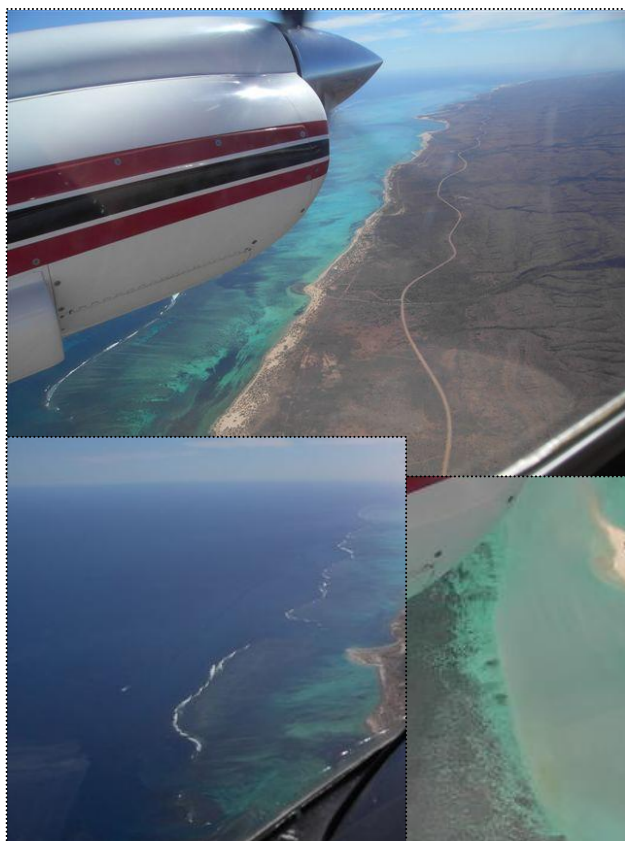
HyMap Image Mosaic of quick look data – area coverage overlaid with planned flight lines and outline of the marine park.



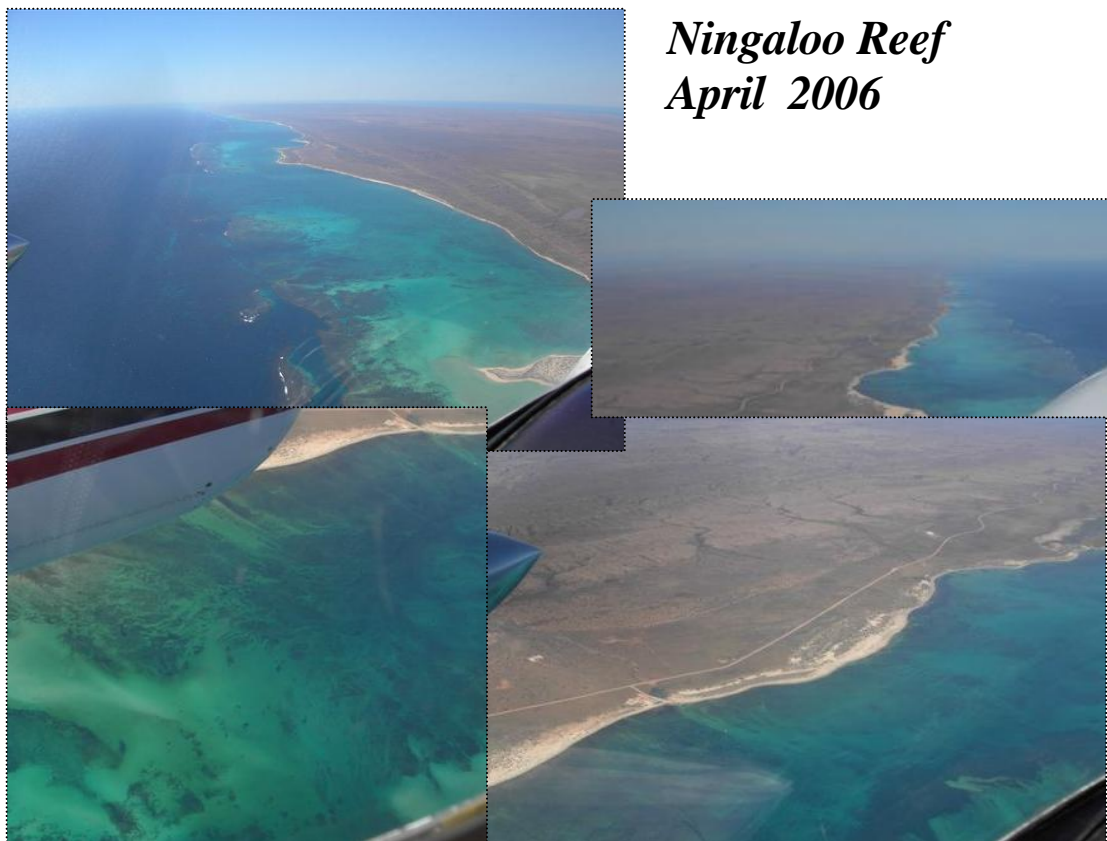
Close up of area coverage:



*Pilot's view - Selected images from the cockpit taken during the survey:
(Courtesy Stuart Criddle – Australian Aerial Surveys – copyright 2006)*



*Ningaloo Reef
April 2006*



*Ningaloo Reef
April 2006*

Annex 1 Description of file extensions for HyVista L2/L3 processing

- _geo** : data is geo-corrected using a HyMap glt (geometric lookup table) file. (See ENVI manual for detailed description)
- _rad** : radiance data – calibrated both spectrally and radiometrically using permission calibration files.
- _ref** : reflectance data – atmospherically corrected : standard processing uses HyCorr
- _h2o** : water vapour file derived from atmospheric correction (e.g. HyCorr)
(details for the parameters used can be found in *_hycorr_settings.txt)
- _effort** : effort processing applied (See ENVI manual for detailed description) *[usually to reflectance data – will smooth out residual atmospheric influences common to all the data in an image cube.]*
- _sub** : processing result is from a spatial subset *[info can usually be found in header]*
- _ss** : processing result is from a spectral subset
_ss2345: using specific spectral channel subset *[can be also found in header]*
- _mnf** : MNF transformation results (See ENVI manual for detailed description)
_mnf 98123 : using specific spectral channel subset to create the MNF transformation
- _pc** : PC transformation results (See ENVI manual for detailed description)
- _unmix****: un-mixing results using ** spectral edge members *[for example or mineral maps]*
_unmix.sli**: spectral library related to un-mixing results
- _xtr** : x-track (BRDF) corrected results - *[removing illumination variations common to one survey line]*
- _b***** : band number *** of HyMap channel
- _dc*******: de-correlation stretch of HyMap channel numbers following the dc
- _LS_**_**_****: Landsat equivalent HyMap bands or ratios, single digits = bands , double digits = ratio's
- _albedo_*** : results displayed on an albedo backdrop image
- _unmasked** : results not masked
- _masked** : results masked

Spectral feature maps:

- _al-oh** : AL-OH (Clay) relevant spectral index using the 2.2 μm absorption feature *[info can be also found in header]*
- _fe-ox** : Fe-Ox (Iron Oxide) relevant spectral index using the 0.9 μm absorption feature *[info can be also found in header]*
- _carb-chlo**: Carbonate / Chlorite relevant spectral index using the 2.3 μm absorption feature *[info can be also found in header]*
- _cellu** : Cellulose spectral index (dry vegetation) using the 2.05 μm absorption feature *[info can be also found in header]*
- _ndvi** : NDVI spectral index (healthy vegetation) using the .9 / 0.65 μm developed index from Landsat- however single spectral channels *[info can be also found in header]*
- _wat** : Water spectral index using the strong SWIR absorption feature and wavelengths at 0.5 and 1.6 μm *[info can be also found in header]*
- _hem-goe**: Spectral index separating Hematite and Goethite rich areas – needs Fe-Ox index as subset *[info can be also found in header]*
- _hydriron**: Spectral index separating utilizing the water big absorption to map hydrated iron – needs fe-ox index as subset *[info can be also found in header]*

Note: a lot of these indexes need masks applied for further processing. For example before using the Carb/Chlo index it is wise to apply a green/dry vegetation mask to avoid false positives and unnecessary confusion.

APPENDIX B

Ningaloo Hyperspectral Processing EoMap report

REPORT

MIP data processing Ningaloo Reef: 2006 HYMAP survey

Prepared for:

Murdoch University



Murdoch University
South St,
WA Australia 6150

Phone: +61 8 93602411
Fax: +61 8 9310 4997
Email: H.Kobryn@murdoch.edu.au
Web: www.murdoch.edu.au

by

EOMAP GmbH & Co.KG



EOMAP GmbH & Co.KG
Special Airport Oberpfaffenhofen
Friedrichshafener Str. 1
82205 Gilching
GERMANY

Phone: +49-8105-370 778-0
Fax: +49-8105-370 778-9
Email: heege@eomap.de
Web: www.eomap.de

REPORT

MIP data processing Ningaloo Reef: **2006 HYMAP survey**

Content

1. Summary
2. Data base and site specific conditions
 - 2.1. HyMap data
 - 2.2. Environmental conditions
3. Data processing methodology
 - 3.1. Data processing strategy
 - 3.2. Basics of physics based product retrieval using MIP
4. Deliverables
 - 4.1. Data naming convention
 - 4.2. Additional deliverables
5. Results
 - 5.1. Sea floor products
 - 5.2. Bathymetry
 - 5.3. Conclusion
6. Appendix
 - 6.1. References

1. Summary

The HyMap hyperspectral remote sensing data was collected for the Ningaloo Collaboration Cluster, in April and May 2006 over Ningaloo Reef. The full size survey area of about 3500 sq.km was ordered for detailed shallow water processing. The main objective for the specialized water processing was to improve the shallow water mapping and habitat classification, by retrieving the spectral sea floor characteristics and sea floor type probabilities from the HyMap data. The environmental conditions for the survey were largely good, but of course with some varieties of water turbidity, of the recording geometry and related sunglitter conditions as expected for such a large survey. Atmospheric transparency was very high and the water turbidity was comparatively low, but flight line dependent increased sunglitter reflections were observed and corrected. All 67 lines were processed in an operational standardized approach, including correction for atmosphere, sunglitter and in water conditions, to retrieve the sea floor albedo and water depth up to just under 18 m depth. The sea floor albedo is used as base for an extended sea floor classification performed by the Murdoch University.

The comparison with independently retrieved water depth demonstrated a high correlation between both data sets and therefore the physical consistence of the applied approach for sea floor mapping. Data were processed with a standardized data processing approach using the Modular and Inversion System MIP, which was initially developed at the German Aerospace Centre and is now marketed through EoMap (Heege et al. 2000, 2003, Heege & Fisher 2004, Pinnel 2007). The product generation was performed independently from external ground truth data.

2. Data base and site specific conditions

2.1. HyMap data

The HyMap data were collected over six days in eleven connected, contiguous, sequentially flown segments, each containing 4-11 flight lines. The subsequent data processing, sunglitter and atmospheric corrections were performed on the individual lines and combined to data blocks (cubes) after calculation of the subsurface reflectance. The water column correction, water depth retrieval and classification were carried out on the individual data blocks. All the blocks were subsequently processed with the same input spectral signatures of the specific in-water and seafloor optical properties, in order to achieve homogenous seafloor classification results across data block boundaries.

2.2. Environmental conditions

The survey was taken at clear atmospheric conditions. The atmospheric properties derived by the remote sensing data are characterized by quite low aerosol optical depth between 0.02 and 0.05 (AOD at 550nm). The highest values of optical depth were retrieved in block H (0.07 AOD).

All lines were somewhat affected by sunglitter. The sunglitter impact varies heavily inner and between different flight lines and blocks due to very different conditions of sea state, sun altitude and observation geometry (Fig. 2.1). Therefore, the correction of sunglitter is most important in order to retrieve reasonable physical values of underwater properties. Almost all blocks are affected, with very high sunglitter radiances in several lines of blocks F, G, H, J and K. However, sunglitter effects could be corrected as part of the standard processing procedure without essential impact on the later retrieved products. Some residuals are visible in deeper water areas of block F and G, were also a significant impact of foam is observed. Few areas were also affected by organic material floating on the water surface, e.g. in block K. However, most areas affected and observed were outside of the relevant shallow water areas.

Water turbidity was quite low at values about 0.05 – 0.3 mg/l for total suspended matter, 0.1 – 0.5 µg/l (Chlorophyll *a*/Phytoplankton) and 0.02 1/m (Coloured dissolved organic material absorption at 440nm). These values were derived directly from the HyMap data and no comparison to real measurements could be carried out. Spatial patterns of in-water turbidity and chlorophyll are the second important factor affecting homogeneous results of sea floor reflectance and reducing the detectable contrast of the sea floor reflectance. In relation to the total area of shallow water habitats, only a small portion of few percent was affected. However, we expected a remarkable impact in some of the coral opening areas at the border line to the open sea, e.g. in block G1. Most effects were observed in the southern part of block K. Even if the error introduced by varying in-water turbidity decreases with decreasing depth, we observed several resuspension hot spots with a dominant impact also in very shallow water areas in the very southern end of block C, or northern part of F2.

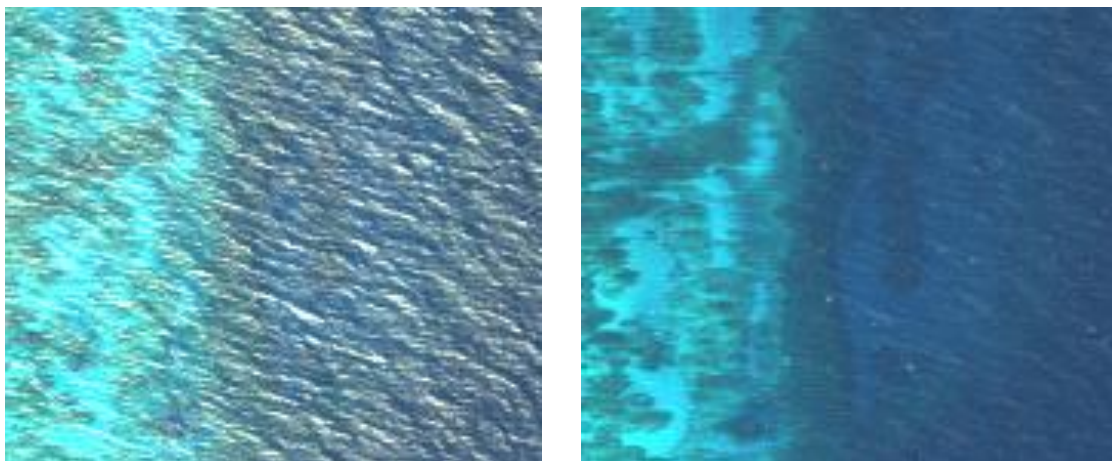


Fig. 2.1: Sensor radiance detail in line F27, channels 13, 9 and 5 (RGB):
Left image original values, right side after sunglitter correction.

3. Data processing methodology

3.1. Data processing strategy

Data processing for the generation of sea floor products from the calibrated sensor radiance images (see HyVista data report) was performed using the EOMAP software system Inversion and Processing System MIP (Heege et al. 2000, 2003, Heege & Fischer 2004, Pinnel 2007). HyMap-Channels 1 – 85 (wavelength from 450 nm to 1700 nm) were used for the product generation in MIP. Channels 1-21 were left unchanged, but several channels in the infrared region, between channels 23 and 85, were merged into specific, combined channels with wider band width in order to enhance the signal-to-noise ratio for these bands.

After image conversion and spectral transformation of the HyMap data the processing was performed in four main steps:

- a) All single flight lines were corrected for sunglitter, atmospheric, and bidirectional above- and underwater effects using the MIP system on a pixel-by-pixel basis.
- b) The resulting *subsurface irradiance reflectance* data files were geo-referenced and mosaiced into blocks, often called cubes, based on their temporal coherence - in this case, recorded sequentially on the same day.
- c) The image cubes of the subsurface irradiance reflectance were then processed to correct for all water column-related effects and to retrieve water depth, the sea floor spectral characteristics, and sea floor type probabilities.
- d) In a second processing run, all the spectral classes from the individual processing runs were combined. A unified set was used for a final classification of the whole area.

The geo-referencing and mosaicking of the individual flight lines was performed and conducted by HyVista Corp using a HyVista proprietary software package.

3.2. Basics of physics-based product retrieval using MIP

The generation of thematic products for aquatic systems from calibrated HyMap radiances was performed using the Modular Inversion and Processing System MIP. MIP is designed for the physics-based recovery of hydro-biological parameters from multi- and hyperspectral remote sensing data and can be used for environmental mapping of shallow and deep inland waters, coastal zones, and wetlands. The architecture of the program correlates a set of general and transferable computational schemes in a chain, connecting bio-physical parameters, such as chlorophyll content or dissolved organic matter in the water column, with the measured sensor radiances.

The physical background of the hyperspectral and fully transferable system incorporates the Finite Element Method for forward calculations of the radiative transfer in a multilayer atmosphere-ocean system (Kisselev & Bulgarelli 2004). It is used for the atmospheric-, sunglitter-, water surface-, and Q-factor-corrections of the underwater light field as explained in Heege & Fischer (2004). The different program modules support transferable algorithms. The adjustment of algorithms to sensor

specifications and recording conditions is supported automatically in MIP. The inversion itself is based on a spectral matching and regulated optimization technique.

The individual program modules inside MIP provide the retrieval of aerosols, pixel-by-pixel sunglitter correction, atmosphere and water surface corrections, and retrieval of water constituents in optically deep waters. In shallow waters, it allows the classification of substrates such as coral reef, seagrass vegetation, and bottom sediments, after an appropriate water column correction procedure (Pinnel 2007, Pinnel et al. 2004, Heege et al. 2004). The processing system has been tested and validated in many surveys and satellite data verifications over German and other European inland waters, as well as Indonesian and Australian coastal zones for both airborne and satellite sensor data. (e.g. Pinnel et al. 2004, Harvey et al. 2007).

Land/water and water/cloud discrimination is performed as part of the sunglitter correction data processing step, performed in the atmospheric correction module, according to typical features of water subsurface reflectance in various channels between 680 and 800 nm. The output files contain unchanged, at-sensor radiances from the respective input datasets over water and zero values over land.

3.2.1. Sunglitter correction

The HyMap sensor has a number of spectral channels in the SWIR (Short Wave Infra-Red) – a spectral region in which the solar irradiance is completely absorbed by the water – thus one can safely assume that no water-leaving radiance is present. The only signal contributions would come from atmospheric scattering or reflected radiation from floating surface materials. Utilising such knowledge, we can devise a sun glint correction algorithm using the signal from the SWIR channels and perform a sun glint removal. With a first approximation of the atmospheric conditions and the use of the radiative transfer data, the radiances at sensor altitude can be corrected for sunglitter individually for each pixel (Heege & Fischer 2000). This is done by calculating and subtracting sunglitter radiances. At first, values of modelled ‘flat-surface case’-radiances (from the database) are subtracted from the measured radiance in the shortwave infrared region. The second step is the calculation of sunglitter radiances in all the other bands in the visible region. Here, the relationship between atmospheric transmissions at different wavelengths is taken into consideration. This module is applied iteratively in combination with the aerosol retrieval.

3.2.2. Aerosol retrieval and atmospheric correction

The resulting radiance at sensor altitude can be converted into subsurface reflectance, if the aerosol concentrations are known. The aerosol calculation is performed using HyMap data from clear, deep water areas and is usually conducted only on the basis of one flight line and one retrieval area per image block. Aerosol concentrations are retrieved using an inversion procedure of atmospheric properties and water constituents according to Odermatt et al. (2008) and Heege & Fischer (2004).

The conversion from radiance to underwater reflectance is performed using a radiative transfer model (Kisselev & Bulgarelli 2004), applying a multi-dimensional interpolation from a customized database containing the relevant radiative transfer relations in atmosphere and water. An additional correction based on the radiative transfer model is applied, commonly called the Q-correction, which corrects for the bidirectional underwater light field contributions (Heege & Fischer 2004). The water constituent concentrations are calculated twice: the first approximation is done according to Heege & Fischer (2004) over deep-water areas and a second adjustment over medium deep benthic substrates is performed in the frame of the sea floor classification and bathymetry retrieval.

3.2.3. Sea floor coverage and bathymetry retrieval

The transformation of subsurface reflectance to the bottom albedo (overall reflectance) was carried out based on the equations published by Albert and Mobley (2003). The unknown input value of depth is calculated iteratively in combination with the spectral un-mixing of the respective bottom reflectance. The un-mixing procedure produces the sea floor coverage of three main bottom components and the residual error between the model bottom reflectance and the calculated reflectance. The final depth, bottom reflectance, and bottom coverage is achieved at the minimum value of the residual error.

The final step of the thematic processing classifies the bottom reflectance due to the spectral signature of different bottom types and biota using a 'Fuzzy Logic' method. Individual probability functions are assigned for each defined sea floor component. The bottom reflectance were approximated during this inversion process as a linear combination of three main component spectra. For the final sea floor classification, separate sea floor classes were identified based on their spectral signatures. The 'Fuzzy Logic' method combined the identification of different spectral features for each sea floor class and calculated probabilities for each of those features. All features related to one specific sea floor class resulted in one mean probability (by taking into account individually calculated weights for each single feature probability) (Heege et al. 2007).

The MIP processing was performed independently of any spectral data collected in the field, such as optical properties of the water constituents, or specific reflectance properties of the sea floor classes. All spectra for the sea floor classification were derived by extracting the spectral sea floor characteristics from different areas over the survey site. This was done by analyzing the statistical variation within each group and inspecting the spectral overlaps between the groups. According to the class specific spectral features, configuration settings for the 'Fuzzy Logic' discrimination of classes were established.

Uncertainties in the optical properties of the water column, which were retrieved solely from the HyMap data, may require a few comparative measurements of water depth at approx. 10-15m depth in order to recalibrate the data and avoid errors. Water depth values retrieved for Ningaloo were accordingly adjusted by factor 1.6.

4. Deliverables

4.1. Data naming convention

Product products were delivered via DVD and FTP-Server in binary BIL –ENVI-format as unsigned integers. All image products are delivered including MIP-Aux-meta-file and ENVI-header for further details. The sea floor reflectance and sea floor product images are also supplemented each by a .log- file containing the description and units for each channel.

All image product files are following a standardized naming convention:

- First three letters of data files denote the survey area Ningaloo: **nin**
- Letters 4-9 denote the record date: YYMMDD, e.g. **060422**
- Letters 10-11 denote the sensor Hymap: **hym**
- The subsequent 1-3 letters denote the image cube X (**A, ... K**)
X = Block name: **A,B,C,D,E,F11,F12,F21,F22,G1,G2,H,I,J,K**
- and/or the flight line number NN (**01 .. 67**)

Example: **nin060422hymK**

- Sequentially product type names are separated by a dot: .
- Radiance data of the first 27 channels including first 21 unchanged channels and 6 spectrally merged channels 22-27: **.rad27**
Scaling: 0.01 mW/sr/m²/nm per DN
- Sun glitter corrected radiance images: **.rad27.sgf**
Scaling: 0.01 mW/sr/m²/nm per DN
- Subsurface irradiance reflectance: **.rad27.sgf.refq.w**
Non-water pixels are masked with value 0
Scaling: 0.0001 per DN
- Sea floor albedo: **.rad27.sgf.refq.w.bref**
Scaling: 0.0001 per DN
- Sea floor products: **.rad27.sgf.refq.w.bot**
Including sea floor coverage maps, water depth and miscellaneous spatial information layers (see meta description file *bot.inf* in each image folder)
 - Channel 1-3: Bottom coverage in [%] of sediment, vegetation type 1 and 2
 - Channel 4-6: same as channel 1-3, but multiplied by factor 1.5 (chan. 4) and 2 (channels 5,6)
 - Channel 7: Scaling factor of the total coverage, multiplied by 100
 - Channel 8: Bottom depth at acquisition time, scaling 0.1m = 1 DN
 - Channel 9: Standard adjusted bottom depth, scaling 0.1m = 1 DN
 - Channel 10: Key of most probable image class
 - Channel 11: Key of most probable sediment class
 - Channel 12: Key of most probable vegetation 1 class
 - Channel 13: Key of most probable vegetation 2 class
 - Channel 16: Error residuum
 - Channel 17: Channel quality
 - Channel 18: First channel with significant signal from the sea floor
 - Channel 19: Last channel with significant signal from the sea floor
 - Channel 20+N: Probability of sea floor class N in percent

Example: *nin060422hymK.rad27.sgf.refq.w*
Block K, subsurface irradiance reflectance

Delivered data are stored in packed *.zip-files

4.2. Additional deliverables

X = Block name: A,B,C,D,E,F11,F12,F21,F22,G1,G2,H,I,J,K

4.2.1. RGB Composites

BREF for Bottom Reflectance, RGB of channels 9,6,4, gain 400
X.bref_9R400_6G400_4B400.tif

REFQ for Subsurface Reflectance (Q-corrected), RGB of channels 15,9,3.
Gain settings are 6500, 1200 and 1500 for channels 15, 9 and 3.
X.refq_15R6500_9G1200_3B1500.tif

5. Results

The derivation of the bathymetry and seafloor characteristics from the HyMap data depends on the exact MIP processing system configuration. The most important controlling factors for the optimization procedure and the product retrieval hereby are the in-water optical properties and the spectral characteristics of the three, basic sea floor components used for the spectral un-mixing approach. The SR processing was performed with uniform, basic sea floor components, uniform spectral classification features, and water constituent concentrations adapted specifically to each image cube. Hence each cube required a dedicated parameter adjustment and computer processing run.

Overall, the SR standard data processing with MIP was completed without any unexpected complications or unforeseen results.

5.1. Sea floor products

The detailed sea floor product generation is currently executed by the Murdoch University and ongoing supported by EOMAP. Due to the decreased visibility of the seafloor reflectance with depth especially in the red spectrum of the light, some of the spectral classes can only be defined for wavelengths shorter than 600nm depending on the depth range where the spectral class appeared. For the same reason, areas down to 13m depth contained very well distinguishable spectral sea floor characteristics. Below 13m, we expect an increasing overlap of some spectral sea floor classes due to the decreasing available spectral information.

5.2. Bathymetry

The water depth product shows reasonable depth distributions for the first 18 meters, allowing good sea floor classification in all cubes.

We conducted a short comparison to echo sounding retrieved water depth provided by the Murdoch University team, which was collected during field campaigns. Independently derived water depth data and MIP/HYMAP retrieved water depth maps were compared by linear regression. Tidal effects were just corrected in a pragmatic manner: we introduced a constant offset value by levelling the 2m water depth ground truth and remote sensing retrieved depth at acquisition time.

We selected approximate 13 300 values. As precondition for the automatic value selection, we allowed a specific maximum spatial heterogeneity in an environment of 4 pixels around the matching points. For the remote sensing retrieved water depth values, we used the mean value inside this filter box. With this, we avoided errors introduced by geolocation mismatches in spatially highly variable areas. Figure 5.2.1 shows the path of the echo sounding boat and both echo sounding and MIP retrieved water depth values side on side.

The comparison results in a correlation coefficient of 0.9 for the depth range from 2 to 20m and a standard error of 10 % (Fig. 5.2.2.). Beyond 18 m, the MIP-HYMAP values become very noisy. Even if no validation points were available beyond 20m, we have the impression that values beyond 22m are underestimated.

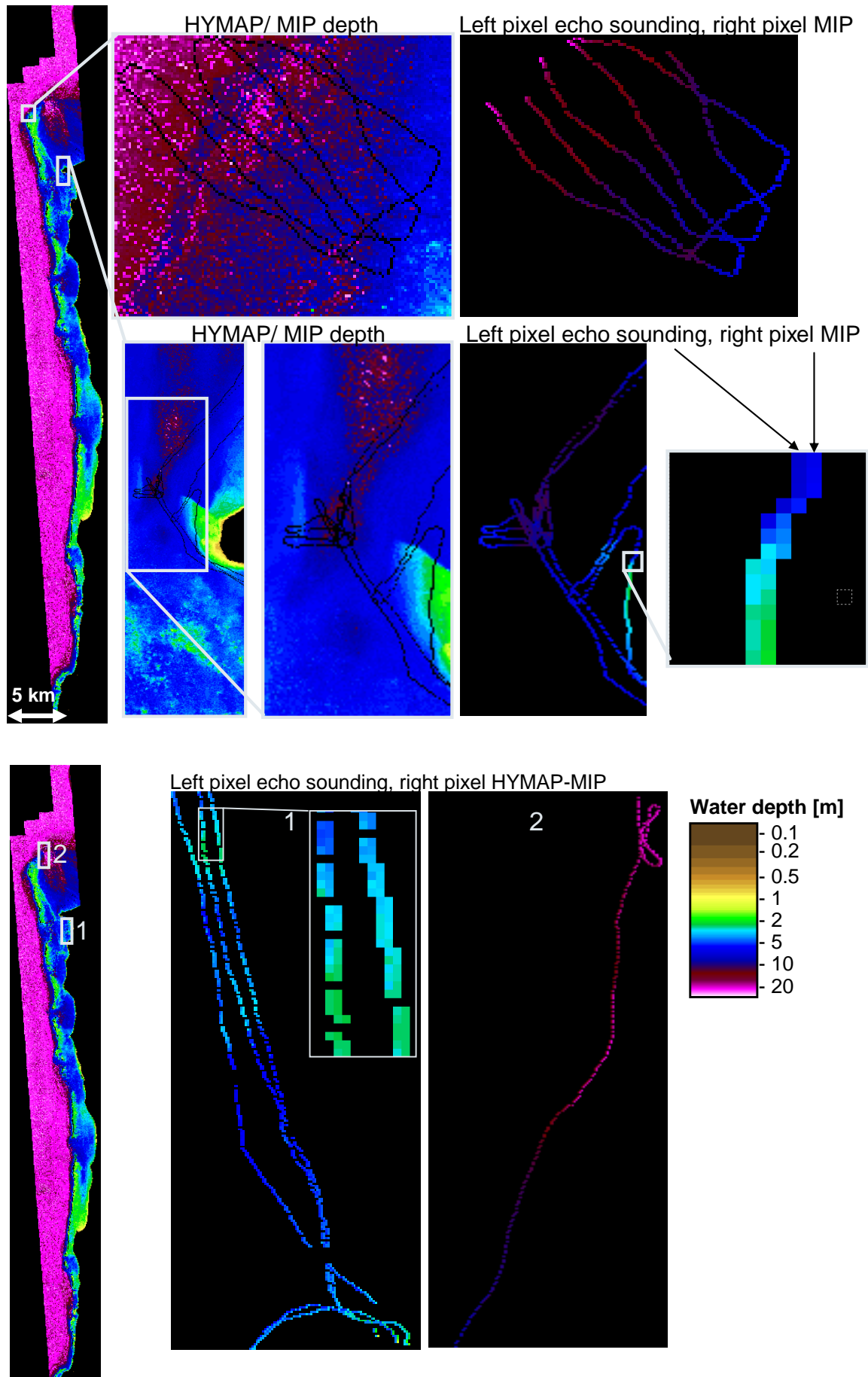


Fig. 5.2.1: Comparison details of ground truth and Hymap retrieved bathymetry

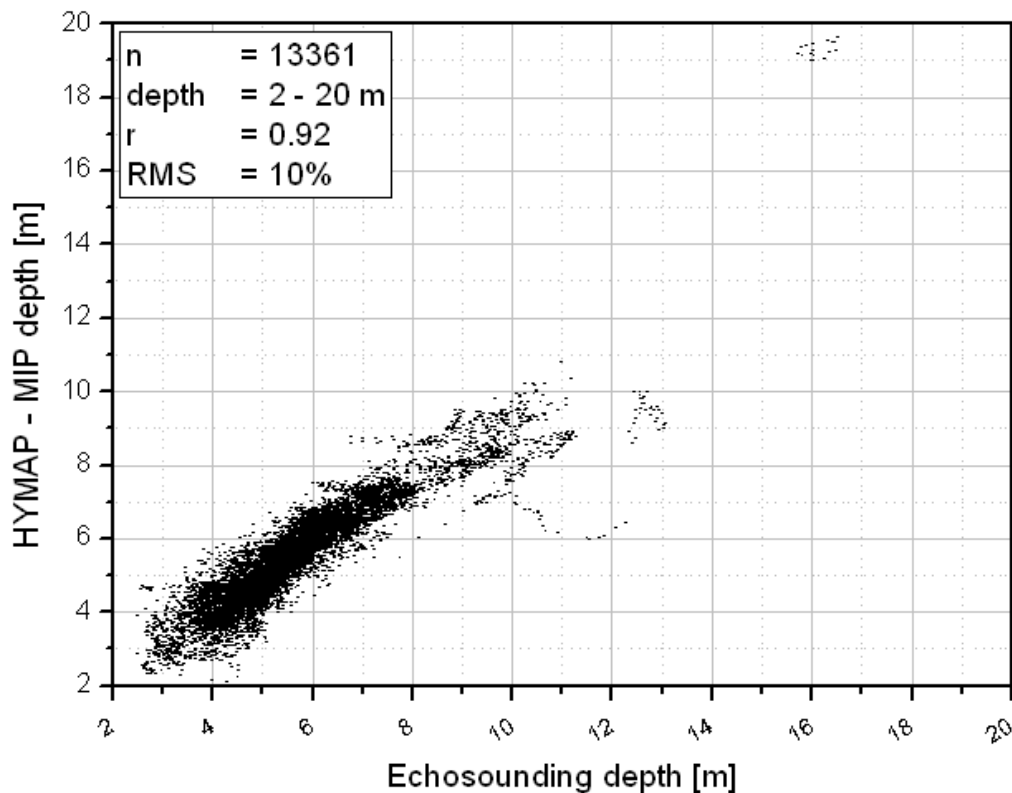


Fig. 5.2.2.: Correlation of echosounding MIP-Hymap retrieved bathymetry

5.3. Conclusion

The hyperspectral survey and shallow water product generation for the Ningaloo Reef area allowed high quality sea floor classification and bathymetry products to be generated. The subsequent translation and synthesis of these spectral classes into ecological relevant and meaningful habitats is performed by the Murdoch University team, in order to take the full advantage of these geospatial data sets and their spectral signatures. Moreover, this data set can be used as base line survey for future temporal repeated remote sensing and ground truth based mappings. This is possible, since we applied a fully physical based and sensor independent approach using the MIP processing system. The spectral definition of the classes found can be used also for the configuration with different data sets from other satellite and airborne sensors as demonstrated with the Quickbird retrieved sea floor products for Rottnest Island. Further investigations for the validation of all product types including independent spectral and echo sounding ground truth measurements would help to prove the new technology as valuable coastal monitoring tool. At any time can the data be re-processed and re-validated should additional information become available. Timeline data can be processed with the same parameters to allow detailed comparisons and change detection over time.

6. Appendix

6.1. References

- Albert, A., & Mobley, C. D. (2003): An analytical model for subsurface irradiance and remote sensing reflectance in deep and shallow case-2 waters. *Optics Express*, 11(22), 2873 -2890.
- Harvey, M., Kobryn, H., Beckley, L., Heege, T., Hausknecht, P., Pinnel, N. (2007): Mapping the shallow marine benthic habitats of rotnnest island, Western Australia Proceedings 3th EARSeL Workshop Remote Sensing of the Coastel Zone. Bozen, Italy, June 7-9 2007, p. 1-12
- Heege, T., & Fischer, J. (2000): Sun glitter correction in remote sensing imaging spectrometry. SPIE Ocean Optics XV Conference, Monaco, October 16-20.
- Heege, T., & Fischer, J. (2004): Mapping of water constituents in Lake Constance using multispectral airborne scanner data and a physically based processing scheme. *Can. J. Remote Sensing*, Vol. 30, No. 1, pp. 77-86
- Heege, T., Bogner, A., Häse, C., Albert, A., Pinnel, N., & Zimmermann, S. (2003): Mapping aquatic systems with a physically based process chain. Proc. 3rd EARSeL Workshop on Imaging Spectroscopy, Herrsching, 13-16 May 2003. Edited by M. Habermeyer, A. Müller, S. Holzwarth. ISBN 2-908885-26-3, pp. 415-422.
- Heege, T., Bogner, A., & Pinnel, N. (2004): Mapping of submerged aquatic vegetation with a physically based process chain. *Remote Sensing of the Ocean and Sea Ice 2003*. Editors: Charles R. Bostater, Jr. & Rosalia Santoleri. Proc. of SPIE Vol. 5233 (SPIE, Bellingham, WA, 2004). ISBN: 0-8194-5116-9 pp. 43-50.
- Heege, T., Hausknecht, P. & Kobryn, H. (2007): Hyperspectral seafloor mapping and direct bathymetry calculation using HyMap data from the Ningaloo reef and Rottneest Island areas in Western Australia. Proceedings 5th EARSeL Workshop on Imaging Spectroscopy. Bruges, Belgium, April 23-25 2007, p. 1-8.
- Kisselev, V., & Bulgarelli, B. (2004): Reflection of light from a rough water surface in numerical methods for solving the radiative transfer equation. *J. Quant. Spectrosc. Ra.*, 85:419–435, 2004.
- Odermatt, D., Heege, T., Nieke, J., Kneubühler, M., & Itten, K. (2008): Water quality monitoring for Lake Constance with a physically based algorithm for MERIS data. *Sensors*, Special Issue on Ocean Remote Sensing, Vol. 8, No. 8, pp. 4582-4599.
- Odermatt, D., Heege, T., Nieke, J., Kneubühler, M., & Itten, K.I. (2008): MERIS Chl-a Time series of Lake Constance 2003-2006, in IEEE Geoscience and Remote Sensing Symposium (IGARSS 2008), IEEE Boston (USA), CD-ROM.
- Pinnel, N., Heege, T., & Zimmermann, S. (2004): Spectral Discrimination of Submerged Macrophytes in Lakes Using Hyperspectral Remote Sensing Data. SPIE Proc. Ocean Optics XVII, October 25-29, Fremantle. SPIE - The International Society for Optical Engineering, CD-ROM proceedings, pp 1-16.
- Pinnel, N. (2007): A method for mapping submerged macrophytes in lakes using hyperspectral remote sensing. Dissertation Technische Universität München.

APPENDIX C

Checklist and a summary of data correction and adjustments undertaken on the field data describing marine habitats at Ningaloo from combined data sources and all field trips (Murdoch University and CSIRO).

- Geographic coordinates from the field GPS unit were changed from degree-minute-second units into decimal degrees and projected coordinates (WGS84) Easting/Northing were added into the database (UTM Zones 49 and 50)
- Several points that included incorrect or unknown benthic codes were modified, this was facilitated by visual analysis of photos taken at sites
- Location names and comments were added to data points where missing
- Obviously incorrect coordinates as a result of GPS error were deleted, for instance some points plotted at the previous day's location
- Points with an obvious GPS error of several pixels) were deleted, if the correct location could not be determined from the HyMap image and thus could not be assigned to a neighbouring pixel
- Points with an obvious GPS error of several pixels that could be assigned to a neighbouring pixel as determined from the HyMap image were shifted to their correct location (for example data collected over a bommie or along the edge of a limestone platform)
- Points referring to a landmark, sanctuary border or similar or with no benthic cover percentages were deleted
- Multiple points within same megaquadrat (10 m x10 m) deleted, as their individual GPS location had not been measured
- Points assigned a high percentage cover of algae, but on visual analysis of the HyMap image had the appearance of abiotic substrate and vice versa as a result of the seasonality of certain algal types were deleted
- Benthic cover percentages were added to points lacking percentages but describing the benthic cover in the 'Comments' field, e.g. describing a boundary between 2 substrates could be changed to 50 % of the one and 50 % of the other substrate
- Points with percentage cover not adding up to 100% were corrected where possible or deleted
- Points including other or additional categories either not existing in the benthic codes list or not used in the majority of points, e.g. "Bommies", were deleted
- As CSIRO data consisted of transects and not single points, only "continuous cover" data points could be used, i.e. points with one category > 95 %, where the assumption could be made that the starting point of the transect would be representative of the dominant category. The cut-off was selected at 95 %, in order to include as many data points as possible of areas not included in the Murdoch data. In order to ensure that the data point representing the start point of the transect would not represent the remaining percentage category (e.g. the remaining 5%), the image spectra of the point was at a later stage compared to other parts of the transect and other points of the same class
- For combining CSIRO and Murdoch data, the CSIRO data structure was adapted to the Murdoch data structure (i.e. divided into up to 9 benthic cover categories and respective percentage cover values).

APPENDIX D

Hymap land report Curtin University

Hymap Ningaloo Corrected Reflectance Dataset Report: Land Reflectance

Data Release V1.0 June 2007

Mark A Gray mark.gray@postgrad.curtin.edu.au

Land Reflectance Correction

Summary

This report summarizes the land data atmospheric correction of April/May 2006 HyMap observation of the Ningaloo Marine Park and nearby areas. HyMap flight tracks have been masked for land and atmospherically corrected using TAFKAA 6S (ATREM 4.0) using observed meteorology. This report summarizes parameters used and computed during processing and outlines the processing steps undertaken.

Processing

Roughly 70% of all flight tracks contain in excess of 5% land (table 1). All flight tracks have been processed with TAFKAA 6S regardless of the land coverage using land masks generated from normalized difference vegetation index calculations. Non-land areas have a reflectance set to -1.0. The land mask data set is very simple: a value of 0 denotes water and a value of 100 denotes land.

Currently end to end processing of the entire data set consumes approximately 12 hours of CPU time.

Data Formats

Corrected reflectance and land mask data is delivered in ENVI data format, a flat binary format in BIL or BSQ ordering with a simple text header in a separate *.hdr file. The files can be accessed using standard programming tools.

Meteorology

Aerosol loading

An AERONET sun photometer was located in the Ningaloo area for the duration of the HyMap flights. 550 μ m transmittance from this sensor is aerosol measurement used to determine the atmospheric aerosol loading (table 2). These data are publicly available at <http://aeronet.gsfc.nasa.gov>

Column Water Vapor

Radiosondes at 0Z and 12Z are launched from Learmonth. The 0Z is used to calculate the column water vapor and this value is used for the entire track (table 2). TAFKAA 6S computes the water vapor beneath the instrument based on this, the altitude and the atmospheric profile (set to the 'Mid Latitude Summer' standard profile for all flight tracks). Sensitivity tests performed during processing have shown that the atmospheric correction is insensitive to the selected profile.

These data are available at <http://weather.uwyo.edu/upperair/sounding.html>

Ozone

Total column ozone is measured daily by the NASA TOMS instrument. Ozone for any recent day, time and location is available at http://toms.gsfc.nasa.gov/teacher/ozone_overhead_v8.html. Values used are summarized in table 2.

Remote Sensing and Satellite Research Group

Flight Track	Fractional Land Coverage
Blk A 01	4.63E-02
Blk A 02	0.3145941
Blk A 03	0.7956949
Blk A 04	0.9628332
Blk B 05	1.32E-02
Blk B 06	0.2253254
Blk B 07	0.692734
Blk B 08	0.8947484
Blk C 09	9.80E-04
Blk C 10	0.1999441
Blk C 11	0.7172551
Blk C 12	0.9994916
Blk D 13	6.64E-02
Blk D 14	0.1179425
Blk D 15	0.2971862
Blk D 16	0.4842899
Blk E 17	0.5612277
Blk E 18	0.1082192
Blk E 19	0.1187839
Blk E 20	0.1850896
Blk E 21	0.3788051
Blk E 22	0.9362414
Blk E 23	1
Blk F 24	7.89E-07
Blk F 25	9.36E-05
Blk F 26	6.33E-05
Blk F 27	1.05E-03
Blk F 28	3.13E-03
Blk F 29	4.78E-02
Blk F 30	8.32E-02
Blk F 31	0.1550743
Blk F 32	0.4426598
Blk F 33	0.8712289
Blk F 34	0.9999995
Blk G 35	1.77E-05
Blk G 36	8.85E-05
Blk G 37	5.08E-02
Blk G 38	0.2742838
Blk G 39	0.7659695
Blk G 40	0.9996023
Blk H 41	5.86E-05
Blk H 42	6.03E-02
Blk H 43	0.4188039
Blk H 44	0.6575004
Blk H 45	0.733219
Blk H 46	0.6618091
Blk I 47	1.76E-04
Blk I 48	2.01E-05
Blk I 49	1.03E-05
Blk I 50	8.93E-02
Blk I 51	0.5154994
Blk I 52	0.9589667
Blk J 53	2.98E-04
Blk J 54	7.26E-02
Blk J 55	8.02E-02
Blk J 56	6.52E-02
Blk J 57	3.38E-02
Blk J 58	5.34E-05
Blk K 59	0.9925665
Blk K 60	0.8290047
Blk K 61	0.6988035
Blk K 62	0.3877163
Blk K 63	0.2631001
Blk K 64	0.295511
Blk K 65	6.81E-02
Blk K 66	2.72E-04
Blk K 67	7.61E-05

Table 1. Fractional land coverage for all flight tracks

Flight Day	Ozone (Dobson Units)	Column Water Vapor (cm)	Tau 500µm
April 21 2006	271	3.762	.05
April 22 2006	262	2.936	.05
April 23 2006	264	3.240	.04
April 24 2006	260	2.735	.04
April 25 2006	269	2.456	.04
April 28 2006	265	0.822	04
May 1 2006	271	1.151	.04

Table 2. Meteorology used for TAFKAA 6S runs for all flight days

APPENDIX E

Frequency of marine habitat classes used for classification in the field database.

Frequency	Class name
233	Continuous-S
80	Equal-LP/Equal-S
80	Dom-S/MA
80	Continuous-HC_withHC=Continuous-CT
79	Continuous-LP
75	Dom-LP/HC_withHC=Equal-CD/Equal-CT
52	Equal-LP/Equal-MA/Equal-S
47	Equal-MA/Equal-S
47	Equal-HC/Equal-S_withHC=Equal-CB/Equal-CT/Equal-CF/Equal-CM/Equal-CS
45	Equal-HC/Equal-S_withHC=Continuous-CT
37	Continuous-SC
37	Dom-LP/S
32	Dom-LP/HC/MA/TA_withHC=Continuous-CD
31	Continuous-IDC
27	Continuous-HC_withHC=Dom-CT/CD
26	Dom-LP/MA
21	Continuous-MA
21	Continuous-HC_withHC=Continuous-CB
20	Equal-LP/Equal-R/Equal-S
20	Continuous-HC_withHC=Continuous-CD
20	Equal-HC/Equal-LP_withHC=Continuous-CT
18	Dom-MA/R
18	Continuous-HC_withHC=Continuous-CM
17	Dom-LP/MA/S
16	Dom-LP/HC/MA/S_withHC=Continuous-CD
16	Dom-SC/HC/LP_withHC=Continuous-CD
15	Continuous-HC_withHC=Continuous-CBT
14	Equal-HC/Equal-LP_withHC=Continuous-CD
13	Equal-LP/Equal-MA
13	Dom-HC/S_withHC=Continuous-CBT
13	Equal-HC/Equal-IDC_withHC=Continuous-CBT
12	Equal-HC/Equal-IDC_withHC=Continuous-CM
12	Equal-HC/Equal-LP_withHC=Dom-CT/CD
11	Dom-LP/TA
11	Dom-MA/LP
11	Dom-MA/S
10	Continuous-HC_withHC=Continuous-CF
10	Continuous-R
10	Equal-HC/Equal-IDC_withHC=Equal-CD/Equal-CT
10	Equal-HC/Equal-IDC_withHC=Continuous-CD
10	Equal-HC/Equal-IDC_withHC=Continuous-CT
10	Equal-HC/Equal-S_withHC=Continuous-CD

9	Equal-HC/Equal-S_withHC=Dom-CT/CBT/CD
9	Equal-HC/Equal-S_withHC=Dom-CT/CD/CS
8	Dom-HC/IDC_withHC=Continuous-CT
8	Dom-HC/LP_withHC=Dom-CT/CD/CE/CS
8	Equal-HC/Equal-IDC/Equal-S_withHC=Continuous-CBT
8	Equal-HC/Equal-S_withHC=Equal-CD/Equal-CT
8	Equal-HC/Equal-S_withHC=Continuous-CB
7	Dom-S/HC/IDC_withHC=Continuous-CB
6	Continuous-HC_withHC=Equal-CB/Equal-CT
6	Continuous-HC_withHC=Equal-CD/Equal-CT/Equal-CE/Equal-CF/Equal-CS
6	Dom-SC/HC/LP/MA_withHC=Continuous-CD
5	Dom-SC/HC/LP/MA_withHC=Equal-CD/Equal-CT
5	Equal-HC/Equal-IDC/Equal-S_withHC=Dom-CBT/CD
4	Continuous-HC_withHC=Dom-CT/CM/CS
4	Continuous-HC_withHC=Equal-CD/Equal-CT
4	Dom-IDC/HC_withHC=Continuous-CM
3	Continuous-HC_withHC=Equal-CB/Equal-CF
3	Dom-HC/IDC_withHC=Dom-CM/CD
3	Dom-HC/IDC_withHC=Continuous-CD
3	Dom-HC/S_withHC=Continuous-CD
3	Dom-HC/S_withHC=Continuous-CM
3	Dom-IDC/HC_withHC=Dom-CD/CT
3	Dom-IDC/HC_withHC=Continuous-CD
3	Dom-IDC/HC_withHC=Continuous-CT
3	Dom-S/HC/IDC_withHC=Continuous-CT
Sum = 1512	

APPENDIX F

R code for calculating JM distance

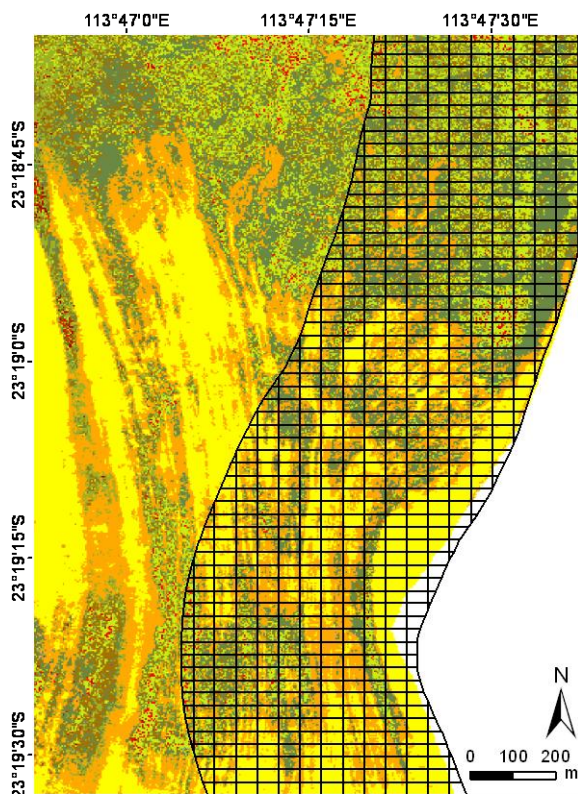
```
library(MASS)
# define new function
dJM <- function(Y, X){
  # column-wise mean and cov for PRE
  m.y <- colMeans(Y)
  c.y <- cov(Y)
  # column-wise mean and cov for POST
  m.x <- colMeans(X)
  c.x <- cov(X)
  # mean difference and its transpose matrix
  m.diff <- as.matrix(m.y - m.x)
  m.diff.t <- t(m.diff)
  # halfsum of covariances
  C <- (c.y + c.x)/2
  # the index
  index <- sqrt( 2 * (1 - exp(-(0.125 * m.diff.t %*% ginv(C) %*% m.diff + 0.5 *
  log(det(C)/sqrt(det(c.y)*det(c.x)))))))
  # print result
  index
}
dJM(Y,X)
dJM(Y,X)^2
```

APPENDIX G

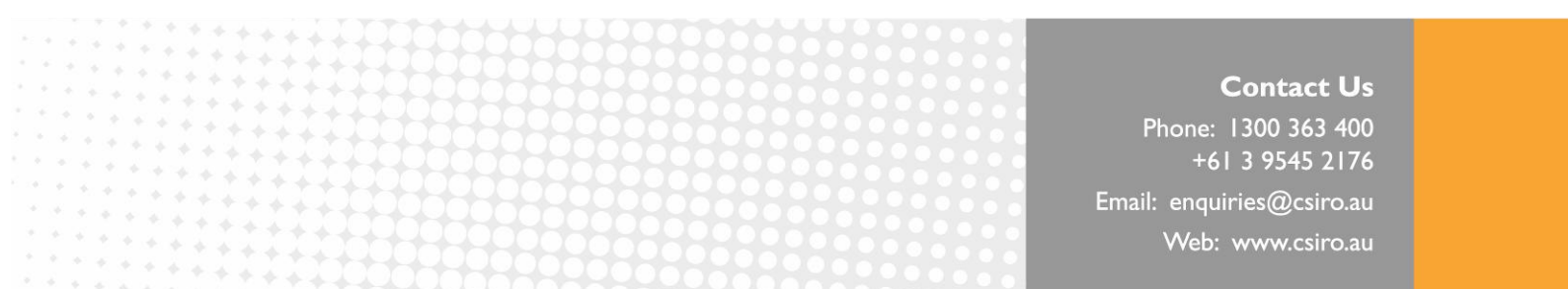
Additional processing was performed on the habitat classification data to support various biodiversity studies (University of Queensland, Murdoch University and CSIRO). The support work consisted of generating a buffer of a fixed distance from the shore (600m) over the marine habitats and creating a sampling grid within that polygon. The aim was to create centroids for each cell to extract geographic coordinates used as input to field GPS units. This was followed by overlaying the grid over generalised habitat maps of two mosaics (dominated by either coral or macroalgae communities) and randomly extracting habitat labels for 20% of the cells.

Other tasks included:

- Overlaying the grid over habitat maps and extracting habitat labels
- Randomly (within each class of the coral and macroalgae dominated mosaics) selecting 20% of points which could then be used by the field crew to access from the shore
- Plotting GPS locations of the field sites
- Plotting field data and extracting habitat information over areas identified as possible fish grazing halos



Example of a 30 by 50m grid superimposed over habitat map to support field sampling.



Contact Us

Phone: 1300 363 400

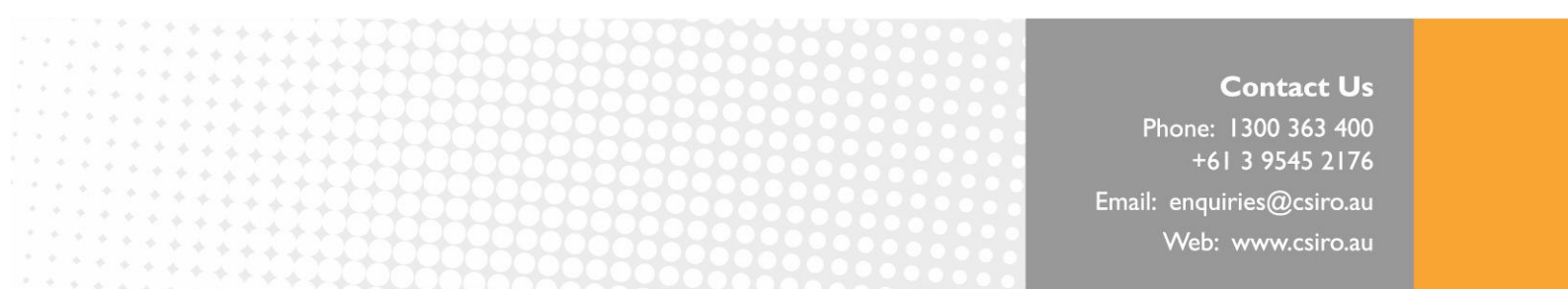
+61 3 9545 2176

Email: enquiries@csiro.au

Web: www.csiro.au

Your CSIRO

Australia is founding its future on science and innovation. Its national science agency, CSIRO, is a powerhouse of ideas, technologies and skills for building prosperity, growth, health and sustainability. It serves governments, industries, business and communities across the nation.



Contact Us

Phone: 1300 363 400

+61 3 9545 2176

Email: enquiries@csiro.au

Web: www.csiro.au

Your CSIRO

Australia is founding its future on science and innovation. Its national science agency, CSIRO, is a powerhouse of ideas, technologies and skills for building prosperity, growth, health and sustainability. It serves governments, industries, business and communities across the nation.